

UNIVERSITAT POLITÈCNICA DE VALÈNCIA

DOCTORADO EN INGENIERÍA Y PRODUCCIÓN INDUSTRIAL



UNIVERSITAT
POLITÈCNICA
DE VALÈNCIA



TESIS DOCTORAL

"Utilización de aceite de semilla de algodón como materia base renovable para la optimización de formulaciones de polímeros de alto rendimiento medioambiental"

Autor

Alfredo Carbonell Verdú

Dirigida por

Dr. Rafael Antonio Balart Gimeno

Dra. Lourdes Sánchez Nacher

Septiembre 2018

UNIVERSITAT POLITÈCNICA DE VALÈNCIA

DOCTORADO EN INGENIERÍA Y PRODUCCIÓN INDUSTRIAL



**UNIVERSITAT
POLITÈCNICA
DE VALÈNCIA**

ITM



INSTITUTO DE TECNOLOGÍA DE MATERIALES

TESIS DOCTORAL

"Utilización de aceite de semilla de algodón como materia base renovable para la optimización de formulaciones de polímeros de alto rendimiento medioambiental"

Alfredo Carbonell Verdú

A GRADECIMIENTOS.

Son tantas las personas que, de una manera u otra, han estado involucradas en tan ardua tarea que cuesta no emocionarse al redactar este apartado. Cualquier trabajo de esta índole conlleva un gran esfuerzo y dedicación, también algunas veces cierta frustración, pero las siguientes personas siempre han estado a mi lado apoyándome ya sea en lo académico o personal y, por consiguiente, merecen un reconocimiento más que merecido entre estas líneas.

En primer lugar, quiero expresar mi más profundo agradecimiento a mis directores de tesis, los catedráticos Rafael Antonio Balart Gimeno y Lourdes Sánchez Nácher. Sin ellos nada de esto habría sido posible pues han estado presentes, no solo como guías y apoyo fundamental en la tesis, sino durante toda mi formación universitaria. Formación durante la cual, además de conceptos, fórmulas e investigaciones me han enseñado a mimar la ciencia y a querer formar parte de ella. Siempre os estaré agradecido. Gracias por ser mi referencia y haber creído en mí en todo momento.

Al catedrático Juan López Martínez por hacerme partícipe de todos sus proyectos; algunos de los cuales nos han llevado incluso a tierras orientales en búsqueda de nuevos materiales. 非常感謝你

Al profesor Luigi Torre y a su grupo de investigación de la Università degli Studi di Perugia (Terni, Italia) y en especial a Franco Dominici quien, además de por sus acertados consejos científicos, me hizo sentir como un miembro más de su familia. Grazie mille e molti altri anni di amicizia.

A los profesores David García Sanoguera, Octavio Ángel Fenollar, Emilio Rayón, Teodomiro Bonorat y Néstor Montañés por sus aportaciones y colaboraciones durante estos años. Y como no mencionar a los técnicos de laboratorio Matías, Javi y Rafa por sus apoyos técnicos. Muchas gracias.

Cómo olvidar a esa gran familia forjada en el laboratorio entre probetas, risas, ensayos y confidencias. Más allá de simples compañeros habéis sido un pilar

fundamental durante todos estos años. Mado, Dani, Pelayo, Vicent y Marina: gracias por estar siempre a mi lado y por momentos inolvidables que dejan huella. Luis, Miguel, David y Leandro gracias por enriquecer todos esos recuerdos con vuestra esencia.

Más allá de las paredes del ámbito académico, este trabajo se ha gestado durante muchas horas en casa donde mis padres Beatriz y Alfredo y en especial a mi hermano Óscar quien ha vivido de primera mano mis alegrías y logros, pero también mis frustraciones y nervios. Gracias a todos. Sin vuestra ayuda no hubiese sido posible.

Por último, y no por ello menos importante,

Gracias por los recursos y ayudas ofertadas, pero también por habernos dado un marco en el cual hemos podido crear una comunidad científica fundamentada en el rigor y la amistad en la cual poder aportar nuestro granito de arena a la investigación por y para una mejor sociedad:

Al Instituto de Tecnología de Materiales (ITM) de la Universidad Politécnica de València.

A la Universitat Politècnica de València por el apoyo financiero a través de la ayuda otorgada de la beca FPI

Al Ministerio de Economía y Competitividad (MINECO) por el soporte financiero de este trabajo (MAT2014-59242-C2-1-R MAT2017-84909-C2-2-R.)

A la Conselleria d'Educació, Cultura y Esports por el soporte financiero de este trabajo (GV/2014/008).

RESUMEN.

“Utilización de aceite de semilla de algodón como materia base renovable para la optimización de formulaciones de polímeros de alto rendimiento medioambiental”

En la última década se ha producido un cambio social de gran relevancia en el ámbito del medio ambiente. Nuestra sociedad es cada vez más consciente del concepto de desarrollo sostenible. Aspectos como la economía circular están adquiriendo gran importancia y ello implica un uso adecuado de los recursos naturales y de los residuos que se generan en diversas actividades empresariales.

La industria del algodón siempre ha tenido como producto principal la fibra de algodón; no obstante, la planta del algodón también incluye el tallo y las semillas. Parte de las semillas se emplean para re-siembra, pero el resto da lugar a un subproducto de grandes volúmenes que se emplea como complemento alimenticio para animales. La semilla de algodón es rica en ácidos grasos insaturados, proteínas y componentes lignocelulósicos. Si bien es posible obtener aceite de semilla de algodón para uso alimenticio, los procesos de refino son complejos y caros y, dado que el principal producto de la industria algodonera es la fibra, los cultivos de esta planta no están sujetos a las restrictivas reglamentaciones de otros cultivos utilizados, principalmente, en alimentación.

Esta tesis doctoral explora las posibilidades de las semillas de algodón como material base para la obtención de polímeros y aditivos de polímeros para el desarrollo de formulaciones de plásticos más respetuosas con el medio ambiente.

En la presente tesis doctoral se exploran diversas posibilidades de modificación del aceite de semilla de algodón para la obtención de resinas termoestables, aditivos plastificantes para polímeros termoplásticos, agentes compatibilizantes y harinas de refuerzo para compuestos.

Dado el perfil lipídico del aceite de semilla de algodón, con alto contenido en ácidos grasos monoinsaturados y poliinsaturados, es posible llevar a cabo diversas modificaciones químicas. Se ha trabajado en el proceso de epoxidación con el empleo de

peroxoácidos generados *in situ* y se ha procedido a optimizar los parámetros de dicho proceso con el fin de obtener el mayor rendimiento de epoxidación. Estos aceites epoxidados se han utilizado como resinas termoestables (resinas con funcionalidad de tipo epoxi) y como plastificantes en diversos polímeros como el poli(cloruro de vinilo) (PVC) y el ácido poliláctico (PLA).

Otro de los procesos de modificación que se ha desarrollado y optimizado es la maleinización del aceite de semilla de algodón en presencia de anhídrido maleico. Una vez obtenidos estos aceites modificados, se ha validado su uso en formulaciones de polímeros de alto rendimiento medioambiental, tanto en formato pieza como en formato film o película.

Finalmente, con el fin de llevar a cabo un máximo aprovechamiento de la semilla de algodón, se ha trabajado en el desarrollo de compuestos con base de ácido poliláctico y refuerzos/rellenos de harina de semilla de algodón, con el empleo de agentes compatibilizantes derivados del aceite de semilla de algodón.

Con esta tesis doctoral, se abren nuevas posibilidades dirigidas hacia la revalorización de un subproducto de la industria algodonera a través de la extracción y modificación química de los aceites de la semilla y aprovechamiento de los residuos de la extracción como rellenos o refuerzos en compuestos que imitan la madera. De esta manera, a la vez que se ofrece una solución a la gran cantidad de residuos de semilla de algodón a nivel mundial, se valida la utilidad de los diferentes materiales derivados de la semilla de algodón en la obtención de formulaciones de plásticos industriales de alto rendimiento medioambiental.

RESUM.

“Utilització d’oli de llavor de cotó com a materia base renovable per a l’optimització de formulacions de polímers d’alt rendiment mediambiental”

En l’última dècada s’ha produït un canvi social de gran rellevància en l’àmbit del medi ambient. La nostra societat és, cada vegada, més conscient del concepte de desenvolupament sostenible. Aspectes com ara l’economia circular estan adquirint gran importància i això implica un ús adequat dels recursos naturals i dels residus que es generen en diverses activitats empresarials.

La indústria del cotó sempre ha tingut com a producte principal la fibra de cotó; no obstant això, la planta de cotó també inclou la tija i les llavors. Part de les llavors s’utilitzen en el procés de sembra, però la resta constitueix un subproducte de gran volum que s’utilitza com a complement alimentari per a animals. La llavor de cotó és rica en àcids grassos saturats, proteïnes i components lignocel·lulòsics. Si bé és cert que es pot obtenir oli de llavor de cotó per a ús alimentari, els processos de refinament son complexes i cars i, donat que el principal producte de la indústria del cotó és la fibra, els cultius d’aquesta planta no estan subjectes a les restrictives reglamentacions d’altres cultius utilitzats, principalment, en alimentació.

Aquesta tesi doctoral explora les possibilitats de les llavors de cotó com a material base per a l’obtenció de polímers i additius de polímers per al desenvolupament de formulacions de plàstics més respectuoses amb el medi ambient.

En la present tesi doctoral, s’exploren diverses possibilitats de modificació de l’oli de la llavor de cotó per a l’obtenció de resines termoestables, additius plastificants per a polímers termoplàstics, agents compatibilitzants i farines de reforç per a compostos.

Donat el perfil lipídic de l’oli de llavor de cotó, amb un alt contingut d’àcids grassos mono insaturats i poli insaturats, és possible dur a terme diferents modificacions químiques. S’ha treballat en el procés d’epoxidació amb la utilització de peroxyàcids generats *in situ* i s’ha procedit a optimitzar els paràmetres de l’esmentat procés amb la finalitat d’obtenir el major rendiment d’epoxidació. Aquestsolis epoxidats s’han utilitzat

com a resines termoestables (resines amb funcionalitat de tipus epoxi) i com a plastificants en diversos polímers com ara el poli(clorur de vinil) (PVC) i l'àcid polilàctic (PLA).

Altre procés de modificació que s'ha desenvolupat i optimitzat és la maleinització de l'oli de llavor de cotó en presència d'anhidrid maleic. Una vegada obtinguts aquests olis modificats, s'ha validat el seu ús en formulacions de polímers d'alt rendiment mediambiental, tant en forma de peces com en format de film o pel·lícula.

Finalment, amb la finalitat d'aprofitar al màxim la llavor de cotó, s'ha treballat en el desenvolupament de compostos amb base àcid polilàctic i reforços/càrregues de farina de llavor de cotó, amb la utilització d'agents compatibilitzants derivats de l'oli de llavor de cotó.

Amb aquesta tesi doctoral, s'obrin noves possibilitats dirigides cap a la revalorització d'un subproducte de la indústria del cotó mitjançant de l'extracció i modificació química dels olis de llavor i aprofitament dels residus de l'extracció com a càrregues o reforços en compostos que imiten la fusta. D'aquesta manera, al mateix temps que s'ofereix una solució a la gran quantitat de residus de llavors de cotó a nivell mundial, es valida la utilitat dels diferents materials derivats de la llavor de cotó en l'obtenció de formulacions de plàstics industrials d'alt rendiment mediambiental.

SUMMARY.

“Use of cottonseed oil as renewable base material for the optimization of high environmentally friendly polymer formulations”

In the last decade a social change of great relevance in the field of environment has been detected. Our society is increasingly aware of the concept of sustainable development. Some topics such as the circular economy are gaining great importance and this implies a proper use of natural resources and an appropriate waste management.

The main product of the cotton industry has been traditionally the cotton fiber; However, the cotton plant also includes the stem and seeds. Part of the seeds are used for re-seeding, but the rest results in a by-product of large volumes which is used as a food supplement for animals. The cottonseed contains high amounts of unsaturated fatty acids, proteins and lignocellulosic components. While it is possible to obtain oil from cottonseed for alimentary use, the refining processes are complex and expensive, and since the main product of the cotton industry is fiber, the crops of this plant are not subjected to the restrictive regulations of other crops whose main market is food industry.

This doctoral thesis explores the possibilities of cottonseed as a base renewable material for obtaining polymers and polymer additives for the development industrial of formulations more respectful with the environment.

In the present thesis different possibilities of modification of cottonseed oil are explored with the aim of obtaining thermosetting resins, plasticizer additives for thermoplastics polymers, compatibilizers agents and flours/powder for reinforcement in composites.

Given the lipid profile of cottonseed oil, with high content of monounsaturated and polyunsaturated fatty acids, it is possible to carry out different chemical modifications. One of these processes is epoxidation using peroxy acids generated *in-situ* which has been optimized in terms of process parameters in order to obtain the best

epoxidation yielding. These epoxidized oils have been used as thermosetting resins (resins with epoxy type functionality) and as plasticizers in several polymers such as poly(vinyl chloride) (PVC) and poly (lactic acid) (PLA).

Another chemical modification of cottonseed oil developed and optimized in this thesis is maleinization in the presence of maleic anhydride. Once obtained these modified oils, it has been validated their potential use in polymer formulations characterized by high environmental efficiency, both in format piece format and film.

Finally, with the aim of maximizing the use of cottonseed, poly(lactic acid) composites with cottonseed oil wastes (in the form of powder or flour) have been manufactured and compatibilized with modified vegetable oils derived from cottonseed.

With this doctoral thesis, new opportunities focused on upgrading of a by-product of the cotton industry have been proposed, through the extraction and chemical modification of the seed oil and by using the wastes obtained from the oil extraction as fillers or reinforcements in wood like composites. Therefore, this thesis provides solution to two important problems: on one hand, it gives a solution to the large amounts of generated waste coming from the cottonseed industry worldwide and, on the other hand, new environmentally friendly materials can be obtained by using cottonseed-derived materials, mainly modified oils and particle fillers.

Tabla de contenidos.

LISTADO DE FIGURAS.	25
LISTADO DE TABLAS.	33
I. INTRODUCCIÓN.....	37
I.1. ACEITES VEGETALES EN INGENIERÍA.....	39
I.1.1. Estructura.	42
I.1.2. Propiedades.	45
I.2. ACEITE DE SEMILLA DE ALGODÓN (CSO).	53
I.2.1. Producción mundial de CSO.	54
I.2.2. Composición de CSO.	56
I.2.3. Composición y propiedades de CSO.	56
I.3. POLÍMEROS DE ALTO RENDIMIENTO MEDIOAMBIENTAL.	57
I.3.1. Polímeros termoplásticos.....	58
I.3.1. Polímeros termoestables.	64
I.4. TERMOESTABLES DERIVADOS DE ACEITES VEGETALES.....	75
I.4.1. Resinas derivadas de aceites vegetales epoxidados.	75
I.4.2. Resinas derivadas de aceites vegetales epoxidados-acrilados....	76
I.4.3. Resinas derivadas de aceites vegetales maleinizados.....	77
I.5. PLASTIFICANTES DERIVADOS DE ACEITES VEGETALES.....	78
I.5.1. Aceites vegetales epoxidados.	79
I.5.2. Aceites vegetales maleinizados.	79
I.5.3. Aceites vegetales epoxidados-acrilados.	80
I.6. REFERENCIAS.....	81
II. INVESTIGACIÓN PREVIA.....	99
II.1. MARCO DE LA INVESTIGACIÓN.	101
II.2. Development of slate fiber reinforced high density polyethylene composites for injection molding.	113
Abstract.	115
Keywords.....	115

II.2.1. Introduction.	116
II.2.2. Experimental.	117
II.2.3. Results and Discussion.	121
II.2.4. Conclusions.	130
Acknowledgements.	130
References.	131
II.3. Wet-laid technique with <i>Cyperus esculentus</i>: Development, manufacturing and characterization of a composite.	137
Abstract.	139
Keywords.	139
II.3.1. Introduction.	140
II.3.2. Experimental.	143
II.3.3. Results and discussion.	148
II.3.4. Conclusions.	156
References.	158
II.4. Development and characterization of a new natural fiber reinforced thermoplastic (NFRP) with <i>Cortaderia selloana</i> (Pampa grass) short fibers.	163
Abstract.	165
Keywords.	165
II.4.1. Introduction.	166
II.4.2. Experimental.	168
II.4.3. Results and discussion.	172
II.4.4. Conclusions.	185
Acknowledgements.	186
References.	187
III. OBJETIVOS Y PLANIFICACIÓN	191
 III.1. HIPÓTESIS Y OBJETIVOS.	193
 II.1.1. Objetivo general.	195
 II.1.2. Objetivos particulares.	195
 III.2. METODOLOGÍA Y PLANIFICACIÓN.	197
IV. RESULTADOS Y DISCUSIÓN	213
RESUMEN	215

IV.1. Development of Environmentally Friendly Composite Matrices from Epoxidized Cottonseed Oil.....	219
Abstract	221
Keywords.....	221
IV.1.1. Introduction.....	222
IV.1.2. Experimental.	225
IV.1.3. Results and discussion.	229
IV.1.4. Conclusions.	241
Acknowledgements.	242
References.	243
IV.2. A new biobased plasticizer for poly (vinyl chloride), PVC base on epoxidized cottonseed oil (ECSO).....	249
Abstract	251
Keywords.....	251
IV.2.1. Introduction.	252
IV.2.2. Experimental.	254
IV.2.3. Results and discussion.....	257
IV.2.4. Conclusions.	272
Acknowledgements.	273
References.	274
IV.3. Plasticization effect of epoxidized cottonseed oil (ECSO) on poly(lactic acid).....	279
Abstract	281
Keywords.....	281
IV.3.1. Introduction.	282
IV.3.2. Experimental.	284
IV.3.3. Results and discussion.....	288
IV.3.4. Conclusions.	300
Acknowledgements.	301
References.	302
IV.4. PLA films with improved flexibility properties by using maleinized cottonseed oil.	309
Abstract	311
Keywords.....	311
IV.4.1. Introduction.	312
IV.4.2. Experimental.	315

IV.4.3. Results and discussion.....	320
IV.4.4. Conclusions.....	331
Acknowledgements.....	332
References.....	333
IV.5. Manufacturing and compatibilization of PLA/PBAT binary blends by cottonseed oil-based derivatives.....	341
Abstract	343
Keywords.....	343
IV.5.1. Introduction.....	344
IV.5.2. Experimental.....	347
IV.5.3. Results and discussion.....	353
IV.5.4. Conclusions	367
Acknowledgements.....	368
References.....	369
IV.6. Processing and characterization of environmentally friendly composites from poly(lactic acid) and cottonseed waste materials.	377
Abstract	378
Keywords.....	378
IV.6.1. Introduction.	379
IV.6.2. Experimental.....	381
IV.6.3. Results and discussion.....	386
IV.6.4. Conclusions.....	399
Acknowledgements.....	400
References.....	401
V. CONCLUSIONES.....	407
V.1. CONCLUSIONES PARCIALES.....	409
V.1.1. Respecto a termoestables derivados del aceite de semilla de algodón epoxidado.	409
V.1.2. Respecto a los plastificantes derivados de aceite de semilla de algodón con aplicaciones en termoplásticos.	410
V.1.3. Respecto a los efectos de aceites vegetales derivados de semilla de algodón en compatibilización y optimización de formulaciones derivadas de ácido poli(láctico).	413
V.2. CONCLUSIONES FINALES.....	416

ABREVIATURAS Y TÉRMINOS.

1-MI	1-metil imidazol
AA	ácido acrílico
AESO	aceite de soja epoxidado acrilado
AEVO	aceite vegetal epoxidado acrilado
AEW	peso equivalente en anhídrido
ASA	anhídrido alquenil succínico
ATBC	acetil tributil citrato
BioPA	poli(amida) de origen renovable total o parcial
BioPC	poli(carbonato) de origen renovable total o parcial
BioPE	poli(etíleno) de origen renovable total o parcial
BioPET	poli(etilén tereftalato) de origen renovable total o parcial
BPA	bisfenol A
BioPP	poli(propileno) de origen renovable total o parcial
BioPUR	poli(uretano) de origen renovable total o parcial
BBP	butil bencil ftalato
bioPE	poli(etíleno) procedente de recursos renovables
BPH	hexafluoroantimonato de N-benzilpirazinio
C16:0	ácido palmítico
C18:1	ácido oleico
C18:2	ácido linoleico
CNSL	líquido de la vaida del anacardo
CoPA	copolí(amida)

CS	<i>Cortaderia selloana</i>
CSF	harina de semilla de algodón
CSO	aceite de semilla de algodón
δ	ángulo de desfase ($^{\circ}$)
DBP	di- <i>n</i> -butil ftalato
DDSA	anhídrido dodecenil succínico
DEHA	di-2etilhexil adipato
DEHP	bis(2-ethylhexil) ftalato
DETA	dietilén triamina
DGEBA	diglicidil éter de bisfenol A
DGEBF	diglicidil éter de bisfenol F
ΔH_{cc}	entalpía de cristalización en frío ($J\ g^{-1}$)
ΔH_m	entalpía de fusión ($J\ g^{-1}$)
$\Delta H_{m(100\%)}$	entalpía de fusión teórica, polímero 100% cristalino ($J\ g^{-1}$)
DIBP	diisobutil ftalato
DIDP	diisodecil ftalato
DINP	diisononil ftalato
DIOP	diisoctil ftalato
DMTA	análisis térmico mecánico-dinámico
DOA	di-2-ethylhexil adipato
DPHP	di-2-propilheptil ftalato
DSC	calorimetría diferencial de barrido
DTBP	di(tert-butilperoxi isopropil) benceno
DTBH	2,5-dimetil-2,5-(t-butilperoxi) hexano

DTG	derivada curva termogravimétrica
DVB	divinil benceno
ϵ_b	alargamiento a la rotura por tracción (%)
ECO	aceite de ricino epoxidado
ECSO	aceite de semilla de algodón epoxidado
EEW	peso equivalente en epóxido
E_f	módulo a flexión (MPa)
ELO	aceite de linaza epoxidado
E_t	módulo elástico a tracción (MPa)
EP	resina epoxi
EPO	aceite de palma epoxidado
EPSO	aceite de palma y de soja epoxidado
ESBO	aceite de soja epoxidado
ETC	cámara de ensayo ambiental
EVO	aceite vegetal epoxidado
FESEM	microscopía electrónica de barrido con emisión de campo
FTIR	espectroscopía infrarroja por transformada de Fourier
γ	deformación de cortadura (%)
G'	módulo de almacenamiento (MPa)
G''	módulo de pérdidas (MPa)
GRAS	generalmente reconocido como seguro
HDPE	polietileno de alta densidad
HDT	temperatura de flexión bajo carga (°C)
HS _D	dureza Shore D

ICAC	comité asesor internacional sobre el algodón
L*	luminancia (%)
L*a*b*	coordenadas de color
LCA	análisis de ciclo de vida
LDPE	poli(etileno de baja densidad)
LO	aceite de linaza
MA	anhídrido maleico
MCSO	aceite de semilla de algodón maleinizado
MLO	aceite de linaza maleinizado
MDI	metilén difenil diisocianato
MF	resina de melanina-formaldehído
MHHPA	anhídrido metil hexahidroftálico
MHO	aceite de semilla de cáñamo maleinizado
MNA	anhídrido metil nádico
MTHPA	anhídrido metil tetrahidroftálico
MXDA	<i>m</i> -xiléndiamina
MVO	aceite vegetal maleinizado
NFRP	plásticos reforzados con fibras naturales
OLA	oligómero de ácido láctico
OOC	contenido en oxígeno oxiránico (%)
OTR	velocidad de transmisión de oxígeno
OR	reometría oscilatoria
PA	anhídrido ftálico
PA6	poli(amida) 6

PAI	poli(amida imida)
PBA	poli(butil acrilato)
PBAT	poli(butilén adipato- <i>co</i> -tereftalato)
PBS	poli(butilén succinato)
PBSA	poli(butilén succinato- <i>co</i> -adipato)
PBT	poli(butilén tereftalato)
PC	poli(carbonato)
PCL	poli(ϵ -caprolactona)
PE	poli(etileno)
PEG	poli(etilén glicol)
PE- <i>g</i> -MA	copolímero de injerto de etileno y anhídrido maleico
PEK	poli(éter cetona)
PEEK	poli(éter éter cetona)
PEI	poli(éter imida)
PEO	poli(óxido de etileno)
PES	poli(éter sulfona)
PET	politileno tereftalato
PDO	propanodiol
PF	resina fenólica
PGA	ácido poli(glicólico)
PHA	poli(hidroxi alcanoato)
PHB	poli(3-hidroxibutirato)
PHBV	poli(3-hidroxi butirato- <i>co</i> -3-hidroxi valerato)
PLA	ácido poli(láctico)

PMMA	poli(metil metacrilato)
POM	poli(óxido de metileno)
PTMS	propil trimetoxisilano
PP	poli(propileno)
P-PVC	poli(cloruro de vinilo) plastificado
PS	poli(estireno)
PVA	poli(vinil alcohol)
PVC	poli(cloruro de vinilo)
θ	ángulo de contacto
ROP	polimerización por apertura de anillo
RTM	moldeo por transferencia de resina
SBO	aceite de semilla de soja
SEM	microscopía electrónica de barrido
SF	fibra de pizarra
σ_f	tensión de rotura a flexión (MPa)
σ_t	tensión de rotura a tracción (MPa)
$\tan \delta$	factor de pérdidas
$T_{5\%}$	temperatura para una pérdida de masa de 5% ($^{\circ}\text{C}$)
$T_{50\%}$	temperatura para una pérdida de masa de 50% ($^{\circ}\text{C}$)
TAc	triacetina
TBC	tributil citrato
T_{cc}	temperatura de cristalización en frío ($^{\circ}\text{C}$)
T_g	temperatura de transición vítrea ($^{\circ}\text{C}$)
TETA	trietilén triamina

TGA	análisis termogravimétrico
T _m	temperatura de fusión (°C)
TPP	trifenil fosfito
TPS	almidón termoplástico
UHMWPE	poli(etileno) de peso molecular ultra alto
UF	resina de urea-formaldehído
UP	resina de poli(éster insaturado)
UV	ultravioleta
VE	resina de vinil éster
VO	aceite vegetal
VOC	compuesto orgánico volátil
VST	temperatura de reblandecimiento Vicat (°C)
W _t	índice de yodo
WCA	ángulo de contacto con agua (°)
WPC	compuesto plástico de madera
WPLA	porcentaje en peso de ácido poliláctico
X _c	grado de cristalinidad (%)

LISTADO DE FIGURAS.

Figura I.1.1. Representación gráfica de los niveles de producción mundial de los principales aceites. <i>Adaptado de [11]</i>	40
Figura I.1.2. Gráfico comparativo de los principales países productores de aceites y grasas. <i>Adaptado de [12]</i>	41
Figura I.1.3. Representación esquemática de la estructura química de triglicérido formado por el anclaje de tres ácidos grasos a una estructura básica de glícerol.	42
Figura I.1.4. Representación esquemática de la estructura Química de diversos ácidos grasos saturados (mirístico, palmítico, margárico, esteárico, araaquídico), monoinsaturados (miristoleico, palmitoleico, oleico) y poliinsaturados (linoleico, linolénico).....	44
Figura I.1.5. Representación esquemática del proceso de epoxidación con la incorporación de peróxido de hidrógeno y ácido acético para la generación de ácido peroxyacético <i>in situ</i> en presencia de medio ácido.....	47
Figura I.1.6. Representación esquemática del proceso de acrilación en dos etapas.....	49
Figura I.1.7. Representación esquemática del proceso de maleinización de un aceite vegetal mediante reacción con anhídrido maleico a elevada temperatura.....	50
Figura I.1.8. Representación esquemática del proceso de hidroxilación de un aceite vegetal epoxidado (EVO mediante reacción con un alcohol orgánico, en medio ácido.....	52
Figura I.2.1. Representación esquemática de la estructura química del gosipol, polifenol de gran presencia en la semilla de algodón.....	53
Figura I.3.1. Clasificación de materiales poliméricos termoplásticos en función de su respuesta medioambiental en origen (petroquímico o renovable) y al final del ciclo de vida (biodegradable o no).	59
Figura I.3.2. Clasificación de los polímeros termoplásticos en función de sus aplicaciones técnicas	60
Figura I.3.3. Estructura química de diversos poliésteres de origen petroquímico y/o potencialmente biodegradables.....	61
Figura I.3.4. Estructura química de diversos poliésteres obtenidos mediante fermentación bacteriana.	63
Figura I.3.5. Representación esquemática de la formación de una estructura de red tridimensional de naturaleza termoestable.....	65

Figura I.3.6. Representación esquemática de las estructuras químicas de diversos tipos de resinas termoestables ampliamente utilizadas en la fabricación de materiales compuestos.....	66
Figura I.3.7. Representación esquemática de la estructura del aceite de vernonia con ácido vernólico que presenta grupos epóxido de forma natural sin modificación química.	68
Figura I.3.8. Representación esquemática de las estructuras químicas de los principales componentes de los residuos líquidos de la industria del anacardo (CNSL).	74
Figura II.1.1. Esquema de las líneas de investigación activas en el grupo de Investigación en Polímeros y Compuestos Ecológicos (GiP-Eco) y Grupo de Investigación en Procesos de Modificación de Superficies (GiPROSUP) en el que se ha desarrollado la presente tesis doctoral.....	110
Figure II.2.1. SEM images of fractured surface (1000X) of HDPE-SF composites with different compatibilization systems: a) untreated slate fiber (SF), b) untreated slate fiber and use of 2 wt.% PE-g-MA copolymer (SF-MA), c) slate fiber subjected to silane treatment with propyltrimethoxy silane (SF-PTMS) and d) slate fiber subjected to silane treatment with propyltrimethoxy silane (SF-PTMS) in combination with 2 wt.% PE-g-MA copolymer (SF-PTMS-MA).	123
Figure II.2.2. Plot evolution of the storage modulus (G') of HDPE-SF at a fixed slate fiber content of 20 wt.% for different compatibilizing systems.....	124
Figure II.2.3. Plot evolution of mechanical properties of HDPE-SF composites in terms of the slate fiber content (wt.%) a) tensile modulus, tensile strength and elongation at break, b) flexural modulus and flexural strength and c) Charpy's impact energy.	126
Figure II.2.4. SEM images of fractured surface from impact tests (400X) for HDPE-SF composites with different wt.% of slate fiber coupled with propyltrimethoxy silane, PTMS: a) 5 wt.%, b) 10 wt.%, c) 20 wt.% and d) 30 wt.%.....	128
Figure II.2.5. Plot evolution of the storage modulus (G') of HDPE-SF composites containing different wt. % of slate fiber (silanized with propyltrimethoxy silane, PTMS).....	129
Figure II.3.1. (a) Tiger nut tuber. (b) Waste generated in the manufacture of horchata.	141
Figure II.3.2. Tiger nut particles from the manufacture of "Horchata" (8X).....	143
Figure II.3.3. General outline of the process of obtaining nonwovens with wet laid technology.	145
Figure II.3.4. Nonwoven sheet rich in natural fiber rolled up, obtained by wet laid technology.	146
Figure II.3.5. SEM micrographs of the nonwoven surface. (a) 80%wt tiger nut + 10%wt Lyocell+10%wt PA6/CoPA, 320X. (b) 80%wt tiger nut + 10%wt Lyocell+10%wt	

PA6/CoPA, 700X. (c) 80%w flax fiber + 10%wt Lyocell +10%wt HDPE, 320X. (d) 80%w flax fiber + 10%wt Lyocell +10%wt HDPE, 700X.....	149
Figure II.3.6. Flexural modulus of the biocomposites with high natural fiber content (80% wt), based on different binders and thermo-bondings. ..	150
Figure II.3.7. Flexural strength of the biocomposites with high natural fiber content (80% wt), based on different binders and thermo-bondings. ..	151
Figure II.3.8. Variation of the energy absorbed in the impact test of the biocomposites with high natural fiber content (80% wt), based on different binders and thermo-boundings.	154
Figure II.3.9. SEM micrographs of the impact fracture surface of biocomposites with 80% wt waste tiger nut. (a) 80%wt tiger nut + 10%wt Lyocell+10%wt PLA, 300x. (b) 80%wt tiger nut + 10%wt Lyocell+10%wt PA6/CoPA, 300x. (c) 80%wt tiger nut + 10%wt Lyocell +10%wt HDPE, 300x. (d) 80%wt tiger nut + 10%wt Cotton +10%wt PLA, 300X. (e) 80%wt tiger nut + 10%wt Cotton+10%wt PA6/CoPA, 300x.....	155
Figure II.4.1. Comparative plot of the differential scanning calorimetry thermograms (DSC) of unfilled bio-HDPE and bio-HDPE/CS composites with different compatibilizing system.....	172
Figure II.4.2. Comparative plot of the thermogravimetric curves (TGA) of <i>Cortaderia selloana</i> (CS) fiber, unfilled bio-HDPE and bio-HDPE/CS composites with different compatibilizing system.....	173
Figure II.4.3. Tensile properties of bio-HDPE/CS with different compatibilizing system: a) Bio-HDPE/CS-UT; b) Bio-HDPE/CS-NaOH; c) Bio-HDPE/CS-MA; d) Bio-HDPE/CS-Silane.	175
Figure II.4.4. SEM images (2000x) of fractured surfaces from tensile tests of bio-HDPE/CS composites with different compatibilizing system: a) Bio-HDPE/CS-UT untreated fiber, b) Bio-HDPE/CS-NaOH; c) Bio-HDPE/CS-MA; d) Bio-HDPE/CS-Silane.	176
Figure II.4.5. Flexural properties of Bio-HDPE/CS with different compatibilizing system: a) Bio-HDPE/CS-UT; b) Bio-HDPE/CS-NaOH; c) Bio-HDPE/CS-MA; d) Bio-HDPE/CS-Silane.	177
Figure II.4.6. Physical morphology of <i>Cortaderia selloana</i> fibers (10x): a) without treatment; b) alkali treatment with NaOH.....	179
Figure II.4.7. Thermogravimetric (TGA) curves of raw <i>Cortaderia selloana</i> fiber and bio-HDPE/CS composites with different <i>Cortaderia selloana</i> content.	180
Figure II.4.8. Mechanical properties of bio-HDPE/CS composites in terms of the wt.% of <i>Cortaderia selloana</i> content.	181
Figure II.4.9. SEM images (500x) of fractured surfaces from tensile tests of bio-HDPE/CS composites with different <i>Cortaderia selloana</i> content: a) 7.5 wt.%; b) 15 wt.%; c) 30 wt.%.....	182

Figure II.4.10. Variation of the water uptake as a function of the treatment time for bio-HDPE/CS composites with different compatibilizing system.....	184
Figure II.4.11.- Variation of the water uptake as a function of the treatment time for bio-HDPE/CS composites with different <i>Cortaderia selloana</i> content	185
Figura III.2.1. Representación esquemática de la fase de investigación de la tesis doctoral centrada en el aprovechamiento de residuos de semilla de algodón	212
Figure IV.1.1. Schematic representation of the epoxidation process from cottonseed oil (CSO).	222
Figure IV.1.2. Schematic representation of different components used to crosslink epoxidized cottonseed oil.	226
Figure IV.1.3. Influence of peroxide to oil ratio on a) oxirane oxygen change index during epoxidation of cottonseed oil and b) iodine index change during the epoxidation reaction.	230
Figure IV.1.4. Plot evolution of the crosslinking of epoxidized cottonseed oil (ECSO) with mixtures of dodecenylsuccinic anhydride (DDSA) and methyl nadic anhydride (MNA) at a constant EEW:AEC of 1 in terms of the variation of the ionic mobility with time a) 110 °C and b) 120 °C.	233
Figure IV.1.5. Comparative plot of the dynamic DSC curing curves of epoxidized cottonseed oil (ECSO) with mixtures of dodecenylsuccinic anhydride (DDSA) and methyl nadic anhydride (MNA) at a constant EEW:AEC of 1.....	234
Figure IV.1.6. Comparative plot of the evolution of the storage modulus (G') for the curing of epoxidized cottonseed oil (ECSO) with mixtures of dodecenylsuccinic anhydride (DDSA) and methyl nadic anhydride (MNA) at a constant EEW:AEC of 1, obtained by plate-plate oscillatory rheometry at a constant temperature of a) 110 °C and b) 120 °C.	235
Figure IV.1.7. Comparative plot of the evolution of the phase angle (γ) for the curing of epoxidized cottonseed oil (ECSO) with mixtures of dodecenylsuccinic anhydride (DDSA) and methyl nadic anhydride (MNA) at a constant EEW:AEC of 1, obtained by plate-plate oscillatory rheometry at a constant temperature of a) 110 °C and b) 120 °C.	237
Figure IV.1.8. SEM images of the fractured surfaces from Charpy test corresponding with different DDSA:MNA mixture impact fracture of the curing with a) 100% DDSA, x200, b) 100% DDSA, x500, c) 50% DDSA:50% MNA, x200, d) 50% DDSA:50% MNA, x500, e) 100% MNA, x200, f) 100% MNA, x500.....	239
Figure IV.1.9. Plot evolution of the storage modulus (G') and $\tan \delta$ for solid ECSO-based thermosetting resins cured with different DDSA:MNA mixture hardeners in terms of temperature.....	241

Figure IV.2.1. Mechanical properties of PVC plastisols plasticized with epoxidized cottonseed oil (ECSO) in terms of the curing time for different isothermal curing temperatures a) tensile strength, b) elongation at break, c) Young's modulus.....	259
Figure IV.2.2. SEM images (250x) of surfaces of fractured samples from tensile tests of cured PVC plastisols subjected to curing cycles of 7.5 min and temperatures of a) 160 °C, b) 175 °C, c) 190 °C, d) 205 °C and e) 220 °C.....	262
Figure IV.2.3. SEM images (250x) of surfaces of fractured samples from tensile tests of cured PVC plastisols subjected to curing cycles of 17.5 min and temperatures of a) 160 °C, b) 175 °C, c) 190 °C, d) 205 °C and e) 220 °C.....	262
Figure IV.2.4. (1/2) Migration levels (weight percentage gain) of cured PVC plastisols with ECSO plasticizer subjected to different curing cycles at different migration temperatures a) 30 °C and b) 40 °C	264
Figure IV.2.4. (2/2) Migration levels (weight percentage gain) of cured PVC plastisols with ECSO plasticizer subjected to different curing cycles at different migration temperatures, c) 50 °C and d) 60 °C	265
Figure IV.2.5. Comparative DSC curves of cured PVC plastisols plasticized with ECSO subjected to different curing cycles.	268
Figure IV.2.6. Optical photographs of cured PVC plastisols with ECSO plasticizer subjected to different curing conditions in terms of the isothermal curing temperature and curing time.	269
Figure IV.2.7. Contour plot of the luminance of cured PVC plastisols with ECSO plasticizer in terms of the isothermal curing temperature and curing time.	271
Figure IV.2.8. Variation of the color coordinates a*b* of cured PVC plastisols with ECSO plasticizer subjected to different curing conditions.....	272
Figure IV.3.1. Schematic representation of the chemical structure of a) poly(lactic acid)-PLA and b) epoxidized cottonseed oil (ECSO).....	285
Figure IV.3.2. Plot evolution of the impact absorbed energy measured by the Charpy's test for plasticized PLA formulations with different weight % of epoxidized cottonseed oil (ECSO).	291
Figure IV.3.3. FESEM images of fractured surfaces from impact tests corresponding to plasticized PLA formulations with different weight % of epoxidized cottonseed oil (ECSO) at 2000x: a) neat PLA, b) 2.5 wt.% ECSO, c) 5.0 wt.% ECSO, d) 7.5 wt.% ECSO and e) 10 wt.% ECSO.....	292
Figure IV.3.4. Plot evolution of the storage modulus (G') as function of temperature for plasticized PLA formulations with different weight % of epoxidized cottonseed oil (ECSO).	294

Figure IV.3.5. Plot evolution of the damping factor ($\tan \delta$) as function of temperature for plasticized PLA formulations with different weight % of epoxidized cottonseed oil (ECSO).....	295
Figure IV.3.6. Comparative plot of the DSC heating thermograms of neat PLA and plasticized PLA formulations with different weight % of epoxidized cottonseed oil (ECSO).	297
Figure IV.3.7. Plasticizer migration levels by the solvent extraction test on plasticized PLA formulations with different weight % of epoxidized cottonseed oil (ECSO).....	300
Figure IV.4.1. Schematic representation of the maleinization process of cottonseed oil.	314
Figure IV.4.2. Effect of temperature and time on the efficiency of the maleinization process of cottonseed oil with maleic anhydride.	320
Figure IV.4.3. Influence of the reaction temperature and time on the colour during maleinization process of cottonseed oil, a) 180 °C – 60 min, b) 200 °C – 60 min, c) 220 °C – 60 min.	321
Figure IV.4.4. Plot evolution of mechanical properties of plasticized PLA films as a function of the wt% of MCSO and MLO, a) elongation at break, b) tensile strength and c) Young's modulus.	323
Figure IV.4.5. FESEM images (5000x) of the cross section of plasticized PLA films with different maleinized vegetable oils, a) unplasticized PLA, b) PLA with 5 wt% MLO, c) PLA with 7.5 wt% MLO, d) PLA with 5 wt% MCSO and e) PLA with 7.5 wt% MCSO.	324
Figure IV.4.6. Visual aspect of plasticized PLA films with maleinized oils in terms of the oil content and disintegration time (the initial size of all films was 25 x 25 mm ²).	330
Figure IV.5.1. Schematic representation of the chemical structure of a) base polymers, <i>i.e.</i> poly(lactic acid) – PLA and poly(butylene adipate – co – terephthalate) – PBAT and b) epoxidized cottonseed oil – ECSO, maleinized cottonseed oil – MCSO and epoxy styrene-acrylic oligomer Joncrys® (generic structure).	348
Figure IV.5.2. Comparative bar plot of tensile properties, <i>i.e.</i> Young's modulus, tensile strength and elongation at break, of neat PLA, neat PBAT and PLA/PBAT blends with and without compatibilizers.	353
Figure IV.5.3. Schematic representation of a) ECSO compatibilized PLA/PBAT blend, b) MCSO compatibilized PLA/PBAT blend and c) Joncrys®-compatibilized PLA/PBAT blend.	355
Figure IV.5.4. FESEM images of the cryofractured films at 10000x, a) neat PLA b) uncompatibilized PLA/PBAT c) PLA/PBAT (80/20 wt/wt) compatibilized with 1 wt% Joncrys®, d) PLA/PBAT (80/20 wt/wt) compatibilized with 1 wt% ECSO e) PLA/PBAT (80/20 wt/wt) compatibilized with 1 wt% MCSO, f) PLA/PBAT (80/20 wt/wt) compatibilized with 7.5 wt% ECSO and g) PLA/PBAT (80/20 wt/wt) compatibilized with 7.5 wt% MCSO.	357

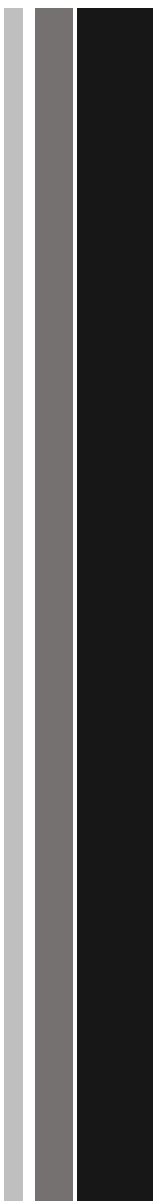
Figure IV.5.5. Differential scanning calorimetry (DSC) thermograms for neat PLA and PBAT.....	358
Figure IV.5.6. Comparative plot of the DSC thermograms of uncompatibilized PLA/PBAT blend (80/20 wt/wt) and the same blend compatibilized with different amounts of Joncrys®, ECSO and MCSO.....	359
Figure IV.5.7. Plot comparison of a) storage modulus, G' and b) damping factor, $\tan \delta$ of neat PLA, PBAT and PLA/PBAT blend (80/20 wt/wt) without and with different compatibilizers. — PLA; - - - PBAT, - - - PLA/PBAT; PLA/PBAT/1 Joncrys®; - - - PLA/PBAT/1 ECSO; - - - PLA/PBAT/1 MCSO; - - - PLA/PBAT/7.5 ECSO; - - - PLA/PBAT/7.5 MCSO	361
Figure IV.5.8. Comparative plot of the TGA thermograms of neat PLA, PBAT and PLA/PBAT blend (80/20 wt/wt) without and with different compatibilizers, a) TGA and b) first derivative DTG.....	363
Figure IV.5.9. Qualitative assessment of the disintegration in controlled compost soil of neat PLA, PBAT and PLA/PBAT blend (80/20 wt/wt) without and with 1 wt% different compatibilizers.....	366
Figure IV.6.1. Images of a) the waste generated during the cold press extraction of cottonseeds and b) micronized cottonseed waste after milling and sieving.....	382
Figure IV.6.2. Schematic plot of the chemical structure of epoxidized and maleinized cottonseed oil, ECSO and MCSO respectively.....	383
Figure IV.6.3. Field emission scanning electron microscopy (FESEM) images at different magnifications (1000x, left column and 2000x, right column) corresponding to neat PLA – a) & b), PLA with 7.5 wt.% ECSO – c) & d) and PLA with 7.5 wt.% MCSO – e) & f).	392
Figure IV.6.4. Field emission scanning electron microscopy (FESEM) images at 1000x corresponding to PLA composites with 15 wt.% CSF – a) & b), PLA composites with 15 wt.% CSF plus 7.5 wt.% ECSO – c) & d) and PLA composites with 15 wt.% CSF plus 7.5 wt.% MCSO – e) & f).	393
Figure IV.6.5. Plot evolution of the storage modulus, G' (red) and damping factor, $\tan \delta$ (blue) corresponding to a) PLA and PLA with 7.5 wt% ECSO and 7.5 wt% MCSO) and b) PLA composites with 15 wt% CSF with additional 7.5 wt% ECSO or 7.5 wt% MCSO.	398

LISTADO DE TABLAS.

Tabla I.1.1. Producción mundial de aceites vegetales a partir de plantas oleaginosas. <i>Adaptado de Tabio García [6]</i>	42
Tabla I.1.2. Distribución de ácidos grasos en varios aceites vegetales, adaptado de Khot S. N., 2001 [16].....	43
Tabla I.2.1. Producción mundial de aceites, adaptado de Ramli, N, 2015 [66].....	55
Table II.2.1. Chemical composition of slate fiber obtained by X-ray fluorescence spectroscopy.	118
Table II.2.2. Composition of HDPE-slate fiber composites and their code.	119
Table II.2.3. Mechanical properties of HDPE-slate fiber composites obtained by tensile, flexural and impact tests in terms of the compatibilizing system for a constant slate fiber content of 20 wt.%.....	121
Table II.3.1. Materials for manufacturing of the nonwoven sheets.	145
Table II.3.2. Values of Shore D hardness of the biocomposites of high content of natural fiber (80% wt), based on different binders and thermo-bondings.	153
Table II.4.1. Composition and designation of the four different formulations of Bio-PE/ <i>Cortaderia selloana</i> composites.....	169
Table II.4.2. Impact resistance values of Bio-PE/CS composites with different compatibilizing system.....	178
Table II.4.3. Effect of <i>Cortaderia selloana</i> content on thermal properties of Bio-HDPE/CS composites obtained by differential scanning calorimetry (DSC).	180
Table IV.1.1. Gel time values at isothermal conditions for the crosslinking of epoxidized cottonseed oil (ECSO) with mixtures of dodecenylsuccinic anhydride (DDSA) and methyl nadic anhydride (MNA) at a constant EEW:AEW of 1.	232
Table IV.1.2. Results of mechanical properties of the ECSO cured resin during bending and impact tests.....	238
Table IV.2.1. Comparison of the mechanical properties of cured PVC plastisols with different plasticizers: epoxidized cottonseed oil (ECSO), epoxidized linseed oil (ELO), epoxidized soybean oil (ESBO), diisononyl phthalate (DINP), bis(2-ethylhexyl) phthalate (DEHP) and dioctyl phthalate (DOP).	260
Table IV.2.2[a]. Percentage plasticizer migration for PVC cured plastisols subjected to different a curing cycle of 7.5 min at 160 °C, in terms of the solvent extraction test with <i>n</i> -hexane in terms of migration time and temperature.	266

Table IV.2.2[b]. Percentage plasticizer migration for PVC cured plastisols subjected to different a curing cycle of 7.5 min at 175 °C, in terms of the solvent extraction test with <i>n</i> -hexane in terms of migration time and temperature.....	266
Table IV.3.1. Composition of ECSO plasticized PLA materials and labelling.....	285
Table IV.3.2. Summary of mechanical properties from tensile and flexural tests of plasticized PLA formulations with different weight % of epoxidized cottonseed oil (ECSO).	289
Table IV.3.3. Summary of thermomechanical properties, Vicat softening temperature (VST) and heat deflection temperature (HDT) of plasticized PLA formulations with different weight % of epoxidized cottonseed oil (ECSO).....	296
Table IV.3.4. Main degradation parameters obtained by thermogravimetric analysis (TGA) for plasticized PLA formulations with different weight % of epoxidized cottonseed oil (ECSO).....	298
Table IV.4.1. Composition and labelling of the plasticized PLA formulations with different maleinized vegetable oils.....	317
Table IV.4.2. Summary of the main thermal properties of neat PLA and plasticized PLA films with maleinized oils, obtained by differential scanning calorimetry – DSC and thermogravimetric analysis – TGA.	326
Table IV.4.3. Barrier properties against oxygen measured as the product between the oxygen transmission rate – OTR and the average thickness (<i>OTR</i> · <i>e</i>) and water contact angle (θ_{water}) measurements for plasticized PLA formulations with maleinized oils.	329
Table IV.5.1. Composition and coding of PLA/PBAT binary blends compatibilized with cottonseed oil derivatives.....	349
Table IV.5.2. Summary of the main results of the thermal degradation of neat PLA, PBAT and PLA/PBAT blend (80/20 wt/wt) without and with different compatibilizers.	364
Table IV.5.3. Summary of some surface properties, <i>i.e.</i> water contact angle and luminance (L*) for neat PLA, PBAT and PLA/PBAT blend (80/20 wt/wt) without and with different compatibilizers.....	365
Table IV.6.1. Composition of the PLA-cottonseed composites with different loads of cottonseed oil (epoxidized-ECSO or maleinized-MCSO), and cottonseed flour (CSF).....	384
Table IV.6.2. Mechanical properties, tensile modulus (E _t), tensile strength (σ _t) and elongation at break (ε _b), of PLA-cottonseed composites with different loads of cottonseed oil (epoxidized-ECSO or maleinized-MCSO), and cottonseed flour (CSF).....	387
Table IV.6.3. Flexural properties, flexural modulus (E _f) and flexural strength (σ _f), of PLA-cottonseed composites with different loads of cottonseed oil (epoxidized-ECSO or maleinized-MCSO), and cottonseed flour (CSF).....	388

Table IV.6.4. Impact strength by Charpy impact test and Shore D hardness of PLA-cottonseed composites with different loads of cottonseed oil (epoxidized-ECSO or maleinized-MCSO), and cottonseed flour (CSF).	390
Table IV.6.5. Thermal properties obtained by differential scanning calorimetry (DSC) of PLA-cottonseed composites with different loads of cottonseed oil (epoxidized-ECSO or maleinized-MCSO), and cottonseed flour (CSF).....	395
Table IV.6.6. Summary of some thermomechanical properties, <i>i.e.</i> glass transition temperature (T_g) and storage modulus (G') obtained by dynamic mechanical thermal analysis (DMTA) on PLA formulations with cottonseed derivatives (CSF, ECSO and MCSO).	399



I. INTRODUCCIÓN



I.1. ACEITES VEGETALES EN INGENIERÍA.

Durante los últimos años la presencia de los aceites vegetales se ha incrementado en la elaboración de productos alimentarios, cosméticos, médicos, farmacéuticos y en la fabricación de biocombustibles [1-5]. Los aceites vegetales se obtienen principalmente mediante la extracción mecánica o el prensado de algunas partes de las plantas entre las cuales destacan, especialmente, las semillas. Con el objetivo de incrementar y favorecer un mayor rendimiento de extracción de aceite también se recurre al uso de disolventes como el hexano [6]. En el caso del aceite de linaza la extracción ha sido llevada principalmente a cabo mediante disolvente y extracción mecánica, logrando una composición química similar del aceite con el empleo de ambos métodos [7].

Los aceites vegetales están constituidos por esteres de ácidos grasos saturados o insaturados. Los ácidos grasos más comunes son el palmítico, oleico, linoleico, linolénico y esteárico. Algunos aceites como el de maíz, girasol o soja con altos contenidos en ácidos grasos poliinsaturados (linoleico y linolénico) o como el de oliva y canola, con ácidos grasos monoinsaturados (oleico), son preferibles para el consumo humano frente a las grasas. Estos ácidos grasos favorecen la disminución del colesterol LDL, manteniendo la salud cardiovascular y por lo tanto demostrando sus efectos beneficiosos sobre la salud. Sin embargo, aceites como el de coco y palma, que son ricos en grasas saturadas (palmítico y esteárico), incrementan el riesgo de enfermedades cardiovasculares [8].

Solamente algunos de estos aceites vegetales resultan pues totalmente recomendables para el consumo humano. Es el caso del polémico aceite de palma omnipresente en muchos de los productos alimenticios que consumimos en la actualidad y cuya plantación se encuentra detrás de la deforestación masiva de amplias zonas selváticas tropicales y hábitats naturales situados especialmente en Asia [9, 10]. La utilización de los aceites vegetales ha generado, por tanto, un gran impacto mediático entre los consumidores mientras los investigadores buscan dar salidas alternativas tanto a estos aceites como a los excedentes generados en su producción. Resultado de esta controversia ha sido la utilización de estos aceites vegetales en otros sectores como el industrial, en el cual los aceites vegetales se llevan manipulando desde finales del siglo XIX como bien atestigua la empresa Tarkett en la producción de una gran variedad de

suelos donde destaca su producto linoleum como uno de los suelos más sostenibles y naturales del mercado.

Atendiendo a los datos de la **Figura I.1.1**, la producción mundial de aceites vegetales está encabezada por el de palma que, con un 29,9 %, representa casi un tercio de la producción global total. Por orden le siguen el aceite de soja, colza, girasol, coco y semilla de palma.

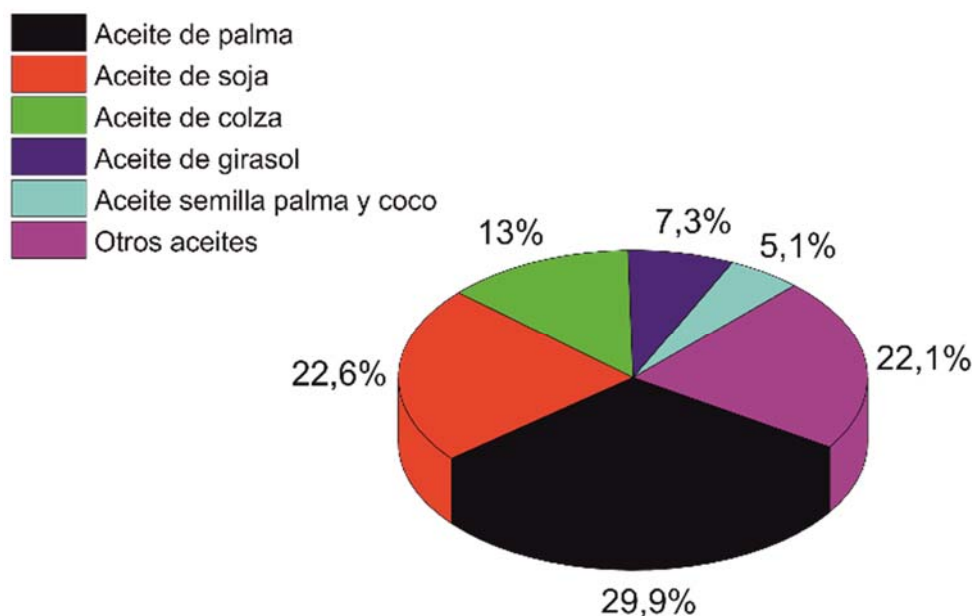


Figura I.1.1. Representación gráfica de los niveles de producción mundial de los principales aceites. *Adaptado de [11]*.

Ahondando en la cuestión, en la **Figura I.1.2** se analizan las principales áreas mundiales productoras de aceites y grasas, entre los que se incluyen los de origen vegetal (aceite de soja, girasol, colza, maíz y el fruto de la palma) y los de origen animal. Llama especialmente la atención el caso de países asiáticos como Indonesia donde la palma ha dejado de ser un mero producto de subsistencia de las poblaciones locales para convertirse, en las últimas décadas, en un producto muy explotado ante la ingente demanda de su aceite por los países desarrollados occidentales; países que aprovechan los bajos costes de este producto y la rapidez de crecimiento de esta planta. La gran demanda también ha acentuado el cultivo de la palma ilegal con tan solo un 20 % de las plantaciones permitidas y reguladas por el ministerio de silvicultura [9].

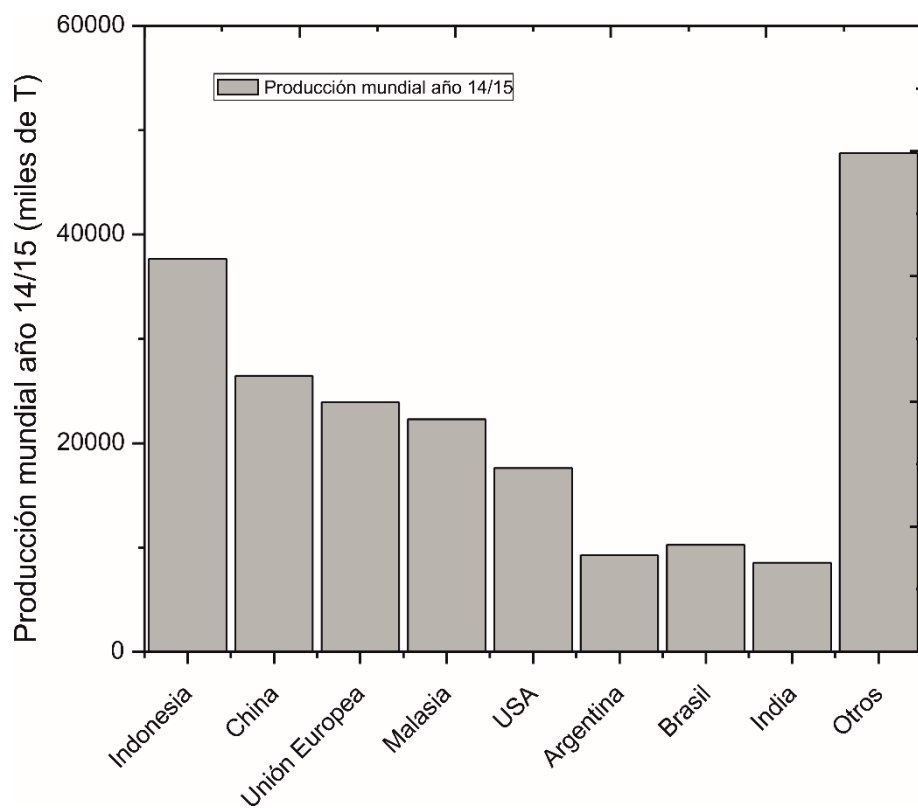


Figura I.1.2. Gráfico comparativo de los principales países productores de aceites y grasas. *Adaptado de [12]*.

En referencia al aceite de palma, si bien Indonesia se postula como el mayor productor en volumen, analizando los valores de extracción de aceite por hectárea, Malasia es más eficiente [13]. En la **Tabla I.1.1** se observa la producción de aceites vegetales donde el aceite de palma con sus cifras corrobora los resultados mencionados anteriormente en la **Figura I.1.1**.

Tabla I.1.1. Producción mundial de aceites vegetales a partir de plantas oleaginosas.
Adaptado de Tabio García [6].

Aceite	Producción (1 ha ⁻¹ año ⁻¹)	Índice de yodo (g de I/100 g de aceite)
Palma aceitera	5550	5 - 50
Coco	2510	---
Jatropha curcas	1590	50 - 100
Ricino	1320	161
Moringa oleífera	1000-1700	60 - 70
Colza *	1100	50 - 100
Maní	990	---
Girasol	890	100 - 150
Soja	420	100 - 150

* Índice de yodo aceite de colza por extracción en prensa 122,9.

* Índice de yodo aceite de colza por extracción con disolvente 97,9.

I.1.1. Estructura.

Los aceites vegetales y las grasas están principalmente constituidos por triglicéridos, localizándose en la mayoría de los aceites en torno al 95 % y solamente un 5 % de ácidos grasos libres [6]. Los aceites son compuestos estables, pero con el tiempo se deterioran químicamente debido a su oxidación o hidrólisis. Estas alteraciones reciben el nombre de rancidez o enranciamiento y afectan al sabor de los aceites.

Los triglicéridos están formados por tres ácidos grasos y se mantienen anclados por una molécula de glicerol, tal y como se observa en la **Figura I.1.3**. El glicerol es un alcohol con tres grupos hidroxilos (-OH) presente en todos los aceites y grasas.

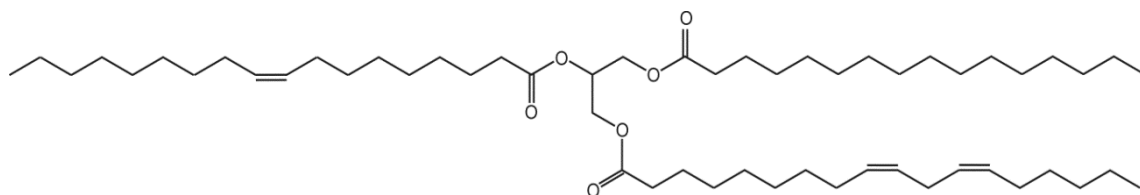


Figura I.1.3. Representación esquemática de la estructura química de triglicérido formado por el anclaje de tres ácidos grasos a una estructura básica de glicerol.

Los ácidos grasos presentes en la naturaleza constan de un solo grupo carboxilo en el extremo de una cadena lineal y contienen, habitualmente, un número par de átomos de carbono (C), dado que las cadenas se forman en unidades C-C [15]. Estos pueden ser saturados o insaturados dependiendo del tipo de enlace entre carbono – carbono. A su vez los ácidos insaturados se dividen en ácidos grasos monoinsaturados y poliinsaturados. A mayor número de dobles enlaces, más insaturados y reactivos son los dobles enlaces. Por lo tanto, los ácidos grasos insaturados poseen dobles enlaces carbono – carbono mientras que los ácidos grasos saturados poseen enlaces simples entre carbono – carbono (**Tabla I.1.2**). En esta tabla se observa cómo los ácidos grasos de algunos aceites contienen entre 0 y 3 dobles enlaces C=C y una longitud entre 14 y 24 átomos de carbono.

Tabla I.1.2. Distribución de ácidos grasos en varios aceites vegetales, adaptado de Khot S. N., 2001 [16].

Ácido graso	C:DE ^(a)	Canola	Maíz	Algodón	Linaza	Oliva	Palma	Colza	Soja
Mirístico	14:0	0,1	0,1	0,7	0,0	0,0	1,0	0,1	0,1
Miristoleico	14:1	0,0	0,0	0,0	0,0	0,0	0,0	0,0	0,0
Palmítico	16:0	4,1	10,9	21,6	5,5	13,7	44,4	3,0	11,0
Palmitoleico	16:1	0,3	0,2	0,6	0,0	1,2	0,2	0,2	0,1
Margárico	17:0	0,1	0,1	0,1	0,0	0,0	0,1	0,0	0,0
Margaroleico	17:1	0,0	0,0	0,1	0,0	0,0	0,0	0,0	0,0
Esteárico	18:0	1,8	2,0	2,6	3,5	2,5	4,1	1,0	4,0
Oleico	18:1	60,9	25,4	18,6	19,1	71,1	39,3	13,2	23,4
Linoleico	18:2	21,0	59,6	54,4	15,3	10,0	10,0	13,2	53,2
Linolénico	18:3	8,8	1,2	0,7	56,6	0,6	0,4	9,0	7,8
Araquídico	20:0	0,7	0,4	0,3	0,0	0,9	0,3	0,5	0,3
Gadoleico	20:1	1,0	0,0	0,0	0,0	0,0	0,0	9,0	0,0
Eicosadienoico	20:0	0,0	0,0	0,0	0,0	0,0	0,0	0,7	0,0
Behénico	22:0	0,3	0,1	0,2	0,0	0,0	0,1	0,5	0,1
Erúcico	22:1	0,7	0,0	0,0	0,0	0,0	0,0	49,2	0,0
Lignocérico	24:0	0,2	0,0	0,0	0,0	0,0	0,0	1,2	0,0
Media DE /triglicérido	3,9	4,5	3,9	6,6	2,8	1,8	3,8	4,6	

(a) Número de Carbono (C): Número de dobles enlaces (DE)

En la **Figura I.1.4** se muestra la estructura química de algunos de estos ácidos grasos.

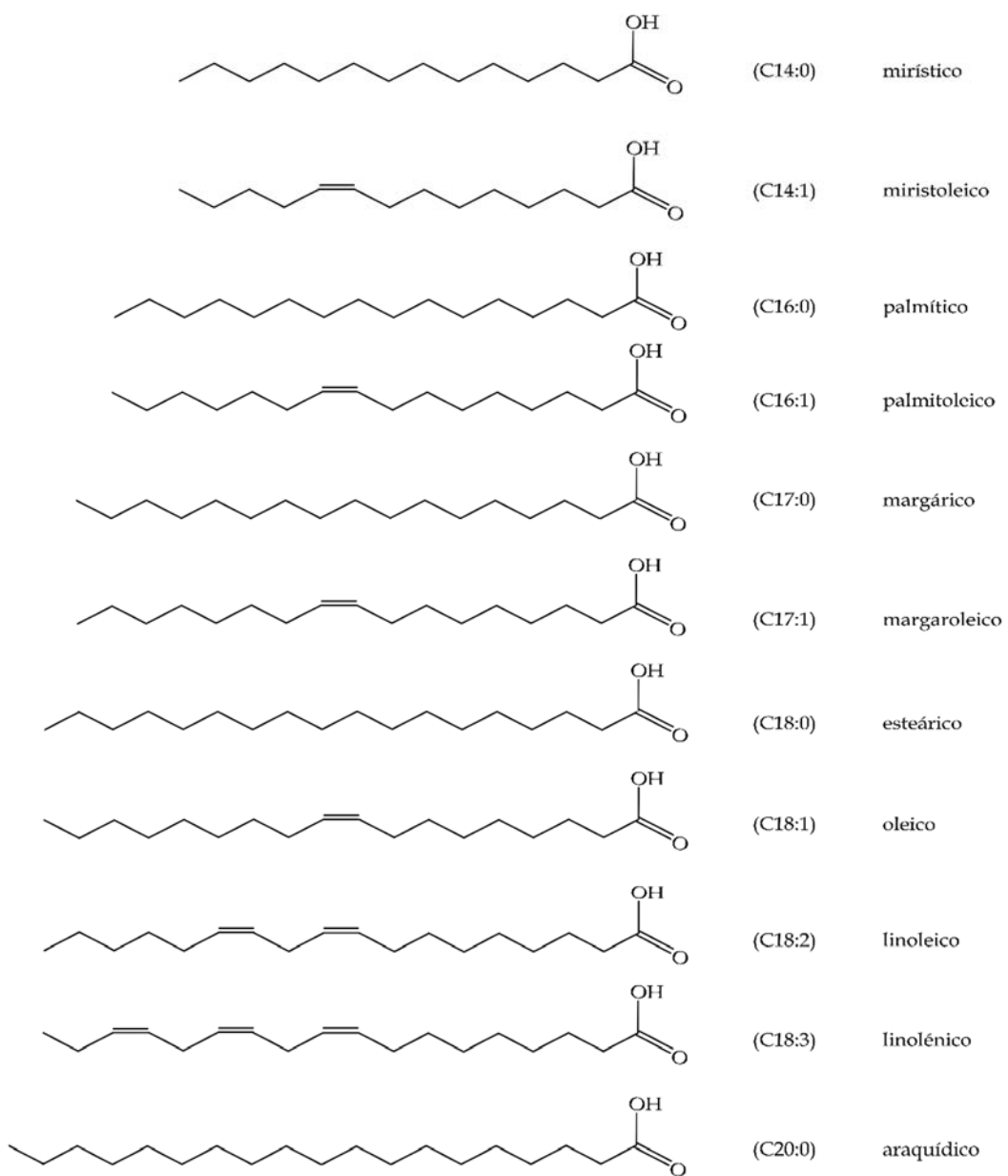


Figura I.1.4. Representación esquemática de la estructura Química de diversos ácidos grasos saturados (mirístico, palmítico, margárico, esteárico, araaquídico), monoinsaturados (miristoleico, palmitoleico, oleico) y poliinsaturados (linoleico, linolénico).

I.1.2. Propiedades.

Los aceites vegetales de por sí son poco reactivos ya que los sitios activos están aislados en su mayoría. No obstante, a través de modificaciones químicas se pueden alterar sus grupos reactivos y por lo tanto representan una interesante alternativa frente a los productos obtenidos a partir del petróleo [17].

Aunque la mayoría de los triglicéridos contienen insaturaciones, son pocos los que contienen otro tipo de grupos y por consiguiente no son atractivos para sectores industriales. Por lo tanto, los aceites con un mayor número de insaturaciones o dobles enlaces son los más propicios para su modificación. El número de dobles enlaces se puede conocer mediante la caracterización del índice de yodo. Esta caracterización nos indica el número de insaturaciones de los ácidos grasos [18], siendo el valor de 0 para los aceites totalmente saturados. En la **Tabla I.1.1** se observan los valores del índice de yodo de algunos aceites, destacando el de soja y girasol con elevados valores. Resulta curioso el caso del aceite de palma, el cual presenta una alta saturación. Pese a ello, ha sido empleado con éxito en gran variedad de aplicaciones industriales como jabones, detergentes, lubricantes e incluso en la elaboración de poliuretanos [19].

El índice de yodo también puede emplearse como un parámetro de control de la calidad del aceite durante su almacenaje. Una disminución del índice es atribuida a la destrucción de los dobles enlaces de los ácidos grasos insaturados por el ataque de radicales libres [20].

Para incrementar su viabilidad fuera de sectores como el de la alimentación o cosmética es necesario modificar su estructura química mediante procesos de epoxidación, acrilación, maleinización e hidroxilación.

Epoxidación.

Durante los últimos años, se han obtenido aceites vegetales epoxidados mediante diferentes procesos de epoxidación, siendo los más utilizados el aceite de soja con una producción de 200000 t año^{-1} [21] y el aceite de linaza. Desde el punto de vista del índice de yodo, el aceite de soja y linaza se presentan como excelentes candidatos por sus elevados valores comprendidos entre 130 y 175 respectivamente. A nivel industrial, empresas como tarkett emplean entre sus formulaciones el aceite de lino para la elaboración de suelos, apostando por su producto y abarcando una gran parte del mercado. No obstante, también se ha encontrado en bibliografía información sobre el uso de otros tipos de aceites epoxidados como el aceite de pescado [22], maíz [23], ricino [24, 25], neem [26], girasol [27, 28], jatropha curcas [29] e incluso el de palma a pesar de poseer en torno a un 50% de ácidos grasos saturados entre los cuales destaca el palmítico y esteárico [30].

Existen varias tecnologías para realizar la epoxidación, entre las que destacaremos:

- a) Epoxidación con peróxidos orgánicos e inorgánicos.
- b) Epoxidación con ácidos percarboxílicos.
- c) Epoxidación con halohidrinas.
- d) Epoxidación con oxígeno molecular.

El rendimiento de un aceite vegetal durante el proceso de epoxidación está directamente relacionado con el índice de yodo o el contenido de ácidos grasos insaturados que pueden ser convertidos en anillos oxiranos. La epoxidación de un ácido graso insaturado (doble enlace carbono carbono) presente en el triglicérido con la reacción de oxígeno activo, da como resultado la adición de un átomo de oxígeno, el cual convierte el doble enlace original en un anillo epóxido (oxirano) (**Figura I.1.5**) [26].

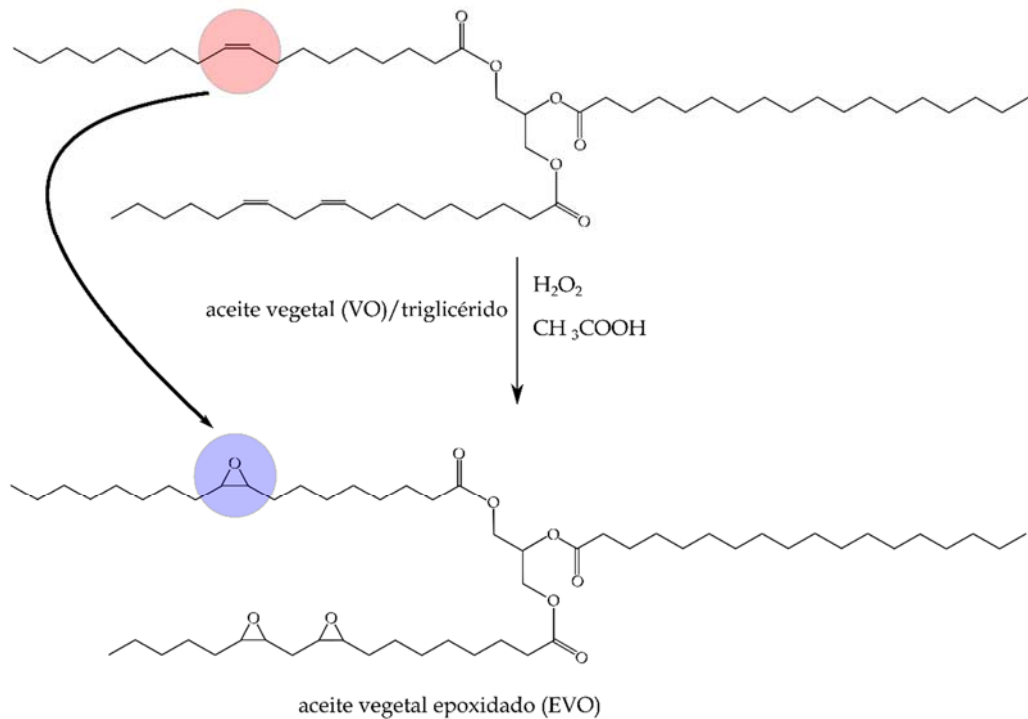


Figura I.1.5. Representación esquemática del proceso de epoxidación con la incorporación de peróxido de hidrógeno y ácido acético para la generación de ácido peroxyacético *in situ* en presencia de medio ácido.

La epoxidación de aceites vegetales a escala industrial se puede llevar a cabo mediante la reacción de Prilezhaev [31]. Durante la reacción, el ácido graso insaturado reacciona con el ácido percarboxílico obtenido previamente *in situ*. Por seguridad y para evitar mezclas explosivas, se recomienda obtenerlo *in situ* mediante la reacción del ácido acético o fórmico [32, 33] con peróxido de hidrógeno, en presencia de un ácido mineral como el sulfúrico. En cuanto al uso de ácido fórmico o acético, tanto por economía como seguridad, se recomienda el uso del ácido acético [34, 35]. En bibliografía también se ha encontrado el uso de otros catalizadores como el ácido fosfórico durante la epoxidación del aceite de ricino [25] y el uso de Amberlite IR 120H para epoxidar aceite de maíz [23].

A causa de su elevado rendimiento catalítico y su bajo coste, se está utilizando como catalizador ácido sulfúrico a nivel industrial. Por otra parte, los niveles de conversión en grupos epóxidos son muy aceptables, sin utilizar catalizadores metálicos o disolventes que dificultarán la posterior separación una vez epoxidado el aceite [36].

Como aplicaciones de los aceites epoxidados han sido numerosas las investigaciones realizadas hasta el momento y diversos autores han publicado sus trabajos. Pese a que se ha trabajado a nivel experimental con aceites epoxidados de girasol [37], semilla de algodón [38] y palma [39], a nivel industrial y disponible en el mercado se encuentra aceite epoxidado de linaza (ELO) [40] y soja (ESBO) [41, 42] con la nomenclatura de Vikoflex 7190 y Vikoflex 7170 respectivamente [43]. Si hablamos de las aplicaciones de los aceites epoxidados destaca su empleo como plastificante de PVC en la realización de plástisoles [44, 45]; como plastificante de polímeros principalmente de origen bio y biodegradable como el PLA [30, 42, 46] así como en la realización de materiales termoestables [38] e incluso como compatibilizante de mezclas de distintos polímeros [47].

Acrilación.

De igual manera que la epoxidación, la acrilación es necesaria para incrementar la reactividad de los aceites vegetales. La acrilación presenta, no obstante, el inconveniente de requerir normalmente de dos etapas, siendo necesario primeramente la epoxidación del aceite y posteriormente la operación de acrilación. Este incremento de medios también se ve favorecido con el logro de un aceite con grupos oxiranos derivados de la epoxidación y acrilatos adquiridos durante la segunda etapa. A nivel industrial, se comercializa el aceite de soja epoxidado-acrilado (AESO) bajo el nombre de Ebecryl 860 [43].

Durante el proceso de acrilación la estructura acrílica es generalmente introducida a través de la apertura de los anillos oxiranos de grupos epoxis logrados previamente durante el proceso de epoxidación (**Figura I.1.6**) [17] aunque también se puede lograr acrilar un aceite en una sola etapa mediante la adición catalítica por ácido de Lewis [48] o reacción de Ritter [49].

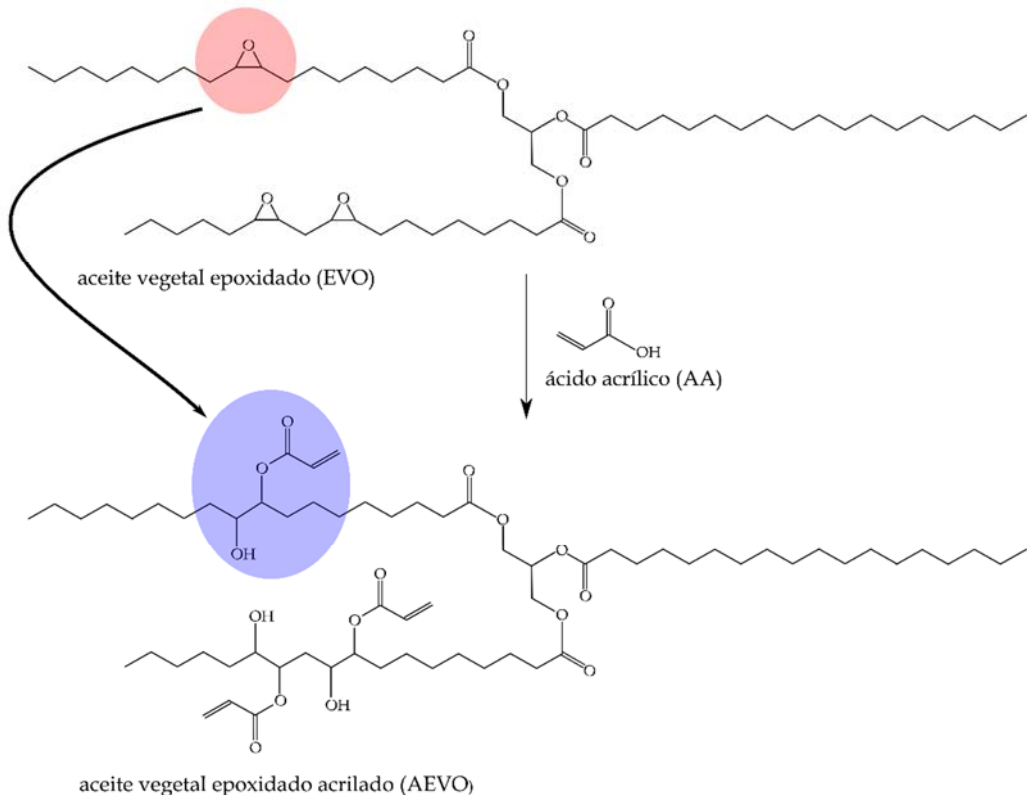


Figura I.1.6. Representación esquemática del proceso de acrilación en dos etapas.

■ Maleinización.

La acrilación presenta, no obstante, el igual que la epoxidación, el proceso de maleinización normalmente se lleva a cabo durante una única etapa. En cuanto a los aceites maleinizados y disponibles en el mercado se pueden encontrar de soja [50, 51] y linaza [52]. También se ha encontrado en bibliografía información sobre el uso de aceites maleinizados como el de semilla de caucho [53], tung [54] y ricino [55].

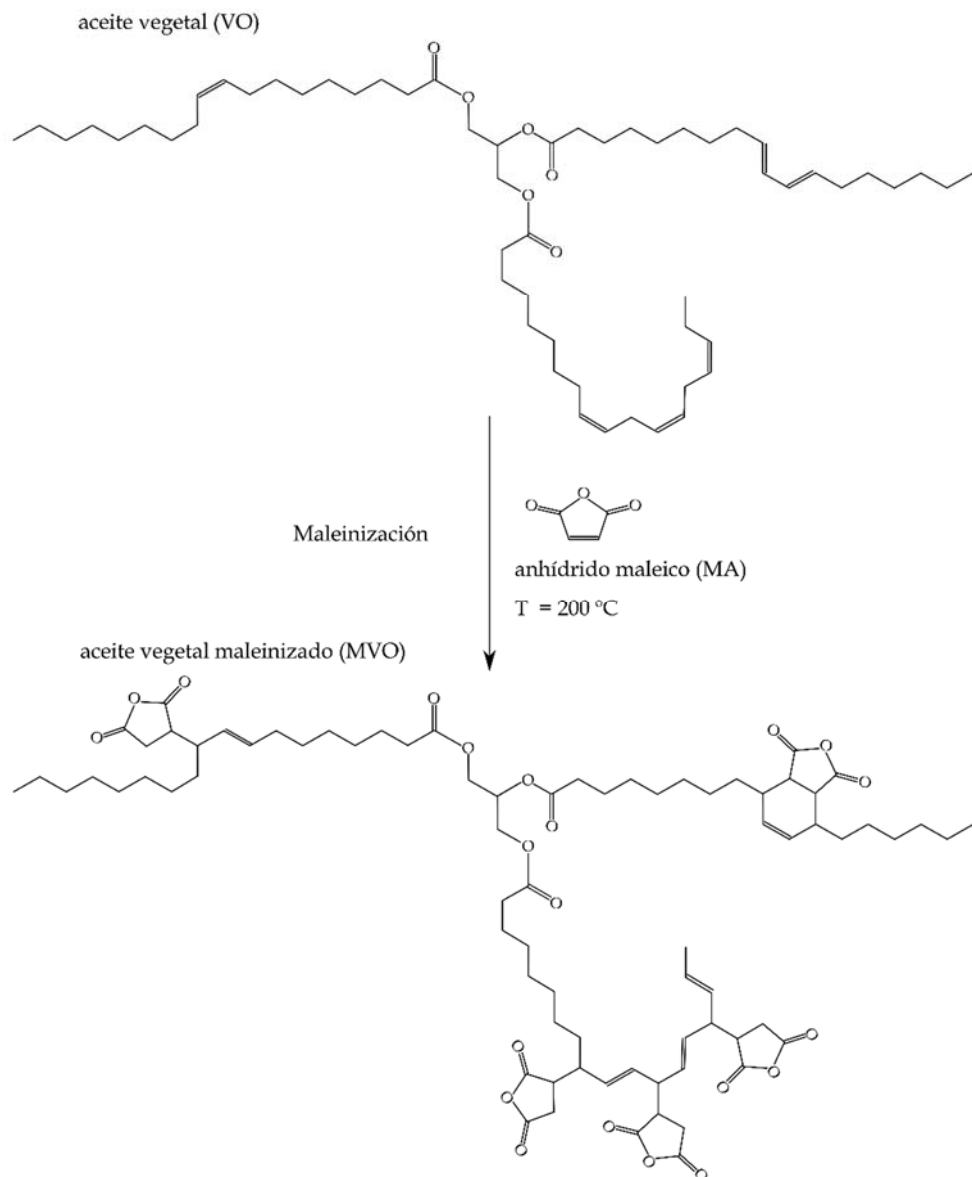


Figura I.1.7. Representación esquemática del proceso de maleinización de un aceite vegetal mediante reacción con anhídrido maleico a elevada temperatura.

La maleinización se realiza principalmente mediante la adición de anhídrido maleico e incorporaciones escalonadas de ácido maleico a temperaturas cercanas a los 200 °C durante un espacio de tiempo de 3 horas. La cantidad de ácido maleico requerida se calcula a partir del número de dobles enlaces obtenidos durante el análisis del perfil lipídico del aceite [52]. Aunque otros autores, con un método similar, emplearon otras

temperaturas para lograr maleinizar el aceite de ricino, siendo la máxima temperatura de 130 °C [55]. No obstante, en bibliografía se pueden consultar métodos mucho más rápidos como el estudiado por Chengguo *et al.* que logran maleinizar el aceite de Tung tan solo en 4 minutos y sin la utilización de ningún iniciador, catalizador o disolvente, usando un sintetizador de microondas. Al comparar el calentamiento por microondas con el calentamiento convencional se observan ventajas como mayores rendimientos y tiempos más cortos. El aceite de tung reaccionó con el anhídrido maleico a través de la copolimerización de radicales libres y la reacción de Diels-Alder [54].

Durante la maleinización de los aceites se lleva a cabo el mecanismo de reacción “eno”. Esta reacción química producida a elevadas temperaturas, por encima de los 200 °C, sucede en la posición alílico del ácido graso con la adición de un grupo de anhídrido [56]. Luego, el número de dobles enlaces, calculado mediante el índice de yodo juega un importante papel en el proceso de maleinización. Aunque el número de dobles enlaces es importante conocerlo antes de realizar la maleinización, durante el proceso de maleinizado no es recomendado calcularlo, ya que durante la maleinización la adición de anhídrido maleico no permite ver la disminución de los dobles enlaces.

Por otro lado, el valor del índice de acidez, el cual indica los miligramos de KOH necesarios para neutralizar los ácidos grasos libres en el aceite, es el indicativo de la maleinización de los aceites. Como ejemplo de aceite comercializado a nivel industrial la empresa Vandeputte dispone de aceite de semilla de linaza maleinizado (MLO) y aceite de soja maleinizado (MSO) al precio de 1,5 € kg⁻¹ y un mínimo de 150 Kg por lote (datos adquiridos en el año 2015). Como valor del índice de acidez se dispone el del MLO con un valor proporcionado por Vandeputte de 120 mg KOH g⁻¹.

Entre las principales aplicaciones de los aceites maleinizados, si bien en bibliografía no se encuentran tantas publicaciones como en el caso de los aceites epoxidados, existen algunas aplicaciones. Ferri *et al.* introdujeron aceite de semilla maleinizado como plastificante de PLA logrando mejorar su ductilidad [57]. A.I. Aigbodion *et al.* lograron valores de acidez de 75,81 mg KOH g⁻¹ con aceite de semilla de caucho maleinizado y lo usaron como aglutinante en recubrimientos a base de agua [53].

Hidroxilación.

La hidroxilación del aceite es una modificación llevada a cabo en dos etapas. Primeramente, es necesario epoxidar el aceite para posteriormente llevar a cabo la hidroxilación. Diferentes publicaciones se pueden encontrar al realizar una revisión bibliográfica sobre los aceites epoxidados e hidroxilados. Tanto el aceite de ricino epoxidado [25], aceite de soja epoxidado [26, 58] como el aceite del árbol *Balanites roxburghii* [59] fueron hidroxilados con la incorporación de hidróxido de sodio (NaOH).

Durante las reacciones de hidroxilación anteriormente citadas, muchas de ellas utilizan unas condiciones similares. Si destacamos el trabajo llevado a cabo por Xujuan *et al.* a partir del aceite de ricino epoxidado incorporando solución de NaOH y a una temperatura de 100 °C con agitación durante 12 horas [25]. También es posible obtener el correspondiente aceite hidroxilado a partir del correspondiente aceite epoxidado mediante reacción con alcohol orgánicos en medio ácido (**Figura I.1.8**).

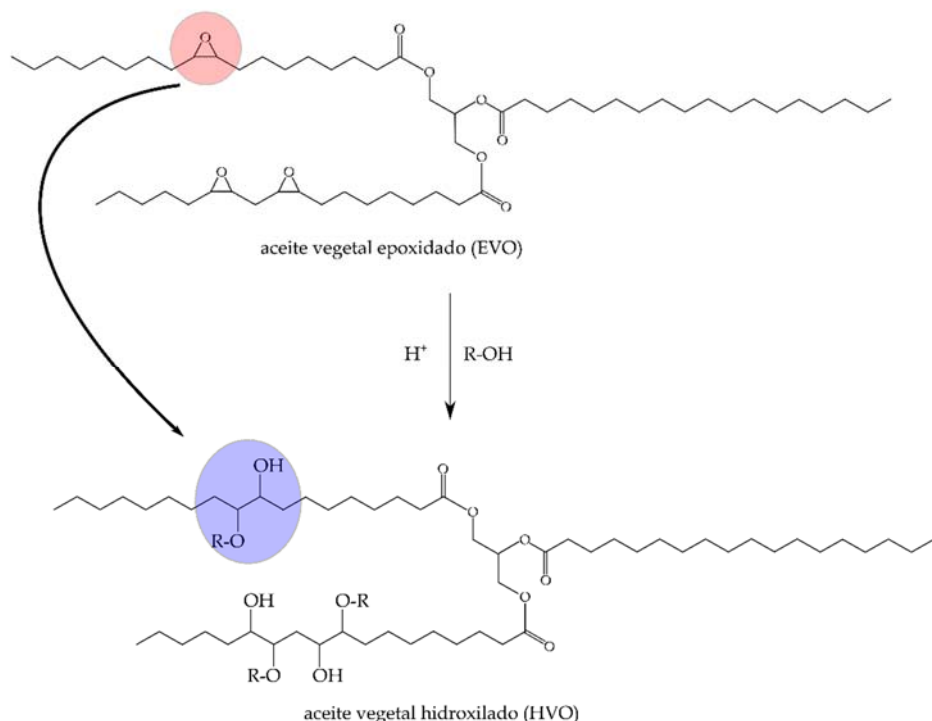


Figura I.1.8. Representación esquemática del proceso de hidroxilación de un aceite vegetal epoxidado (EVO) mediante reacción con un alcohol orgánico, en medio ácido.

I.2. ACEITE DE SEMILLA DE ALGODÓN (CSO).

El algodón es una planta de la familia de las malváceas. Esta planta contiene las semillas de algodón en su interior con una cobertura rodeada por fibras ricas en celulosa, siendo el principal recurso empleado de la planta conocida como *Gossypium*. Por lo tanto, el aceite de semilla de algodón es considerado como un subproducto de la industria algodonera donde el principal producto es la fibra de algodón. El aceite de semilla de algodón, al igual que la mayoría de los destinados al sector alimenticio, se extrae mediante procesos mecánicos de prensado en frío. No obstante, existen otros métodos de extracción del aceite mediante el uso de disolventes. Aunque el aceite de semilla de algodón puede ser considerado como un aceite comestible usado en muchos productos existe cierta controversia sobre sus efectos para la salud por la presencia de componentes como el gosipol [60].

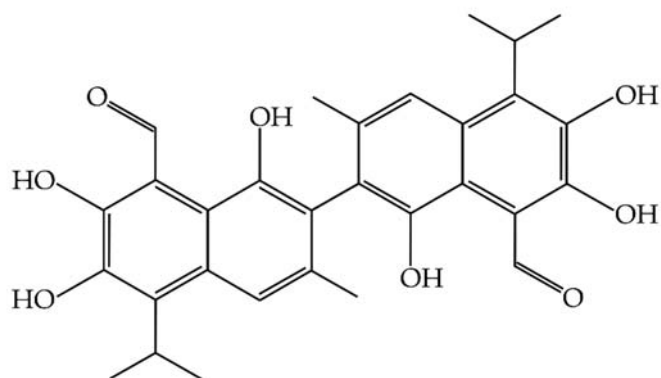


Figura I.2.1. Representación esquemática de la estructura química del gosipol, polifenol de gran presencia en la semilla de algodón.

El polifenol (conocido como gosipol) (**Figura I.2.1**) es una sustancia tóxica que se encuentra presente en todas las partes de la planta lo cual queda patente al utilizar las semillas donde el gosipol se halla en cantidades comprendidas entre el 0,3 y 20 g kg⁻¹. Dicha sustancia actúa como un plaguicida eficaz disuasivo de los insectos y se reconoce durante la extracción del aceite por la tonalidad rojiza que le confiere. Cabe destacar la posibilidad de dotar al aceite de la característica tonalidad amarillenta mediante un proceso de desacidificación [61]. La desacidificación o neutralización del aceite tiene

como objetivo además de otorgarle el color amarillento, extraer los ácidos libres contenidos en el aceite mediante procedimientos físicos sin modificar la estructura glicerídica inicial. El contenido de ácidos libres y su calidad depende de las condiciones de humedad a las que sea sometida la planta tras pasar el periodo de madurez, favorecida por un clima seco.

La semilla de algodón es utilizada como alimento en las vacas lecheras por sus altas concentraciones de proteína cruda, fibra y energía, pero la presencia del gosipol limitan la cantidad que pueden ingerir los rumiantes debido a que tiene propiedades oxidantes que podrían causar daños en los tejidos del animal y reaccionar con ciertos aminoácidos (especialmente lisina) disminuyendo la disponibilidad de los mismos. Pero no solamente afectan a los animales puesto que en las investigaciones realizadas se ha podido observar que afecta a los órganos reproductores, corazón e hígado de los humanos [62]. Por lo tanto, la gran problemática presentada por la sustancia gosipol en diversos usos de los productos derivados de la planta del algodón han derivado en investigaciones para su eliminación de las semillas del algodón, conservando el gosipol en el resto de la planta para preservar su capacidad plaguicida. Thomas Wedegaertner y Keerti Rathore produjeron una planta que conserva su mecanismo de defensa natural en toda la planta excepto en la semilla [63].

Aunque el gosipol se ha considerado una sustancia tóxica, también aparece su vertiente más favorable aplicada en medicina. Michael K. Dowd *et al.* encontraron en el pigmento propiedades antivirales y antitumorales. Por lo tanto, para ellos es importante extraer el máximo porcentaje de gosipol de las semillas de algodón. En su investigación lograron recuperar un $57,0 \pm 2,5\%$ durante un tiempo de reacción de 1 hora con ácido fosfórico [64].

I.2.1. Producción mundial de CSO.

Si se diferencia entre la fibra y la semilla que se obtienen del algodón bruto, a pesar de ser la fibra el principal producto por el cual se cultiva la planta del algodón, esta tan solo representa el 42% de la planta y su destino es íntegramente el sector textil. En cuanto a la semilla de algodón (el cual representa el 58%) sus aplicaciones son más

diversas: elaboración de aceite, siembra y forraje. Incluso, la pasta resultante del proceso de extracción de aceite también es empleada como forraje para rumiantes [65].

Tal y como se observa en la **Tabla I.2.1**, la producción de la mayoría de tipos de aceites presenta un aumento progresivo con el paso de los años. No obstante, el mayor aceite que se produce a nivel mundial es el de palma con una producción en el año 2015 de 62,79 millones de toneladas y seguido del aceite de soja con 48,72 millones de toneladas. Si observamos el aceite de semilla de algodón, tan solo fue de 4,72 millones de toneladas, aunque la producción fue prácticamente doblada en comparación con un aceite muy conocido por los españoles como es el de oliva [66].

Tabla I.2.1. Producción mundial de aceites, adaptado de Ramli N. 2015 [66].

Aceite/grasa ('ooo Toneladas)	2010	2011	2012	2013	2014	2015
Aceite de palma	46.246	50.886	53.849	56.270	59.657	62.792
Aceite de semilla de soja	40.104	41.443	41.736	42.754	45.240	48.720
Aceite de colza	24.259	24.113	24.917	25.493	27.040	26.130
Aceite de girasol	12.455	13.103	14.998	13.976	16.140	14.970
Aceite de germen de palma	5.105	5.546	5.926	6.240	6.540	6.820
Aceite de semilla de algodón	4.499	4.849	5.108	4.990	4.880	4.720
Aceite de maní	4.159	4.217	3.970	3.901	3.920	3.680
Aceite de maíz	2.411	2.617	2.845	3.038	3.150	3.200
Aceite de coco	3.604	2.981	3.241	3.339	3.020	2.980
Aceite de oliva	3.322	3.448	3.526	2.826	3.140	2.860
Aceite de sésamo	800	837	811	777	790	810
Aceite de linanza	580	559	617	597	650	710
Aceite de ricino	645	646	698	674	630	670
Total Aceites Vegetales	148.189	155.245	162.242	164.875	174.797	179.062

I.2.2. Composición de CSO.

Entre las propiedades del aceite de algodón, destaca el índice de yodo y la densidad, con valores del índice de yodo entre comprendidos entre 109 y 120 y una densidad de 0,92 g cm⁻³. El perfil de ácidos grasos general del aceite de semilla de algodón consiste tan solo en un 25 % de saturados (principalmente palmítico y esteárico) y en un 75 % aproximadamente de ácidos grasos insaturados (incluyendo monoinsaturados, oleico, y poliinsaturados, linoleico) siendo el ácido linoleico el principal ácido graso poliinsaturado presente en el aceite de algodón con un 48,9 % en peso.

I.2.3. Composición y propiedades de CSO.

El aceite de algodón puede ser utilizado en infinidad de industrias, en la fabricación de jabón, cosméticos y productos farmacéuticos, así como materia prima en la fabricación de plásticos, fungicidas, papel, textiles, combustibles, etc. [67, 68] Aunque ya se han comentado anteriormente las controversias del uso del aceite de semilla de algodón como uso alimenticio, el ácido linoleico es el principal ácido graso poliinsaturado presente en el aceite. Se considera un aceite “naturalmente hidrogenado” debido a sus niveles de ácidos oleico, palmítico y esteárico; lo que le lleva a ser un aceite de fritura estable sin la necesidad de ser sometido a un procesado adicional que pudiera conducir a la formación de ácidos grasos –trans. Pero también se presenta como un aceite interesante para usos industriales. La epoxidación es otra manera de usar este aceite con un elevado y prometedor potencial en la industria de los composites y plastificantes. El aceite de semilla de algodón es excelente para epoxidar, ya que un 75% de sus ácidos grasos corresponden a insaturados, con dobles enlaces entre sus cadenas. La elevada cantidad de dobles enlaces permitirán conseguir un gran número de grupos epóxidos para incrementar su rendimiento en posteriores usos como curado con anhídridos, plastificante de PLA y plastificante de PVC para la elaboración de plastisoles entre otros.

I.3. POLÍMEROS DE ALTO RENDIMIENTO MEDIOAMBIENTAL.

En la actualidad los residuos poliméricos presentan una grave problemática medioambiental debido al gran volumen de productos que se genera. Desde la aparición de los plásticos se estima que se han producido más de 8000 millones de toneladas de polímeros termoplásticos y termoestables a nivel mundial [69]. Pero lo más alarmante es el aumento del uso llevado a cabo durante los últimos años, con una producción de 4000 millones de toneladas durante los últimos 13 años [70] de los cuales 8 millones anuales fueron a parar al mar, generando grandes aglomeraciones de residuos contaminantes en las cuales los animales pueden quedar atrapados. Asimismo, los seres vivos marinos ingieren estos plásticos y en estudios realizados se puede comprobar como casi un tercio de los ejemplares capturados en el mar habían ingerido plásticos, pero este número se incrementó al 100 % en las capturas en agua dulce y más concretamente en el Rio de la Plata [71, 72]. Realmente aquí no termina el problema ya que la mayor parte de los materiales poliméricos son de lenta degradación y perduran durante muchos años. Atendiendo a los datos disponibles, el reciclaje del resto de plástico resulta escaso. Del total de los plásticos generados a partir de 2015 solamente un 9% fueron reciclados [69] y el resto de residuos se acumularon en vertederos o se incineraron con la consiguiente liberación de gases tóxicos a la atmósfera.

Por todas estas razones están proliferando leyes para minimizar el problema generado por los materiales poliméricos convencionales, con la implantación de normativas para instaurar el uso de polímeros biodegradables. Aunque algunos países ya están tomando medidas para paliar la problemática y en países como Italia ya es posible adquirir cubiertos biodegradables en los supermercados, en España parece que se tardarán algunos años en tomar la problemática en serio y solamente parecen intentarlo con las bolsas de plástico que, desde el 1 de julio de 2018, son cobradas en todos los establecimientos de manera obligatoria. Francia también está concienciada y para 2020 los cubiertos de plástico tendrán que estar fabricados en un 50 % con material biodegradable y en 2025 en un 60 %.

I.3.1. Polímeros termoplásticos.

Los polímeros termoplásticos tradicionales, a pesar de presentar la virtud de poderse fundirse y moldearse varias veces, también generan problemas de contaminación, ya que durante el proceso repetido de fusión se debilitan sus enlaces y disminuyen sus propiedades, llegando a terminar en vertederos o en los mares. Este problema podría mitigarse con la utilización de materiales biodegradables. No obstante, por otra parte, se añade la problemática suscitada por la gran mayoría de los termoplásticos procedentes del petróleo. A ello cabe sumar el cercano agotamiento del petróleo si bien se están aplicando nuevas tecnologías para su localización y extracción a mayores profundidades tales como la fracturación o estimulación hidráulica que, a su vez, también genera problemas para el ecosistema con usos abusivos de agua y productos químicos que provocan que esté prohibida en Europa y muchas regiones del mundo [73]. Cobran importancia por lo tanto las investigaciones que actualmente se están llevando a cabo sobre la obtención de materiales íntegramente derivados de recursos renovables y biodegradables.

Si se emplea el término de bioplástico, según la European Bioplastics es aquel que tiene una base biológica (derivado de la biomasa), es biodegradable o presenta ambas propiedades. La fabricación de bioplásticos en 2014 fue de 1,7 millones de toneladas, pero con respecto a los plásticos obtenidos a partir del petróleo fue una insignificante parte puesto que en el año 2015 se produjeron 300 millones de toneladas. En cuanto a la utilización de los bioplásticos, en el año 2014, casi el 75 % del total se destinó al mercado del envasado [74].

Aunque se está avanzando en el desarrollo de materiales a partir de fuentes renovables, a nivel industrial según los datos aportados por Lligadas *et al.* sitúan su producción en valores inferiores al 5 % principalmente por su elevado precio e inferiores propiedades con respecto a los polímeros petroquímicos [75]. Este hecho supone un reto para la industria de los polímeros renovables. Dada su relevancia se explicarán los cuatro grupos de materiales según su procedencia y biodegradabilidad.

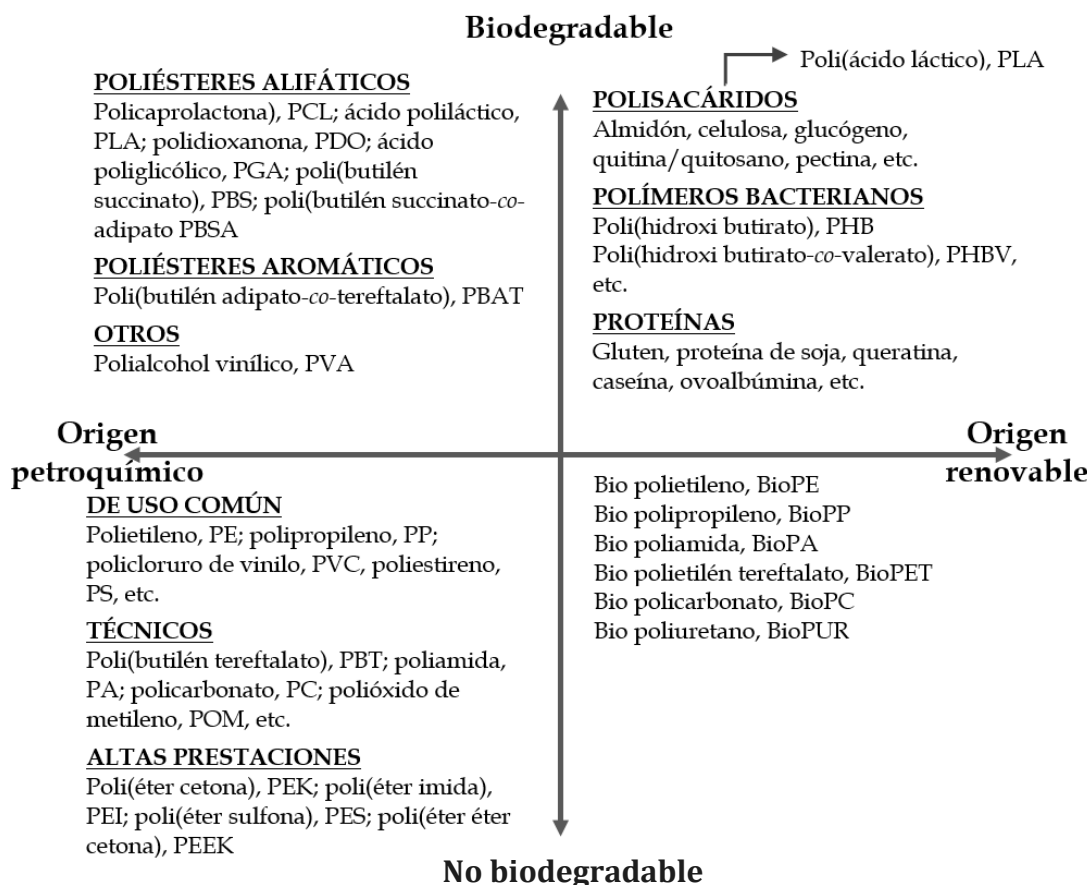


Figura I.3.1. Clasificación de materiales poliméricos termoplásticos en función de su respuesta medioambiental en origen (petroquímico o renovable) y al final del ciclo de vida (biodegradable o no).

■ Polímeros petroquímicos/no biodegradables.

Los polímeros provenientes del petróleo son ampliamente empleados en la industria por su gran disponibilidad, bajo coste y buenas propiedades barrera. Sin embargo, problemas medioambientales como el calentamiento global y el efecto invernadero son causados por la producción de polímeros a partir de recursos fósiles [75]. Existen infinidad de polímeros obtenidos a partir del petróleo y no biodegradables, entre los cuales encontramos poli(etileno) (PE), poli(propileno) (PP), poli(estireno) (PS), poli(cloruro de vinilo) (PVC), y poli(etilén tereftalato) (PET). Estos son los más representativos de los plásticos de uso común. No obstante, en este grupo también se contemplan los plásticos técnicos y los de altas prestaciones (**Figura I.3.2**).

I. Introducción.

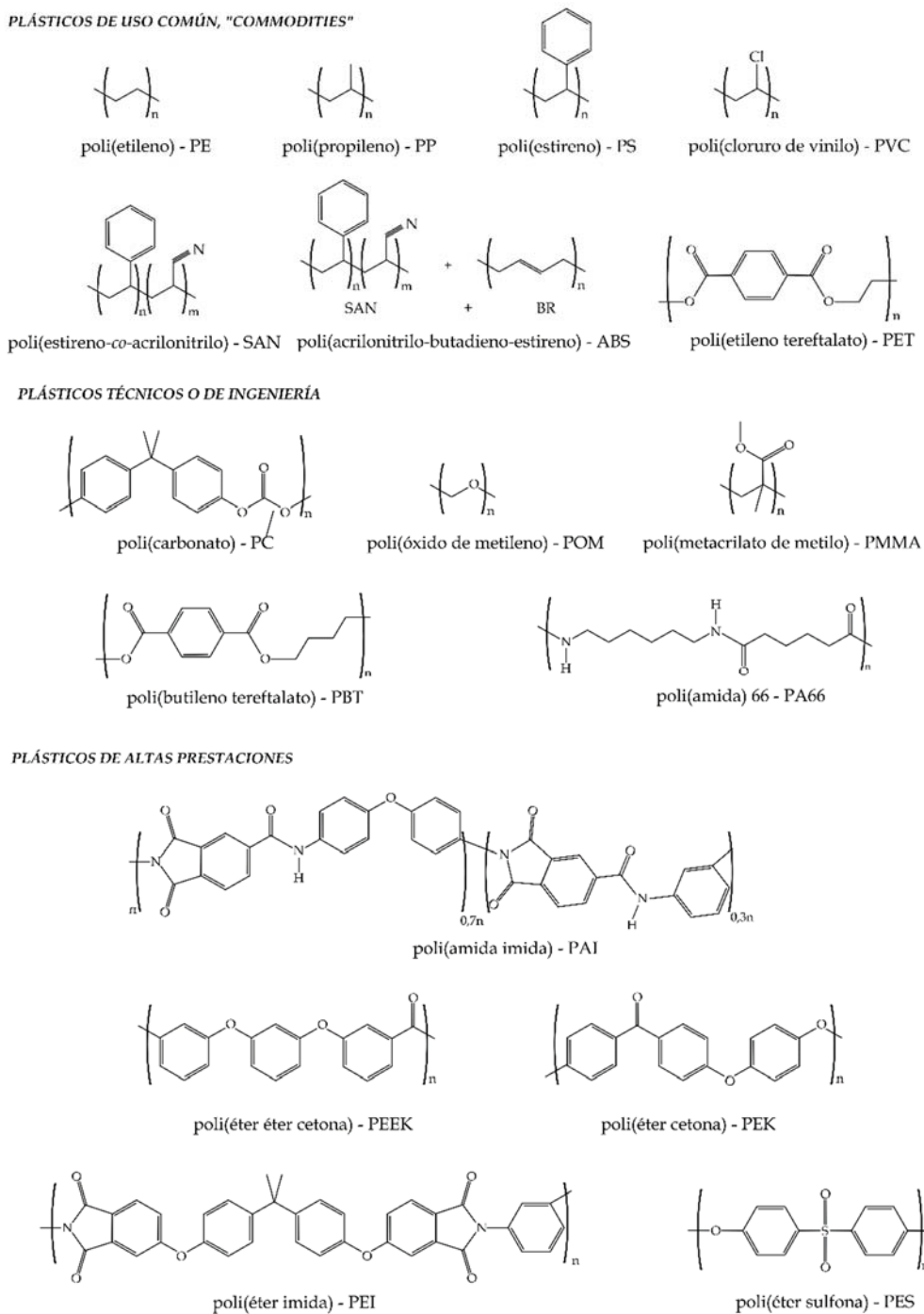


Figura I.3.2. Clasificación de los polímeros termoplásticos en función de sus aplicaciones técnicas.

█ Polímeros petroquímicos/biodegradables.

Los polímeros de origen petroquímico y biodegradables se presentan como una interesante alternativa a corto plazo para paliar la contaminación que generan los productos al finalizar su vida útil si bien, tanto el aumento del precio del petróleo como su agotamiento en el futuro, los hacen poco atractivos y por lo tanto no se presentan como la solución definitiva para los problemas medioambientales.

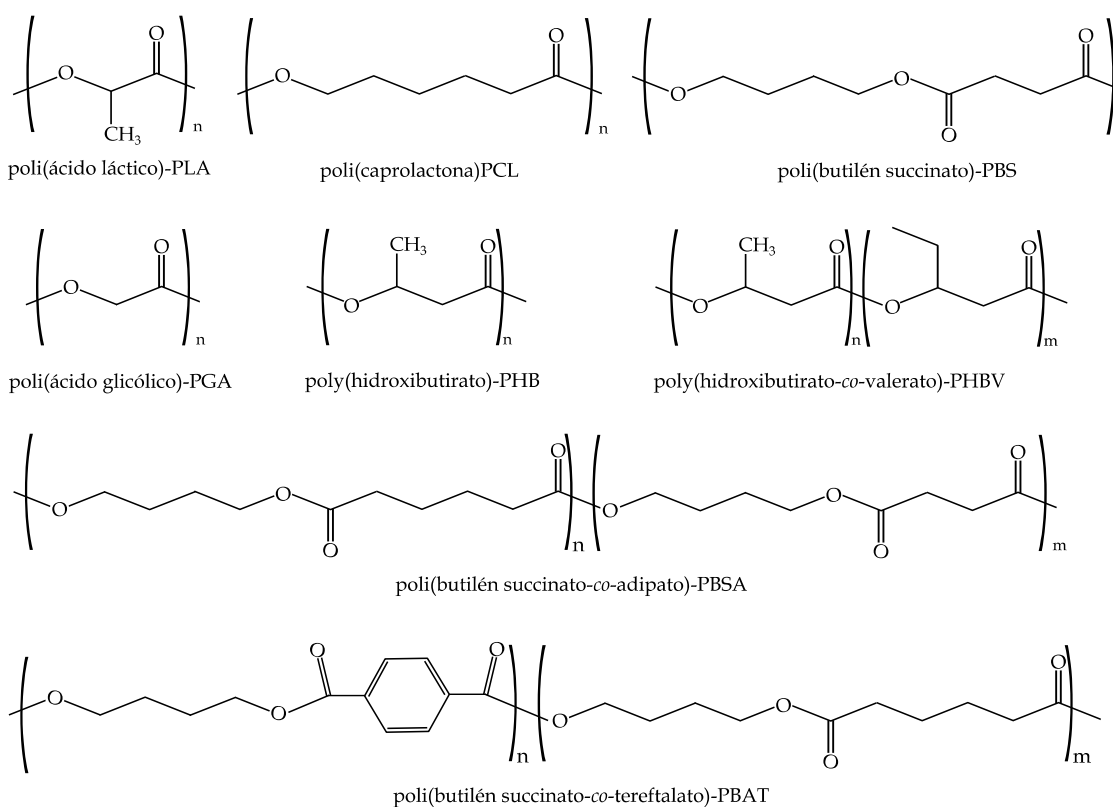


Figura I.3.3. Estructura química de diversos poliésteres de origen petroquímico y/o potencialmente biodegradables.

Entre los polímeros biodegradables (**Figura I.3.3**) logrados a partir del petróleo encontramos dos grupos: los poliésteres alifáticos y los aromáticos. Como poliésteres alifáticos se dispone la poli(caprolactona) – PCL, ácido poliglicólico – PGA, poli(butilén succinato) – PBS, y poli(butilén succinato-*co*-adipato) – PBSA [76, 77]. Y como poliéster aromático biodegradable se encuentra un polímero con una alta ductilidad conocido

como poli(butilén adipato-co-tereftalato) – PBAT [78]. Estos polímeros son capaces de biodegradarse gracias a las reacciones de hidrólisis, las cuales actúan bajo unas condiciones apropiadas en la desintegración de los poliésteres alifáticos e incluso algunos aromáticos como el PBAT. Aunque no todos los poliésteres aromáticos son biodegradables, el politereftalato de butilenglicol (PBT) y el politereftalato de etilenglicol (PET) con altos puntos de fusión no lo son. Por el contrario, la policaprolactona es biodegradable, pero presenta problemas en muchas aplicaciones debido a su bajo punto de fusión en torno a 60 °C aunque su biocompatibilidad ha propiciado su estudio en los campos biomédicos [79].

Polímeros renovables/no biodegradables.

Este tipo de polímeros no provienen del petróleo y tienen un origen a partir de fuentes renovables como las plantas, animales o microorganismos. Por lo tanto, su procedencia en mayor parte a partir de la biomasa producida por la agricultura les otorga el nombre de agropolímeros. Estos polímeros obtenidos a partir de recursos renovables pueden competir o incluso aventajar a los polímeros provenientes del petróleo en sustitución parcial o total de los polímeros tradicionales [75]. Pero estos polímeros, a pesar de ser más sostenibles, continúan presentando la problemática para gestionarlos al finalizar su ciclo de vida. Entre los polímeros renovables, pero no biodegradables encontramos el bio-poli(etileno) (BioPE), bio-poli(propileno) (BioPP), bio-poliamida (BioPA), bio-poli(etilén tereftalato) (BioPET), bio-poli(carbonato) (BioPC), bio-poli(uretano) (BioPUR). Pero entre los nombrados el más conocido es el bio-poli(etileno) (BioPE), logrado a partir de la caña de azúcar y producido en gran volumen por la empresa Braskem.

Polímeros renovables/biodegradables.

Para solucionar los incesantes aumentos de la contaminación ambiental, las investigaciones se están centrando en obtener materiales biodegradables e íntegramente

de recursos renovables. En la actualidad existe una gran diversidad de este tipo de polímeros para conseguir polisacáridos, polímeros bacterianos y proteínas a partir de microorganismos y plantas. Los polisacáridos permiten lograr entre otros homopolisacáridos como el almidón, la celulosa, la quitina y los quitosanos o heteropolisacáridos como pectinas y gomas naturales [80]. Entre los homopolisacáridos destacamos el almidón termoplástico (TPS) [81, 82] y los quitosanos adquiridos a partir de los exoesqueletos de crustáceos [83].

Los polímeros bacterianos (**Figura I.3.4**) o poliésteres alifáticos pueden ser producidos a partir de la síntesis de monómeros naturales como el ácido poliláctico (PLA) o a partir de microorganismos como el polihidroxibutirato (PHB) [83] y el polihidroxibutirato-co-valerato (PHBV) [84, 85]. Entre los poliésteres alifáticos, aunque el PHB se presenta como un interesante biopolímero por su facilidad para biodegradarse y por su biocompatibilidad, su elevado coste limita su aplicación [86] y a día de hoy a nivel industrial para la producción de piezas en serie solamente puede competir el PLA con los polímeros tradicionales, a pesar de sus problemas de fragilidad.

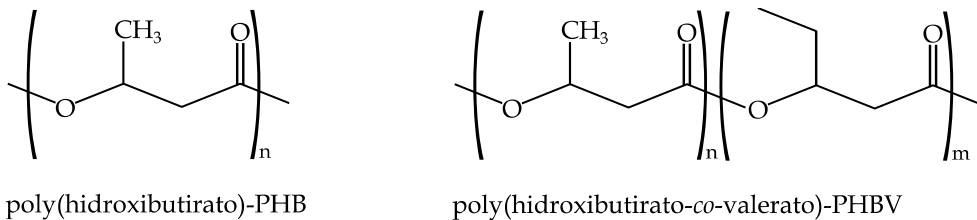


Figura I.3.4. Estructura química de diversos poliésteres obtenidos mediante fermentación bacteriana.

El PLA ha sido producido a gran escala durante los últimos años; muestra de ello lo reflejan las grandes cantidades que se producen, así como los diferentes grados existentes en el mercado para la producción de infinidad de productos. Los sectores en los que se encuentra el PLA son muy variados y van desde el sector médico, envase embalaje, sector textil, sector agrícola y como filamento para impresoras 3D [87-91]. El PLA se obtiene a partir de la fermentación de productos agrícolas tales como el maíz o la caña de azúcar [92]. Además, posee buenas propiedades barrera y propiedades mecánicas a la carta dependiendo del grado seleccionado. Los diferentes grados permiten obtener PLA desde el estado amorfo hasta el semicristalino, modificando las

composiciones de L-ácido láctico y D-ácido láctico, la copolimerización y los pesos moleculares [93]. Por lo tanto, un PLA amorfico presenta un contenido de D-ácido láctico superior al 7% mientras que en un PLA semicristalino los valores son inferiores. Un PLA amorfico se suele utilizar para la producción de films y filamentos, ya que un PLA de menor peso molecular facilita el procesado y permite lograr productos más dúctiles. En cambio, el PLA semicristalino es interesante para productos que requieren altas propiedades mecánicas. En función del grado podemos encontrar PLA para la producción de productos por inyección, extrusión y filamento.

Finalmente, el grupo de las proteínas, se dividen en vegetales y animales. Entre las de origen vegetal, obtenidas a partir de las plantas, se encuentran el gluten y la soja. Entre las de origen animal se dispone de la caseína, el colágeno y la gelatina.

I.3.1. Polímeros termoestables.

Si bien, los desarrollos en el campo de los polímeros termoplásticos “bio” ya son una realidad, el campo de los polímeros termoestables ecológicos o “bio” no está tan desarrollado, sobre todo a nivel comercial debido a la naturaleza de estas resinas. Se ha trabajado intensamente en los últimos años en el desarrollo de polímeros termoestables a partir de recursos renovables, pero a nivel comercial son escasas las iniciativas y, el coste de estos materiales, está todavía muy lejos de ofrecer precios competitivos. Los materiales termoestables se caracterizan por elevados grados de entrecruzamiento que se consiguen cuando la funcionalidad de los monómeros es superior a 2, de tal manera que la estructura puede crecer en diferentes direcciones dando lugar a la formación de redes tridimensionales altamente tupidas.

En la **Figura I.3.5** se muestra de forma esquemática el proceso de formación de una red termoestable o plástico reticulado a partir de monómeros con funcionalidad superior a 2.

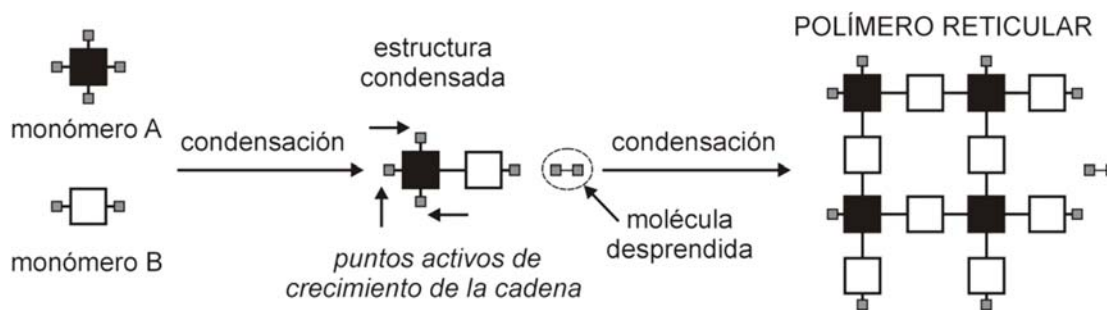


Figura I.3.5. Representación esquemática de la formación de una estructura de red tridimensional de naturaleza termoestable.

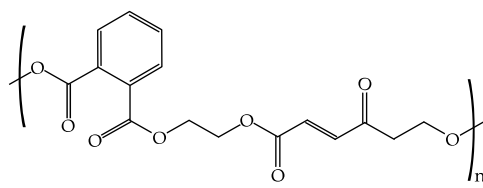
En general la formación de redes termoestables se basa en la reactividad de determinados grupos funcionales que en determinadas condiciones pueden dar lugar a reacciones químicas de condensación, adición y combinadas; teniendo en cuenta que se trata de monómeros con funcionalidad superior a 2, el crecimiento de la estructura se lleva a cabo en las 3 dimensiones dando lugar a la típica red tridimensional mediante procesos de adición, de condensación y combinados.

Desde un punto de vista industrial, las resinas termoestables que mayor aplicación encuentran a nivel industrial son las siguientes:

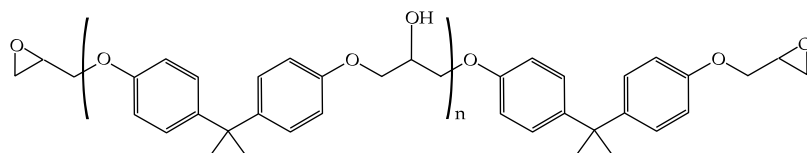
- Epoxi (EP).
- Poliéster insaturado (UP).
- Resinas de vinil-éster (VE).
- Fenol-formaldehído (PF).
- Melamina-formaldehído (MF).
- Urea-formaldehído (UF).

Muchas de estas resinas encuentran importantes usos como adhesivos, recubrimientos, barnices, lacas, aglomerantes o “binders”, etc. No obstante, su versatilidad se ha ampliado de forma notable con el desarrollo de materiales compuestos con refuerzo de fibra, donde el empleo de resinas epoxídicas (EP), vinil-éster (VE) y

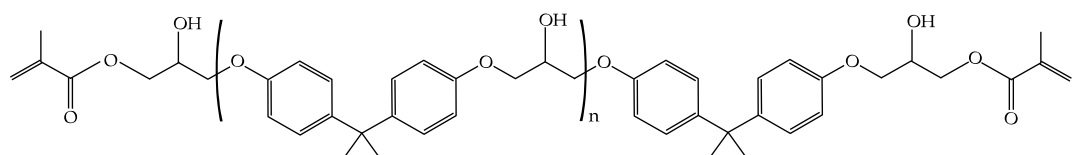
poliéster insaturado (UP) está ampliamente extendido por la versatilidad en cuanto a procesado que ofrecen (resinas de colada a temperatura ambiente) y el equilibrio de propiedades que aportan (**Figura I.3.6**). En general, las resinas de poliéster insaturado se emplean en aplicaciones corrientes ya que se trata de resinas con un buen equilibrio entre propiedades y coste. Por su parte, las resinas epoxídicas ofrecen mayor calidad y se emplean en aplicaciones donde se requiere mayor responsabilidad técnica; ahora bien, el coste de las resinas epoxi supera de forma importante el de las resinas de poliéster insaturado. Las resinas de vinil-éster son resinas con procesos de entrecruzamiento similares a los de las resinas de poliéster insaturado, pero no se sintetizan de la misma manera ya que proceden de la reacción de resinas epoxídicas con diversos tipos de ácidos acrílicos.



resina de poliéster insaturado (UP)



resina epoxi (EP) derivada de diglicidil éter de bisfenol A (DGEBA)



resina de vinil éster (VE) derivada de DGEBA

Figura I.3.6. Representación esquemática de las estructuras químicas de diversos tipos de resinas termoestables ampliamente utilizadas en la fabricación de materiales compuestos.

Resinas epoxi de alto rendimiento medioambiental.

Las resinas epoxi son un importante grupo a resaltar puesto que representan el 70% del mercado de resinas termoestables [95]. Su producción se inició a mediados del siglo XX evolucionando con el paso de los años e introduciéndose en mayor número de sectores industriales como los materiales compuestos, pinturas, adhesivos, aplicaciones náuticas, sistemas eléctricos y electrónicos entre otros debido a sus excelentes propiedades mecánicas, eléctricas, resistencia química y mínima contracción después del curado [96, 97]. Pero dichas ventajas están favorecidas tanto por la estructura química de las resinas epoxi como por la correcta elección de los aditivos necesarios (agentes de reticulación, pigmentos, materiales de relleno, plastificantes, catalizadores, etc.) [14, 98]. Aunque un importante inconveniente es su fragilidad debido a la alta densidad de reticulación [55].

Las resinas epoxis a partir de recursos bio presenta ventajas como la ausencia de bisfenol A en su formulación. Aunque el diglicidil éter de bisfenol A (DGEBA) es el monómero más empleado para la elaboración de epóxidos debido a su precio y versatilidad. El DGEBA puede ser sintetizado a partir de epiclorhidrina y Bisfenol A en presencia de hidróxido de sodio, y el producto resultante, posee un grupo epoxi en cada uno de los extremos de la cadena. Pero el Bisfenol A proveniente de recursos fósiles es el que se encuentra en mayor proporción y representa más del 67% de la masa molar de DBEBA [95]. Pero sumado al problema medioambiental se encuentra su efecto negativo sobre la salud [99-101].

Las resinas epoxi contienen al menos dos grupos epóxido o también conocidos como oxirano o glicidilo. Los monómeros epoxídicos se pueden curar utilizando diferentes agentes de curado como anhídridos o ácidos, aminas alifáticas o aromáticas y alcoholes mediante homopolimerización catiónica o aniónica por ellos mismos [94, 102]. Los aditivos o rellenos también se suelen emplear durante la mezcla para lograr las propiedades y procesamiento deseado, aunque el ratio resina – reactivo (agente de curado) y la temperatura de curado marcará claramente las propiedades finales de las resinas epoxídicas.

Una de las líneas de investigación más interesante en el campo de las resinas epoxi es la que plantea el empleo de epóxidos derivados de aceites vegetales para la

formación de resinas termoestables mediante procesos de curado con diferentes agentes de entrecruzamiento. Algunos aceites vegetales, como el aceite de vernonia, presentan en su estructura algún grupo epóxido, lo cual lo convierte en una resina epoxi natural (**Figura I.3.7**). No obstante, son pocos los grupos epoxi que aparecen en la molécula de triglicérido de tal manera que su eficiencia como resina epoxi para matrices en compuestos es muy baja. Con aproximadamente 3 grupos epoxi por triglicérido, el aceite de vernonia se puede entrecruzar mediante polimerización catiónica con ácido fluorosulfónico a temperaturas relativamente bajas. Los materiales así obtenidos pueden emplearse como espesantes en formulaciones de lubricantes [103].

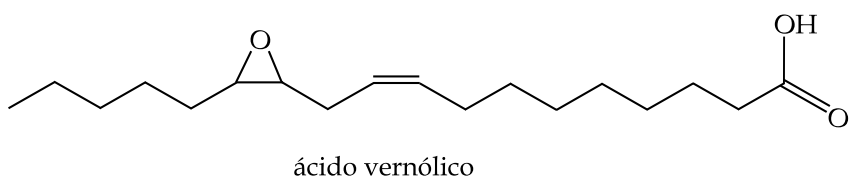


Figura I.3.7. Representación esquemática de la estructura del aceite de vernonia con ácido vernólico que presenta grupos epóxido de forma natural sin modificación química.

Por ello, se prefiere trabajar con aceites epoxidados, aceites vegetales en los que se consigue la incorporación de grupos epóxido en los dobles enlaces que presentan los diferentes ácidos grasos. El aceite de soja y el aceite de linaza ofrecen un elevado número de insaturaciones en la estructura y mediante un proceso de epoxidación adecuado, es posible obtener el derivado epoxidado correspondiente. De hecho, comercialmente es fácil encontrar aceite de linaza y de soja epoxidado, ELO y ESBO respectivamente. Este tipo de aceites epoxidados encuentran muchas aplicaciones en el campo de la plastificación y estabilización de formulaciones de termoplásticos y su empleo en materiales compuestos no es extensivo.

Industrialmente, el proceso de epoxidación de triglicéridos es bien conocido y en la actualidad se pueden encontrar numerosos proveedores de diferentes aceites epoxidados, fundamentalmente aceite de soja, ESBO, de linaza, ELO y de ricino, ECO. Los aceites de linaza y de soja epoxidados son los que mayores posibilidades ofrecen en la preparación de resinas epoxi derivadas de triglicéridos ya que el número de insaturaciones presentes en las estructuras es elevado y ello permite obtener elevados grados de epoxidación. Aunque se han descrito diversos procesos de epoxidación [104-

107], el proceso más empleado a escala industrial emplea peroxiácidos generados *in situ* (ver sección I.1).

Normalmente, las resinas epoxi se emplean en aplicaciones bastante técnicas debido a la calidad intrínseca de este grupo de resinas de colada. Por ello, se está empezando a trabajar en el desarrollo de resinas ecológicas mediante mezclado de resinas convencionales derivadas del petróleo (fundamentalmente derivadas del bisfenol A) con resinas epoxi derivadas de triglicéridos o, lo que es lo mismo, aceites vegetales epoxidados.

Entre las soluciones con cierto contenido ecológico, algunas investigaciones se centran en la obtención de resinas epoxi mediante mezclado en diferentes proporciones de epoxi derivada del petróleo y epoxis derivadas de aceites vegetales epoxidados. Algunos autores han trabajado con mezclas de resina epoxi derivada del bisfenol A (DGEBA) con epoxis derivadas de aceites de soja y de ricino epoxidados con el empleo de hexafluoroantimonato de N-benzilpirazinio (BPH) [108, 109]. Estos aceites epoxidados pueden ofrecer posibilidades interesantes como diluyentes reactivos pudiendo adaptar las características del producto entrecruzado. Destaca el empleo de aceite de maíz epoxidado, ECO como diluyente reactivo de compuestos derivados de la reacción entre resinas epoxi petroquímicas derivadas de DGEBA con ácido pimárico derivado de la colofonia [110]. Otras investigaciones han desarrollado resinas de elevado interés tecnológico con el empleo de resinas epoxi derivadas del bisfenol F (DGEBF - diglicidil éter del bisfenol F) con aceite de linaza y de soja epoxidados. El proceso de curado se lleva a cabo con anhídridos cíclicos como el anhídrido metil tetrahidroftálico (MTHPA) en presencia de un acelerador del tipo imidazol. La presencia de los aceites vegetales funcionalizados incide de forma positiva en la mejora de las propiedades a impacto de estas resinas debido a la estructura de los aceites [111]. Por otro lado, el tipo de agente de curado (amina, anhídrido, mercaptano, ácido carboxílico, etc.) afecta de forma decisiva las prestaciones finales de estas resinas curadas [112, 113]. Entre otros agentes de curado, se han empleado con éxito aminas como dietilén triamina (DETA) y la trietilén tetramina (TETA), algunas polialquilén aminas, anhídridos cíclicos, etc. dando lugar a materiales entrecruzados con propiedades que abarcan amplios rangos [114, 115]. Concretamente este tipo de compuestos con ESO y THPE-GE se han procesado de forma satisfactoria mediante un proceso de compresión en caliente previa eliminación de burbujas resultantes del mezclado mediante vacío.

Otros autores han trabajado en el estudio del proceso de curado de resinas epoxídicas derivadas de aceites vegetales mediante el empleo de agentes de curado de tipo anhídridos de diferentes ácidos dicarboxílicos en presencia de catalizadores de curado como aminas terciarias, imidazol, etc [116-120]. Los resultados previos con estas resinas de colada demuestran que se consiguen materiales con propiedades interesantes, pero con transiciones vítreas en el rango de 43-73 °C, algo inferiores a muchas de las resinas industriales con T_g superior a 100 °C. Con el empleo de anhídrido maleico y anhídrido isoftálico se consiguen estas resinas de tipo rígido. Con el empleo de otros anhídridos como los del ácido hexahidroftálico y del ácido succínico se obtienen materiales con comportamiento elastomérico con valores de T_g inferiores a la temperatura ambiente [121]. En esta misma línea de trabajo, también se han obtenido compuestos con matrices de aceite de soja epoxidado curado con anhídrido maleico y refuerzos de fibras naturales. Con ello, se obtienen compuestos completamente ecológicos que incluso se pueden procesar mediante técnicas típicas de materiales compuestos como RTM [122]. Las resinas empleadas han sido fundamentalmente aceite de soja epoxidado como componente principal y otras resinas derivadas del aceite de soja. Otros autores han trabajado con mezclas de resinas epoxi y fenólicas a las que se incorpora aceite de linaza para formar redes de interpenetración con buenas propiedades globales. No obstante, las propiedades finales están algo lejos de las que se obtienen con el empleo de resina epoxi sin mezclar [123].

Entre las resinas epoxi de alto rendimiento medioambiental comerciales, podemos encontrar Greenpoxy, Ecopoxy y Super Sap entre otras. Aunque en bibliografía se contempla como se realizan resinas epoxi a partir de materiales bio-basados. Tanto el ácido maleopimárico o ácido abiético que se encuentran en la colofonia y el ácido ferúlico disponible en diversas fuentes biológicas no comestibles pueden ser utilizados para sintetizar polímeros termoestables con buenas propiedades [103-105].

Resinas de poliéster insaturado de alto rendimiento medioambiental.

Las resinas de poliéster insaturado son ampliamente utilizadas en la industria por sus excelentes propiedades. A parte su gran versatilidad en los métodos de fabricación y composición de las resinas, permiten lograr productos con las propiedades deseadas y generalmente más económicas y sencillas de procesar que las resinas epoxi. Para lograr las insaturaciones en el poliéster se realiza una reacción de esterificación al hacer reaccionar anhídridos o ácidos con un grupo de alcoholes denominados polioles. La reactividad de la resina o rigidez del material curado dependerá de la cantidad de anhídrido o ácido saturado incorporado. Como entrecruzador, el más común es el estireno ya que mejora las propiedades finales de los productos y es económico, aunque su fuerte olor, volatilidad y toxicidad genera preocupación y se necesita una alternativa [127].

Al igual que las resinas epoxi, las resinas de poliéster insaturado (UP) representan un elevado consumo en el mercado de los termoestables para materiales compuestos. Las resinas de poliéster insaturado se obtienen mediante un proceso combinado de policondensación seguido de un proceso de entrecruzamiento por poliadición con estireno (St). Los componentes principales de las resinas de poliéster insaturado son: glicoles, ácidos carboxílicos saturados y ácidos carboxílicos insaturados.

Las iniciativas ecológicas en el campo de las tecnologías de resinas de poliéster insaturado se han centrado en la substitución de algún componente por otros de origen renovable. Así, es posible encontrar resinas de poliéster insaturado en los que parte del glicol petroquímico se ha substituido por 1,3 propanodiol de origen 100% renovable (Bio PDO). Otro diol con interesantes aplicaciones en la síntesis de resinas de poliéster insaturado es la isosorbida que se obtiene a partir de la glucosa [129]. Diversas resinas de poliéster insaturado se han obtenido tomando como base la isosorbida y bio PDO en combinación con diversos ácidos dicarboxílicos tales como el ácido sebácico, adípico, succínico (como ácidos saturados) y ácido itacónico, ácido fumárico [130-132].

Los aceites vegetales son interesantes para la sustitución del problemático estireno puesto que son triglicéridos con gran cantidad de sitios potencialmente reactivos

y sin toxicidad. Autores como Yili Wu *et al.* han sustituido el estireno por aceite de soja acrilado (AESO) en una resina comercial de poliéster insaturado [127]. Yeong Jung *et al.* prepararon biopolíester a partir de la lignina epoxidada que usaron como un macromonomero de lignina reactiva. Pero las resinas de base biológica también pueden ser utilizadas en aplicaciones como materiales compuestos a partir de fibra de vidrio con resultados comparables a las resinas de poliéster insaturado [128]. En el mercado existen resinas de poliéster insaturado, bajo el nombre comercial de Envirez 5000, con una parte de materiales renovables [43].

Otra de las líneas ligadas a los poliésteres insaturados ecológicos se centra en la substitución del estireno como agente de entrecruzamiento ya que este presenta alta volatilidad junto con una importante toxicidad. Así pues, se ha substituido por diversos monómeros vinílicos como divinilbenceno (DVB). Sin embargo, estas acciones simplemente ofrecen, en su mayoría, una reducción de los compuestos orgánicos volátiles (VOCs) emitidos, pero no incrementan el contenido renovable en la resina. Algunos autores han desarrollado nuevos monómeros acrílicos a partir de recursos renovables que contribuyen de forma doblemente positiva a la obtención de resinas de poliéster insaturado ecológicas [129-131].

■ Resinas fenólicas de alto rendimiento medioambiental.

Las resinas fenólicas se obtienen por policondensación de fenoles con el formaldehido, aunque se puede sustituir el fenol por xilenol o m-cresol. Si nos remontamos a los inicios de las resinas fenólicas encontramos la bakelita usada en aplicaciones como teléfonos o radios. Estos elementos construidos con bakelita disponían de buena estabilidad térmica y elevada dureza. En la actualidad las resinas fenólicas son ampliamente utilizadas en aplicaciones donde se requiere aislamiento eléctrico y térmico (inflamable), resistencia al agua (tanto dulce como salada) y resistencia a la radiación UV. En la actualidad se fabrican enchufes, interruptores, aparatos de soldadura, mangos de paellas, ceniceros para coches, etc. mediante técnicas de inyección, prensado y laminado.

La resina fenólica es un agente de curado macromolecular que puede proporcionar propiedades ignífugas. Por lo tanto Peng Deng *et al.* en su investigación utilizaron resina fenólica e incrementaron sus propiedades ignífugas al incorporar fósforo para curar resina epoxi y lograr incrementar aún más sus propiedades ignífugas [96].

Al igual que ocurre con las resinas citadas en anteriores apartados, las resinas fenólicas también presentan su vertiente realizada con recursos renovables y más concretamente los aceites. Investigaciones como las llevadas por Jiaxi Li *et al.* utilizaron aceite de soja como plastificante sostenible para caucho curado con resinas fenólicas. Los autores indicaron que cantidades inferiores al 10 phr de aceite de soja sería un buen sustituto para el plastificante a base de petróleo curado con resinas fenólicas [136].

Merece la pena destacar el interés del “cashew nut shell liquid”, CNSL que está compuesto fundamentalmente por cardanol, cardol y ácido anacárdico. El principal interés que presenta el empleo de CNSL es que presenta diversas funcionalidades y ello permite llevar a cabo una amplia gama de reacciones químicas: hidroxilo, ácido e insaturaciones en las cadenas alifáticas que permiten que estos productos se utilicen como resinas o agentes de entrecruzamiento [137-139] tal y como se aprecia en la **Figura I.3.8.**

Las resinas de CNSL pueden polimerizarse de diferentes maneras atendiendo a la funcionalidad principal. Es posible polimerizar estas resinas con compuestos que presenten hidrógenos activos, como el formaldehído en las posiciones “orto” y “para” de los anillos fenólicos en condiciones ácidas (ácido sulfúrico, por ejemplo) o incluso en condiciones alcalinas. Variando la proporción entre CNSL y el formaldehído es posible obtener novolacas (1: >1) o resoles (1: <1) [140-142]. Recientemente se han empleado aminas para llevar a cabo el entrecruzamiento de estas resinas epoxídicas derivadas de CNSL y ofrecer productos libres de formaldehído [139, 143, 144].

Se han realizado algunos trabajos sobre el empleo de este tipo de matriz para compuestos de alto rendimiento medioambiental [145, 146] y además se ha estudiado el papel que desempeñan estas resinas en el proceso de curado/entrecruzamiento de resinas comerciales como las resinas epoxi.

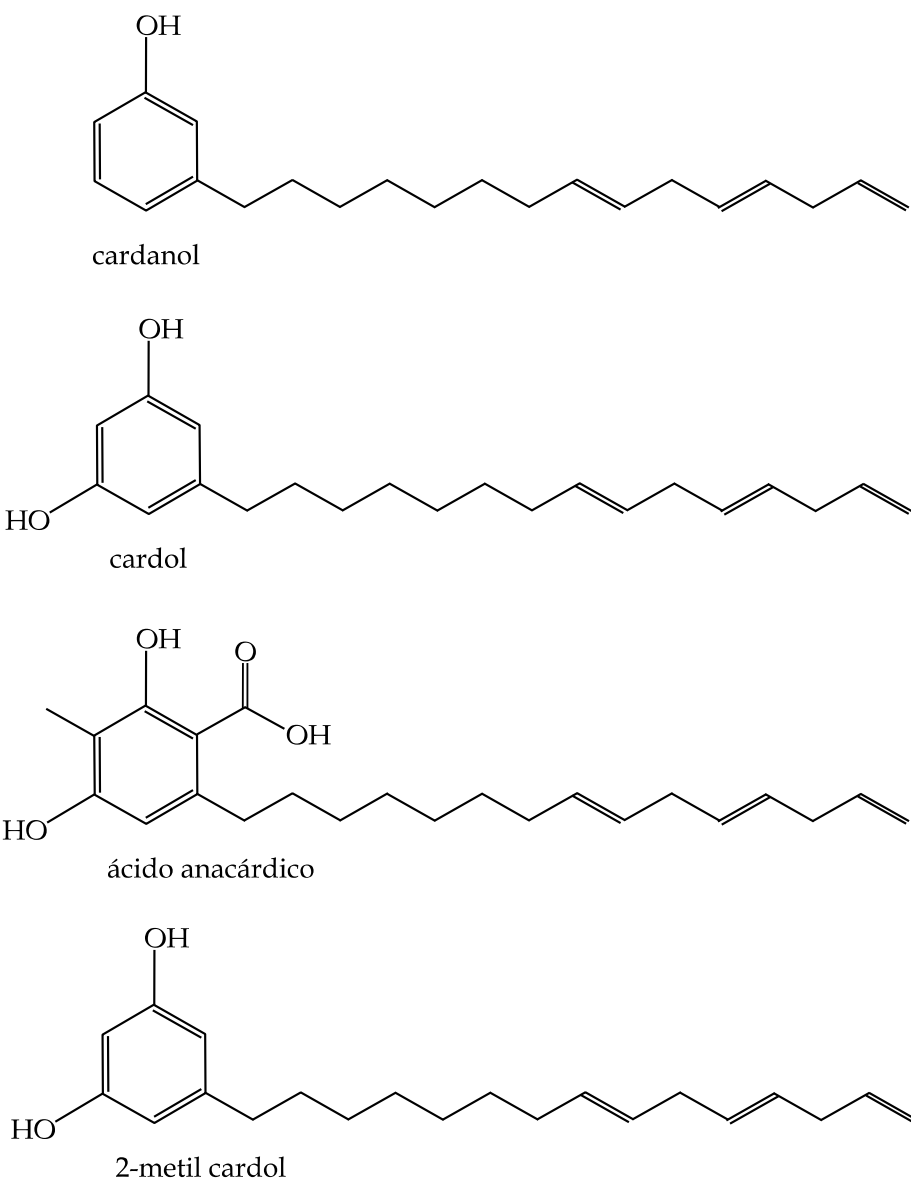


Figura I.3.8. Representación esquemática de las estructuras químicas de los principales componentes de los residuos líquidos de la industria del anacardo (CNSL).

I.4. TERMOESTABLES DERIVADOS DE ACEITES VEGETALES.

En la actualidad son muchas las investigaciones que se focalizan en lograr productos a partir de recursos renovables. Prueba de ello se hace visible en las innumerables publicaciones donde se logran resinas formadas principalmente por aceites modificados químicamente. Estos productos tendrán un origen respetuoso, más sostenible y se postulan como una atractiva alternativa ante el posible agotamiento o encarecimiento del petróleo si bien se debe tener en cuenta que no comprenderán la solución definitiva a la problemática medioambiental dado que los productos no serán biodegradables.

Hoy en día los aceites vegetales se utilizan como resinas termoestables para aplicación en recubrimientos, materiales compuestos, etc. Pero no todos los aceites son viables para su uso industrial ya que han de ser modificados químicamente para aumentar su reactividad. Los procesos usados para lograrlo son la epoxidación, acrilación y maleinización.

I.4.1. Resinas derivadas de aceites vegetales epoxidados.

Actualmente algunos aceites vegetales, y más concretamente el aceite de soja epoxidado (ESO), mejoran las propiedades de la resina epoxídica, logrando un producto final con un alto contenido bio [147]. No obstante, es fácil encontrar investigaciones donde el uso de otros aceites epoxidados como el de maíz se utiliza para la elaboración de resinas [110]. Consultando la bibliografía, autores como Sudheer Kumar *et al.* lograron buenas propiedades al reemplazar un 20 % de Diglicidil Éter de Bisfenol A (DGEBA) por aceite de soja epoxidado (ESO) usando anhídrido metil hexahidroftálico (MHHPA) como agente de curado y como catalizador 2-metil imidazol (2-MI). Un 20 %

de ESO incrementó la resistencia a la tracción en más de un 13 % y mejoras tanto en la tenacidad a la fractura como en calorimetría diferencial de barrido [148].

En otras investigaciones se utilizó el ESO como carga del Diglicidil Éter de Bisfenol A (DGEBA) curado con ácido sebálico por su bajo coste, comparado con endurecedores de aminas, y su capacidad de reaccionar con la resina epoxi y los grupos oxiranos. Se estudió la energía de activación en las distintas mezclas (DGEBA – ácido sebálico) con la adición de 10, 20 y 30 % en peso de ESO. Hallando una mayor energía de activación durante el proceso de curado con la adición de un 30 % de ESO [147].

Durante muchos años la elaboración de materiales compuestos se ha investigado en la creación de biocompuestos a partir de fibras de plantas, pero como fase matriz se ha utilizado la resina epoxi [149]. No obstante, autores como M.D. Samper *et al.* realizaron materiales compuestos laminados usando como matriz aceite de linaza (ELO) y aceite de soja epoxidado (ESBO) con fibra pizarra mediante la técnica RTM obteniendo materiales compuestos con propiedades mecánicas superiores a materiales tradicionales epoxi-fibra de vidrio [150]. En otras investigaciones se emplearon fibras de sisal y aceite de soja epoxidado (ESO) para incrementar tanto el módulo como la resistencia a la tracción con el aporte de un 15 % en peso de fibra [151].

I.4.2. Resinas derivadas de aceites vegetales epoxidados-acrilados.

En referencia a los aceites acrilados, también han sido usados en diferentes aplicaciones. En los últimos años el AESO se ha convertido en una de las resinas industriales de base biológica que pueden ser curadas con radiación ultravioleta (UV). Bowen Dong *et al.* utilizaron aceite de soja acrilado (AESO) como recubrimiento usando la técnica de curado mediante radiación UV. Pero también incorporaron grafeno funcionalizado para mejorar tanto las propiedades mecánicas como térmicas, logrando mejorar las propiedades con un 1% de carga de grafeno [152]. El curado con UV ha

experimentado un gran auge en la industria de los recubrimientos puesto que es respetuoso con el medio ambiente y no emite compuestos orgánicos volátiles durante el proceso de curado [153]. Además de poseer ventajas como bajo consumo de energía y alta velocidad de curado, en comparación con los métodos de recubrimiento tradicionales [154].

También ha sido estudiado por otros autores el efecto del contenido de AESO en presencia de diferentes endurecedores sobre las propiedades mecánicas y térmicas. Suheyla Kocaman *et al.* en su investigación lograron incrementar el alargamiento a la rotura al incorporar AESO a la resina epoxi diglicidil éter de bisfenol (DGEBA) con respecto a la resina pura de DGEBA. Para demostrar la resistencia química la resina epoxi modificada con AESO se curó con cinco endurecedores, logrando las pruebas más satisfactorias con los agentes de curado MXDA- *m*-xilendiamina y anhídrido MA-maleico [155].

I.4.3. Resinas derivadas de aceites vegetales maleinizados.

En referencia a los aceites maleinizados también existen diversas publicaciones sobre su uso como recubrimiento. Dan Rosu *et al.* emplearon el aceite de ricino maleinizado como reticulante de diglicidil eter de bisfenol A (DGEBA) en presencia de cloruro de bencil trimetil amonio para su uso como recubrimiento [14, 55].

I.5. PLASTIFICANTES DERIVADOS DE ACEITES VEGETALES.

La principal función de los plastificantes es proporcionar ductilidad o flexibilidad. Por lo tanto, aumentan el índice de fluidez y mejoran la procesabilidad del material. Desde un punto de vista más técnico, su incorporación favorece la cristalización en frío y reduce la temperatura donde el material se reblandece (T_g) [156]. Repercutiendo en un menor coste de energía y de maquinaria debido al descenso de la temperatura de procesabilidad.

Habitualmente, los plastificantes están compuestos por pequeñas moléculas orgánicas y con baja volatilidad. A nivel molecular, el plastificante se sitúa entre las cadenas disminuyendo la interacción entre estas y facilitando su movimiento, y por lo tanto disminuyendo la rigidez de la estructura. Para dar una explicación al fenómeno de plastificación existen las siguientes teorías: teoría del volumen libre, teoría del gel y la teoría de la lubricación.

La teoría del volumen libre ocurre cuando el plastificante se intercala entre las cadenas poliméricas. A mayor volumen libre se logrará mayor flexibilidad y menor T_g , debido a la facilidad en el movimiento de las cadenas. Aunque la eficiencia de uno u otro plastificante dependerá de la compatibilidad con la matriz polimérica y la estructura química de su molécula.

La teoría del gel se basa en el debilitamiento que el plastificante ejerce sobre las fuerzas intermoleculares. De esta forma, el plastificante dificulta las interacciones moleculares entre las cadenas y, por lo tanto, el material polimérico se hace más procesable y dúctil. Esta teoría se aplica a polímeros amorfos.

La teoría de la lubricación, tal y como la misma palabra apunta, se basa en el uso del plastificante como un lubricante que disminuye la fricción intermolecular de las cadenas y por lo tanto facilita su movimiento.

Aunque existen diferentes tipos de plastificantes como los monoméricos, oligoméricos y poliméricos en función de su estructura y peso molecular, nos centraremos en los siguientes plastificantes derivados de los aceites vegetales.

I.5.1. Aceites vegetales epoxidados.

En la actualidad se han demostrado los buenos resultados logrados con aceites epoxidados como plastificantes de PLA y PVC [156]. Entre los usos del PLA plastificado con aceites epoxidados destacan sus aplicaciones alimentarias debido a su baja toxicidad y gran abundancia [157]. Tanto los aceites epoxidados de soja (ESBO) [158], palma (EPO) [159], semilla de girasol [160] y semilla de algodón (ECSO) [46] han indicado un incremento de la flexibilidad del PLA. Pero también se ha demostrado que la adición del plastificante logra materiales más estables térmicamente [157].

En cuanto al uso de los aceites vegetales como plastificantes de PVC la principal aplicación se produce en la elaboración de plásticos sin ftalatos con baja toxicidad y bajo impacto ambiental. La problemática de la migración de los ftalatos y sus problemas de toxicidad han limitado su uso en aplicaciones que estén en contacto con juguetes, alimentos, elementos médicos, etc [44]. Consultando en bibliografía se han realizado plásticos con aceites epoxidados de linaza (ELO) [44], semilla de algodón (ECSO) [161] y soja (ESBO) [162] con un contenido de plastificante entre 50 y 80 phr y unas temperaturas de curado comprendidas entre los 160 °C y 220 °C con tiempos de curado entre los 6 y 17,5 min. La investigación llevada a cabo por Fenollar *et al.* rechazó los mejores resultados con una temperatura de curado de 70 phr durante 8 min y 220 °C, mientras que la investigación desarrollada con ECSO indicó como resultados óptimos de curado los logrados durante 15 min a 205 °C con el mismo porcentaje de plastificante. En el caso del PVC plastificado con ESBO el porcentaje de plastificante se redujo a 50 phr y las condiciones de curado óptimas se consiguieron durante 8 min a 170 °C [161].

I.5.2. Aceites vegetales maleinizados.

Los aceites maleinizados también se presentan como una interesante alternativa, a partir de recursos renovables, para incrementar y mejorar la flexibilidad del PLA. En el trabajo llevado a cabo por Ferri *et al.* se observó como la incorporación de un 15-20 phr de MLO a la matriz de PLA incrementaba durante los ensayos de tracción el alargamiento por encima del 1000 % debido a la reducción de las fuerzas intermoleculares, el efecto de

la lubricación y el incremento del volumen libre propiciado por un elevado phr de plastificante, el cual conduce a una mayor movilidad de las cadenas [163].

Otro aceite maleinizado que presenta buenos resultados como plastificante de PLA es el de semilla de cáñamo. En la investigación llevada a cabo por Quiles-Carrillo *et al.* la acción plastificante de dicho aceite mejora tanto la resistencia al impacto y el alargamiento a la rotura como la resistencia a la tracción y el módulo elástico. También observaron una disminución de la temperatura de transición vítrea desde valores de 62,8 °C para el PLA puro hasta 59,8 °C al incorporar un 10 % phr de aceite de cáñamo maleinizado. Estos hechos, están provocados por la extensión, ramificación o reticulación de los grupos hidroxilos de las cadenas de PLA con los grupos de anhídrido maleico del MHO [164].

I.5.3. Aceites vegetales epoxidados-acrilados.

En relación al empleo de aceites acrilados se encuentra el uso del aceite de soja epoxiado acrilado (AESO) como plastificante con la virtud de poseer grupos epoxi, hidroxilo y acrilato [165]. Si recordamos cuando se trató la acrilación, esta podía ser lograda directamente en una sola etapa o mediante una previa epoxidación y posterior apertura del anillo oxirano para incorporar la estructura acrílica.

Autores como Sheli C. Mauck *et al.* emplearon el aceite de soja epóxido y acrilado (AESO) con el objetivo de incrementar la dureza del PLA. Aunque los resultados muestran como la matriz de PLA se endureció, también el efecto plastificante se demostró. Las muestras de PLA puro son frágiles y presentan un pobre alargamiento con valores del 4,1 % mientras que la incorporación de un 5 % en peso propició valores del 31 % [51].

I.6. REFERENCIAS.

- [1] N. Khalid, R.S. Khan, M.I. Hussain, M. Farooq, A. Ahmad, I. Ahmed, "*A comprehensive characterisation of safflower oil for its potential applications as a bioactive food ingredient - A review*", Trends in Food Science & Technology (2017) **66**, 176-186.
- [2] A. Zielinska, I. Nowak, "*Abundance of active ingredients in sea-buckthorn oil*", Lipids in Health and Disease (2017) **16**, 95.
- [3] M. Musil, F. Skopal, M. Hájek, A. Vavra, "*Butanolysis: Comparison of potassium hydroxide and potassium tert-butoxide as catalyst for biodiesel preparing from rapeseed oil*", Journal of Environmental Management (2018) **218**, 555-561.
- [4] M. Lapuerta, M. Villajos, J.R. Agudelo, A.L. Boehman, "*Key properties and blending strategies of hydrotreated vegetable oil as biofuel for diesel engines*", Fuel Processing Technology (2011) **92**, 2406-2411.
- [5] A. Wibowo, I.N.G. Wardana, S. Wahyudi, D.W. Yanuriyawan, "*A comparative analysis of spray combustion of kapok seed oil and jatropha oil as an alternative biofuel*", Journal of Engineering Science and Technology (2018) **13**, 1111-1121.
- [6] D. Tabio García, Y. Díaz Domínguez, M. Rondón Macias, E. Fernández Santana, R. Piloto-Rodríguez, *Extracción de aceites de origen vegetal*. Monografía. Universidad Tecnológica de La Habana "José Antonio Echeverría" (2017), DOI: 10.13140/RG.2.2.11047.55201.
- [7] D.M. Kasote, Y.S. Badhe, M.V. Hegde, "*Effect of mechanical press oil extraction processing on quality of linseed oil*", Industrial Crops and Products (2013) **42**, 10-13.
- [8] F. Lu, G.K. Kuhnle, Q.F. Cheng, "*Vegetable oil as fat replacer inhibits formation of heterocyclic amines and polycyclic aromatic hydrocarbons in reduced fat pork patties*", Food Control (2017) **81**, 113-125.
- [9] A.C. Hughes, "*Have Indo-Malaysian forests reached the end of the road?*", Biological Conservation (2018) **223**, 129-137.

- [10] G. Manoli, A. Meijide, N. Huth, A. Knohl, Y. Kosugi, P. Burlando, J. Ghazoul, S. Faticchi, "Ecohydrological changes after tropical forest conversion to oil palm", *Environmental Research Letters* (2018) **13**, 064035.
- [11] T. Mielke. *Palm oil the leaer in global oils and fast supply* (2013).
- [12] B.d.c.d. Rosario, *Aceites y grasas*, J. Calzada, Editor. 2016: https://www.bcr.com.ar/Pages/Publicaciones/informativosemanal_noticias.aspx?pIdNoticia=636.
- [13] H. Varkkey, A. Tyson, S.A.B. Choiruzzad, "Palm oil intensification and expansion in Indonesia and Malaysia: Environmental and socio-political factors influencing policy", *Forest Policy and Economics* (2018) **92**, 148-159.
- [14] D. Rosu, F. Mustata, N. Tudorachi, C.D. Varganici, L. Rosu, V.E. Musteata, "A study on coating properties of an epoxy system hardened with maleinized castor oil", *Progress in Organic Coatings* (2016) **99**, 480-489.
- [15] A.E. Bailey, *Aceites y Grasas Industriales*. (1984), Ed. Reverté.
- [16] S.N. Khot, J.J. Lascala, E. Can, S.S. Morye, G.I. Williams, G.R. Palmese, S.H. Kusefoglu, R.P. Wool, "Development and application of triglyceride-based polymers and composites", *Journal of Applied Polymer Science* (2001) **82**, 703-723.
- [17] Z. Sotoodeh-Nia, A. Hohmann, A. Buss, R.C. Williams, E.W. Cochran, "Rheological and physical characterization of pressure sensitive adhesives from bio-derived block copolymers", *Journal of Applied Polymer Science* (2018) **135**, 46618.
- [18] J. Deng, Q. Liu, Q. Zhang, C. Zhang, D. Liu, D. Fan, H. Yang, "Comparative study on composition, physicochemical and antioxidant characteristics of different varieties of kiwifruit seed oil in China", *Food Chemistry* (2018) **264**, 411-418.
- [19] P.K.S. Pillai, S. Li, L. Bouzidi, S.S. Narine, "Metathesized palm oil & novel polyol derivatives: Structure, chemical composition and physical properties", *Industrial Crops and Products* (2016) **84**, 205-223.

- [20] F.T. Djikeng, H.M. Womeni, E. Anjaneyulu, M.S.L. Karuna, R.B.N. Prasad, M. Linder, "*Effects of natural antioxidants extracted from Cameroonian ginger roots on the oxidative stability of refined palm olein*", European Food Research and Technology (2018) **244**, 1015-1025.
- [21] C.S. Cai, H.G. Dai, R.S. Chen, C.X. Su, X.Y. Xu, S. Zhang, L.T. Yang, "*Studies on the kinetics of in situ epoxidation of vegetable oils*", European Journal of Lipid Science and Technology (2008) **110**, 341-346.
- [22] D.W. Marks, R.C. Larock, "*The conjugation and epoxidation of fish oil*", Journal of the American Oil Chemists Society (2002) **79**, 65-68.
- [23] F. Mustata, T. Nita, L. Bicu, "*The curing reaction of epoxidized methyl esters of corn oil with Diels-Alder adducts of resin acids. The kinetic study and thermal characterization of crosslinked products*", Journal of Analytical and Applied Pyrolysis (2014) **108**, 254-264.
- [24] S. Sinadinovic-Fiser, M. Jankovic, O. Borota, "*Epoxidation of castor oil with peracetic acid formed in situ in the presence of an ion exchange resin*", Chemical Engineering and Processing (2012) **62**, 106-113.
- [25] X.J. Huang, H. Liu, S.B. Shang, Z.S. Cai, J. Song, Z.Q. Song, "*Synthesis and characterization of castor oil-based polymeric surfactants*", Frontiers of Agricultural Science and Engineering (2016) **3**, 46-54.
- [26] P.K. Gamage, M. O'Brien, L. Karunananayake, "*Epoxidation of some vegetable oils and their hydrolysed products with peroxyformic acid - optimised to industrial scale*", Journal of the National Science Foundation of Sri Lanka (2009) **37**, 229-240.
- [27] M.T. Benaniba, N. Belhaneche-Bensemra, G. Gelbard, "*Epoxidation of sunflower oil with peroxyoacetic acid in presence of ion exchange resin by various processes*", Energy Education Science and Technology (2008) **21**, 71-82.
- [28] A.I. Hashem, W.S.I. Abou Elmagd, A.E. Salem, M. El-Kasaby, A.M. El-Nahas, "*Conversion of some vegetable oils into synthetic lubricants*", Energy Sources Part a-Recovery Utilization and Environmental Effects (2013) **35**, 397-400.

- [29] B.W. Chieng, N.A. Ibrahim, Y.Y. Then, Y.Y. Loo, "Epoxidized jatropha oil as a sustainable plasticizer to poly(lactic acid)", *Polymers* (2017) **9**, 204.
- [30] B.W. Chieng, N.A. Ibrahim, Y.Y. Then, Y.Y. Loo, "Epoxidized vegetable oils plasticized poly(lactic acid) biocomposites: mechanical, thermal and morphology properties", *Molecules* (2014) **19**, 16024-16038.
- [31] S. Ranganathan, V. Sieber, "Development of semi-continuous chemo-enzymatic terpene epoxidation: combination of anthraquinone autoxidation and the lipase-mediated epoxidation process", *Reaction Chemistry & Engineering* (2017) **2**, 885-895.
- [32] Y.L. Wu, A.L. Li, K.C. Li, "Development and evaluation of pressure sensitive adhesives from a fatty ester", *Journal of Applied Polymer Science* (2014) **131**, 41143.
- [33] J. Wang, Y. Liu, Z. Zhou, Y. Fu, J. Chang, "Epoxidation of soybean oil catalyzed by deep eutectic solvents based on the choline chloride–carboxylic acid bifunctional catalytic system", *Industrial & Engineering Chemistry Research* (2017) **56**, 8224-8234.
- [34] M.B.M. Serrano, "Obtención de polioles a partir de aceites vegetales para la fabricación de poliuretano", Tesis doctoral (2008)
- [35] L.A. Rios, P. Weckes, H. Schuster, W. Hölderich, "Mesoporous and amorphous Ti-silicas on the epoxidation of vegetable oils", *Journal of Catalysis* **232** (2005) 19-26.
- [36] T.T. Kouroosh Saremi, Alireza SHakeri, Ahmad Babanalbandi "Epoxidation of soybean oil", *Annals of Biological Research* **3** (2012) 4254-4258.
- [37] M.M. Wadhi, R. Weliam, "Effect of epoxidized sunflower oil on polylactic acid properties", *Research on Chemical Intermediates* (2014) **40**, 399-406.
- [38] A. Carbonell-Verdu, L. Bernardi, D. Garcia-Garcia, L. Sanchez-Nacher, R. Balart, "Development of environmentally friendly composite matrices from epoxidized cottonseed oil", *European Polymer Journal* (2015) **63**, 1-10.
- [39] Y.B. Tee, R.A. Talib, K. Abdan, N.L. Chin, R.K. Basha, K.F.M. Yunos, "Comparative study of chemical, mechanical, thermal, and barrier properties of poly(lactic acid) plasticized with epoxidized soybean oil and epoxidized palm oil", *Bioresources* (2016) **11**, 1518-1540.

- [40] J. Alam, M. Alam, M. Raja, Z. Abduljaleel, L.A. Dass, "MWCNTs-reinforced epoxidized linseed oil plasticized polylactic acid nanocomposite and its electroactive shape memory behaviour", International Journal of Molecular Sciences (2014) **15**, 19924-19937.
- [41] S. Vijayarajan, S.E.M. Selke, L.M. Matuana, "Continuous blending approach in the manufacture of epoxidized soybeanplasticized poly(lactic acid) sheets and films", Macromolecular Materials and Engineering (2014) **299**, 622-630.
- [42] C. Xing, L.M. Matuana, "*Epoxidized soybean oil-plasticized poly(lactic acid) films performance as impacted by storage*", Journal of Applied Polymer Science (2016) **133**, 43201.
- [43] D. Ray, S. Sain, *3 - Thermosetting bioresins as matrix for biocomposites*, in Biocomposites for High-Performance Applications, D. Ray, Editor. (2017), Woodhead Publishing. p. 57-80.
- [44] O. Fenollar, D. Garcia-Sanoguera, L. Sanchez-Nacher, J. Lopez, R. Balart, "*Effect of the epoxidized linseed oil concentration as natural plasticizer in vinyl plastisols*", Journal of Materials Science (2010) **45**, 4406-4413.
- [45] A. Carbonell-Verdu, D. Garcia-Sanoguera, A. Jordá-Vilaplana, L. Sanchez-Nacher, R. Balart, "*A new biobased plasticizer for poly(vinyl chloride) based on epoxidized cottonseed oil*", Journal of Applied Polymer Science (2016) **133**, 43642.
- [46] A. Carbonell-Verdu, M.D. Samper, D. Garcia-Garcia, L. Sanchez-Nacher, R. Balart, "*Plasticization effect of epoxidized cottonseed oil (ECSO) on poly(lactic acid)*", Industrial Crops and Products (2017) **104**, 278-286.
- [47] A. Carbonell, J. Ferri, F. Dominici, T. Boronat, L. Sanchez-Nacher, R. Balart, L. Torre, "*Manufacturing and compatibilization of PLA/PBAT binary blends by cottonseed oil-based derivatives*". Express Polymer Letters (2018) **12**, 808-823.
- [48] P. Zhang, J.N. Xin, J.W. Zhang, "Effects of catalyst type and reaction parameters on one-step acrylation of soybean oil", Acs Sustainable Chemistry & Engineering (2014) **2**, 181-187.
- [49] C.G. Liu, Q.Q. Shang, P.Y. Jia, Y. Dai, Y.H. Zhou, Z.S. Liu, "Tung oil-based unsaturated co-ester macromonomer for thermosetting polymers: synergistic synthesis and

- copolymerization with styrene", Acs Sustainable Chemistry & Engineering (2016) **4**, 3437-3449.
- [50] J.R. Ernzen, F. Bondan, C. Luvison, C.H. Wanke, J.D. Martins, R. Fiorio, O. Bianchi, "Structure and properties relationship of melt reacted polyamide 6/maleinized soybean oil", Journal of Applied Polymer Science (2016) **133**, 43050.
- [51] S.C. Mauck, S. Wang, W. Ding, B.J. Rohde, C.K. Fortune, G. Yang, S.-K. Ahn, M.L. Robertson, "Biorenewable tough blends of polylactide and acrylated epoxidized soybean oil compatibilized by a polylactide star polymer", Macromolecules (2016) **49**, 1605-1615.
- [52] A. Carbonell-Verdu, D. Garcia-Garcia, F. Dominici, L. Torre, L. Sanchez-Nacher, R. Balart, "PLA films with improved flexibility properties by using maleinized cottonseed oil", European Polymer Journal (2017) **91**, 248-259.
- [53] A.I. Aigbodion, F.E. Okieimen, E.O. Obazee, I.O. Bakare, "Utilisation of maleinized rubber seed oil and its alkyd resin as binders in water-borne coatings", Progress in Organic Coatings (2003) **46**, 28-31.
- [54] C. Liu, Z. Liu, B.H. Tisserat, R. Wang, T.P. Schuman, Y. Zhou, L. Hu, "Microwave-assisted maleation of tung oil for bio-based products with versatile applications", Industrial Crops and Products (2015) **71**, 185-196.
- [55] D. Rosu, F. Mustata, N. Tudorachi, V.E. Musteata, L. Rosu, C.D. Varganici, "Novel bio-based flexible epoxy resin from diglycidyl ether of bisphenol A cured with castor oil maleate", Rsc Advances (2015) **5**, 45679-45687.
- [56] T. Eren, S.H. Kusefoglu, R. Wool, "Polymerization of maleic anhydride-modified plant oils with polyols", Journal of Applied Polymer Science (2003) **90**, 197-202.
- [57] J.M. Ferri, D. Garcia-Garcia, N. Montanes, O. Fenollar, R. Balart, "The effect of maleinized linseed oil as biobased plasticizer in poly(lactic acid)-based formulations", Polymer International (2017) **66**, 882-891.

- [58] X.J. Huang, H. Liu, S.B. Shang, X.P. Rao, J. Song, "preparation and characterization of polymeric surfactants based on epoxidized soybean oil grafted hydroxyethyl cellulose", Journal of Agricultural and Food Chemistry (2015) **63**, 9062-9068.
- [59] D.S. Tathe, R.N. Jagtap, "Design novel polyhydroxyl fatty amide based on *Balanites roxburgii* oil and its application for coating", Designed Monomers and Polymers (2014) **17**, 717-725.
- [60] I.C.N. Gadelha, N.B.S. Fonseca, S.C.S. Oloris, M.M. Melo, B. Soto-Blanco, "Gossypol toxicity from cottonseed products", Scientific World Journal (2014), 231635.
- [61] R. Plank, El empleo del frío en la industria de la alimentación (1963), ed. S.A. Editorial Reverté.
- [62] H.K. Knutsen, L. Barregard, M. Bignami, B. Brueschweiler, S. Ceccatelli, M. Dinovi, L. Edler, B. Grasl-Kraupp, C. Hogstrand, L. Hoogenboom, C.S. Nebbia, I.P. Oswald, A. Petersen, M. Rose, A.C. Roudot, T. Schwerdtle, C. Vleminckx, G. Vollmer, H. Wallace, J. Alexander, B. Cottrill, K. Mackay, E.P.C.F. Chain, "Presence of free gossypol in whole cottonseed", EFSA Journal (2017) **15**, 15.
- [63] T. Wedegaertner, K. Rathore, *Elimination of gossypol in cottonseed will improve its utilization*, in Agriculture and Climate Change - Adapting Crops to Increased Uncertainty, D. Edwards and G. Oldroyd, Editors. (2015), Elsevier Science Bv: Amsterdam. p. 124-125.
- [64] M.K. Dowd, S.M. Pelitire, "Recovery of gossypol acetic acid from cottonseed soapstock", Industrial Crops and Products (2001) **14**, 113-123.
- [65] Monografía de cultivos (2011).
- [66] N. Ramli. *World production of 17 oils & fats* (2015).
- [67] N. Hoda, "Optimization of biodiesel production from cottonseed oil by transesterification using naoh and methanol", Energy Sources Part a-Recovery Utilization and Environmental Effects (2010) **32**, 434-441.
- [68] W.W. Song, K.B. He, J.X. Wang, X.T. Wang, X.Y. Shi, C. Yu, W.M. Chen, L. Zheng, "Emissions of EC, OC, and PAHs from Cottonseed oil biodiesel in a heavy-duty diesel engine", Environmental Science & Technology (2011) **45**, 6683-6689.

- [69] R. Geyer, J.R. Jambeck, K.L. Law, "Production, use, and fate of all plastics ever made", *Science Advances* (2017) 3, 1700782.
- [70] E. Jiménez. *¿Cuánto plástico hay en el mundo?* 2017; Available from: <http://archivos.es.greenpeace.org/espana/es/Blog/cuento-plastico-hay-en-el-mundo/blog/59905/>.
- [71] R.S. Pazos, T. Maiztegui, D.C. Colautti, A.H. Paracampo, N. Gomez, "Microplastics in gut contents of coastal freshwater fish from rio de la plata estuary", *Marine Pollution Bulletin* (2017) **122**, 85-90.
- [72] C. Alomar, A. Sureda, X. Capo, B. Guijarro, S. Tejada, S. Deudero, "Microplastic ingestion by *Mullus surmuletus Linnaeus, 1758* fish and its potential for causing oxidative stress", *Environmental Research* (2017) **159**, 135-142.
- [73] M. Xavier, N.V. Goethem, A.A. Novotny, "A simplified model of fracking based on the topological derivative concept", *International Journal of Solids and Structures* (2018) **139-140**, 211-223.
- [74] D. Gere, T. Czigany, "Rheological and mechanical properties of recycled polyethylene films contaminated by biopolymer", *Waste Management* (2018) **76**, 190-198.
- [75] G. Lligadas, J.C. Ronda, M. Galià, V. Cádiz, "Renewable polymeric materials from vegetable oils: a perspective", *Materials Today* (2013) **16**, 337-343.
- [76] X. Zhang, X. Wang, "Polybutylene succinate/cellulose nanocrystals: Role of phthalic anhydride in squeeze oriented bionanocomposites", *Carbohydrate polymers* (2018) **196**, 254-261.
- [77] D.M. Abou-Zeid, R.J. Muller, W.D. Deckwer, "Biodegradation of aliphatic homopolymers and aliphatic - aromatic copolymers by anaerobic microorganisms", *Biomacromolecules* (2004) **5**, 1687-1697.
- [78] D.B. Rocha, J.S. de Carvalho, S.A. de Oliveira, D.D. Rosa, "A new approach for flexible PBAT/PLA/CaCO₃ films into agriculture", *Journal of Applied Polymer Science* (2018) **135**, 46660.

- [79] A.R.P. Figueiredo, A.J.D. Silvestre, C.P. Neto, C.S.R. Freire, "In situ synthesis of bacterial cellulose/polycaprolactone blends for hot pressing nanocomposite films production", Carbohydrate Polymers (2015) **132**, 400-408.
- [80] A. Rajan, J.D. Sudha, T.E. Abraham, "Enzymatic modification of cassava starch by fungal lipase", Industrial Crops and Products (2008) **27**, 50-59.
- [81] H.B. Li, M.A. Huneault, "Effect of chain extension on the properties of PLA/TPS blends", Journal of Applied Polymer Science (2011) **122**, 134-141.
- [82] J.M. Ferri, D. Garcia-Garcia, L. Sanchez-Nacher, O. Fenollar, R. Balart, "The effect of maleinized linseed oil (MLO) on mechanical performance of poly(lactic acid)-thermoplastic starch (PLA-TPS) blends", Carbohydrate Polymers (2016) **147**, 60-68.
- [83] R. Grande, A.J.F. Carvalho, "Compatible ternary blends of chitosan/poly(vinyl alcohol)/poly(lactic acid) produced by oil-in-water emulsion processing", Biomacromolecules (2011) **12**, 907-914.
- [84] V. Jost, O. Miesbauer, "Effect of different biopolymers and polymers on the mechanical and permeation properties of extruded PHBV cast films", Journal of Applied Polymer Science (2018) **135**, 46153.
- [85] V. Jost, "Packaging related properties of commercially available biopolymers - An overview of the status quo", Express Polymer Letters (2018) **12**, 429-435.
- [86] M.P. Arrieta, J. López, D. López, J.M. Kenny, L. Peponi, "Biodegradable electrospun bionanocomposite fibers based on plasticized PLA-PHB blends reinforced with cellulose nanocrystals", Industrial Crops and Products (2016) **93**, 290-301.
- [87] I. Chiulan, A.N. Frone, C. Brandabur, D.M. Panaiteescu, "Recent advances in 3D Printing of aliphatic polyesters", Bioengineering (Basel, Switzerland) (2017) **5**, 10002.
- [88] D. da Silva, M. Kaduri, M. Poley, O. Adir, N. Krinsky, J. Shainsky-Roitman, A. Schroeder, "Biocompatibility, biodegradation and excretion of polylactic acid (PLA) in medical implants and theranostic systems", Chemical Engineering Journal (2018) **340**, 9-14.

- [89] E. Lopez-Alba, S. Schmeer, F. Diaz, "Energy absorption capacity in natural fiber reinforcement composites structures", Materials (Basel, Switzerland) (2018) **11**, 418.
- [90] M. Patricia Arrieta, M. Dolores Samper, M. Aldas, J. Lopez, "On the use of PLA-PHB blends for sustainable food packaging applications", Materials (2017) **10**, 1008.
- [91] B. Tyler, D. Gullotti, A. Mangraviti, T. Utsuki, H. Brem, "Polylactic acid (PLA) controlled delivery carriers for biomedical applications", Advanced Drug Delivery Reviews (2016) **107**, 163-175.
- [92] M.L. Sanyang, S.M. Sapuan, M. Jawaid, M.R. Ishak, J. Sahari, "Development and characterization of sugar palm starch and poly(lactic acid) bilayer films", Carbohydrate Polymers (2016) **146**, 36-45.
- [93] D.D.A. López, A.F. Vela, J.Z. Cano, A.G. Murillo, A.L. Marure, F.C. Romo, "Estudio y síntesis en la producción de pla (ácido poliláctico)", III encuentro Participación de la Mujer en la Ciencia (2009).
- [94] R. Auvergne, S. Caillol, G. David, B. Boutevin, J.-P. Pascault, "Biobased thermosetting epoxy: present and future", Chemical Reviews (2014) **114**, 1082-1115.
- [95] S.Q. Ma, T.T. Li, X.Q. Liu, J. Zhu, "Research progress on bio-based thermosetting resins", Polymer International (2016) **65**, 164-173.
- [96] P. Deng, Y.S. Liu, Y. Liu, C.G. Xu, Q. Wang, "Preparation of phosphorus-containing phenolic resin and its application in epoxy resin as a curing agent and flame retardant", Polymers for Advanced Technologies (2018) **29**, 1294-1302.
- [97] F.-L. Jin, S.-J. Park, "Impact-strength improvement of epoxy resins reinforced with a biodegradable polymer", Materials Science and Engineering: A (2008) **478**, 402-405.
- [98] C.L. Dong, A. Wirasaputra, Q.Q. Luo, S.M. Liu, Y.C. Yuan, J.Q. Zhao, Y. Fu, "Intrinsic flame-retardant and thermally stable epoxy endowed by a highly efficient, multifunctional curing agent", Materials (2016) **9**, 1008.

- [99] N.M. O'Boyle, I.B. Niklasson, A.R. Tehrani-Bagha, T. Delaine, K. Holmberg, K. Luthman, A.T. Karlberg, "Epoxy resin monomers with reduced skin sensitizing potency", Chemical Research in Toxicology (2014) **27**, 1002-1010.
- [100] S. Solouki, M.R. Fazeli, S. Solouki, "Efficiency of multispecies probiotic supplements in bioremoval of bisphenol a: an in vitro study", Applied Food Biotechnology (2018) **5**, 37-46.
- [101] X. Li, L. Wang, F. Shen, Q. Zhou, X. Huang, "Impacts of exogenous pollutant bisphenol A on characteristics of soybeans", Ecotoxicology and environmental safety (2018) **157**, 463-471.
- [102] S. Ma, D.C. Webster, "Naturally occurring acids as cross-linkers to yield VOC-free, high-performance, fully bio-based, degradable thermosets", Macromolecules (2015) **48**, 7127-7137.
- [103] A. Biswas, H.N. Cheng, K.T. Klasson, Z.S. Liu, J. Berfield, F.O. Ayorinde, "Direct polymerization of vernonia oil through cationic means", Journal of the American Oil Chemists Society (2014) **91**, 2111-2116.
- [104] K. Malarczyk, E. Milchert, "Methods for epoxidation of vegetable oils on heterogenous catalysts", Przemysl Chemiczny (2015) **94**, 412-415.
- [105] S.D. Miao, P. Wang, Z.G. Su, S.P. Zhang, "Vegetable-oil-based polymers as future polymeric biomaterials", Acta Biomaterialia (2014) **10**, 1692-1704.
- [106] E. Milchert, K. Malarczyk, M. Klos, "Technological aspects of chemoenzymatic epoxidation of fatty acids, fatty acid esters and vegetable oils: a review", Molecules (2015) **20**, 21481-21493.
- [107] S.G. Tan, W.S. Chow, "Biobased epoxidized vegetable oils and its greener epoxy blends: a review", Polymer-Plastics Technology and Engineering (2010) **49**, 1581-1590.
- [108] F.L. Jin, S.J. Park, "Thermomechanical behavior of epoxy resins modified with epoxidized vegetable oils", Polymer International (2008) **57**, 577-583.
- [109] S.J. Park, F.L. Jin, J.R. Lee, "Effect of biodegradable epoxidized castor oil on physicochemical and mechanical properties of epoxy resins", Macromolecular Chemistry and Physics (2004) **205**, 2048-2054.

- [110] F.R. Mustata, N. Tudorachi, I. Bicu, "Biobased epoxy matrix from diglycidyl ether of bisphenol A and epoxidized corn oil, cross-linked with diels-alder adduct of levopimamic acid with acrylic acid", Industrial & Engineering Chemistry Research (2013) **52**, 17099-17110.
- [111] H. Miyagawa, M. Misra, L.T. Drzal, A.K. Mohanty, "Fracture toughness and impact strength of anhydride-cured biobased epoxy", Polymer Engineering and Science (2005) **45**, 487-495.
- [112] H. Miyagawa, A.K. Mohanty, M. Misra, L.T. Drzal, "Thermo-physical and impact properties of epoxy containing epoxidized linseed oil, 1 - Anhydride-cured epoxy", Macromolecular Materials and Engineering (2004) **289**, 629-635.
- [113] H. Miyagawa, A.K. Mohanty, M. Misra, L.T. Drzal, "Thermo-physical and impact properties of epoxy containing epoxidized linseed oil, 2(a) - Amine-cured epoxy", Macromolecular Materials and Engineering (2004) **289**, 636-641.
- [114] J.D. Earls, J.E. White, L.C. Lopez, Z. Lysenko, M.L. Dettloff, M.J. Null, "Amine-cured omega-epoxy fatty acid triglycerides: Fundamental structure-property relationships", Polymer (2007) **48**, 712-719.
- [115] J.D. Espinoza-Perez, B.A. Nerenz, D.M. Haagenson, Z.G. Chen, C.A. Ulven, D.P. Wiesenborn, "Comparison of curing agents for epoxidized vegetable oils applied to composites", Polymer Composites (2011) **32**, 1806-1816.
- [116] C. Ding, G.M. Tian, A. Matharu, "Adipic acid - glutaric anhydride - epoxidised linseed oil biobased thermosets with tunable properties", Materials Today Communications (2016) **7**, 51-58.
- [117] J.M. Espana, L. Sanchez-Nacher, T. Boronat, V. Fombuena, R. Balart, "Properties of biobased epoxy resins from epoxidized soybean oil (ESBO) cured with maleic anhydride (MA)", Journal of the American Oil Chemists Society (2012) **89**, 2067-2075.
- [118] A.R. Mahendran, G. Wuzella, A. Kandelbauer, N. Aust, "Thermal cure kinetics of epoxidized linseed oil with anhydride hardener", Journal of Thermal Analysis and Calorimetry (2012) **107**, 989-998.

- [119] J.M. Pin, N. Sbirrazzuoli, A. Mija, "From epoxidized linseed oil to bioresin: an overall approach of epoxy/anhydride cross-linking", Chemsuschem (2015) **8**, 1232-1243.
- [120] M.D. Samper, V. Fombuena, T. Boronat, D. Garcia-Sanoguera, R. Balart, "Thermal and mechanical characterization of epoxy resins (ELO and ESO) cured with anhydrides", Journal of the American Oil Chemists Society (2012) **89**, 1521-1528.
- [121] J. Rosch, R. Mulhaupt, "Polymers from renewable resources - polyester resins and blends based upon anhydride-cured epoxidized soybean oil", Polymer Bulletin (1993) **31**, 679-685.
- [122] P. Tran, D. Graiver, R. Narayan, "Biocomposites synthesized from chemically modified soy oil and biofibers", Journal of Applied Polymer Science (2006) **102**, 69-75.
- [123] J.C. Munoz, H. Ku, F. Cardona, D. Rogers, "Effects of catalysts and post-curing conditions in the polymer network of epoxy and phenolic resins: Preliminary results", Journal of Materials Processing Technology (2008) **202**, 486-492.
- [124] A.-L. Brocas, A. Llevot, C. Mantzaridis, G. Cendejas, R. Auvergne, S. Caillol, S. Carlotti, H. Cramail, "Epoxidized rosin acids as co-precursors for epoxy resins", Designed Monomers and Polymers (2014) **17**, 301-310.
- [125] R. Menard, S. Caillol, F. Allais, "Ferulic acid-based renewable esters and amides-containing epoxy thermosets from wheat bran and beetroot pulp: Chemo-enzymatic synthesis and thermo-mechanical properties characterization", Industrial Crops and Products (2017) **95**, 83-95.
- [126] R. Li, P. Zhang, T. Liu, B. Muhunthan, J. Xin, J. Zhang, "Use of hempseed-oil-derived polyacid and rosin-derived anhydride acid as cocuring agents for epoxy materials", Acs Sustainable Chemistry & Engineering (2018) **6**, 4016-4025.
- [127] Y.L. Wu, K.C. Li, "Acrylated epoxidized soybean oil as a styrene replacement in a dicyclopentadiene-modified unsaturated polyester resin", Journal of Applied Polymer Science (2018) **135**, 46212.
- [128] J.M. Sadler, F.R. Toulan, A.P.T. Nguyen, R.V. Kayea, S. Ziae, G.R. Palmese, J.J. La Scala, "Isosorbide as the structural component of bio-based unsaturated polyesters for use as thermosetting resins", Carbohydrate Polymers (2014) **100**, 97-106.

- [129] T.J. Farmer, R.L. Castle, J.H. Clark, D.J. Macquarrie, "Synthesis of unsaturated polyester resins from various bio-derived platform molecules", International Journal of Molecular Sciences (2015) **16**, 14912-14932.
- [130] A.C. Fonseca, I.M. Lopes, J.F.J. Coelho, A.C. Serra, "*Synthesis of unsaturated polyesters based on renewable monomers: Structure/properties relationship and crosslinking with 2-hydroxyethyl methacrylate*", Reactive & Functional Polymers (2015) **97**, 1-11.
- [131] C.M. Hong, X.J. Wang, Z.G. Pan, Y.F. Zhang, "*Curing thermodynamics and kinetics of unsaturated polyester resin with different chain length of saturated aliphatic binary carboxylic acid*", Journal of Thermal Analysis and Calorimetry (2015) **122**, 427-436.
- [132] A. Campanella, R.P. Wool, M. Bah, S. Fita, A. Abuobaid, "*Composites from northern red oak (*Quercus robur*) leaves and plant oil-based resins*", Journal of Applied Polymer Science (2013) **127**, 18-26.
- [133] S. Cousinet, A. Ghadban, I. Allaoua, F. Lortie, D. Portinha, E. Drockenmuller, J.P. Pascault, "*Biobased vinyl levulinate as styrene replacement for unsaturated polyester resins*", Journal of Polymer Science Part a-Polymer Chemistry (2014) **52**, 3356-3364.
- [134] S. Cousinet, A. Ghadban, E. Fleury, F. Lortie, J.P. Pascault, D. Portinha, "*Toward replacement of styrene by bio-based methacrylates in unsaturated polyester resins*", European Polymer Journal (2015) **67**, 539-550.
- [135] J.M. Sadler, A.P. Nguyen, S.M. Greer, G.R. Palmese, J.J. La Scala, "*Synthesis and characterization of a novel bio-based reactive diluent as a styrene replacement*", Journal of Biobased Materials and Bioenergy (2012) **6**, 86-93.
- [136] J.X. Li, A.I. Isayev, Q.H. Wang, M.D. Soucek, "*Sustainable plasticizer for butyl rubber cured by phenolic resin*", Journal of Applied Polymer Science (2018) **135**, 45500.
- [137] D. Balgude, A.S. Sabnis, "*CNSL: an environment friendly alternative for the modern coating industry*", Journal of Coatings Technology and Research (2014) **11**, 169-183.
- [138] M. Telascrea, A.L. Leao, M.Z. Ferreira, H.F.F. Pupo, B.M. Cherian, S. Narine, "*Use of a cashew nut shell liquid resin as a potential replacement for phenolic resins in the*

- preparation of panels - a review", Molecular Crystals and Liquid Crystals (2014) **604**, 222-232.
- [139] P. Kasemsiri, A. Neramittagapong, P. Chindaprasirt, "Curing kinetic, thermal and adhesive properties of epoxy resin cured with cashew nut shell liquid", Thermochimica Acta (2015) **600**, 20-27.
- [140] P. Campaner, D. D'Amico, L. Longo, C. Stifani, A. Tarzia, "Cardanol-based novolac resins as curing agents of epoxy resins", Journal of Applied Polymer Science (2009) **114**, 3585-3591.
- [141] M. Lubi, E.T. Thachil, "Particleboard from cashew nut shell liquid", Polymers & Polymer Composites (2007) **15**, 75-82.
- [142] D. Roy, P.K. Basu, P. Raghunathan, S.V. Eswaran, "Cashew nut shell liquid-based tailor-made novolac resins: Polymer morphology quantitation by 1-D and 2-D NMR techniques and performance evaluation", Journal of Applied Polymer Science (2003) **89**, 1959-1965.
- [143] E. Darroman, N. Durand, B. Boutevin, S. Caillol, "Improved cardanol derived epoxy coatings", Progress in Organic Coatings (2016) **91**, 9-16.
- [144] S. Dworakowska, A. Cornille, D. Bogdal, B. Boutevin, S. Caillol, "Formulation of bio-based epoxy foams from epoxidized cardanol and vegetable oil amine", European Journal of Lipid Science and Technology (2015) **117**, 1893-1902.
- [145] A.C.H. Barreto, M.A. Esmeraldo, D.S. Rosa, P.B.A. Fechine, S.E. Mazzetto, "Cardanol biocomposites reinforced with jute fiber: microstructure, biodegradability, and mechanical properties", Polymer Composites (2010) **31**, 1928-1937.
- [146] A.C.H. Barreto, A.E.C. Junior, J.E.B. Freitas, D.S. Rosa, W.M. Barcellos, F.N.A. Freire, P.B.A. Fechine, S.E. Mazzetto, "Biocomposites from dwarf-green Brazilian coconut impregnated with cashew nut shell liquid resin", Journal of Composite Materials (2013) **47**, 459-466.
- [147] G.M. Roudsari, A.K. Mohanty, M. Misra, "Study of the curing kinetics of epoxy resins with biobased hardener and epoxidized soybean oil", Acs Sustainable Chemistry & Engineering (2014) **2**, 2111-2116.

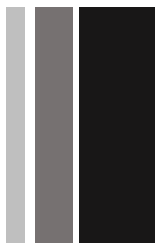
- [148] S. Kumar, S.K. Samal, S. Mohanty, S.K. Nayak, "Epoxidized soybean oil-based epoxy blend cured with anhydride-based cross-linker: thermal and mechanical characterization", Industrial & Engineering Chemistry Research (2017) **56**, 687-698.
- [149] R.D.J. Johnson, V.A. Prabu, P. Amuthakkannan, K.A. Prasath, "A review on biocomposites and bioresin based composites for potential industrial applications", Reviews on Advanced Materials Science (2017) **49**, 112-121.
- [150] M.D. Samper, R. Petrucci, L. Sanchez-Nacher, R. Balart, J.M. Kenny, "New environmentally friendly composite laminates with epoxidized linseed oil (ELO) and slate fiber fabrics", Composites Part B-Engineering (2015) **71**, 203-209.
- [151] S.K. Sahoo, S. Mohanty, S.K. Nayak, "Mechanical, thermal, and interfacial characterization of randomly oriented short sisal fibers reinforced epoxy composite modified with epoxidized soybean oil", Journal of Natural Fibers (2017) **14**, 357-367.
- [152] B.W. Dong, Y. Yuan, J. Luo, L.M. Dong, R. Liu, X.Y. Liu, "Acryloyl-group functionalized graphene for enhancing thermal and mechanical properties of acrylated epoxidized soybean oil UV-curable based coatings", Progress in Organic Coatings (2018) **118**, 57-65.
- [153] S.N.A. Ramlan, W.J. Basirun, S.W. Phang, D.T.C. Ang, "Electrically conductive palm oil-based coating with UV curing ability", Progress in Organic Coatings (2017) **112**, 9-17.
- [154] H.J. Liu, W.C. Lu, S.J. Liu, "Development of acrylated soybean oil-based UV-curable coatings with high impact strength from low viscosity oligomer", Journal of Applied Polymer Science (2018) **135**, 45698.
- [155] S. Kocaman, G. Ahmetli, "A study of coating properties of biobased modified epoxy resin with different hardeners", Progress in Organic Coatings (2016) **97**, 53-64.
- [156] J.F. Balart, V. Fombuena, O. Fenollar, T. Boronat, L. Sanchez-Nacher, "Processing and characterization of high environmental efficiency composites based on PLA and hazelnut shell flour (HSF) with biobased plasticizers derived from epoxidized linseed oil (ELO)", Composites Part B-Engineering (2016) **86**, 168-177.

- [157] V.S.G. Silverajah, N.A. Ibrahim, N. Zainuddin, W. Yunus, H. Abu Hassan, "Mechanical, thermal and morphological properties of poly(lactic acid)/epoxidized palm olein blend", Molecules (2012) **17**, 11729-11747.
- [158] F. Ali, Y.W. Chang, S.C. Kang, J.Y. Yoon, "Thermal, mechanical and rheological properties of poly (lactic acid)/epoxidized soybean oil blends", Polymer Bulletin (2009) **62**, 91-98.
- [159] V.S.G. Silverajah, N.A. Ibrahim, W. Yunus, H. Abu Hassan, C.B. Woei, "a comparative study on the mechanical, thermal and morphological characterization of poly(lactic acid)/epoxidized palm oil blend", International Journal of Molecular Sciences (2012) **13**, 5878-5898.
- [160] N. Prempeh, J.L. Li, D.G. Liu, K. Das, S. Maiti, Y. Zhang, "Plasticizing effects of epoxidized sun flower oil on biodegradable polylactide films: a comparative study", Polymer Science Series A (2014) **56**, 856-863.
- [161] A. Carbonell-Verdu, D. Garcia-Sanoguera, A. Jordà-Vilaplana, L. Sanchez-Nacher, R. Balart, "A new biobased plasticizer for poly(vinyl chloride) based on epoxidized cottonseed oil", Journal of Applied Polymer Science (2017) **134**, 43642.
- [162] C. Bueno-Ferrer, M.C. Garrigos, A. Jimenez, "Characterization and thermal stability of poly(vinyl chloride) plasticized with epoxidized soybean oil for food packaging", Polymer Degradation and Stability (2010) **95**, 2207-2212.
- [163] J.M. Ferri, D. Garcia-Garcia, N. Montanes, O. Fenollar, R. Balart, "The effect of maleinized linseed oil as biobased plasticizer in poly (lactic acid)-based formulations", Polymer International (2017) **66**, 882-891.
- [164] L. Quiles-Carrillo, M.M. Blanes-Martinez, N. Montanes, O. Fenollar, S. Torres-Giner, R. Balart, "Reactive toughening of injection-molded polylactide pieces using maleinized hemp seed oil", European Polymer Journal (2018) **98**, 402-410.
- [165] J. Narewska, L. Lassila, P. Fardim, "Preparation and characterization of new mouldable cellulose-AESO biocomposites", Cellulose (2014) **21**, 1769-1780.



II. INVESTIGACIÓN

PREVIA



II.1. MARCO DE LA INVESTIGACIÓN.

En este apartado se lleva a cabo una descripción breve de la trayectoria del grupo de investigación en el que se ha desarrollado esta tesis doctoral, trayectoria que define el marco en el que se plantea esta investigación.

Reciclado y revalorización de residuos de materiales poliméricos.

Esta representa la primera línea de trabajo en el ámbito de la investigación en la que se integró el doctorando. La razón de ser de esta línea de trabajo se fundamenta en las características del entorno socioeconómico más cercano a la Escuela Politécnica Superior de Alcoy, con un peso muy relevante del sector juguetero y sectores crecientes como el mueble y los accesorios, auxiliar del automóvil, envase y embalaje. En este entorno empiezan a desarrollarse iniciativas empresariales de fuerte implicación medioambiental, ligadas a la revalorización de los residuos de estas industrias. Bajo este marco, el grupo empieza a desarrollar una actividad intensa en el ámbito del reciclado de materiales poliméricos con un marcado enfoque empresarial con el fin de ofrecer una investigación claramente aplicada con potencial de transferencia a nivel de empresa. De hecho, gran parte de los esfuerzos en el seno del grupo van dirigidas hacia la revalorización de residuos de materiales poliméricos de naturaleza técnica (plásticos técnicos o de ingeniería), intentando ofrecer una doble ventaja: dar solución a la problemática ligada a la generación y acumulación de residuos y ofrecer una nueva vida a los residuos de materiales poliméricos en nuevas aplicaciones de ingeniería.

Aditivos funcionales y de bajo impacto medioambiental en materiales poliméricos.

Esta línea de investigación representa una de las principales apuestas del grupo. Se ha trabajado en diversas actuaciones tal y como se resume a continuación:

**"PLASTIFICANTES DE BAJO IMPACTO MEDIOAMBIENTAL
PARA FORMULACIONES DE POLI(CLORURO DE VINILO) (PVC)"**

Por su relevancia a nivel industrial, el grupo siempre ha enfocado su actividad investigadora hacia la resolución de problemas industriales. El sector del poli(cloruro de vinilo) (PVC) es un sector que representa un consumo importante en el global, con amplios usos en la industria de la construcción, sector eléctrico, industria del juguete, etc. Las formulaciones industriales de PVC contienen importantes cantidades de aditivos tales como plastificantes, antioxidantes, colorantes, estabilizantes térmicos, etc. Concretamente, los plastificantes, representan cantidades bastante elevadas en las formulaciones ya que se requieren para aportar flexibilidad al PVC cuya estructura química le confiere alta rigidez y fragilidad. Tradicionalmente, se han empleado productos derivados del petróleo con excelentes resultados de plastificación, siendo los ftalatos los plastificantes que se han empleado de forma extensiva.

El problema del empleo de los plastificantes radica en su potencial migración, sobre todo, en sectores donde se produce un contacto directo del consumidor con el producto (sector de juguetes, mordedores de bebés, sector médico) o bien, un contacto indirecto (sector envase-embalaje). Los problemas ligados a la toxicidad de los productos migrados, ha actuado como fuerza impulsora hacia el desarrollo, uso y validación de nuevos plastificantes para formulaciones industriales de PVC. La experiencia del grupo en el campo del PVC ha permitido abordar estos retos centrando su actividad en el empleo de diferentes tipos de plastificantes de menor impacto medioambiental y menor riesgo toxicológico. Así pues, destacan las actuaciones llevadas a cabo con plastificantes derivados de aceites vegetales y explorando otras alternativas a los plastificantes tradicionales como el empleo de ésteres del ácido cítrico, sebálico, succínico, etc.

**"ADITIVOS FUNCIONALES DERIVADOS DE
NANOPARTÍCULAS"**

Una de las primeras actuaciones que se llevó a cabo en el grupo, en materia de nanopartículas, se centró en el potencial de las nanoarcillas derivadas de montmorillonita modificada (OMM) como aditivo funcional en fibras de polipropileno

obtenidas mediante procesos de hilatura en fundido (“melt spinning”), en colaboración con el Instituto Tecnológico Textil (AITEX). Se trabajó en los procesos de intercalación y/o exfoliación y su efecto sobre las propiedades finales de las fibras obtenidas y los tejidos fabricados con dichas fibras.

Otras actuaciones se han centrado en la encapsulación de pigmentos y colorantes orgánicos en nanopartículas. Los colorantes orgánicos ofrecen una enorme versatilidad en cuanto a posibilidades de color; sin embargo, su naturaleza orgánica conlleva una estabilidad térmica limitada. Con la encapsulación de las moléculas de colorante en el interior de nanopartículas se pretendía mejorar su estabilidad en condiciones térmicas agresivas, incrementando el rango de aplicación de estos colorantes orgánicos.

También en la línea del empleo de nanopartículas en formulaciones de materiales poliméricos, se han desarrollado diversos trabajos en colaboración con el Instituto Tecnológico Textil (AITEX) centrados en el potencial de las nanopartículas conductoras para la mejora de las propiedades de apantallamiento electromagnético y de conductividad eléctrica. Se ha trabajado con nanotubos de carbono de pared simple (SWCNTs) y de pared múltiple (MWCNTs), nanofibras de carbono (CNFs) así como con nanopartículas de óxidos metálicos como el óxido de zinc. Estas nanopartículas se han utilizado para la fabricación de “masterbatches” o concentrados y, posteriormente, se han realizado diluciones de dichos concentrados en diversas matrices poliméricas mediante procesos de “compounding” para su posterior caracterización prestando especial atención al estudio de los procesos de percolación ligados a la conductividad eléctrica proporcionada por las nanopartículas conductoras.

Polímeros biodegradables y aditivos ecológicos.

La optimización de formulaciones de alto rendimiento medioambiental, no solo se ha centrado en el campo del PVC. En los últimos años, el grupo ha realizado importantes esfuerzos en el desarrollo de formulaciones industriales derivadas de polímeros biodegradables (más correctamente, “biocompostables” en condiciones controladas) así como el empleo de aditivos de bajo impacto ambiental y posible origen removable.

“FORMULACIONES DE POLÍMEROS BIODEGRADABLES”

Bajo este marco, se ha trabajado intensamente en formulaciones derivadas de polímeros biodegradables de distinta naturaleza:

i. Polímeros derivados de la biomasa.

En esta categoría se incluyen las investigaciones realizadas con polímeros directamente extraídos de la biomasa como los polisacáridos y su potencial en la fabricación de almidones termoplásticos (TPS), así como los trabajos realizados con estructuras de proteínas como el gluten, proteína de soja, ovoalbúmina, caseína, etc. También se incluye en esta categoría el ácido poliláctico (PLA) obtenido a partir de la fermentación de almidones y posterior polimerización del lactato obtenido.

ii. Polímeros obtenidos mediante fermentación bacteriana.

Se ha trabajado con polihidroxialcanoatos (PHAs) entre los que se incluye el polihidroxibutirato (PHB) y el polihidroxibutirato-co-hidroxivalerato (PHBV).

iii. Poliésteres de origen petroquímico biocompostables.

En esta categoría se incluyen un amplio rango de materiales poliméricos de tipo poliéster que son susceptibles de procesos de biodegradación mediante hidrólisis de los grupos éster. Concretamente se ha trabajado con poli(butilén succinato) (PBS), poli(caprolactona) (PCL), poli(butilén adipato-co-tereftalato) (PBAT), poli(butilén succinato-co-adipato) (PBSA).

Los trabajos desarrollados en el marco de esta línea se han centrado en el desarrollo de formulaciones industriales. Actualmente, a pesar de la amplia variedad de polímeros de alto rendimiento medioambiental, el ácido poliláctico (PLA) es el que está introducido a nivel comercial en mayor intensidad por un excelente equilibrio de propiedades (mecánicas, químicas, barrera), facilidad de procesado y coste. No obstante, la industria del PLA se enfrenta a un importante reto ligado a la escasa capacidad de deformación de este, que se traduce en baja tenacidad, aspecto que limita algunas aplicaciones industriales. En este sentido, numerosas investigaciones a nivel internacional se están llevando a cabo con la finalidad de reducir al máximo la fragilidad intrínseca de los polímeros de PLA.

El grupo en el que el doctorando desarrolla su actividad investigadora ha intensificado acciones para el desarrollo y aplicación de plastificantes de origen renovable derivados de aceites vegetales. En concreto, se ha trabajado con aceites vegetales epoxidados (al igual que se han empleado en las formulaciones de PVC). Sin embargo, el rendimiento de plastificación de los aceites vegetales epoxidados es limitado debido a la separación de fases. Con el objetivo de mejorar las propiedades dúctiles de los polímeros de PLA se ha trabajado con otros plastificantes derivados de aceites vegetales, concretamente en aceites vegetales maleinizados (MVO) obteniendo un rendimiento muy superior a los aceites vegetales epoxidados (EVO). En particular, se han obtenido resultados muy atractivos con aceites maleinizados comerciales como el de linaza (MLO) y otros de síntesis derivados del aceite de semilla de algodón (MCSO).

“ADITIVOS FUNCIONALES DE ORIGEN RENOVABLE”

En el marco de esta actuación se han realizado esfuerzos por incrementar el contenido renovable en las formulaciones de uso industrial de los materiales poliméricos, no solo a nivel de plastificantes, sino a nivel de otros aditivos que, aunque incorporados en cantidades bajas, pueden presentar problemas de toxicidad ligados a su migración. Así, se ha trabajado en el potencial de diversos compuestos orgánicos de origen natural y explotar sus intrínsecas propiedades antioxidantes, antibacterianas, estabilizantes, etc.

Destacan los trabajos realizados con timol y carvacrol como antioxidantes y antibacterianos, así como los resultados obtenidos con α -tocoferol (vitamina E) y ácido tánico en el campo de la estabilización frente a la oxidación con una notable mejora en la estabilidad a altas temperaturas proporcionada por la capacidad de dichos compuestos para la captación de radicales libres formados en los procesos termo-oxidativos. Junto con estas acciones, destacar los excelentes resultados de protección frente a la radiación ultravioleta proporcionados por compuestos orgánicos tipo flavonoides en la estabilización de polímeros como el poli(propileno) (PP) altamente sensible a la fotodegradación.

Materiales compuestos ecológicos.

En el marco de esta línea se contemplan dos actuaciones claramente diferenciadas. Por un lado, el desarrollo de compuestos con matrices de tipo termoplástico y por otro, compuestos con matriz termoestable.

“COMPUESTOS ECOLÓGICOS DE MATRIZ TERMOPLÁSTICA”

Esta línea de investigación inicia su actividad en torno a un trabajo desarrollado en el seno del grupo en el marco de los plastisoles vinílicos o formulaciones de poli(cloruro de vinilo) plastificado (P-PVC). En esta investigación se trabajó en el

desarrollo de materiales que imitaban la madera mediante la incorporación de cáscara de almendra de diferentes granulometrías. En esta investigación se determinó el gran potencial que tenían los materiales poliméricos como matrices para materiales compuestos con acabados similares a la madera (WPC – “wood plastic composites”), con refuerzos de tipo lignocelulósico.

A partir de estas investigaciones, el grupo empieza a hacer extensivo el empleo de residuos de tipo lignocelulósico como refuerzos o cargas funcionales en un amplio rango de matrices poliméricas y se trabaja con materias de tipo lignocelulósico de diferentes naturalezas. Así, se inicia una línea de trabajo con el empleo de refuerzos de origen natural. Bajo este marco, se trabaja con residuos industriales de cáscara de almendra, residuos de fabricación de cerveza, cáscara de avellana, residuos de café, cantueso o tomillo alicantino, cáscara de cacahuete, tegumento de cacahuete y también se desarrollan investigaciones con diversos residuos de biomasa no industrial tales como el plumero de la pampa, pinocha y piñas de pino, residuos de alga de Posidonia oceanica, etc. Junto a estas investigaciones en las que intervienen materiales lignocelulósicos, se amplía el rango de cargas/refuerzos con materiales de naturaleza inorgánica como carbonato cálcico procedente de conchas marinas o el obtenido a partir de las cáscaras de huevo. Entre las matrices poliméricas, se barre un amplio abanico que contempla polímeros derivados del petróleo como el poli(etileno) (PE), poli(propileno) (PP) y, en los últimos años, se amplía el conjunto de matrices con polímeros biodegradables como el ácido poliláctico (PLA), poli(butilén succinato) (PBS), poli(hidroxibutirato) (PHB), estructuras de proteína de gluten y soja, etc. Entre los procesos de fabricación, se trabaja en sistemas de mezclado mediante extrusión y posterior inyección. También se trabaja con el método de termocompresión o prensado en caliente. El principal reto al que se enfrentan el grupo en estas investigaciones se centra en la naturaleza tan dispar de los componentes: por un lado, un polímero altamente hidrofóbico y, por otro lado, una carga lignocelulósica altamente hidrofílica. Con ello, aparecen problemas de concentración de tensiones y efectos de refuerzo de baja intensidad. Con este objetivo se empieza a trabajar en los fenómenos de intensificación de las interacciones polímero-carga celulósica y se aborda el reto desde diferentes planteamientos.

i. Utilización de agentes compatibilizantes.

Derivados de copolímeros de poliolefinas con anhídrido maleico (PE-*g*-MA, PP-*g*-MA, SEBS-*g*-MA) o con monómeros acrílicos como el ácido acrílico (AA), metil metacrilato (MMA), etil acrilato (EA), entre otros, así como síntesis de otros de bajo impacto medioambiental.

ii. Utilización de agentes de acoplamiento.

Se ha trabajado con diversos silanos seleccionados específicamente para intensificar los fenómenos de entrecara y con tratamientos de esterificación de los compuestos lignocelulósicos con compuestos derivados de ácidos grasos como el ácido palmítico con resultados excelentes en cuanto a mejora de las propiedades globales de los compuestos. Además de los ácidos grasos, en los últimos años se ha estado trabajando con aceites vegetales o triglicéridos previamente sometidos a diversas modificaciones químicas como la acrilación, maleinización, etc. y que están siendo validadas en investigaciones actuales en el seno del grupo, a través de diversas tesis doctorales.

Además de la problemática ligada a compatibilidad de los componentes, se ha tenido que abordar un reto adicional ligado a la fragilidad intrínseca de muchos de estos polímeros debido a sus altos niveles de cristalinidad. En el caso de las formulaciones basadas en ácido poliláctico (PLA), se han realizado investigaciones con diferentes compuestos químicos que cumplan, simultáneamente, una función de compatibilización, de extensión de cadena y de plastificación para disponer de materiales de amplias posibilidades en la industria del envase y de la construcción. En relación a los polihidroxi alcanoatos, entre los que destacan los trabajos con poli(3-hidroxibutirato) (P3HB), los retos que se están abordando intentan cubrir diversos frentes. Por un lado, la temperatura de fusión del P3HB se sitúa en torno a 170 °C, muy cercana a la degradación, que comienza a los 180-190 °C dejando una ventana de procesado muy estrecha. Por otro lado, al disponer de una temperatura de transición vítrea muy baja (en torno a 0 °C), se produce un proceso de cristalización fría que conduce a un

envejecimiento físico de los materiales a temperatura ambiente, lo cual repercute en una mayor fragilidad de los materiales.

“COMPUESTOS ECOLÓGICOS DE MATRIZ TERMOESTABLE”

En el ámbito de los compuestos ecológicos con matrices termoestables, la apuesta del grupo es de gran magnitud. Actualmente la mayoría de los materiales compuestos de matriz polimérica se fabrican con matrices termoestables derivadas del petróleo (resinas epoxi-EP, poliéster insaturado-UP, fenólicas-PF, viniléster-VE, etc.) y con fibras de refuerzo que cubren diversos segmentos de mercado: fibra de carbono (CF) cuando se requieren máxima rigidez, fibras de aramida (AF) para aplicaciones que requieren resistencia a impactos y fibra de vidrio (GF) cuando se busca un buen equilibrio entre coste y prestaciones. A lo largo de los años, el grupo ha trabajado con algunos de estos sistemas convencionales, pero en los últimos años, se ha intensificado la investigación en compuestos termoestables ecológicos con diferentes planteamientos.

Se ha trabajado en el desarrollo y optimización de nuevas matrices termoestables de alto rendimiento a partir de aceites vegetales. Una de las líneas más sólidas se ha centrado en el desarrollo de formulaciones altamente eficientes derivadas de aceites vegetales epoxidados (EVOs) tales como el aceite de linaza y de soja epoxidados, ELO y ESBO respectivamente. Se han estudiado los procesos de entrecruzamiento de estos materiales con diferentes anhídridos cílicos, ácidos carboxílicos, aminas y combinaciones con el fin de incrementar el contenido renovable y garantizar niveles de curado o entrecruzamiento adecuados para la industria. En estas investigaciones también se ha trabajado con los sistemas de catálisis e iniciación con el empleo de alcoholes polihidráticos (glicerol, propanodiol, etanodiol) así como regulación de las velocidades de reacción con el empleo de aminas terciarias, fundamentalmente imidazoles. Junto a estos sistemas, se han llevado a cabo investigaciones con resinas de tipo acrílico termoestable con aceite de soja epoxidado-acrilado (AESBO) con diluyentes reactivos de tipo estireno. Además de estos triglicéridos, se ha caracterizado un amplio rango de aceites con potencial uso en la fabricación de termoestables (aceite de cáñamo, jojoba, semilla de uva, etc.).

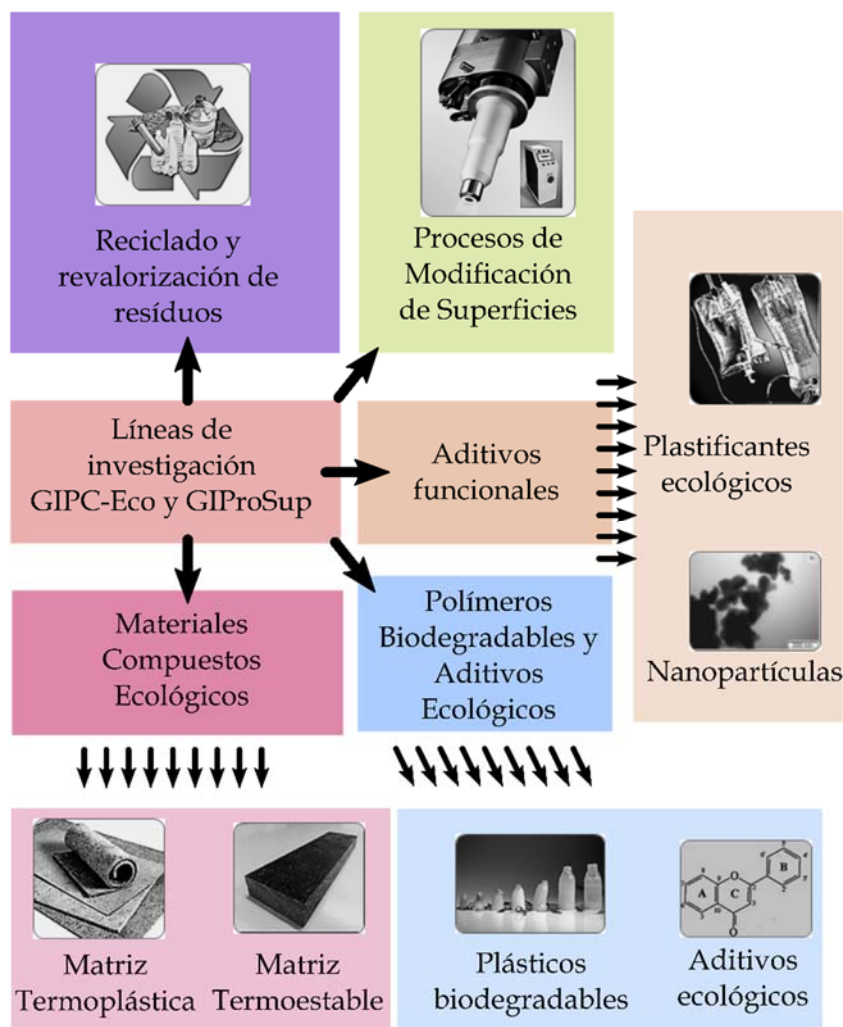


Figura II.1.1. Esquema de las líneas de investigación activas en el grupo de Investigación en Polímeros y Compuestos Ecológicos (GiP-Eco) y Grupo de Investigación en Procesos de Modificación de Superficies (GiPROSUP) en el que se ha desarrollado la presente tesis doctoral.

En cuanto a las fibras de refuerzo, además de las fibras convencionales (carbono, vidrio, basalto, aramida, fundamentalmente), el grupo ha intensificado su investigación en otras fibras para actuar como elemento de refuerzo en materiales compuestos. Estas investigaciones se han dirigido hacia el empleo de fibras naturales como lino, yute, cáñamo, ramio, bambú, entre otras y los procesos de mejora de la interacción matriz-refuerzo con sistemas de acoplamiento, agentes compatibilizantes, modificación de fibras con tecnologías de plasma, etc. Además de estas fibras naturales, se han desarrollado investigaciones con otras fibras de marcado carácter medioambiental, como

es el caso de las fibras de pizarra (SF – “slate fiber”) puesto que se obtienen a partir de los residuos de la industria de la construcción y dan solución al problema de generación de residuos en este sector. En la **Figura II.1.1** se muestra un resumen esquemático de las líneas más relevantes que se desarrollan en el grupo en el que se ha realizado la presente tesis doctoral.

En el marco de estas líneas de investigación, previamente a la realización de la tesis doctoral, el doctorando participó en el desarrollo de formulaciones de materiales compuestos ecológicos con matrices termoplásticas. Concretamente, se trabajó con matrices de biopolietileno (obtenido a partir de la caña de azúcar) y refuerzos de fibras de pizarra, procedentes de residuos de la industria de la pizarra. Estas investigaciones previas pretendían mejorar la interacción entre la matriz de poli(etileno) y las fibras de pizarra. Además de la fibra de pizarra se trabajó con fibras naturales procedentes de una planta invasora, el plumero de la pampa o Cortaderi selliana. En ambos trabajos se evaluó la influencia del contenido en fibra de refuerzo y la necesidad de empleo de agentes de acoplamiento o compatibilizantes para mejorar los fenómenos de entrecara.

Los aspectos más relevantes de esta investigación previa se plasmaron en las siguientes publicaciones, todas ellas con un marcado carácter medioambiental:

Capítulo II.2.

A. Carbonell, D. García-García, A. Jordá, M.D. Samper, R. Balart, “*Development of slate fiber reinforced high density polyethylene composites for injection molding*” Composites Part B. Engineering, (2015) **69**, 460-466.

Capítulo II.3.

A. Carbonell-Verdu, T. Boronat, E. Fages, S. Girones, E. Sanchez-Zapata, J.A. Perez-Alvarez, L. Sanchez-Nacher, D. Garcia-Sanoguera, “*Wet-laid technique with Cyperus esculentus: Development, manufacturing and characterization of a composite*” Materials & Design (2015) **86**, 887-893.

Capítulo II.4.

A. Jordá-Vilaplana, A. Carbonell-Verdu, M.D. Samper, A. Pop, D. García-Sanoguera, “*Development and characterization of a new natural fiber reinforced thermoplastic (NFRP) with Cortaderia selloana (Pampa grass) short fibers*” Composites Science and Technology (2017) **145**, 1-9.

II.2

II.2. Development of slate fiber reinforced high density polyethylene composites for injection molding.

A. Carbonell-Verdu¹, D. García-García¹, A. Jordá², M.D. Samper¹, R. Balart¹

¹ Materials Technology Institute (ITM)

Universitat Politècnica de València (UPV)

Plaza Ferrandiz y Carbonell 1, 03801, Alcoy, Alicante (Spain)

² Departamento de Ingeniería Gráfica

Universitat Politècnica de València (UPV)

Plaza Ferrandiz y Carbonell 1, 03801, Alcoy, Alicante (Spain)

"Development of slate fiber reinforced high density polyethylene composites for injection molding"

Abstract.

During the last decade the use of fiber reinforced composite materials has consolidated as an attracting alternative to traditional materials due to an excellent balance between mechanical properties and lightweight. One drawback related to the use of inorganic fibers such as those derived from siliceous materials is the relative low compatibility with conventional organic polymer matrices. Surface treatments with coupling agents and the use of copolymers allow increasing fiber-matrix interactions which has a positive effect on overall properties of composites. In this research work we report the use of slate fiber treated with different coupling agents as reinforcement for high density polyethylene from sugarcane. A silane (propyltrimethoxy silane; PTMS) and a graft copolymer (polyethylene-graft-maleic anhydride; PE-g-MA) were used to improve fiber-matrix interactions on HDPE-slate fiber. The effect of the different compatibilizing systems and slate fiber content were evaluated by scanning electron microscopy (SEM), dynamic thermo mechanical analysis (DTMA) as well as mechanical properties (tensile, flexural and impact). The results show that the use of silane coupling agents leads to higher fiber-matrix interactions which has a positive effect on overall mechanical properties. Interesting results are obtained for composites containing 30 wt.% slate fiber previously treated with propyltrimethoxy silane (PTMS) with an increase in tensile and flexural strength of about 16% and 18% respectively.

Keywords.

Fibres; mechanical properties; microstructures; injection moulding; thermoplastic resin.

II.2.1. Introduction.

In the last decade a remarkable increase in concern about the environment has been detected and different topics related to petroleum depletion, recycling, biodegradation, waste upgrading, etc. act as leading forces for the development of new and environmentally friendly materials. This situation has been particularly marked in the field of polymers and polymer-based composites which traditionally use petroleum-based polymers characterized by non-biodegradability. In the case of composite materials, research has been focused on the use of low environmental impact polymer matrices and reinforcing fibers [1-5].

Commodity plastics such as polyolefins (polyethylene, polypropylene, etc.) find attracting uses in medium to low technical applications due to excellent balance between overall properties (mechanical, thermal, chemical resistance, etc.) and easy processing by conventional techniques such as extrusion and injection molding. Nevertheless, these polymers do not reach, in general, typical properties of technical or engineering polymers. For this reason, it is quite usual to reinforce commodity plastics (and also, engineering plastics) [6] with short or long fibers such as natural (flax, sisal, coir, jute, henequen, etc.) [7-13], inorganic (glass fiber) [14-17], synthetic (aramid, polyamide, polyester, etc.) [18], carbon fiber [19], etc. in order to provide them with improved properties such as stiffness, thermal resistance, shrinkage reduction, etc. in order to offer materials in the frontier line separation between commodity and engineering/technical plastics. Although glass fiber has been the most used reinforcing fiber for thermoplastics, in the last years new inorganic fibers have invaded the composite's industry as alternatives to glass and carbon fibers for industrial, medical, electrical, etc. applications [20]. This is the case of basalt fiber obtained from widely spread basalt mineral, which offers some advantages with regard to glass fiber by considering Life Cycle Assessment (LCA) approach or nature silica [21-24]. Another recent initiative is the slate fiber (SF) obtained from slate wastes.

Slate is a widely used material for roofing; this industry is characterized by a large waste generation (one-ton end product could generate almost 30 tons of waste) thus leading to a high environmental impact. For this reason, the survival of this industry is directly linked to its capacity to upgrade wastes [25]. Some attempts have been used in

order to upgrade slate powder as filler for polymers [26] or even as a filler for thermosetting resins such as unsaturated polyesters or epoxies. Galicia is one of the largest producers of slate in Europe with about 90% production in Europe. Being aware of the high environmental impact of the generated slate wastes, important efforts focused on slate waste upgrading have been made in the last years. Mifibra is a Galician company which commercializes a novel fiber obtained from slate wastes with potential uses in composite's industry (pultruded bars and profiles, fabrics for laminates, isolation panels, twisted yarns, etc.). This contributes twice to environment: on one hand the large volume amounts of slate wastes are reduced and on the other hand, wastes represent the base material for fiber production with new and attractive industrial and technical uses.

The main aim of this work is manufacturing of new environmentally friendly thermoplastic reinforced composites by using high density polyethylene from sugarcane and slate fiber from slate wastes. Slate fibers treated with a hydrophobic silane namely, propyltrimethoxy silane (PTMS) are used in combination with and without conventional compatibilizer copolymer (polyethylene graft maleic anhydride, PE-g-MA) to evaluate the influence on overall properties for a fixed slate fiber content of 20 wt.%. In addition, the effect of the slate fiber content in the 5-30 wt.% on mechanical properties of HDPE-slate fiber composites is evaluated.

II.2.2. Experimental.

■ Materials.

Base polymer for composites was high density polyethylene (HDPE) commercial grade SHA7260 from Braskem (BRASKEM, Sao Paulo, Brasil) supplied by FKuR (FKuR Kunststoff GmbH, Willich, Germany) with a minimum biobased content of 94% (as determined by ASTM D6866). It is characterized by a melt flow index (MFI) of 20 g/10 min at 190 °C and a density of 0.955 g cm⁻³. And it is suitable for injection molding.

Slate fiber (SF) from Mifibra (MIFIBRA S.L., Ourense, España) 15 mm in length and a diameter in the 15-23 µm range was used as reinforcing fiber for HDPE-based composites. Before composite manufacturing, slate fibers were washed with distilled water and subsequently they were placed in an oven at 350 °C for 3 h to remove organic sizings. Chemical characterization of slate fiber was carried out with X-ray fluorescence spectroscopy in a sequential X-ray spectrometer PHILIPS MAGIX PRO PW2400 equipped with a rhodium tube and a beryllium window. Results of chemical composition were analyzed by using the SuperQ analytical software. **Table II.2.1** shows a summary of the chemical composition of slate fiber obtained by XRF.

Table II.2.1. Chemical composition of slate fiber obtained by X-ray fluorescence spectroscopy.

Composition	wt. (%)
SiO ₂	53.50
Fe ₂ O ₃	15.70
Al ₂ O ₃	15.11
CaO	10.05
TiO ₂	3.02
K ₂ O	2.38
MnO	0.25

A hydrophobic silane coupling agent was used to improve fiber-matrix interactions: propyl trimethoxy silane; PTMS supplied by Sigma Aldrich (Sigma Aldrich, Madrid, Spain). A typical graft copolymer polyethylene-graft-maleic anhydride; PE-*g*-MA supplied by Sigma Aldrich was also used to increase compatibility between the inorganic slate fiber and the organic HDPE matrix.

■ HDPE-SF composite manufacturing.

Four different HDPE-SF composite formulations were manufactured by varying the compatibilizing system at a constant slate content (see **Table II.2.2**).

Table II.2.2. Composition of HDPE-slate fiber composites and their code.

Code	HDPE (wt.%)	Silane type: Slate fiber content(wt.%)	PE-g-MA (wt.%)
SF	80	Untreated: 20	-
SF-MA	78	Untreated: 20	2
SF-PTMS	80	Silane treated TMPS: 20	-
SF-PTMS-MA	78	Silane treated TMPS: 20	2

Silane treatment was carried out as follows: 1 wt.% silane with respect to the slate fiber to silanize, was dissolved in a 50/50 water/methanol solution and the final solution was stirred for 10 min to ensure homogenization and hydrolysis of alkoxy groups. After this, slate fiber was immersed in this solution for 15 min and subsequently, slate fiber was removed and was washed with distilled water and dried at room temperature for 24 h.

HDPE-SF composites were manufactured with a twin screw extruder with 4 temperature stages (160 °C, 160 °C, 165 °C and 170 °C from the feeding to the dye) at a rotating speed of 40 rpm and subsequently pelletized. Standardized samples for testing were obtained with an injection molding machine Meteor 270/75 (Mateu and Solé, Barcelona, Spain) at an injection temperature of 190 °C.

Mechanical characterization of HDPE-slate fiber composites.

HDPE-SF composites were characterized by standardized mechanical tests: tensile, flexural, hardness and impact. Tensile and flexural tests were carried out at room temperature in a universal test machine Ibertest ELIB 30 (S.A.E. Ibertest, Madrid, España) following the guidelines of the ISO 527-5 and ISO 178 respectively. A 5 kN load cell was used and the crosshead speed was set to 5 mm min⁻¹. At least five samples were tested and average values of different parameters were calculated.

With regard to the impact test, a 1 J Charpy's pendulum (Metrotec S.A., San Sebastián, Spain) was used as indicated in the ISO 179:1993 standard. Five different

notched samples (“V” notch type at 45° with a notch radius of 0.25 mm) were tested and average values of absorbed energy were calculated.

Hardness characterization was obtained with a Shore D durometer 673-D (Instrumentos J. Bot S.A., Barcelona, Spain) following the ISO 868. At least five different measurements were taken and average values were calculated.

Characterization of HDPE-slate fiber fractured surfaces.

Fractured surfaces of HDPE-SF composites from impact tests were analyzed by scanning electron microscopy (SEM) with a FEI mod. Phenom (FEI Company, Eindoven, The Netherlands). All fractured samples were previously coated with a thin gold-palladium alloy with a sputter coater EMITECH model SC7620 (Quorum Technologies, East Suseex, UK).

Dynamic mechanical thermal analysis of HDPE-slate fiber composites.

Mechanical dynamical properties of HDPE-SF composites were evaluated in an oscillatory rheometer AR G2 (TA Instruments, New Castle, EEUU) equipped with a DMA accessory (torsion mode) for solid samples. Samples sizing 40x40x4 mm³ were subjected to a temperature program from -50 °C up to 100 °C at a heating rate of 2 °C min⁻¹ under controlled strain of 0.1% at a frequency of 1 Hz.

II.2.3. Results and Discussion.

■ Study of the effect of compatibilizing system.

Firstly, the effect of the compatibilizing system on overall mechanical properties of HDPE-SF composites was evaluated at a constant slate fiber content of 20 wt.%. **Table II.2.3** shows a summary of the main mechanical properties obtained in tensile and flexural tests and impact tests.

Table II.2.3. Mechanical properties of HDPE-slate fiber composites obtained by tensile, flexural and impact tests in terms of the compatibilizing system for a constant slate fiber content of 20 wt.%.

Property	HDPE	SF	SF-MA	SF-PTMS	SF-PTMS-MA
Tensile strength (MPa)	19.6	20.2	22.7	22.8	21.8
Tensile modulus (MPa)	373	1483	1253	1701	1642
Elongation at break (%)	520	18.7	11.7	12.8	13.1
Flexural strength (MPa)	23	23.2	25.4	26.7	26.3
Flexural modulus (MPa)	805	1707	2554	2622	2558
Charpy impact energy (J m ⁻²)	2.6	3.2	3.2	3.5	3.0

As expected, tensile strength values of HDPE-SF composites are higher for all composites if compared to unreinforced HDPE matrix. In addition, all tensile strength values of compatibilized HDPE-SF composites are higher than the value corresponding to uncompatibilized HDPE-SF composites. Uncompatibilized HDPE-SF composite is characterized by a tensile strength of about 20.2 MPa and this value is increased up to values of 22.8 MPa for composites containing PTMS silane treated slate fiber which represents a percentage increase of about 13% with regard to the uncompatibilized HDPE-SF composite. Silanes can be attached to hydrophilic substrates by reaction of hydrolyzed alkoxy groups with hydroxyl groups such as Si-OH (in slate and other siliceous fibers) and C-OH (in natural fibers) thus leading to tailored functionalities [27-29]. Different research works focused on basalt fiber have shown the effectiveness of a silane treatment to improve fiber-matrix interactions [30-32]. Even in the case of the compatibilizing system consisting on a combination of silane treatment with

propyletrimethoxy silane and a polyethylene-graft-maleic anhydride copolymer (PTMS-MA), the tensile strength is still higher with regard to the uncompatibilized HDPE-SF composite with values of 21.8 MPa (percentage increase of 8%). Some research works have proved the effectiveness of combination of silanes and copolymers to improve interactions between fiber and polymer matrix as in the case of polyethylene and glass fiber or nanoclays [33-35].

As it can be observed, addition of conventional compatibilizer (SF-PTMS-MA) does not lead to an increase in tensile strength but a small decrease can be detected which is accompanied by a slight increase in elongation at break. Obviously, as the elastic modulus is directly related to tensile strength and inversely related to elongation at break, the overall effect of the combination of hydrophobic silane and conventional graft compatibilizer is a slight decrease in elastic modulus.

Regarding the evolution of the tensile modulus, similar tendency can be observed. The only addition of slate fiber without any compatibilizer leads to a remarkable increase in stiffness. The initial elastic modulus of the unreinforced HDPE is close to 373 MPa and this value is increased up to values of about 1483 MPa by the only addition of 20 wt.% uncompatibilized slate fiber. One can observe that the silane treatment (alone or combined with the maleinized copolymer) promotes an increase in stiffness up to values of 1701 and 1642 MPa respectively.

With regard to flexural tests of HDPE-SF composites we observe the same behavior as previous tensile results. Composite samples with slate fiber subjected to silane (PTMS) treatment show the highest flexural strength with values of 26.7 MPa which is slightly higher to the value corresponding to composites with combined compatibilizer system (PTMS silane treatment combined with 2 wt.% polyethylene graft maleic anhydride). In the case of flexural tests, the effectiveness of the compatibilization is clearly evident as both flexural strength and modulus are higher for HDPE-slate fiber composites with different compatibilization systems compared to the uncompatibilized system. The flexural modulus is increased up to values of about 2622 MPa which represents almost 54% higher than uncompatibilized HDPE-SF composites and 325% increase with regard to the unreinforced HDPE matrix.

As expected, the addition of reinforcing fiber into HDPE matrix leads to a remarkable decrease in elongation at break as observed in **Table II.2.3**. Short fibers

randomly dispersed into the HDPE matrix provide good stiffness but they act as stress concentrators thus leading to dramatic decrease in elongation at break.

Concerning to impact energy, all HDPE-SF composites (notched samples) show higher energy absorption than the unreinforced HDPE matrix. HDPE-SF composites with slate fibers subjected to surface treatment with PTMS offer the maximum energy absorption with values of about 3.4 J m^{-2} which represents a percentage increase of 13% with regard to the untreated slate fiber and 35% with regard to unreinforced HDPE matrix.

Scanning electron microscopy can be useful to evaluate interaction phenomena among fiber-matrix. **Figure II.2.1** shows SEM images corresponding to fractured surfaces of HDPE-SF from impact tests.

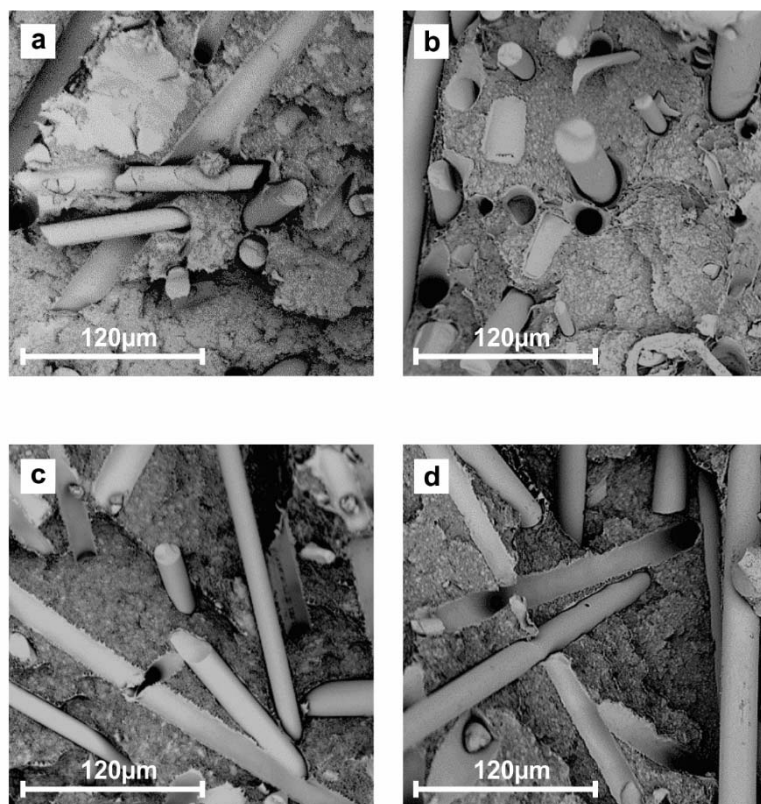


Figure II.2.1. SEM images of fractured surface (1000X) of HDPE-SF composites with different compatibilization systems: a) untreated slate fiber (SF), b) untreated slate fiber and use of 2 wt.% PE-g-MA copolymer (SF-MA), c) slate fiber subjected to silane treatment with propyltrimethoxy silane (SF-PTMS) and d) slate fiber subjected to silane treatment with propyltrimethoxy silane (SF-PTMS) in combination with 2 wt.% PE-g-MA copolymer (SF-PTMS-MA).

As we can see, HDPE-SF composites with untreated slate fiber (SF) are characterized by a very low fiber-matrix interaction as observed in **Figure II.2.1[a]**. This is evidenced by presence of gaps at fiber-matrix interface. In addition, big holes and cavities related to removed slate fiber during impact tests can be observed thus evidencing low interaction between the organic matrix and the inorganic reinforcing fiber. The absence of fiber-matrix interactions does not allow load transfer from the matrix to the fiber so that, the fiber has a stress concentration effect which is responsible for relatively poor mechanical properties. The use of different compatibilizer systems leads improved fiber-matrix interactions as it can be observed in **Figure II.2.1[b], [c] & [d]**. Presence of cavities due to removed slate fiber during fracture is less intense as compared to untreated slate fiber (SF). As a consequence, load transfer between matrix and fiber occurs in a higher extent and this is responsible for higher tensile and flexural strength values for HDPE-SF composites with different compatibilizing systems. This effect is more evident for silane-treated samples as observed in **Figure II.2.1[c] & [d]** since fewer cavities can be detected in the fractured surface. Another evidence of the better interface interaction is the amount of material (HDPE matrix) that remains adhered to the fiber after the fracture by impact; this can be seen in **Figure II.2.1[c] & [d]** in which, a small amount of polyethylene matrix can be detected along the fiber surface. HDPE-SF composites without previous silane treatment offer clean and smooth surfaces representative for low fiber-matrix interaction.

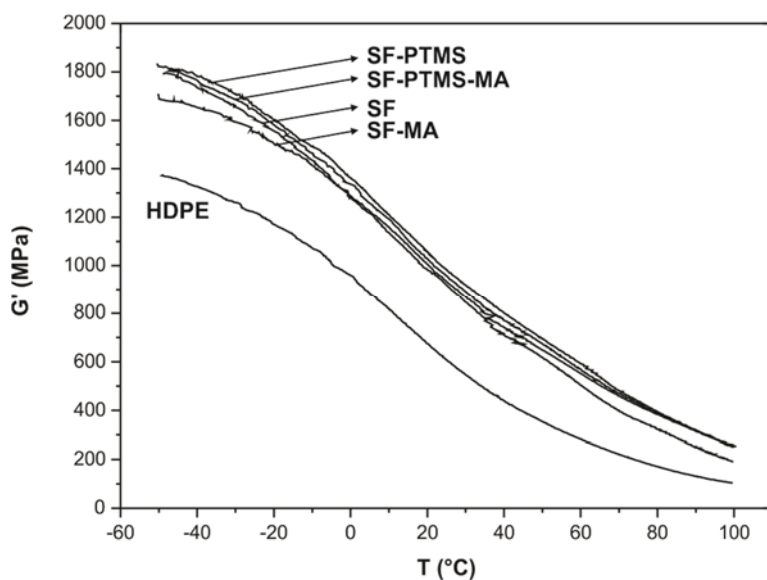


Figure II.2.2. Plot evolution of the storage modulus (G') of HDPE-SF at a fixed slate fiber content of 20 wt.% for different compatibilizing systems.

The effect of the compatibilizing system can also be observed by following the evolution of the storage modulus (G') with temperature. **Figure II.2.2** shows plots evolution of the storage modulus for unreinforced HDPE and HDPE-SF composites with different compatibilizing systems. As it can be observed the only addition of 20 wt.% slate fiber leads to a remarkable increase in G' and this phenomenon is more intense at low temperatures. In general terms we can see that silane-treated slate fiber (alone and combined with PE-*g*-MA) leads to slightly higher G' values which is in total accordance with previous tensile and flexural results. With regard to the use of PE-*g*-MA as unique compatibilizer, once again we observe slightly lower G' values (even lower than the uncompatibilized HDPE-SF composites). The highest G' values for all the temperature range are obtained for HDPE-SF composites with previous silane treatment (PTMS) for slate fibers.

Effect of slate fiber content on properties of HDPE-SF composites.

As we have clearly observed, silane-treated (propyletrimethoxy silane, PTMS) is the best compatibilizing system for the HDPE-slate fiber system. The silane treatment allows chemical anchorage of hydrophobic groups (propyl) as a consequence of the reaction between the hydrolyzed methoxy groups and hydroxyl groups in the topmost layers of the slate fibers thus leading to increase affinity with hydrophobic polyethylene chains. In general terms, propyletrimethoxy silane provides dual functionality to increase polyethylene (hydrophobic)-slate fiber (hydrophilic) interaction.

Once the optimum compatibilizing system has been selected, the influence of the slate fiber content on HDPE-slate fibers was studied by varying the slate fiber content in the 5-30 wt.% range).

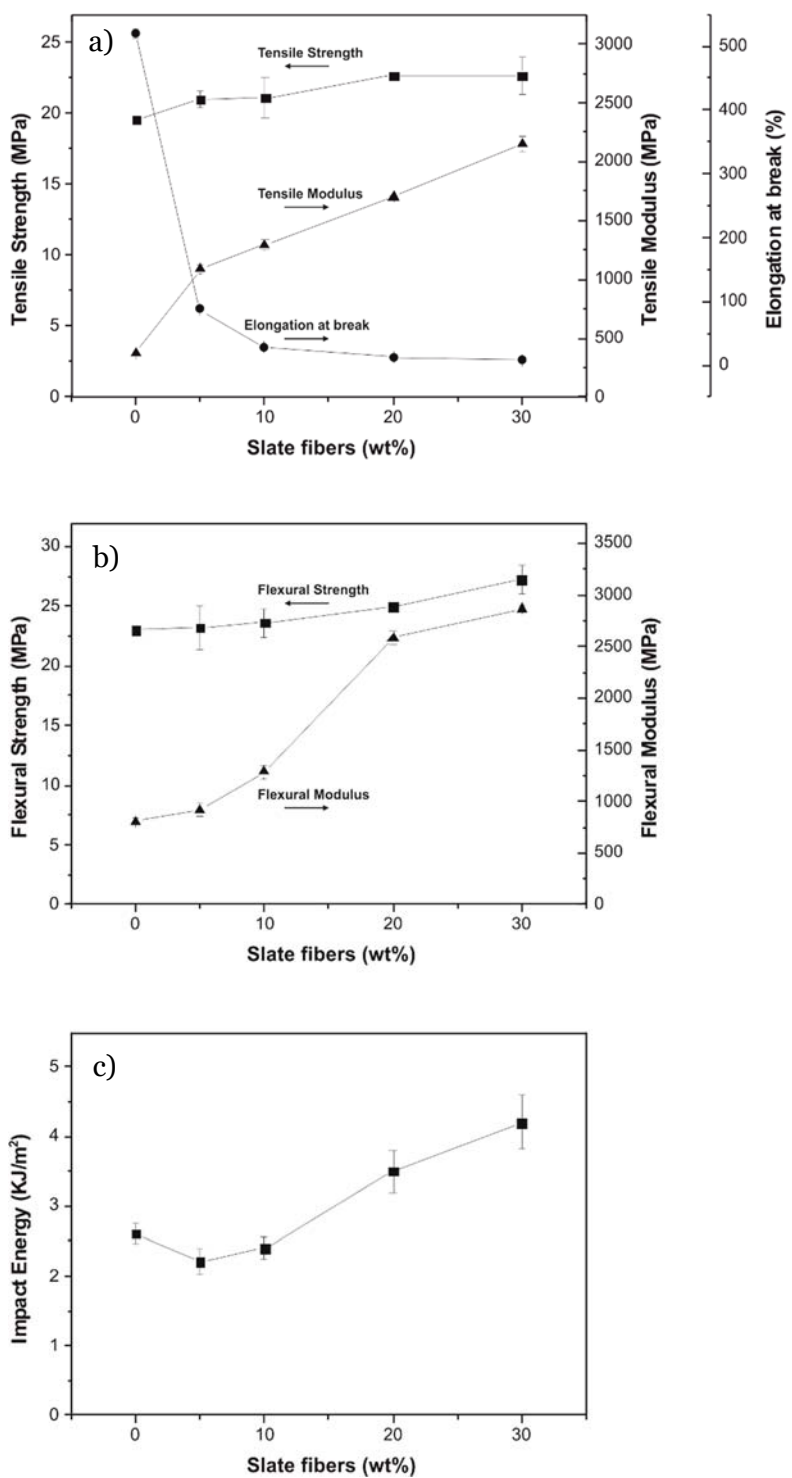


Figure II.2.3. Plot evolution of mechanical properties of HDPE-SF composites in terms of the slate fiber content (wt.%) a) tensile modulus, tensile strength and elongation at break, b) flexural modulus and flexural strength and c) Charpy's impact energy.

Figure II.2.3 shows the plot evolution of different mechanical properties of HDPE-SF composites as a function of the slate fiber content (previously treated with propyletrimethoxy silane, PTMS). With regard to mechanical resistant properties we observe an increase in strength and modulus values (for both tensile and flexural tests) as the slate fiber content increases. By considering the tensile test results, the tensile strength is increased from 19.6 MPa (unreinforced HDPE) up to values of about 22.7 MPa for HDPE-SF composites containing 30 wt.% slate fiber and this represents a percentage increase of about 16%. These values indicate the reinforcing effect of slate fiber. In addition, the addition of slate fiber leads to a remarkable increase in stiffness as detected by the increase in the elastic modulus which changes from 373 MPa (unreinforced HDPE) up to 2150 MPa for HDPE-SF (30 wt.% SF) which represents a percentage increase of almost 476%. This increase in elastic modulus is also a consequence of the decrease in elongation at break which is dramatically reduced from 520% (unreinforced HDPE) up to values of about 10-12% for composites containing 20-30 wt.% slate fiber. If we consider that the elastic modulus relates the strength and elongation in the linear region, an increase in strength and a decrease in elongation at break have a positive effect on increasing stiffness. Similar results are observed for flexural tests. The flexural strength of the unreinforced HDPE is 23 MPa and this value is increased up to values close to 30 MPa for composites containing 20-30 wt.% slate fiber. In a similar way, the flexural modulus suffers a noticeable increase of about 356%, as it changes from 805 MPa (unreinforced HDPE) up to 2864 MPa for HDPE-SF composites containing 30 wt.% slate fiber.

With regard to the ability of the material to absorb energy (impact conditions), we observe a slight decrease in the Charpy's impact energy values for low slate fiber contents in the 5-10 wt.% range. In this case, it seems that it is not possible to transfer impact load from the HDPE matrix to the fiber as slate fiber appears as short dispersed fibers in the HDPE matrix and this low content is not enough to support all the impact stress. On the other hand, composites containing 20 and 30 wt.% slate fiber show a clear increase in the absorbed energy. Charpy's impact energy reaches maximum values for HDPE-SF composites containing 30 wt.% slate fiber with values of about 4.2 kJ m^{-2} which represents a percentage increase of almost 61%.

As we have described previously, the slate fiber content has a positive effect on mechanical resistant properties such as strength, modulus, stiffness but a decrease is

detected for mechanical ductile properties such as elongation at break. **Figure II.2.4** shows different SEM images of fractured surfaces after impact tests for HDPE-SF composites with different slate fiber content. With regard to HDPE-SF composites with 5 wt.% slate fiber, we have previously observed a slight decrease in Charpy's absorbed energy and this can be explained by observing the corresponding fracture surface (**Figure II.2.4[a]**).

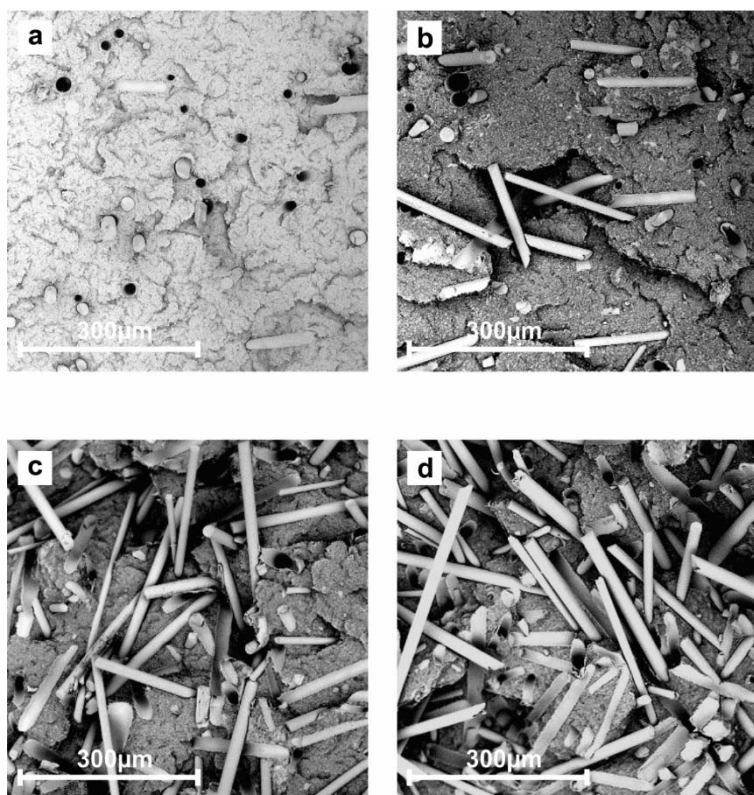


Figure II.2.4. SEM images of fractured surface from impact tests (400X) for HDPE-SF composites with different wt.% of slate fiber coupled with propyltrimethoxy silane, PTMS: a) 5 wt.%, b) 10 wt.%, c) 20 wt.% and d) 30 wt.%.

When impact occurs, the composite is subjected to high stress; then, the matrix tries to transfer load/stress to the stiffer component (slate fiber) but in this case, the slate fiber content is too low to support all the transferred loads so that, the composite breaks with relatively low energy absorption. As the slate fiber content increases, the impact strength is transferred to more slate fibers which can dissipate some additional impact energy thus leading to increased Charpy's absorbed energy values. Fractured surfaces for

HDPE-SF composites with 20-30 wt.% slate fiber (**Figure II.2.4[c] & [d]**) show clear evidence of the potential distribution of the impact stress between a high amount of short slate fibers and this has a positive effect on impact absorbed energy as described before.

The improvement on stiffness is also evident from DMA (torsion) tests as observed in **Figure II.2.5**. The addition of very low weight percentages of slate fiber does not provide reinforcing properties. It is important to take into account the relative density of both components: HDPE (0.955 g cm^{-3}) and slate fiber (2.68 g cm^{-3}); so that 5 wt.% slate fiber represents only a 1.8 v/v %. The non-reinforcing effect can be clearly observed by following the evolution of the storage modulus, G' for HDPE-SF composites containing 5 wt.% slate fiber which overlaps the unreinforced material. The reinforcing effects can be observed for slate fiber contents over 10 wt.% as G' is shifted to higher values.

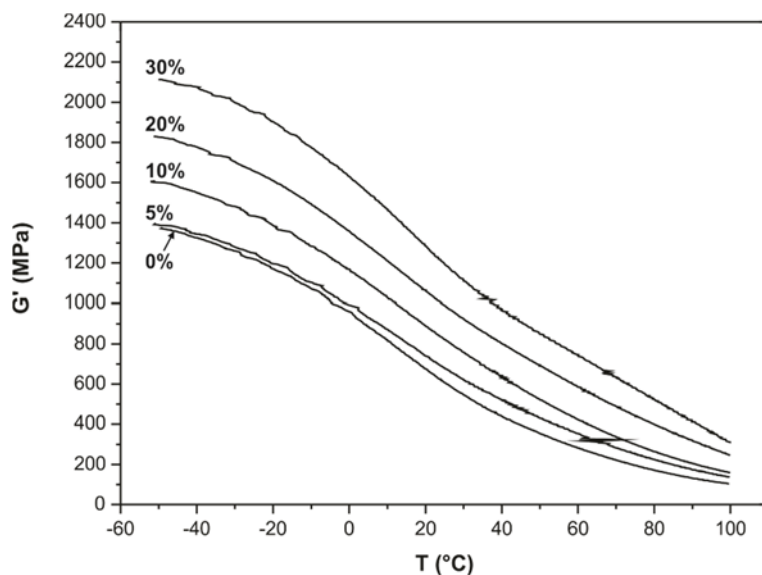


Figure II.2.5. Plot evolution of the storage modulus (G') of HDPE-SF composites containing different wt. % of slate fiber (silanized with propyltrimethoxy silane, PTMS).

II.2.4. Conclusions.

High environmentally friendly thermoplastic composites were manufactured by using high density polyethylene (HDPE) from sugarcane and new siliceous fiber namely slate fiber (SF) from slate wastes. Composites were manufactured by extrusion-compounding followed by injection molding. Different compatibilizing systems were tested in order to improve fiber-matrix interactions: silane treatment with hydrophobic propyltrimethoxy silane (PTMS) and a polyethylene graft maleic anhydride copolymer (PE-g-MA), alone and in combination. Optimum results were obtained for HDPE-SF with silane-treated (PTMS) slate fibers as described by mechanical properties and SEM analysis. On the other hand, the real reinforcing effect of slate fibers can be observed for fiber contents over 10 wt.% slate fiber as all mechanical resistant properties (strength, modulus, stiffness) are remarkably increased but, in addition, the Charpy's absorbed energy is higher than the unreinforced matrix. Due to the nature and density of the slate fiber, it is possible to add it in conventional extrusion and subsequent injection molding processes up to a total content of about 30 wt.% with attraction increase in stiffness. As a general conclusion, we report new attractive materials from technical, economical and environmental points of view which can compete with conventional glass fiber (GF) reinforced petroleum-based polyolefins such as polyethylene and polypropylene but with a marked environmental efficiency as the matrix is obtained from renewable resources and slate fiber gives a solution to an increasing problematic linked to slate wastes accumulation.

Acknowledgements.

Authors thank “Ministerio de Economía y Competitividad” ref: MAT2011-28468-Co2-o2 for financial support.

References.

- [1] G. Koronis, A. Silva, M. Fontul, "*Green composites: A review of adequate materials for automotive applications*", Composites Part B-Engineering (2013) **44**, 120-127.
- [2] M.P.M. Dicker, P.F. Duckworth, A.B. Baker, G. Francois, M.K. Hazzard, P.M. Weaver, "*Green composites: A review of material attributes and complementary applications*", Composites Part a-Applied Science and Manufacturing (2014) **56**, 280-289.
- [3] H.-J. Kwon, J. Sunthornvarabhas, J.-W. Park, J.-H. Lee, H.-J. Kim, K. Piyachomkwan, K. Sriroth, D. Cho, "*Tensile properties of kenaf fiber and corn husk flour reinforced poly(lactic acid) hybrid bio-composites: Role of aspect ratio of natural fibers*", Composites Part B-Engineering (2014) **56**, 232-237.
- [4] O. Faruk, A.K. Bledzki, H.-P. Fink, M. Sain, "*Progress report on natural fiber reinforced composites*", Macromolecular Materials and Engineering (2014) **299**, 9-26.
- [5] J. Ganster, J. Erdmann, H.-P. Fink, "*Biobased composites*", Polimery (2013) **58**, 423-434.
- [6] M.F. Arif, F. Meraghni, Y. Chemisky, N. Despringre, G. Robert, "*In situ damage mechanisms investigation of PA66/GF30 composite: Effect of relative humidity*", Composites Part B-Engineering (2014) **58**, 487-495.
- [7] C. Asasutjarit, S. Charoenvai, J. Hirunlabh, J. Khedari, "*Materials and mechanical properties of pretreated coir-based green composites*", Composites Part B-Engineering (2009) **40**, 633-637.
- [8] A. Balakrishna, D.N. Rao, A.S. Rakesh, "*Characterization and modeling of process parameters on tensile strength of short and randomly oriented Borassus Flabellifer (Asian Palmyra) fiber reinforced composite*", Composites Part B-Engineering (2013) **55**, 479-485.
- [9] P.J. Herrera-Franco, A. Valadez-Gonzalez, "*A study of the mechanical properties of short natural-fiber reinforced composites*", Composites Part B-Engineering (2005) **36**, 597-608.

- [10] H. Ku, H. Wang, N. Pattrachaiyakoop, M. Trada, "A review on the tensile properties of natural fiber reinforced polymer composites", Composites Part B-Engineering (2011) **42**, 856-873.
- [11] L. Yan, N. Chouw, K. Jayaraman, "Flax fibre and its composites - A review", Composites Part B-Engineering (2014) **56**, 296-317.
- [12] Z.L. Yan, J.C. Zhang, G. Lin, H. Zhang, Y. Ding, H. Wang, "Fabrication process optimization of hemp fibre-reinforced polypropylene composites", Journal of Reinforced Plastics and Composites (2013) **32**, 1504-1512.
- [13] R. Chianelli-Junior, J.M.L. Reis, J.L. Cardoso, P.F. Castro, "Mechanical characterization of sisal fiber-reinforced recycled HDPE composites", Materials Research-Ibero-American Journal of Materials (2013) **16**, 1393-1397.
- [14] O.F. Erkendirci, B.Z. Haque, "Quasi-static penetration resistance behavior of glass fiber reinforced thermoplastic composites", Composites Part B-Engineering (2012) **43**, 3391-3405.
- [15] J.H. Santos Almeida Junior, S.C. Amico, E.C. Botelho, F.D. Rico Amado, "Hybridization effect on the mechanical properties of curaua/glass fiber composites", Composites Part B-Engineering (2013) **55**, 492-497.
- [16] N.A. Rahman, A. Hassan, R. Yahya, R.A. Lafia-Araga, "Impact Properties of Glass-fiber/Polypropylene Composites: The Influence of Fiber Loading, Specimen Geometry and Test Temperature", Fibers and Polymers (2013) **14**, 1877-1885.
- [17] R. Huang, X. Xu, S. Lee, Y. Zhang, B.-J. Kim, Q. Wu, "High Density Polyethylene Composites Reinforced with Hybrid Inorganic Fillers: Morphology, Mechanical and Thermal Expansion Performance", Materials (2013) **6**, 4122-4138.
- [18] C. Hintze, R. Boldt, S. Wiessner, G. Heinrich, "Influence of processing on morphology in short aramid fiber reinforced elastomer compounds", Journal of Applied Polymer Science (2013) **130**, 1682-1690.

- [19] Y. Arao, S. Yumitori, H. Suzuki, T. Tanaka, K. Tanaka, T. Katayama, "Mechanical properties of injection-molded carbon fiber/polypropylene composites hybridized with nanofillers", Composites Part a-Applied Science and Manufacturing (2013) **55**, 19-26.
- [20] I. Mokhtar, M.Y. Yahya, M.R.A. Kadir, "Mechanical characterization of basalt/HDPE composite under in-vitro condition", Polymer-Plastics Technology and Engineering (2013) **52**, 1007-1015.
- [21] V. Lopresto, C. Leone, I. De Iorio, "Mechanical characterisation of basalt fibre reinforced plastic", Composites Part B-Engineering (2011) **42**, 717-723.
- [22] V. Manikandan, J.T.W. Jappes, S.M.S. Kumar, P. Amuthakkannan, "Investigation of the effect of surface modifications on the mechanical properties of basalt fibre reinforced polymer composites", Composites Part B-Engineering (2012) **43**, 812-818.
- [23] M.G. Segatelli, I.V. Pagotto Yoshida, M.d.C. Goncalves, "Natural silica fiber as reinforcing filler of nylon 6", Composites Part B-Engineering (2010) **41**, 98-105.
- [24] T. Deak, T. Czigany, M. Marsalkova, J. Militky, "Manufacturing and testing of long basalt fiber reinforced thermoplastic matrix composites", Polymer Engineering and Science (2010) **50**, 2448-2456.
- [25] G. Barluenga, F. Hernandez-Olivares, "Self-levelling cement mortar containing ground slate from quarrying waste", Construction and Building Materials (2010) **24**, 1601-1607.
- [26] G.M.X. de Carvalho, H.S. Mansur, W.L. Vasconcelos, R.L. Orefice, "Composites obtained by the combination of slate powder and polypropylene", Polimeros-Ciencia E Tecnologia (2007) **17**, 98-103.
- [27] M.A. Rodriguez, J. Rubio, F. Rubio, M.J. Liso, J.L. Oteo, "Study of the reaction of gamma-aminopropyltriethoxy silane with slate particles", Boletin De La Sociedad Espanola De Ceramica Y Vidrio (2001) **40**, 101-106.
- [28] Y. Xie, C.A.S. Hill, Z. Xiao, H. Militz, C. Mai, "Silane coupling agents used for natural fiber/polymer composites: A review", Composites Part a-Applied Science and Manufacturing (2010) **41**, 806-819.

- [29] A. El-Sabbagh, "Effect of coupling agent on natural fibre in natural fibre/polypropylene composites on mechanical and thermal behaviour", Composites Part B-Engineering (2014) **57**, 126-135.
- [30] T. Deak, T. Czigany, P. Tamas, C. Nemeth, "Enhancement of interfacial properties of basalt fiber reinforced nylon 6 matrix composites with silane coupling agents", Express Polymer Letters (2010) **4**, 590-598.
- [31] J.M. Espana, M.D. Samper, E. Fages, L. Sanchez-Nacher, R. Balart, "Investigation of the effect of different silane coupling agents on mechanical performance of basalt fiber composite laminates with biobased epoxy matrices", Polymer Composites (2013) **34**, 376-381.
- [32] R.J. Varley, W. Tian, K.H. Leong, A.Y. Leong, F. Fredo, M. Quaresimin, "The effect of surface treatments on the mechanical properties of basalt-reinforced epoxy composites", Polymer Composites (2013) **34**, 320-329.
- [33] D. Bikiaris, P. Matzinos, J. Prinos, V. Flaris, A. Larena, C. Panayiotou, "Use of silanes and copolymers as adhesion promoters glass fiber/polyethylene composites", Journal of Applied Polymer Science (2001) **80**, 2877-2888.
- [34] J. Pascual, E. Fages, O. Fenollar, D. Garcia, R. Balart, "Influence of the compatibilizer/nanoclay ratio on final properties of polypropylene matrix modified with montmorillonite-based organoclay", Polymer Bulletin (2009) **62**, 367-380.
- [35] A.L. Catto, B.V. Stefani, V.F. Ribeiro, R.M.C. Santana, "Influence of coupling agent in compatibility of post-consumer HDPE in thermoplastic composites reinforced with eucalyptus fiber", Materials Research (2014) **17**, 203-209.

II. Investigación previa.

Composites: Part B 69 (2015) 460–466



Development of slate fiber reinforced high density polyethylene composites for injection molding



A. Carbonell-Verdú^a, D. García-García^a, A. Jordá^b, M.D. Samper^a, R. Balart^{a,*}

^a Instituto de Tecnología de Materiales (ITM), Universitat Politècnica de València (UPV), Plaza Ferrandiz y Carbonell 1, 03801 Alcoy, Alicante, Spain
^b Departamento de Ingeniería Gráfica, Universitat Politècnica de València (UPV), Plaza Ferrandiz y Carbonell 1, 03801 Alcoy, Alicante, Spain

ARTICLE INFO

Article history:

Received 7 April 2014

Accepted 13 October 2014

Available online 19 October 2014

Keywords:

- A. Fibres
- B. Mechanical properties
- B. Microstructures
- E. Injection molding
- E. Thermoplastic resin

ABSTRACT

During the last decade the use of fiber reinforced composite materials has consolidated as an attracting alternative to traditional materials due to an excellent balance between mechanical properties and lightweight. One drawback related to the use of inorganic fibers such as those derived from siliceous materials is the relative low compatibility with conventional organic polymer matrices. Surface treatments with coupling agents and the use of copolymers allow increasing fiber-matrix interactions which has a positive effect on overall properties of composites. In this research work we report the use of slate fiber treated with different coupling agents as reinforcement for high density polyethylene from sugarcane. A silane (propyltrimethoxy silane; PTMS) and a graft copolymer (polyethylene-graft-maleic anhydride; PE-g-MA) were used to improve fiber-matrix interactions on HDPE-slate fiber. The effect of the different compatibilizing systems and slate fiber content were evaluated by scanning electron microscopy (SEM), dynamic thermomechanical analysis (DTMA) as well as mechanical properties (tensile, flexural and impact). The results show that the use of silane coupling agents leads to higher fiber-matrix interactions which has a positive effect on overall mechanical properties. Interesting results are obtained for composites containing 30 wt.% slate fiber previously treated with propyltrimethoxy silane (PTMS) with an increase in tensile and flexural strength of about 16% and 18% respectively.

© 2014 Elsevier Ltd. All rights reserved.

1. Introduction

In the last decade a remarkable increase in concern about the environment has been detected and different topics related to petroleum depletion, recycling, biodegradation, waste upgrading, etc. act as leading forces for the development of new and environmentally friendly materials. This situation has been particularly marked in the field of polymers and polymer-based composites which traditionally use petroleum-based polymers characterized by non-biodegradability. In the case of composite materials, research has been focused on the use of low environmental impact polymer matrices and reinforcing fibers [1–5].

Commodity plastics such as polyolefins (polyethylene, polypropylene, etc.) find attracting uses in medium to low technical applications due to excellent balance between overall properties (mechanical, thermal, chemical resistance, etc.) and easy processing by conventional techniques such as extrusion and injection molding. Nevertheless these polymers do not reach, in general,

typical properties of technical or engineering polymers. For this reason, it is quite usual to reinforce commodity plastics (and also, engineering plastics) [6] with short or long fibers such as natural (flax, sisal, coir, jute, henequen, etc.) [7–13], inorganic (glass fiber) [14–17], synthetic (aramid, polyamide, polyester, etc.) [18], carbon fiber [19], etc. in order to provide them with improved properties such as stiffness, thermal resistance, shrinkage reduction in order to offer materials in the frontier line separation between commodity and engineering/technical plastics. Although glass fiber has been the most used reinforcing fiber for thermoplastics, in the last years new inorganic fibers have invaded the composite's industry as alternatives to glass and carbon fibers for industrial, medical, electrical, etc. applications [20]. This is the case of basalt fiber obtained from widely spread basalt mineral, which offers some advantages with regard to glass fiber by considering Life Cycle Assessment (LCA) approach or nature silica [21–24]. Another recent initiative is the slate fiber (SF) obtained from slate wastes.

Slate is a widely used material for roofing; this industry is characterized by a large waste generation (one ton end product could generate almost 30 tons of waste) thus leading to a high environmental impact. For this reason the survival of this industry is directly linked to its capacity to upgrade wastes [25]. Some

* Corresponding author. Tel.: +34 96 652 84 00.

E-mail address: rbalart@mcm.upv.es (R. Balart).

II.3

II.3. Wet-laid technique with *Cyperus esculentus*: Development, manufacturing and characterization of a composite.

A. Carbonell-Verdu¹, T. Boronat¹, E. Fages², S. Girones², E. Sanchez-Zapata³, J.A. Perez-Alvarez³, L. Sanchez-Nacher¹, D. Garcia-Sanoguera¹

¹ Instituto de Tecnología de Materiales (ITM)
Universitat Politècnica de València (UPV)
Plaza Ferrandiz y Carbonell 1, 03801, Alcoy, Alicante (Spain)

² Textile Research Institute (AITEX)
Plaza Emilio Sala 1, 03801, Alcoy, Alicante (Spain)

¹ IPOA Research Group, Agrofood Technology Department
Orihuela Polytechnical High School
Miguel HErández University
Ctra. A Beniel km. 3.2, 03312 Orihuela, Alicante (Spain)

**"Wet-laid technique with *Cyperus esculentus*:
Development, manufacturing and characterization of a
composite"**

Abstract.

Biobased composite were fabricated with waste of tiger nut natural fibers, different binder fibers (Lyocell and Cotton) and thermo-bonding fibers (PLA, HDPE, PA6-CoPA). These composites were processed by wet-laid process and hot-press molding process. The obtained composites were characterized by flexural, hardness and Charpy impact tests. The internal structure of the composite was analyzed by SEM observing a significant heterogeneity. The high fiber content (80% wt) and the absence of a continuous matrix phase makes the mechanical response of the material is not high. Thermo-bonding fibers kind are more influential than the binder fibers. The best mechanical responses were obtained with additions of PLA fibers thermo-bonding fibers. Flexural modulus was maximum (865 MPa) for 80%wt tiger nut/10% wt binder fiber / 10% PLA fiber composite.

Keywords.

Polymer-matrix composites; particle-reinforcement; thermomechanical; thermal properties; tiger nut.

II.3.1. Introduction.

The depletion of oil resources and the stricter environmental regulations, are acting synergistically to boost new materials and products which are compatible with the environment and independent of fossil fuels. In the field of composite materials widely used in engineering, the increasing environmental concerns have encouraged the replacement of synthetic fibers by natural fibers. Natural fibers, as its name suggests, are extracted from natural resources, and may be from mineral, vegetable or animal source. In recent years, there has been substantial growth in the research, development and application of the so-called "biobased composites" or NFRP (Natural Fiber Reinforced Plastics). Such composites are applied in major industrial application sectors such as construction, automobile, interior design, packaging, toy, etc. These materials show interesting characteristics of sustainability, recyclability and even biodegradability.

The global consumption of natural fiber composites reached 2.1 billion in 2010, which represents an annual growth of 5% over the past 5 years. It is forecasted a 10% growing trend until 2016. It is expected to reach a 3.8 trillion dollars consumption volume of such materials in 2016. Cellulosic fibers of kenaf, hemp, flax, sisal, coir, and jute are being used successfully in NFRP. Most of these fibers are readily available, lightweight and inexpensive, and they are generated as waste from various industrial processes. The NFRP offer additional advantages such as low density, high strength/weight ratio, no brittle fracture, and good acoustic and thermal insulation properties. These characteristics make them interesting materials mainly for the construction industry and the automobile [1-5].

On the Mediterranean coast, due to the special nature of the climate, a native variety called "*Cyperus esculentus L.*" is grown. The plant requires sandy soil and a mild climate; as such, Valencia's Mediterranean climate is particularly suitable for its cultivation. This herbaceous plant produces an edible tuber known as tiger nut as shown in **Figure II.3.1[a]**. Its most appreciated use is for the development of a milk-like beverage called "Horchata". For the production of this beverage, the tuber is ground, and after its processing a wet solid waste is generated without any kind of application, as shown in **Figure II.3.1[b]**. For the producers, the residue of ground tiger nut in making horchata is a problem because it generates large volumes without any economic value.

Also, such residue is capable of rapid fermentation. This involves costs for the producer, and environmental damage. According to the data provided by the Regulatory Council 'Chufa de Valencia' (Tiger nut from Valencia) the horchata production is close to 3.3 million euros, equivalent to the generation of 4.2 tons of tiger nut waste.

The tiger nut is also cultivated in areas with temperate climates such as Brazil, Chile, and the states of Louisiana, Florida, Missouri, New Mexico in USA [6-8].



Figure II.3.1. (a) Tiger nut tuber. (b) Waste generated in the manufacture of horchata.

One way to minimize this problem, is the revaluation of this lignocellulosic waste using it as natural fillers on "biobased composites". In order to incorporate very high levels ($\geq 50\%$) of this residue in a polymer matrix it is planned the use of compression molding technique from several layers of nonwoven with high content in tiger nut.

American Standard Test Materials, ASTM, qualifies as nonwoven the textile structures obtained by bonding or cross-linking of fibers, or both at once, achieved by mechanical procedures, dissolution or combination thereof. Papers and tissues that have been obtained by weaving, knitting or felting based wool are expressly excluded. The rapid progress in technological processes for the manufacturing of nonwoven fabrics has allowed them to be incorporated into consumers daily. Such tissue is characterized by very low density, to be porous and be formed of fibers or filaments which are joined by chemical, thermal or mechanical forming network-like structures. Its production cost is low as well as being very versatile materials, easy to form, recyclable, flexible, etc. They are widely used as filters, hygiene and personal care, automotive components, elements

for thermal and acoustic insulation, etc. and every day appear new products which use this type of tissue [4, 9-14].

In this work wet-laid nonwoven processing technology has been chosen in order to obtain fabric using tiger nut waste. The traditional technique of paper processing has been applied and the tiger nut waste in an aqueous medium became a nonwoven sheet.

The Wet-Laid technology is used in order to develop nonwoven composites of all fibers which have the ability to be dispersed in fluids. The Wet-Laid technology lets to produce products with very good homogeneity, versatility in product finish and high production.

In general, the process follows next steps: Fiber dispersion in water, continuous formation of the nonwoven filtering on a mesh, consolidation and drying of the nonwoven. The dispersion of the fibers in a liquid is extremely important in the production method for the nonwoven Wet-Laid technology. Raw materials must be able to be separated homogeneously in loose fibers to form a slurry and remain evenly distributed during its transport to the formation of nonwoven. The mixture of fibers suspended in an aqueous medium is deposited on a porous conveyor belt which allows the pass of water. The conveyor belt transports the nonwoven to the next stage where the material is consolidated by a thermal process.

As a result, it is obtained a uniform sheet of nonwoven fibers that have not been damaged during processing distribution. In addition, this technology is environmentally friendly and lets to produce nonwovens with high volume of fiber and low quantity of matrix, so the final costs are also reduced because the polymeric matrices are expensive [15-20].

These nonwovens are the base of laminated composites by hot pressing of several layers. During the processing, pressure and temperature are applied and the thermo-bonding materials that were added merge in order to unite the composite. Such composites do not have a continuous matrix and are characterized by high amounts of fiber, sometimes they are greater than 90 wt% fiber, but the mechanical behavior is adequate for many technical applications that not require high resistance [1, 4, 21].

Thus, the main objective of this study is to obtain and characterize mechanically the composite material obtained by hot-press molding. The material is made of layers of

nonwoven which are rich in tiger nut waste and are obtained using a wet laid process. The influence of different binding fibers and thermo-bonding over the properties of the material will also be determined. It is intended to determine whether the biocomposite rich in tiger nut residue is suitable for application as technological material.

II.3.2. Experimental.

Materials.

The tiger nut residue from the production of horchata has been provided by the University Miguel Hernández (Elche, Spain). In order to obtain the nonwoven, it is used the wet original waste (without drying) since in the wet laid technology, in the first stage it is mixed with water. The moisture of the tiger nut waste is about 80%, so it is plasticene like. Particles of this residue have an average size of 1.5mm with polygonal shapes, as shown in **Figure II.3.2**.



Figure II.3.2. Tiger nut particles from the manufacture of "Horchata" (8X).

Cotton fibers and Lyocell fibers have been used as binding materials in order to give cohesion to the tiger nut fiber sheet, both supplied by STW Fibers (Schwarzwälder Textil-Werke GmbH, Schenkenzell, Germany). The cotton fibers are natural fibers with reference FB1 / 150 and 1.3 mm in length. Lyocell fibers are spun cellulose fibers,

reference GL1.7 / 4 and a length of 4 mm. It is advisable that the length of the fibers should not exceed 15 mm, since otherwise it is very likely that the dispersion thereof is not adequate and a nonuniform sheet will be obtained with a large number of defects.

Different materials have been used as thermo-bonding component of the composite, such as high density polyethylene (HDPE), polylactic acid fibers (PLA) and bicomponent fibers Polyamide6/Copolyamide.

HDPE has been acquired from the company STW Fibers. The sales reference is FPE 910F. The fiber length is 1.3-2 mm and 30 μm in diameter, with a melt temperature of 132 °C.

PLA fibers were supplied by the company Trevira GmbH (Germany), and its reference is 260, the fiber length is 6mm and melting temperature is 160°C.

The bicomponent fibers PA6/CoPA have been provided by the company EMS-GRILTECH GmbH (EMS-CHEMIE, Neumünster, Germany), whose sales reference is BA 140. They have a core/shell structure in which the fiber core is composed by PA6 and sheath or outer layer is formed by CoPA. The shell or sheath has a melting point of 135°C with 6 mm fiber length.

In addition, flax fiber has been used as reference material in order to compare the characteristics of the obtained composite with tiger nut fiber. STW Fibers also provides the Commercial flax fibers, reference F513, with 6 mm in length and with a diameter between 10 and 500 μm .

Processing of nonwoven sheets.

The formulations proposed for the study of the composite materials with tiger nut are shown in **Table II.3.1**. Each one of these formulations was processed by wet laid technique following the steps shown in **Figure II.3.3**, obtaining nonwoven sheets rich in natural fiber.

Table II.3.1. Materials for manufacturing of the nonwoven sheets.

sample code	natural fibers		binder		thermo-bounding			grammage g.m ⁻²
	tiger nut fiber %wt	flax fiber %wt	lyocell %wt	cotton %wt	PLA %wt	PA6/CoP A %wt	HDPE %wt	
1	80	-	10	-	10	-	-	342
2	80	-	10	-	-	10	-	307
3	80	-	10	-	-	-	10	352
4	80	-	-	10	10	-	-	295
5	80	-	-	10	-	10	-	314
6	80	-	-	10	-	-	10	-
7	-	80	10	-	10	-	-	422
8	-	80	10	-	-	10	-	428
9	-	80	10	-	-	-	10	409
10	-	80	-	10	10	-	-	348
11	-	80	-	10	-	10	-	336
12	-	80	-	10	-	-	10	360
13	40	40	10	-	10	-	-	345
14	40	40	10	-	-	10	-	395
15	40	40	10	-	-	-	10	361
16	40	40	-	10	10	-	-	336
17	40	40	-	10	-	10	-	324
18	40	40	-	10	-	-	10	-

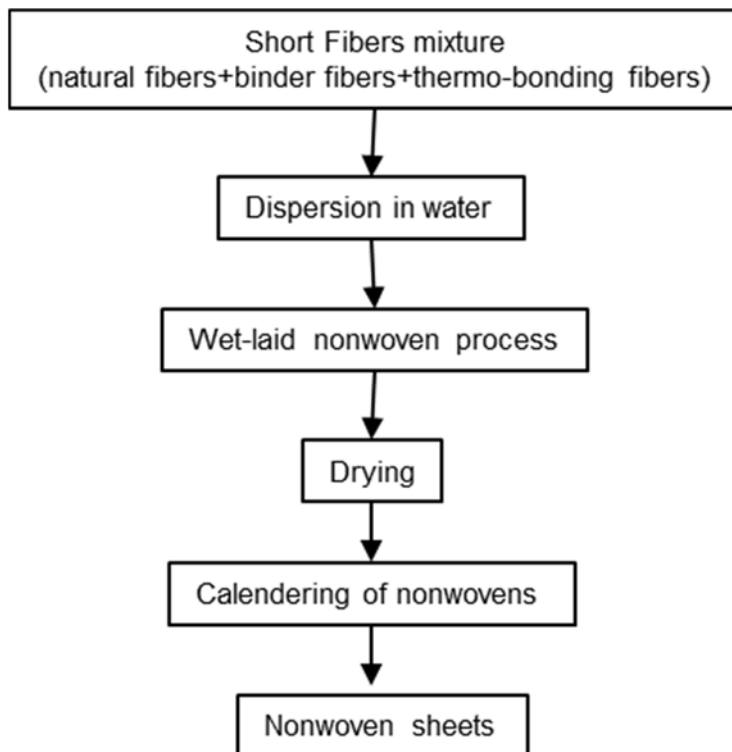


Figure II.3.3. General outline of the process of obtaining nonwovens with wet laid technology.

Each one of the fiber blends proposed in the study, with a dry weight of 800 g, is dispersed in water (1g l^{-1}) in a high shear stirrer in order to separate and uniformly disperse the fibers. The used stirrer was provided by PILL Nassvliestechnik (PILL Nassvliestechnik GmbH, Reutlingen, Germany). It has a capacity of 800 liters, and stirring was performed at 2400 rpm for 10 minutes. Once the fibers are well dispersed in the aqueous medium, the mixture was transported to the area of formation of the nonwoven using of hydraulic pumps.

The fiber/water mixture is deposited on a porous conveyor belt with a feed rate of 1 m min^{-1} which acts as a filter. The porous belt drains water and the fibers remain deposited over the belt forming the nonwoven sheet. The consolidation of the obtained sheet is done in two steps: The first one through a drying oven, and the second one passing the material between two hot rollers that apply pressure and heat to the nonwoven. The drying oven used was supplied by Tacome SA, mod. SDT-600 (Tacome SA, Valencia, Spain). In this first drying step the nonwoven is maintained at 180°C for the PLA blend, 150°C for PA6/CoPA, and the HDPE at 152°C all of them for 10 minutes long. The second process is the calendering of the nonwoven through rollers which are maintained at 200°C with a linear fixed pressure on the sheet of 0.124 MPa m . The calendering is performed in an equipment provided by Tacome SA, mod. CL-600 (Tacome SA, Valencia, Spain). After the consolidation phase, the nonwoven sheet is rolled up on a machine supplied by the same company Tacome SA mod. EN-600, as shown in **Figure II.3.4**. The average thickness of the obtained nonwoven is 1.18 mm, and the grammage for each one of the different formulations is shown in **Table II.3.1**.



Figure II.3.4. Nonwoven sheet rich in natural fiber rolled up, obtained by wet laid technology.

Manufacture of the composite materials.

Composite materials are processed by hot pressing. For the hot pressing 8 sheets sized 12.5x12.5 cm² are superimposed inside the press in order to obtain laminates with 3 mm thickness. The press is set at different temperatures depending on termoconformante used (165 °C PLA, 135 °C PA6/CoPA and 150 °C HDPE) and it is set at a constant pressure of 8T for 8 min. After that the mold is cooled for 20 min at room temperature before demolding the biocomposite. The hot molding press used was supplied by Robima SA (Valencia, Spain).

Characterization of the biocomposites.

The bending tests were performed in a universal testing machine IBERTEST ELIB 30 (SAE Ibertest, Madrid, Spain) according to the UNE EN ISO 178, applying a constant load speed of 2 mm min⁻¹ and a load cell of 5 kN. The specimens used were sized 10x80x3 mm³. Impact tests were performed using a 6J Charpy pendulum manufactured by Metrotect (Metrotect SA, San Sebastian, Spain) following the ISO 179:1993. Biocomposites hardness is determined by a durometer Shore D scale, mod. 673D (J. Bot Instruments SA, Barcelona, Spain) according to the guidelines of the UNE-EN-ISO 868.

The scanning electron microscope SEM used for the morphological characterization of the fracture of the biocomposites obtained by hot pressing, was supplied by FEI Company, model Phenom (FEI Company, Eindhoven, Netherlands). Before the morphological study, samples are coated with a layer of gold-palladium using a sputter coater Emitech mod. SC7620 (Quorum Technologies, UK).

II.3.3. Results and discussion.

■ Nonwoven morphology.

The different biocomposites proposed in this work (Table I) have been obtained in order to determine the influence of different binding and thermo-bonding fibers on the properties thereof. A first series with high content in tiger nut waste (80 wt%) has been produced which is the objective of the work. A second series is formulated with 80% wt of flax as reference material. The bio-component rich in flax lets to compare the mechanical properties and also validate if the composite of tiger nut is optimal for technological applications. The third group (40% wt tiger nut + 40 wt% flax) is used as a comparative reference of the type of natural fibers. It should be noticed that two proposed samples have not been analyzed. The sample number 6 (80% wt tiger nut/10% wt cotton/10% wt HDPE) and the sample number 18 (40% wt tiger nut+40% wt flax/10% wt cotton/10% wt HDPE) lacked consistency after the wet laid process. The sheet obtained with these compositions with cotton and HDPE did not consolidated in the drying process and it breaks down. This problem occurs when HDPE is used as thermoplastic fiber. It may be because the HDPE is in the form of very short fiber, almost powder and hinders the bonding entanglement with tiger nut particles. The other two thermomolders, PLA y PA6/CoPA, are in the form of threads and it is produced a better interaction with the different fibers.

The structure in the obtained sheets by wet laid is characterized by a very heterogeneous appearance, without continuity in matrix form. Due to the use of high contents of natural fiber/particle and low amounts of thermoplastic fiber, the nonwoven consolidation occurs mainly by mechanical entanglement of binder fibers-thermo-bonding fibers together with bonding partial melting of the thermo-bonding fibers, as shown in the examples of **Figure II.3.5**. **Figure II.3.5[a]** shows the irregular particle shape of the tiger nut residue "hooked" on the network formed by the lyocell fibers and bicomponent in a nonwoven with 80 wt% waste of tiger nut. **Figure II.3.5[b]** shows in detail the junctions between the fibers by heat fusing thereof. Comparatively, the SEM image in **Figure II.3.5[c]** of

nonwoven with 80% wt of flax fiber, presents fibers of different thicknesses irregularly distributed. **Figure II.3.5[d]** shows with higher magnification the "links" between fibers, they are caused by thermal fusion of the thermo-bonding fibers during the manufacturing of the nonwoven. From the structural point of view, there is not difference in spatial arrangements of the phases of the composite with tiger nut or with flax. They are structurally equivalent.

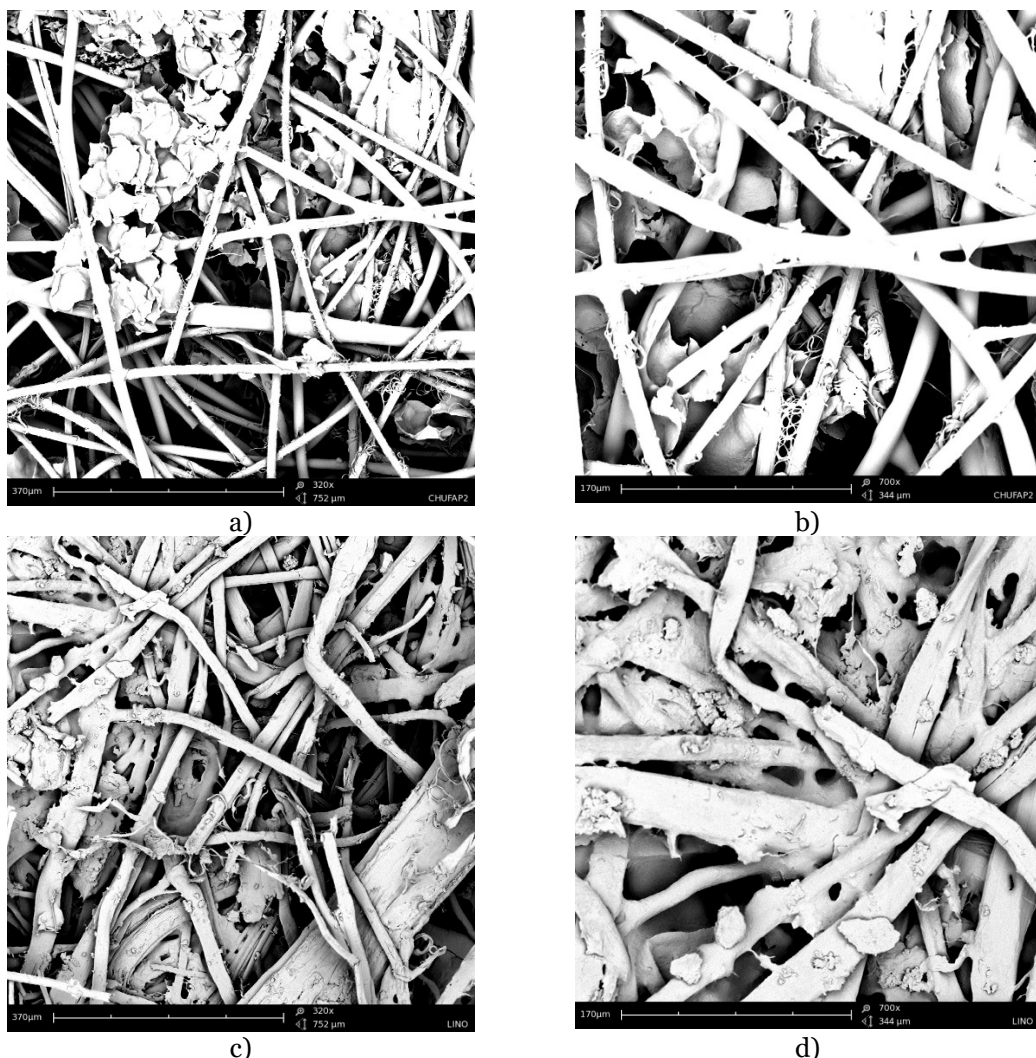


Figure II.3.5. SEM micrographs of the nonwoven surface. (a) 80%wt tiger nut + 10%wt Lyocell+10%wt PA6/CoPA, 320X. (b) 80%wt tiger nut + 10%wt Lyocell+10%wt PA6/CoPA, 700X. (c) 80%w flax fiber + 10%wt Lyocell +10%wt HDPE, 320X. (d) 80%w flax fiber + 10%wt Lyocell +10%wt HDPE, 700X

This type of irregular structures without internal continuity determine the behavior of the biocomposites obtained with these nonwovens. The few unions by thermal fusion of the thermo-bonding fibers give consistency and consolidate the nonwoven for its processing, but also influence in a poor mechanical response of the biocomposite.

■ Biocomposites flexural properties.

Figure II.3.6 depicts the flexural modulus of the bicomposites with high contents of natural fibers (80%wt tiger nut, 80%wt flax, 40%wt tiger nut+ 40%wt flax) for different binders and thermo-boundings used.

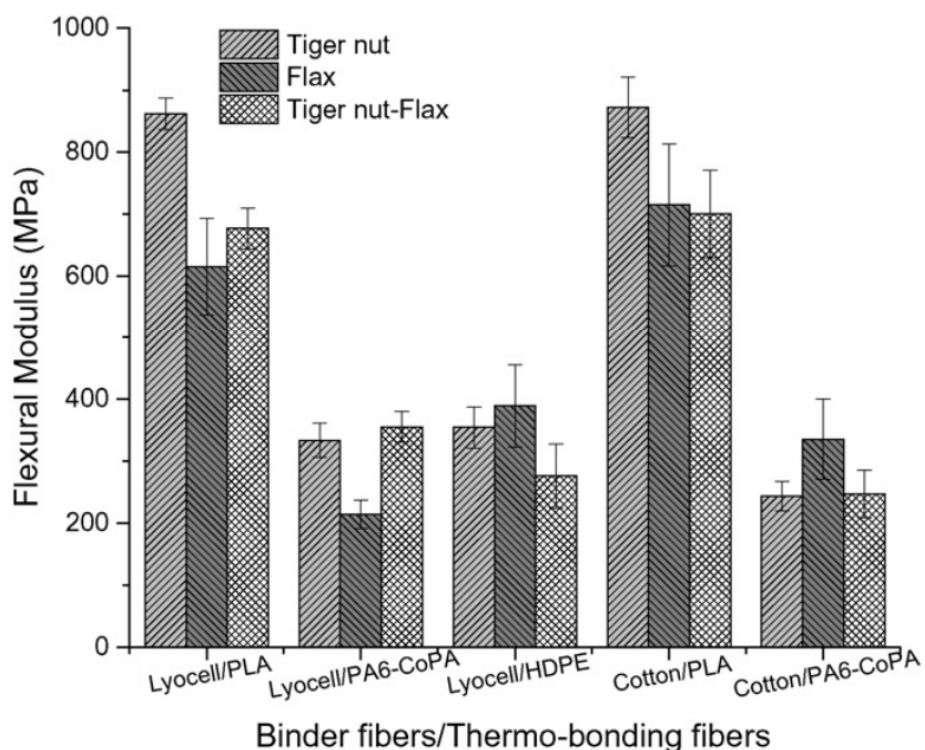


Figure II.3.6. Flexural modulus of the biocomposites with high natural fiber content (80% wt), based on different binders and thermo-bondings.

The behavior for each of the three systems is similar in each mixture binder/thermo-bonding. The higher elastic modulus is obtained using PLA as thermo-bonding, and it presents similar values regardless of the binder fiber used: cotton or Lyocell. The behavior for each one of the three systems is similar for each mixture binder/thermo-bonding. The higher elastic modulus is obtained using PLA as thermo-bounding, and their values are very similar when binder fiber varies: Lyocell or cotton. When PA6/CoPA or HDPE are used as thermo-bounding nonwoven fiber, the flexural modulus values obtained are half or even less of those for the PLA. From the viewpoint of the types of natural fibers, the tiger nut/PLA exhibit the maximum value of flexural modulus. Its flexural modulus is 28% higher for tiger nut/Lyocell/PLA than that obtained in flax/Lyocell/PLA. In the case of using cotton as a binder, this parameter is 18% higher for tiger nut too.

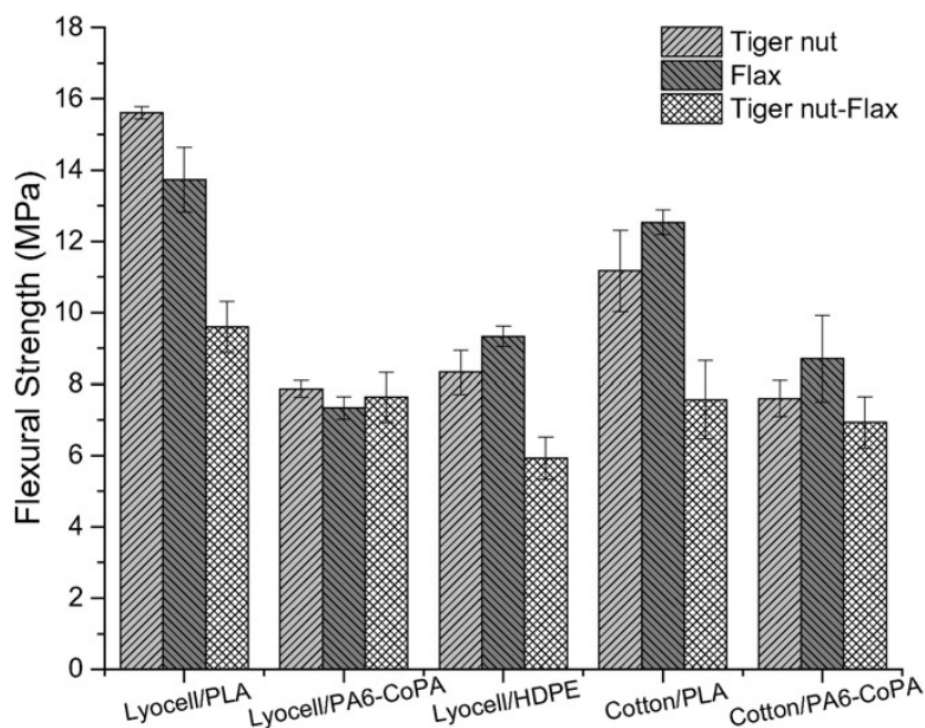


Figure II.3.7. Flexural strength of the biocomposites with high natural fiber content (80% wt), based on different binders and thermo-bondings.

Figure II.3.7 shows the flexural strength of the biocomposites with high natural fiber content in accordance with different binders and thermo-bondings

used. The behavior for each of the three systems is similar for each binder/ thermo-bounding mixture. The greatest resistance against bending are obtained using PLA fibers, and the lowest for the bicomponent fibers PA6/CoPA. The Flexural strength presents similar values to the biocomposites of tiger nut and flax. But, for laminated tiger nut+ flax the flexural strength is lower.

From the viewpoint of the types of natural fibers, the tiger nut/Lyocell/PLA reach the maximum value of flexural strength. Its flexural modulus is 12% higher than that one obtained in flax/Lyocell/PLA. When cotton is used as a binder, this parameter is 10% higher for flax/Lyocell/PLA. It can be concluded that the response to bending stresses in the biocomposites studied, the most influential component is the thermo-bonding used. The use of fibers of PLA provides maximum performance against bending.

It has to be considered that the flax fiber bicomposites are used as benchmark in this paper. Analyzing the graphs, it can be determined that laminates with high contents of tiger nut waste can perfectly replace the rich flax fiber composites since their behavior is very similar.

The hardness obtained for the three systems biocomposite tested: 80%wt Tiger nut, 80%wt Flax, 40%wt Tiger nut+40%wt Flax, is shown in **Table II.3.2**. The Shore D hardness obtained are very similar for all tested samples. Only it is observed a slight increase in hardness with the use of PLA as thermo-bonding.

Table II.3.2. Values of Shore D hardness of the biocomposites of high content of natural fiber (80% wt), based on different binders and thermo-bondings.

Binder/thermo-bonding Fibers	Tiger nut 80% wt		Flax 80% wt		Tiger nut 40% wt + Flax 40% wt	
	Shore D	SD	Shore D	SD	Shore D	SD
Lyocell/PLA	46.3	2.4	45	1.5	47.6	2.3
Lyocell/PA6-CoPA	45.0	0.5	45.3	2.0	44.0	1.7
Lyocell/HDPE	47.0	0.5	38.3	0.8	45.0	2.5
Cotton/PLA	55.3	1.1	55	2.5	45	2.1
Cotton/PA6-CoPA	47.3	1.0	39.3	1.7	37.3	0.3

■ Biocomposites impact properties.

The results obtained for the biocomposites for the Charpy impact test are shown in **Figure II.3.8**. In it is depicted the energy absorbed in the impact test, for the proposed natural fibers: T80%wt Tiger nut, 80%wt Flax, 40%wt Tiger nut+40%wt Flax, based on the various binders and thermo-bonders. Despite the fiber content are very high (80% wt), they are not embedded in a continuous matrix (Figure 9), so the the biocomposites studied absorb low impact energy. Continuous matrices absorb most of the energy before failure, partly because their possibility of deformation when forces are transmitted to the fiber.

The biggest impact energy absorption corresponds to the composites with PA6/CoPA bicomponent as thermo-bonding, they present values above twice the value presented using PLA. HDPE fiber has an intermediate impact behavior regarding the two previous ones. The most fragile composites under impact conditions are those with PLA as thermo-bounding. In such cases there is no significant difference between different natural fibers. The impact resistance is similar in bicomposites with tiger nut fiber, flax fiber or mixture of the both.

Regarding binder fiber used in the nonwoven, Lyocell and cotton, there is no clear influence regarding the impact resistance of the composite. The obtained values are very similar for the two different binders, maintaining the same thermo-bonding.

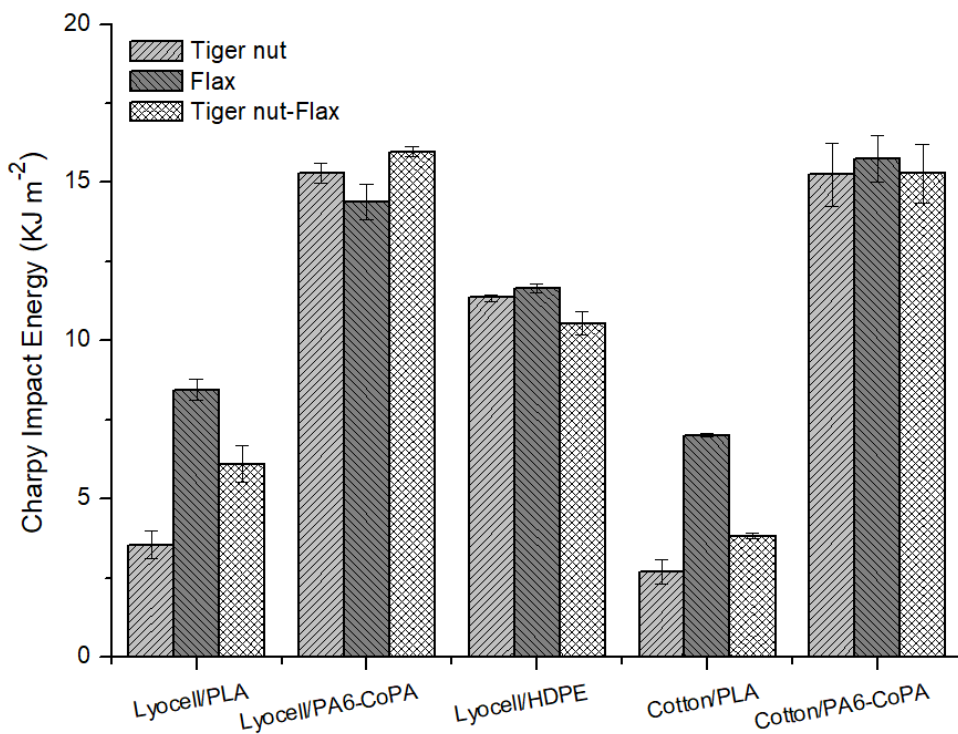


Figure II.3.8. Variation of the energy absorbed in the impact test of the biocomposites with high natural fiber content (80% wt), based on different binders and thermo-boundaries.

The morphology study of the fracture surfaces obtained after the impact test (**Figure II.3.9**) show a lack of continuity in the internal structure of the biocomposites studied.

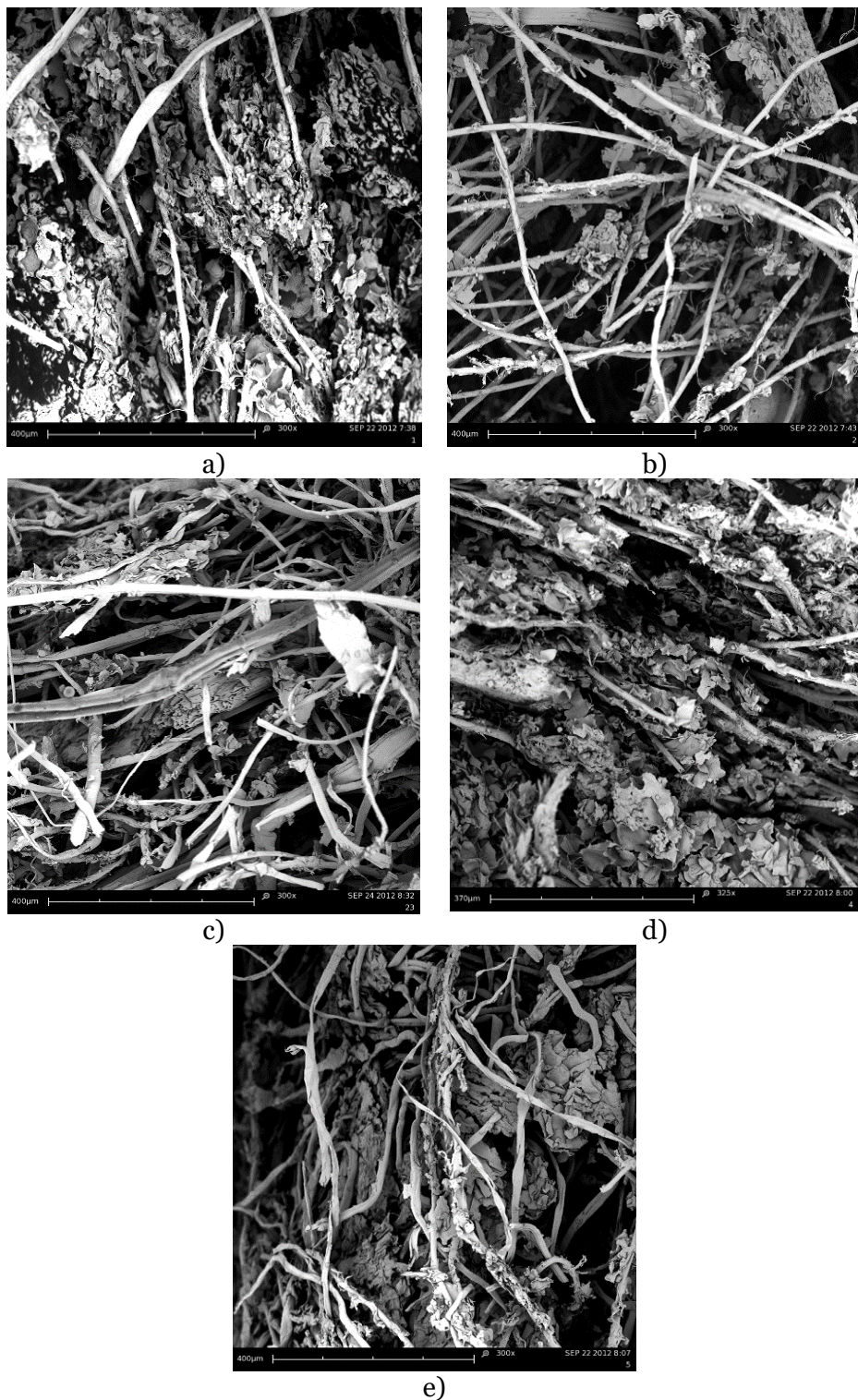


Figure II.3.9. SEM micrographs of the impact fracture surface of biocomposites with 80% wt waste tiger nut. (a) 80%wt tiger nut + 10%wt Lyocell+10%wt PLA, 300x. (b) 80%wt tiger nut + 10%wt Lyocell+10%wt PA6/CoPA, 300x. (c) 80%wt tiger nut + 10%wt Lyocell +10%wt HDPE, 300x. (d) 80%wt tiger nut + 10%wt Cotton +10%wt PLA, 300X. (e) 80%wt tiger nut + 10%wt Cotton+10%wt PA6/CoPA, 300x.

The morphologies of impact fracture surfaces of biocomposites rich in tiger nut residue, are characterized by a very irregular and heterogeneous appearance. The particles of tiger nut are embedded in the fibers used as a binder and thermo-bonding. The fibers do not have a preferred orientation, are disposed in all directions. Due to the length of fibers and its ripple, tiger nut particles remain "trapped" by the effect of entanglement of the fibers. It is not observed a uniform structure by the absence of matrix phase. This discontinuity causes the existence of many voids in the internal structure of biocomposite. Such structures are responsible for the low impact strength of the analyzed composites. This morphology is similar in all samples although the used fibers as binders and/or thermo-bonding are different.

II.3.4. Conclusions.

A nonwoven material has been obtained applying wet-laid technology with high content of tiger nut waste. This technique of obtaining nonwoven in a wet manner presents the advantage that it is possible to use waste in the form of short fibers or particles and only needs water in order to process the material, so it is an eco-efficient technology. The use of such high contents of tiger nut, 80% wt, permits the revaluation of a major industrial waste.

Obtaining wet laid sheets requires the addition of binder fibers, Lyocell and cotton, and thermo-bonding, PLA; HDPE; PA6-CoPA.

The subsequent forming of several layers of nonwoven by thermoconpresion lets to obtain biocomposites. Such composites are characterized by not filing a continuous matrix, which has negative effects on the mechanical response of the material. In the response to the bending stresses in the biocomposites studied, the most influential component is the thermo-bonding used. The use of PLA fibers provides maximum performance against bending. Tiger nut/Lyocell/PLA exhibits the maximum flexural modulus, 861.78 MPa, and 28% higher than that obtained with flax/Lyocell/PLA. In the case of using cotton as a binder, this parameter reaches a value of 872.04 MPa, 18% higher than flax/cotton/PLA.

The results obtained in this study determine that the biocomposites with high contents of tiger nut residue, are suitable materials for many technical applications that not require high strengths. Its manufacturing is optimal using the wet-laid technique and compression molding. This material comes from an agri-food waste and it is very interesting from an environmental and sustainability point of view. It would be suitable for applications such as soundproofing panels or thermal insulation for interior cladding in construction, automotive industry, furniture, etc.

References.

- [1] Q. Cheng, S. Wang, T.G. Rials, K.M. Kit, M. Hansen, "Fabrication optimization of polypropylene composites reinforced with steam-exploded wood flour by wet process", European Journal of Wood and Wood Products (2009) **67**, 449-455.
- [2] S.J. Christian, S.L. Billington, "Mechanical response of PHB- and cellulose acetate natural fiber-reinforced composites for construction applications", Composites Part B-Engineering (2011) **42**, 1920-1928.
- [3] N. El Hajj, B. Mboumba-Mamboundou, R.-M. Dheilly, Z. Aboura, M. Benzeggagh, M. Queneudec, "Development of thermal insulating and sound absorbing agro-sourced materials from auto linked flax-tows", Industrial Crops and Products (2011) **34**, 921-928.
- [4] K.-Y. Kim, S.J. Doh, J.N. Im, W.Y. Jeong, H.J. An, D.Y. Lim, "Effects of binder fibers and bonding processes on pet hollow fiber nonwovens for automotive cushion materials", Fibers and Polymers (2013) **14**, 639-646.
- [5] A.K. Mohanty, M. Misra, L.T. Drzal, "Sustainable bio-composites from renewable resources: Opportunities and challenges in the green materials world", Journal of Polymers and the Environment (2002) **10**, 19-26.
- [6] E. Sanchez-Zapata, J. Fernandez-Lopez, J. Angel Perez-Alvarez, "Tiger nut (*Cyperus esculentus*) commercialization: health aspects, composition, properties, and food applications", Comprehensive Reviews in Food Science and Food Safety (2012) **11**, 366-377.
- [7] E. Sanchez-Zapata, E. Fuentes-Zaragoza, M. Viuda-Martos, J. Fernandez-Lopez, E. Sendra, E. Sayas, J. Angel Perez-Alvarez, "Reclaim of the by-products from "horchata" elaboration process", Food and Bioprocess Technology (2012) **5**, 954-963.
- [8] E.S. Shklavtsova, S.A. Ushakova, V.N. Shikhov, O.V. Anishchenko, "Tolerance of chufa (*Cyperus esculentus* L.) plants, representing the higher plant compartment in bioregenerative life support systems, to super-optimal air temperatures", Advances in Space Research (2013) **51**, 124-132.

- [9] N. Anantharamaiah, S. Verenich, B. Pourdeyhimi, "Durable nonwoven fabrics via fracturing bicomponent islands-in-the-sea filaments", Journal of Engineered Fibers and Fabrics (2008) **3**, 1-9.
- [10] M. Dasdemir, B. Maze, N. Anantharamaiah, B. Pourdeyhimi, "Formation of novel thermoplastic composites using bicomponent nonwovens as a precursor", Journal of Materials Science (2011) **46**, 3269-3281.
- [11] N. Mao, S.J. Russell, "A framework for determining the bonding intensity in hydroentangled nonwoven fabrics", Composites Science and Technology (2006) **66**, 80-91.
- [12] D.V. Parikh, T.A. Calamari, A.P.S. Sawhney, E.J. Blanchard, F.J. Screen, J.C. Myatt, D.H. Muller, D.D. Stryjewski, "Thermoformable automotive composites containing kenaf and other cellulosic fibers", Textile Research Journal (2002) **72**, 668-672.
- [13] D.V. Parikh, Y. Chen, L. Sun, "Reducing automotive interior noise with natural fiber nonwoven floor covering systems", Textile Research Journal (2006) **76**, 813-820.
- [14] B.Y. Yeom, B. Pourdeyhimi, "Aerosol filtration properties of PA6/PE islands-in-the-sea bicomponent spunbond web fibrillated by high-pressure water jets", Journal of Materials Science (2011) **46**, 5761-5767.
- [15] S.J. Doh, J.Y. Lee, D.Y. Lim, J.N. Im, "Manufacturing and analyses of wet-laid nonwoven consisting of carboxymethyl cellulose fibers", Fibers and Polymers (2013) **14**, 2176-2184.
- [16] Y. Du, T. Wu, N. Yan, M.T. Kortschot, R. Farnood, "Fabrication and characterization of fully biodegradable natural fiber-reinforced poly(lactic acid) composites", Composites Part B-Engineering (2014) **56**, 717-723.
- [17] E. Fages, M.A. Cano, S. Girones, T. Boronat, O. Fenollar, R. Balart, "The use of wet-laid techniques to obtain flax nonwovens with different thermoplastic binding fibers for technical insulation applications", Textile Research Journal (2013) **83**, 426-437.
- [18] E. Fages, S. Girones, L. Sanchez-Nacher, D. Garcia-Sanoguera, R. Balart, "Use of wet-laid techniques to form flax-polypropylene nonwovens as base substrates for eco-friendly composites by using hot-press molding", Polymer Composites (2012) **33**, 253-261.

II. Investigación previa.

- [19] M.J. Yoon, S.J. Doh, J.N. Im, "*Preparation and characterization of carboxymethyl cellulose nonwovens by a wet-laid process*", Fibers and Polymers (2011) **12**, 247-251.
- [20] Y.N. Yoon, J.N. Im, S.J. Doh, "*Study on the effects of reaction conditions on carboxymethyl cellulose nonwoven manufactured by wet-laid process*", Fibers and Polymers (2013) **14**, 1012-1018.
- [21] H. Wang, X. Jin, N. Mao, S.J. Russell, "*Differences in the tensile properties and failure mechanism of PP/PE core/sheath bicomponent and PP spunbond fabrics in uniaxial conditions*", Textile Research Journal (2010) **80**, 1759-1767.

II. Investigación previa.



Wet-laid technique with *Cyperus esculentus*: Development, manufacturing and characterization of a new composite



A. Carbonell^a, T. Boronat^{a,*}, E. Fages^b, S. Girones^b, E. Sanchez-Zapata^c, J.A. Perez-Alvarez^c, L. Sanchez-Nacher^a, D. Garcia-Sanoguera^a

^a Instituto de Tecnología de Materiales (ITM), Universidad Politécnica de Valencia (UPV), Plaza Ferrández y Carbonell 1, 03801 Alcoy, Alicante, Spain

^b Textile Research Institute (AITEX), Plaza Emilio Sola 1, 03801 Alcoy, Alicante, Spain

^c IPOA Research Group, Agrofood Technology Department, Orihuela Polytechnical High School, Miguel Hernández University, Ctra. a Beniel Km. 3,2, 03312 Orihuela, Alicante, Spain

ARTICLE INFO

Article history:

Received 6 February 2015

Received in revised form 23 July 2015

Accepted 3 August 2015

Available online 5 August 2015

Keywords:

Polymer-matrix composites

Particle-reinforcement

Thermomechanical

Thermal properties

Tiger nut

ABSTRACT

Bio-based composites were fabricated with waste of tiger nut natural fibers, different binder fibers (lyocell and cotton) and thermo-bonding fibers (PLA, HDPE, PA6-CoPA). These composites were processed by wet-laid process and hot-press molding process. The obtained composites were characterized by flexural, hardness and Charpy impact tests.

The internal structure of the composite was analyzed by SEM observing a significant heterogeneity. The high fiber content (80 wt.%) and the lack of a continuous matrix phase cause mediocre mechanical response of the material. Thermo-bonding fibers are more influential than the binder fibers. The best mechanical responses were obtained with additions of PLA fibers and thermo-bonding fibers. Flexural modulus was maximum (865 MPa) for 80 wt.% tiger nut/10 wt.% binder fiber/10% PLA fiber composite.

© 2015 Elsevier Ltd. All rights reserved.

1. Introduction

The depletion of oil resources and the stricter environmental regulations, are acting synergistically to boost new materials and products which are compatible with the environment and are independent of fossil fuels. In the field of composite materials widely used in engineering, the increasing environmental concerns have encouraged the replacement of synthetic fibers by natural fibers. Natural fibers, as the name suggests, are extracted from natural resources, and may be from mineral, vegetable or animal source. In recent years, there has been substantial growth in the research, development and application of the so-called "biobased composites" or NFRP (Natural Fiber Reinforced Plastics). Such composites are applied in major industrial application sectors such as construction, automobile, interior design, packaging, and toy. These materials show interesting characteristics of sustainability, recyclability and even biodegradability. The NFRP offer additional advantages such as low density, high strength/weight ratio, no brittle fracture, and good acoustic and thermal insulation properties. These characteristics make them interesting materials mainly for the construction and automobile industries [1–5].

On the Mediterranean coast, due to the special nature of the climate, a native variety called "*Cyperus esculentus L.*" is grown. This herbaceous plant produces an edible tuber known as tiger nut as shown in Fig. 1(a).

Its most appreciated use is for the development of a milk-like beverage called "Horchata". For the production of this beverage, the tuber is ground, and after its processing a wet solid waste is generated without any kind of application, as shown in Fig. 1(b). For the producers, the residue of ground tiger nut in making Horchata is a problem because it generates large volumes without any economic value. Also, such residue is capable of rapid fermentation. This involves costs for the producer, and environmental damage.

The tiger nut is also cultivated in areas with temperate climates such as Brazil, Chile, and the states of Louisiana, Florida, Missouri, and New Mexico in the USA [6–8].

One way to minimize this problem, is the revaluation of this lignocellulosic waste using it as natural fillers on "biobased composites". In order to incorporate very high levels ($\geq 50\%$) of this residue in a polymer matrix the use of compression molding technique from several layers of nonwoven with high content in tiger nut is planned. Nonwoven materials are characterized by very low density, to be porous and be formed of fibers or filaments which are joined by chemical, thermal or mechanical forming network-like structures. Its production cost is low as well as being very versatile materials, easy to form, recyclable, flexible, etc. They are widely used as filters, used for hygiene and personal care, automotive components, elements for thermal and acoustic insulation, etc. and new products which use this type of tissue appear every day.

In this work, Wet-Laid nonwoven processing technology has been chosen in order to obtain fabric using tiger nut waste. The traditional

* Corresponding author.
E-mail address: tboronat@dimm.upv.es (T. Boronat).

II.4

II.4. Development and characterization of a new natural fiber reinforced thermoplastic (NFRP) with *Cortaderia selloana* (Pampa grass) short fibers.

A. Jordá-Vilaplana¹, A. Carbonell-Verdu¹, M.D. Samper¹, A. Pop², D. García-Sanoguera¹

¹ **Materials Technology Institute (ITM)**

Universitat Politècnica de València (UPV)
Plaza Ferrandiz y Carbonell 1, 03801, Alcoy, Alicante (Spain)

² **Department of Mechatronics**

University of Oradea
410087, Oradea, Romania

"Development and characterization of a new natural fiber reinforced thermoplastic (NFRP) with *Cortaderia selloana* (Pampa grass) short fibers"

Abstract.

In this work, fully bio-based thermoplastic composites are manufactured with bio-based polyethylene (from sugarcane) and short fibers coming from *Cortaderia selloana* (CS) wastes. These wastes are characterized by high cellulose content, which can provide high stiffness to the polymeric matrix. The effect of *Cortaderia selloana* short fibers on thermal properties has been evaluated by differential scanning calorimetry (DSC) and thermogravimetric analysis (TGA). The effect of the filler load on mechanical properties has also been evaluated by tensile and impact tests as well as the effects of different coupling agents. Fiber-matrix interactions have been studied by scanning electron microscopy (SEM). The addition of 15-30 wt. % *Cortaderia selloana* short fiber leads to high elastic and flexural modulus without remarkable changes in thermal degradation of the polymer composite.

Keywords.

Cortaderia selloana; natural fiber reinforced plastics (NFRP); bio-based polyethylene; mechanical properties.

II.4.1. Introduction.

In recent decades, society has raised awareness regarding the need to preserve the environment. The way of life of modern societies based on consumption is responsible for the high production of wastes from both the manufacturer and the final consumer. This generates significant environmental and pollution problems. Governments in developed countries have the need to implement laws to protect the environment against the generation of waste and allow their controlled management [1, 2]. This is the main aim in the research on biodegradable and environmentally friendly materials.

It is evident that within the industrial sector the largest volume of waste generated will correspond to polymeric materials, mainly for their wide range of applications and their short life cycle, in areas of high consumption of materials like packaging, household goods, toys, leisure, construction, automotive, medical and catering, etc. Taking into account the petrochemical origin of most polymeric materials and their non-biodegradable nature, these become an interesting material to replace. Petroleum depletion is another factor that positive influence on the interest in developing new polymeric materials from renewable sources. Currently polymeric materials from renewable sources (bio-based polymers) are marketed both thermoset and thermoplastic nature. Their properties are virtually the same as petroleum-based polymers, but derived from natural oils, sugars, proteins, starches, polysaccharides, etc. These biopolymers are perfect substitutes for traditional polymers, in any industry and application [3-6].

One of the technological applications with high demand for traditional polymers is as composites matrices. Most industrial composites are constituted by two components: the matrix and the reinforcing fiber. This structure is responsible for its virtually impossible recyclability and therefore it has become an environmental problem.

Thus, the possibility of obtaining materials that do not damage the environment promotes the use of reinforcement fibers from natural origin [7]. Several studies have analyzed the so-called “green composites” made from lignocellulosic fibers such as jute, sisal, flax, sunhemp, pineapple, flax, kenaf, wood, rice or seaweed and different polymer matrices [8-10]. In addition, optimizing the composition of these composites together with its low cost, has led to a new family of composite materials called Natural Fiber

Reinforced Plastics (NFRP) and Wood Plastic Composites (WPC, being wood and wood wastes the lignocellulosic component of the composite) with highest growth in the plastics industry in recent years [11, 12].

Just in the USA, WPC have generated 5.3 billion dollars in revenue and more than 1 billion tons of production. The largest consumer of WPC is USA with 73% of the total, followed by China with 15%. The main applications are in the building industry, which represents almost 70% of total consumption on items such as handrails, railings, deckings, outdoor benches, fences, wall coverings or window frames [12-14]. The European Union has a demand on WPC of about 5% of the global production, mainly for applications in the automotive sector such as side interior panels, dashes, roofs, seats, acoustic panels or glove boxes [15-18].

The most widely used polymer matrix in these commercial WPC is polyethylene (PE), both low density (LDPE) and high density (HDPE), followed by the PP and PVC. In USA the PE use represents 83% of the total, while the PP and PVC represents 9% and 7% respectively.

These thermoplastic matrices give the composite versatility and easy processing. Furthermore, compared with natural wood, WPC have greater dimensional stability and longer service life without maintenance [16, 19].

The main drawback of WPC is the lack of interaction between the lignocellulosic fiber and the polymer matrix. Due to the different hydrophilic behavior of the fiber and the polymer matrix, there is not a good adhesion/interaction between them. The mechanical behavior of the composites depends directly on the matrix-fiber interface [20, 21]. A solution to this problem is the surface pretreatment of the fibers to improve adhesion to the matrix through the use of so-called coupling agents. Recent studies demonstrate the effectiveness of alkaline treatments coupled with isocyanates, acrylates, silanes and peroxides, which enhance matrix-fiber interaction [17, 19, 22, 23].

In the present study, we used natural fiber from the plant *Cortaderia selloana* usually called Pampa Grass. Pampas grass is a hemicryptophyte that develops in clumps up to 3 meters high. It presents inflorescence in white-gray panicles of 60x15 cm high. This kind of natural fiber has been selected to manufacture the composite because it allows revalue the large volume of waste generated by pruning this plant. In addition,

Pampa grass is an allochtoon gramineae, which is considered "invasive species" with strong dominance that can become invasive on important native ecosystems. In addition, it drastically reduces biodiversity, changes the landscape and competes with native species. The most effective method for control is cutting or pruning, which generates large amounts of waste, with no use or value.

This work aims to characterize a new NFRP for uses in the WPC industry based on the use of *Cortaderia selloana* as reinforcing lignocellulosic material into a bio-based high-density polyethylene (HDPE) thermoplastic matrix. The first objective is to analyze the effects of compatibilizers to improve fiber-matrix interface adhesion. Secondly, the influence of the relative amounts of fiber added to the polymeric matrix has been studied.

II.4.2. Experimental.

■ Materials.

The HDPE used in this work as composite matrix was bioPE SHA7260 supplied by Braskem (Braskem Ideasa, Sao Pablo, Brasil). This HDPE is characterized by a minimum of 94 wt% bio-based content measured following the ASTM D6866 standard as indicated by the manufacturer. The melt flow index is the 20 g/10 min at 190 °C and the density is 0.955 g cm⁻³, making it a suitable polymer for injection molding.

The lignocellulosic reinforcing component was *Cortaderia selloana* collected from locally pruning and harvesting on Valencia, Spain. Different coupling systems were used to evaluate their influence on fiber-matrix interactions: a maleated polyethylene copolymer, polyethylene-graft-maleic anhydride (PE-g-MA) CAS 9006-26-2, and previous silanization with a hydrophobic silane, trimethoxy-propyl silane CAS 1067-25-0. Both coupling agents were supplied by Sigma-Aldrich (SIGMA-ALDRICH Chemie GmbH, Steinheim, Germany). Sodium hydroxide, 99% purity, was provided by Scharlab (Shacharlab, SL, Barcelona, Spain) and was used for alkali treatment.

Composite processing.

Firstly, *Cortaderia selloana* fibers were cut in an industrial mill to obtain short fibers. The final length of the fibers was in the 1-4 mm range. After this, they were washed with distilled water and then dried in oven at 60 °C for 24 hours. Different formulations were prepared for manufacturing as described below in **Table II.4.1** together with the corresponding designations.

Table II.4.1. Composition and designation of the four different formulations of Bio-PE/*Cortaderia selloana* composites.

Designation	Bio-PE (wt. %)	<i>Cortaderia selloana</i> fiber		PE-g-MA compatibilizer (wt. %)
		Previous treatment	(wt. %)	
Bio-HDPE/CS-UT	85	Untreated	15	-
Bio-HDPE/CS-NaOH	85	NaOH ^(*)	15	-
Bio-HDPE/CS-MA	82	NaOH	15	3
Bio-HDPE/CS-Silane	85	NaOH+silane ^(**)	15	-

(*) **NaOH treatment.** Treatment of *Cortaderia selloana* fibers in a 5 wt. % NaOH solution with distilled water, for 24 hours with stirring followed by washing with distilled water and subsequent drying in oven at 60 °C for 24 hours.

(**) **NaOH+silane treatment.** Same as NaOH treatment followed by hydrophobic silanization process in a bath containing 3 wt. % trimethoxy-propyl silane in aqueous-alcohol solution (50 wt. % distilled water - 50 wt. % methanol) for 15 minutes with vigorous stirring. Finally, the silanized fiber was washed with distilled water and dried in oven at 60 °C for 24 hours.

The four different formulations were extruded in a twin-screw extruder with the temperature in each of the four heating zones of 155, 160, 165 and 170 °C (from hopper to die) respectively and a screw speed of 30 rpm; finally the extruded material was pelletized. Rectangular samples (80x10x4 mm³) and standard tensile test samples were obtained by injection molding using an injection machine Meteor (Meteor 270/75, Mateu and Sole, Barcelona, Spain) at an injection temperature of 190 °C.

Thermal characterization.

Thermal transitions were studied by differential scanning calorimetry (DSC) using a Mettler-Toledo 821 (Mettler-Toledo Inc., Schwerzenbach, Switzerland). Samples ranging 5-10 mg in weight were used. A heating program from 30 to 300 °C at a heating rate of 10 °C min⁻¹ in an air atmosphere was used for all composites. Thermogravimetric analysis (TGA) was carried out in a TGA/SDTA 851 (Mettler-Toledo Inc., Schwerzenbach, Switzerland) and the temperature ranged from 30 °C to 900 °C with a heating rate of 20 °C min⁻¹. TGA tests were performed in nitrogen environment at a flow rate 60 mL min⁻¹.

Mechanical characterization.

Tensile and flexural properties of the different samples of bio-HDPE/CS were measured with a universal test machine Ibertest Elib 30 (Ibertest S.A.E., Madrid, Spain) with a load cell of 5 kN and crosshead speed of 10 mm min⁻¹ (ISO 527) for tensile test, and 5 mm min⁻¹ crosshead speed for flexural test (ISO 178). Hardness of bio-HDPE/CS composites was measured with a Shore D hardness durometer model 676-D (J. Bot Instruments, Barcelona, Spain) according to the impact energy of notched samples was determined using a 1 J Charpy pendulum following the guidelines of the ISO 179 standard.

Fractography by Scanning Electron Microscopy (SEM).

Fractured surfaces from impact tests of bio-HDPE/CS composites were observed with a scanning electron microscope (SEM) model Phenom (FEI Company, Eindhoven, Netherlands). Before observation, samples, mounted on a conductive adhesive tape, were covered with a thin gold-palladium layer. The coating process lasted 120 seconds using a sputter-coater Emitech mod. SC 7620 (Quorum Technologies Ltd, East Sussex, UK).

Water uptake characterization of bio-HDPE/CS composites.

Water uptake of bio-HDPE/CS composites was determined with samples sizing 80 x 10 x 4 mm³. Three different samples were tested to obtain average values. Prior to the water uptake test, HDPE/CS composite samples were dried at 80 °C for 4 h. After this, samples were immersed in distilled water at room temperature for a period of 60 days. The percentage water uptake was calculated by using the following expression:

$$\text{Water Uptake (\%)} = \frac{(M_f - M_i)}{M_i} \times 100 \quad \text{Equation II.4.1}$$

Where M_f is the final weight after a certain immersion period and M_i is the initial weight of the sample before immersion.

II.4.3. Results and discussion.

Effect of compatibilizing system on the bio-HDPE/CS composite properties.

Figure II.4.1 shows the DSC calorimetric curves of the bio-HDPE/CS composites using different compatibilizing system.

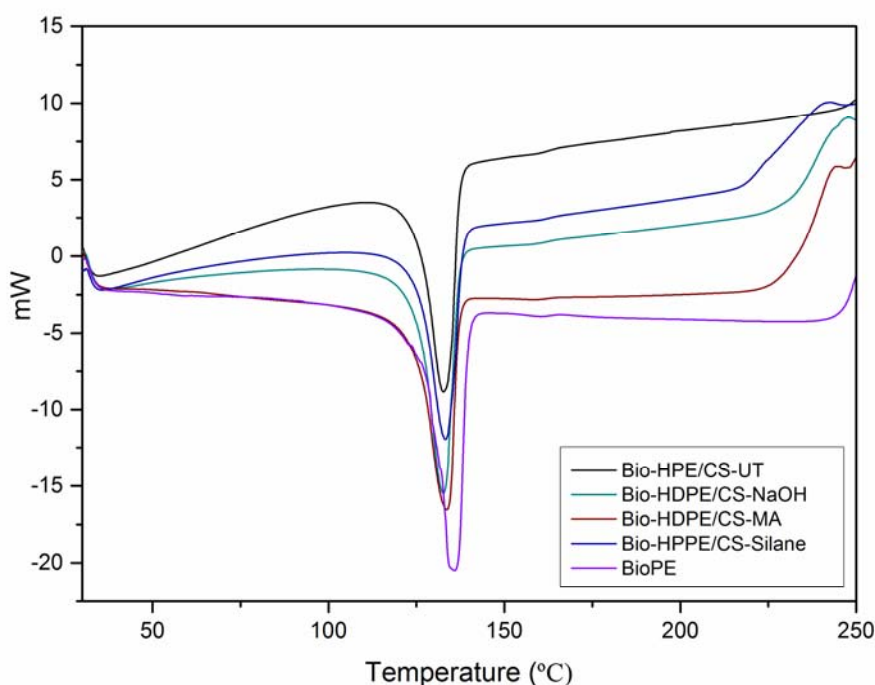


Figure II.4.1. Comparative plot of the differential scanning calorimetry thermograms (DSC) of unfilled bio-HDPE and bio-HDPE/CS composites with different compatibilizing system.

As it can be observed, the compatibilizing system does not significantly modify the melting temperature (T_m) and the degradation onset. Bio-HDPE from natural resources shows a melt peak at 135 °C, and this is decreased to 132.8 °C with the addition of 15 wt% of CS fiber without treatment, probably due to the nucleating effect of the filler. Compatibilizing system maintain the melt peak between 132 °C and 133 °C, so that they

have no effect on T_m . The same applies to the degradation temperature, as no significant changes are observed. Furthermore, the addition of CS fiber without treatment and with PE-g-MA, has no influence on the thermal behavior of bio-HDPE/CS composite [24].

Regarding to results obtained by thermogravimetric analysis of bio-HDPE/CS composites, **Figure II.4.2** shows similar behavior for the different compatibilizing system used. Degradation of unfilled bio-HDPE occurs in the 350-520 °C range and above 520 °C the amount of residual char is very small, since the degradation of polyethylene generates large amount of gaseous products by its organic nature. With regard to *Cortaderia selloana*, thermogravimetric curve is the typical of a lignocellulosic material: at a relative low temperatures (50-150 °C), residual moisture evaporation takes place. At intermediate temperatures ranging from 220 °C to 350 °C decomposition of low molecular weight species (hemicelluloses, glycosidic bonds typical of cellulose and other volatile compounds) are removed and a remarkable weight loss takes place (about 40-50 wt.%). Finally, thermal degradation of cellulose occurs and lignin degradation proceeds slowly with final residual char of about 20 wt.%.

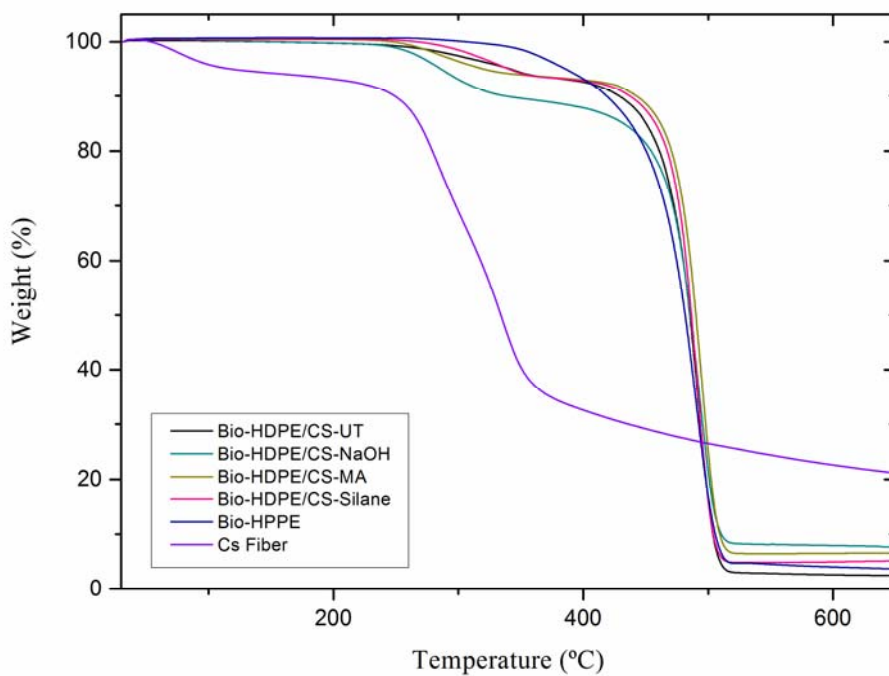


Figure II.4.2. Comparative plot of the thermogravimetric curves (TGA) of *Cortaderia selloana* (CS) fiber, unfilled bio-HDPE and bio-HDPE/CS composites with different compatibilizing system.

Bio-HDPE/CS composites show the typical degradation steps of both components, but in the thermograms, we can observe two main different steps: the first one corresponds to a temperature range 250-350 °C and it is attributable to degradation of the reinforcement fiber. The second main step is located in the 350-500 °C temperature range, which corresponds to the degradation of polyethylene. In general terms, the compatibilizing system does not affect the thermal stability at high temperatures although some delay is achieved by silane and PE-g-MA compatibilizing system. As expected, the residual char in bio-HDPE/CS composites increases from 2.05 wt.% (raw unfilled bio-HDPE) up to values in the 5-6 wt.% range due to char formation from lignocellulosic component [19, 25].

Figure II.4.3 and **Figure II.4.4** show the effect of the treatment on tensile and flexural properties respectively. In general terms, very small differences are detected. With regard to tensile modulus, the maximum values are reached for untreated bio-HDPE/CS (559 MPa). This value is higher to unfilled bio-HDPE with typical values of 373 MPa. It is important to remark that all composites (with same *Cortaderia selloana* content and different compatibilizing system) are stiffer than unfilled bio-HDPE. By analyzing tensile strength results, we observe similar values in the 17.4 – 20.1 MPa for untreated fiber (bio-HDPE/CS-UT) and fiber subjected to NaOH treatment followed by silanization respectively (bio-HDPE/CS-Silane).

Unfilled polyethylene shows a tensile strength of about 19.6 MPa and, as we can see, composites show similar tensile strength values independently of the compatibilizing system. Nevertheless, elongation at break is highly affected by presence of the reinforcing filler. Unfilled bio-HDPE is characterized by high plastic deformation with elongation at break values of about 520%. Nevertheless, all composites are characterized by a high embrittlement process with very low elongation at break values, even with different compatibilizing system, with values around 1.5%. This is due to the high stiffness of the lignocellulosic particles if compared to polyethylene and, mainly, due to lack of interactions between the particles and surrounding polymer matrix.

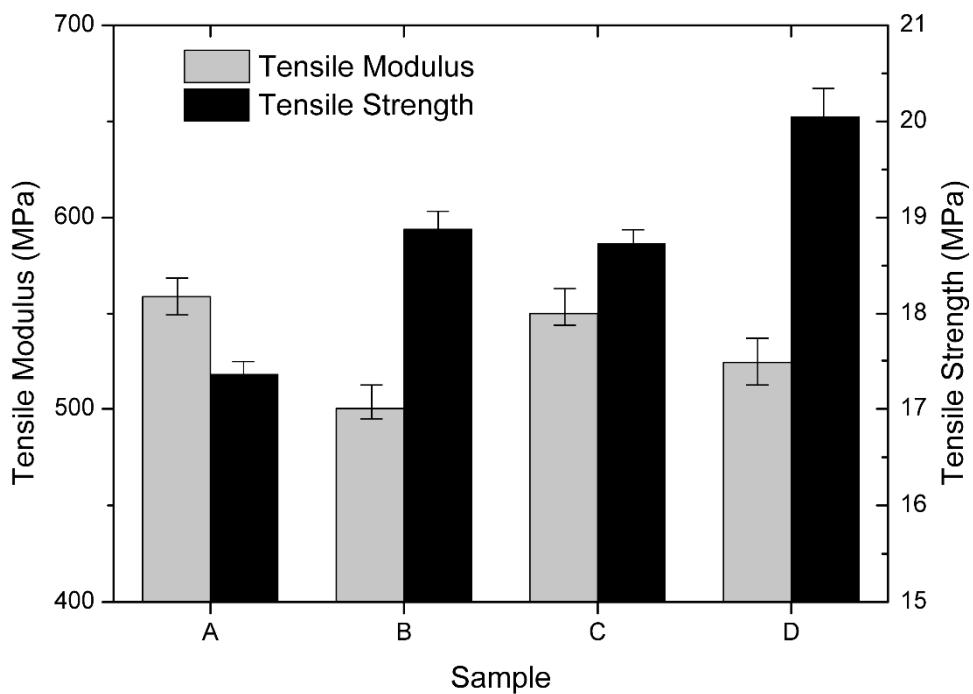


Figure II.4.3. Tensile properties of bio-HDPE/CS with different compatibilizing system: a) Bio-HDPE/CS-UT; b) Bio-HDPE/CS-NaOH; c) Bio-HDPE/CS-MA; d) Bio-HDPE/CS-Silane.

This fact can be easily observed in **Figure II.4.4**, which shows detailed images corresponding to fractured surfaces. We can clearly observe absence of matrix-filler continuity even with the use of compatibilizing system. We observe typical gaps around the particle perimeter. These gaps are representative for low particle-matrix interactions. Lead to stress concentration phenomena thus leading to microcracks formation and subsequent crack growth, and promote early fracture of the composite. All composites break in a typical fragile way, almost without plastic deformation. The use of the different compatibilizing system does not show remarkable differences if compared to composite with untreated fibers [9, 18, 26].

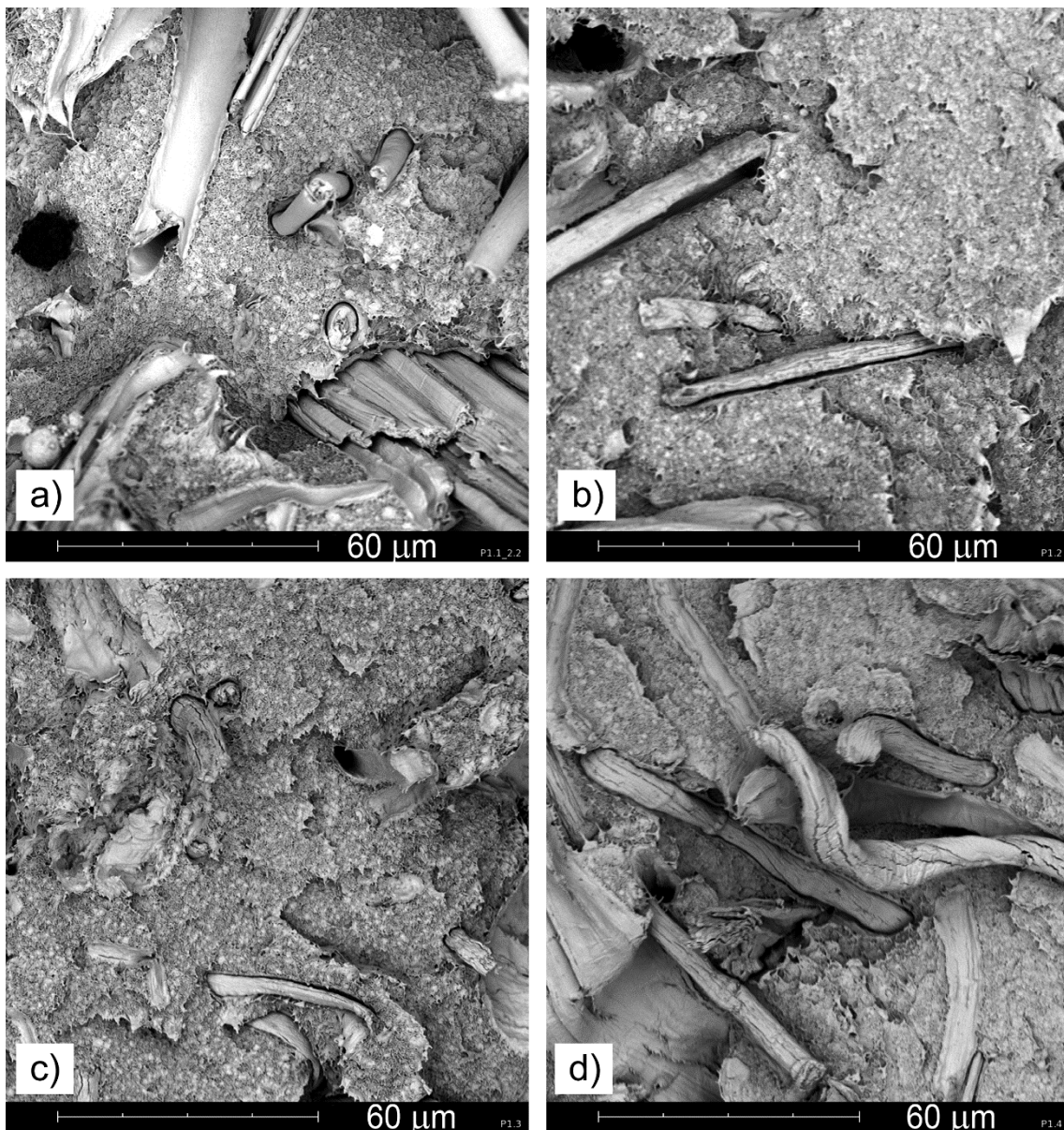


Figure II.4.4. SEM images (2000x) of fractured surfaces from tensile tests of bio-HDPE/CS composites with different compatibilizing system: a) Bio-HDPE/CS-UT untreated fiber, b) Bio-HDPE/CS-NaOH; c) Bio-HDPE/CS-MA; d) Bio-HDPE/CS-Silane.

With regard to flexural properties, similar behavior to tensile properties can be observed. The flexural modulus of unfilled bio-HDPE is increased by 60% up to values of 1290 MPa for bio-HDPE/CS-UT composite without previous treatment. With respect to flexural strength, an average percentage increase of 13% is detected for all composites

with values in the 46-47 MPa range. Once again, in the case of *Cortaderia selloana* fibers, the compatibilizing system do not lead to remarkable differences in composites' response.

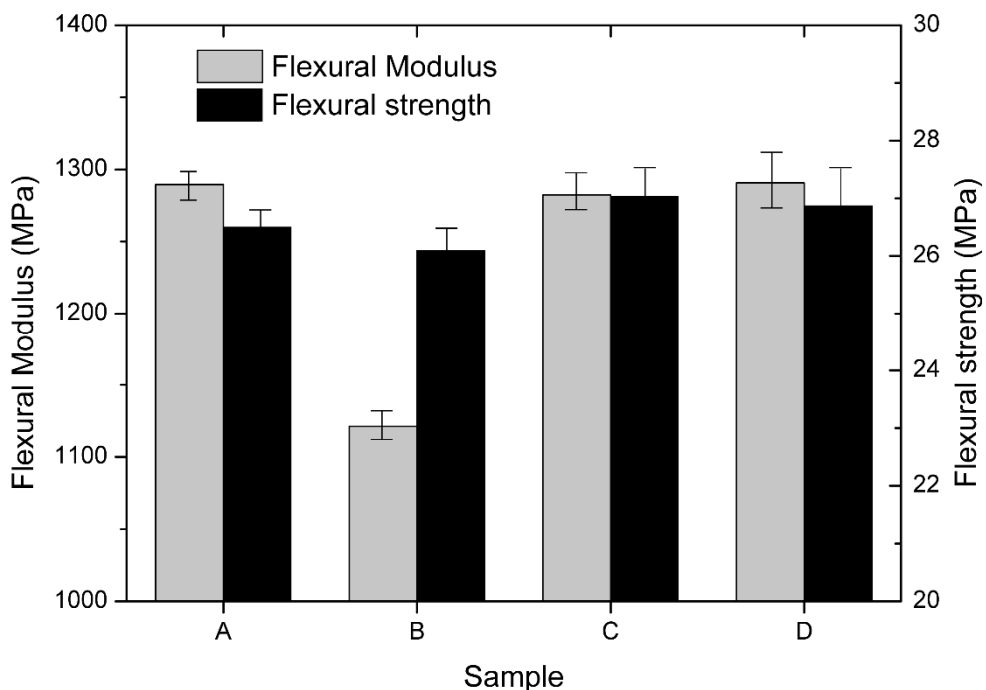


Figure II.4.5. Flexural properties of Bio-HDPE/CS with different compatibilizing system: a) Bio-HDPE/CS-UT; b) Bio-HDPE/CS-NaOH; c) Bio-HDPE/CS-MA; d) Bio-HDPE/CS-Silane.

On the other hand, the impact resistance is not remarkably affected by the use of different compatibilizing system as it can be observed in **Table II.4.2**. It is important to remark that unnotched HDPE does not break due to the high plastic deformation that can support. All results showed in **Table II.4.2** are obtained, thus, using notched sample. Noteworthy that sample Bio-HDPE/CS-UT, carried out using a CS filler without compatibilizing treatment, obtained the lowest values of impact resistance. This due to the poor compatibility between polymeric matrix and the used cellulosic filler. On the other hand, when different compatibilizing systems are used this impact resistance are increased, even above to Bio-HDPE. Nevertheless, this increment is reduced (around

9%). As to the different compatibilizing systems used, negligible differences are obtained, thus the compatibilizing system choosed does not play a key role on impact resistances as observed previously with flexural and tensile properties.

Table II.4.2. Impact resistance values of Bio-PE/CS composites with different compatibilizing system.

Sample	Impact resistance (kJ mm ⁻²)	SD
Bio-HDPE	2.75	0.23
Bio-HDPE/CS-UT	2.33	0.52
Bio-HDPE/CS-NaOH	3.00	0.25
Bio-HDPE/CS-MA	3.00	0.05
Bio-HDPE/CS-Silane	3.00	0.25

These results show that the different compatibilizing system do not play a key role in improving the overall performance of bio-HDPE/CS composites. This fact could be directly related to the physical morphology of the fibers themselves.

Figure II.4.6[a] shows the typical appearance of untreated *Cortaderia selloana* fibers with a feather like morphology, with very thin outstretched fibers characterized by very high surface area. **Figure II.4.6[b]** corresponds to the same fibers subjected to alkali treatment with NaOH. We can clearly see the difference in morphology between the untreated and NaOH-treated fibers. In the case of the NaOH-treated fibers we can see that the linear fiber shapes have disappeared and new aggregates can be detected with more compact fibers and, subsequently, with lower surface area due to the aggregation state. Although some fiber-matrix interactions can be achieved by the different compatibilizing system, the treatment leads to breakages of the feather-like structure and low surface area is obtained thus leading to lower fiber-matrix interactions. For this reason, we evaluate the influence of the *Cortaderia selloana* content in composites without previous treatment and/or compatibilizer as we have corroborated that the different compatibilizing system do not improve mechanical and thermal behaviour of bio-HDPE/CS composites.

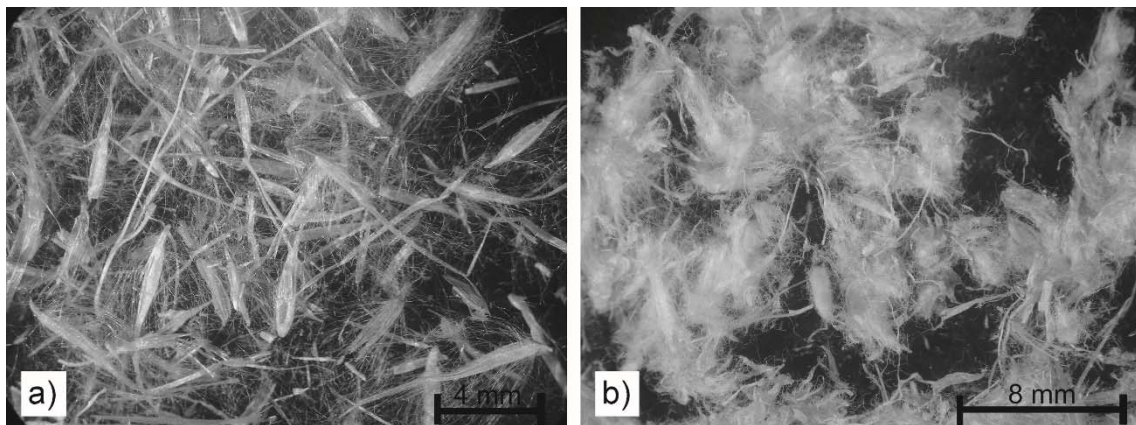


Figure II.4.6. Physical morphology of *Cortaderia selloana* fibers (10x): a) without treatment; b) alkali treatment with NaOH.

Effect of *Cortaderia selloana* content on bio-HDPE/CS composite properties.

Differential scanning calorimetry (DSC) results are summarized in **Table II.4.3**. The melting peak is slightly reduced as the fiber content increases due to the nucleating effect provided by the lignocellulose component. With regard to the onset degradation temperature it is important to note the remarkable increase in thermal stability as the *Cortaderia selloana* content increases. The onset degradation temperature of the raw unfilled bio-HDPE is located at about 232.5 °C and this is remarkably increased up to values of 265 °C for composites containing 30 wt.% CS. DSC study reveals a clear stabilizing effect against thermo-oxidative processes due to presence of intrinsic antioxidant components in *Cortaderia selloana*.

Although addition of *Cortaderia selloana* leads to a clear thermal stabilization effect at moderate temperatures, thermal degradation of bio-HDPE/CS composites is slightly reduced at moderate-high temperatures due to lignocellulosic components degradation [24]. Thermogravimetric analysis (TGA) of bio-HDPE/CS composites is shown in **Figure II.4.7**. *Cortaderia selloana* degradation mainly occurs in the 250-350

°C range with a slight weight loss around 100 °C due to removal of residual water and quite residual ash at high temperatures (close to 20 wt.%).

Table II.4.3. Effect of *Cortaderia selloana* content on thermal properties of Bio-HDPE/CS composites obtained by differential scanning calorimetry (DSC).

wt.% <i>Cortaderia selloana</i> fiber	Melt Temperature (°C)	Onset degradation temperature (°C)
0	135.0	232.5
7.5	133.1	233.6
15.0	132.8	255.1
30.0	131.9	265.1

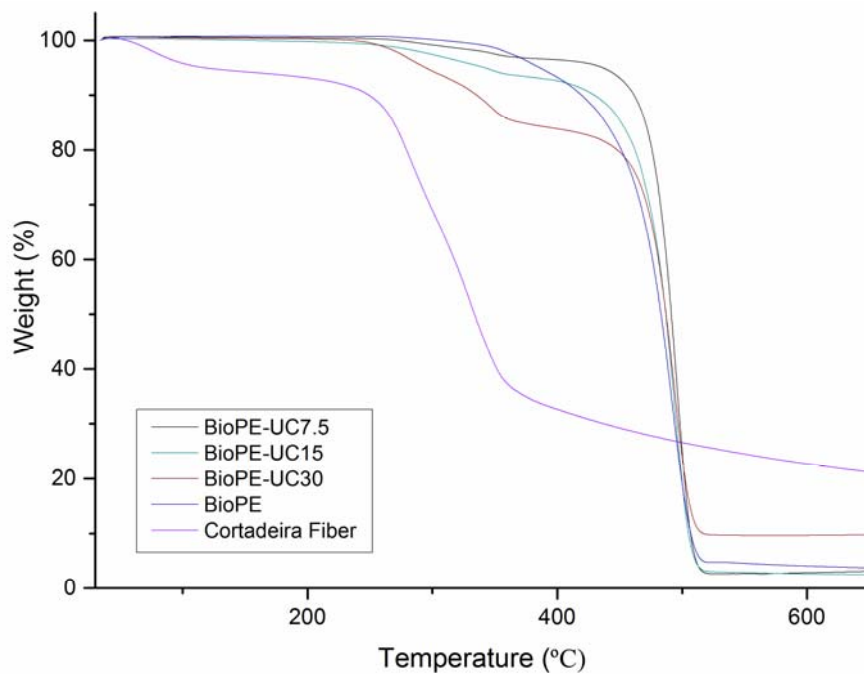


Figure II.4.7. Thermogravimetric (TGA) curves of raw *Cortaderia selloana* fiber and bio-HDPE/CS composites with different *Cortaderia selloana* content.

With regard to unfilled bio-HDPE, degradation occurs in the 350-500 °C range in a single step process with very low char formation. With regard to bio-HDPE/CS

composites, degradation occurs in two clearly detectable stages. The first stage is located in the 250 °C-350 °C and corresponds to degradation of lignocellulosic components and other organic constituents [27-29]. The second stage is directly related to polyethylene degradation and we can clearly see the stabilizing effect provided by *Cortaderia selloana* fibers as the onset degradation temperature of the second stage is higher than unfilled polyethylene. In addition, as expected, the weight loss of the first degradation step is directly related to the total amount of *Cortaderia selloana* fibers. Moreover, the residual char increases with the total amount of *Cortaderia selloana* changing from 2.05 wt.% (composites with 7.5 wt.% CS) up to 11.4 wt.% for composites containing 30 wt.% CS.

The effect of the fiber content on mechanical response can be observed in **Figure II.4.8**. As the fiber content increases, both the tensile and flexural modulus increase. In the case of tensile modulus, it increases by 86% for composites containing 30 wt.% CS with regard to unfilled HDPE. The flexural modulus increases up to twice the initial value of unfilled HDPE for composites with 30 wt.% CS. Addition of short dispersed fiber leads to a dramatic decrease in plastic deformation.

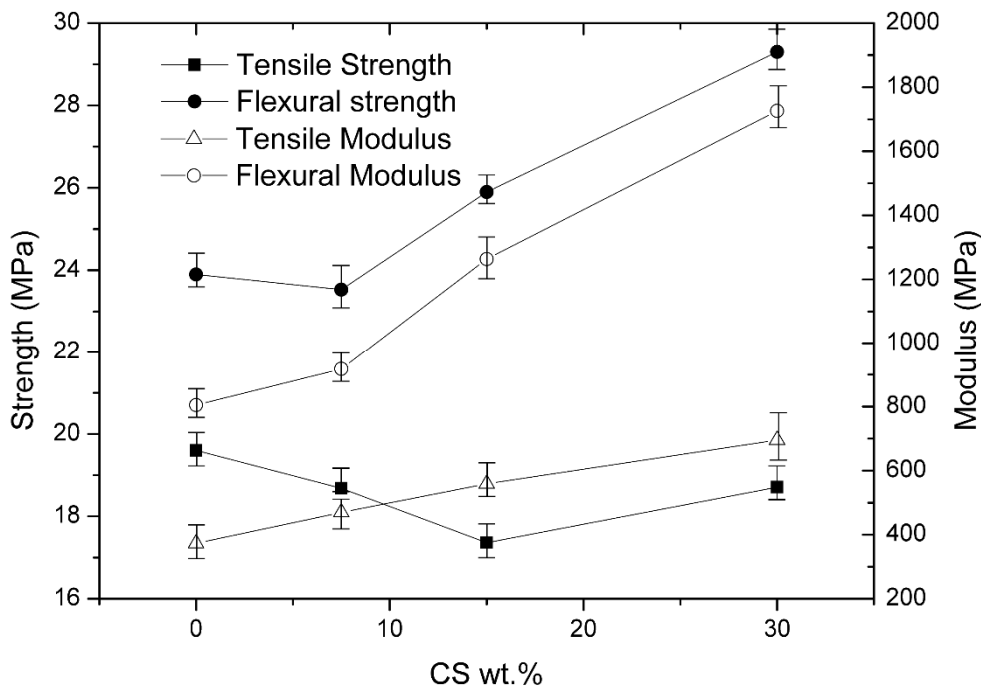


Figure II.4.8. Mechanical properties of bio-HDPE/CS composites in terms of the wt.% of *Cortaderia selloana* content.

The modulus can be defined as a ratio between stress and deformation (in tensile and flexural conditions). As we can see, the strength values are not highly reduced but the elongation at break is reduced to minimum values. For this reason, the stress/elongation ratio increases thus indicating more stiffness; so that, addition of *Cortaderia selloana* fibers leads to a clear reinforcing effect [19, 24]. With regard to tensile and flexural strength it is important to remark that the fiber content does not produce important changes in their values.

The evolution of the elongation at break is similar to that observed in the previous section with a clear embrittlement effect due to a dramatic decrease in elongation at break values. The total content on reinforcement fiber does not have significant effects on elongation at break and very low values, near 1.5%, are obtained for all composites. **Figure II.4.9** shows the fractured surfaces from tensile tests for different fiber content. As indicated previously, morphologies are characterized by lack of interaction among the fiber-matrix interface. Obviously, as the fiber content increases, the total amount of fibers in the fractured surfaces is more evident.

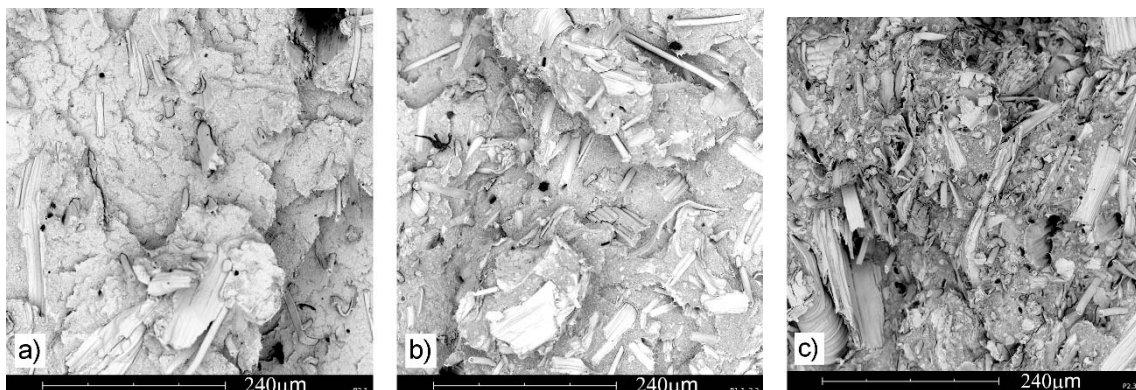


Figure II.4.9. SEM images (500x) of fractured surfaces from tensile tests of bio-HDPE/CS composites with different *Cortaderia selloana* content: a) 7.5 wt.%; b) 15 wt.%; c) 30 wt.%.

■ Water uptake of bio-HDPE/Cortaderia fibre composites.

Differential scanning calorimetry (DSC) results are summarized in **Table II.4.3**. The melting peak is slightly reduced as the fiber content increases due to the nucleating effect.

Figure II.4.10 shows the time dependences of water uptake for the different bio-HDPE/CS composites using various coupling agents. bio-HDPE absorbed only 0.021 wt% of water after 60 days, due its hydrophobic character. It was found that the composite of unfilled bio-HDPE with untreated fiber exhibits very low water uptake even after 60 days. Comparatively, the fibers with coupling agents show a higher water absorption levels. The composite unfilled bio-HDPE with fibers pre-treated with NaOH and PE-g-MA submits values of water uptake of 6.2 wt%, while in composite of unfilled bio-HDPE with untreated fiber is only 0.844 wt%, after 60 days. For the other fiber treatment studied, also increases the amount of water absorbed. These results show that in the bio-HDPE/CS system studied, coupling agents worsen the water absorption behavior of the material. This phenomenon is due to the certain natural hydrophobic character of the *Cortaderia selloana* fibers. While NaOH bath favors a more hydrophilic behavior of the composite material as shown in Figure 10. These considerations show that the composite unfilled bio-HDPE with untreated Cortaderia fiber unfilled bio-HDPE has the best behavior in water uptake phenomenon.

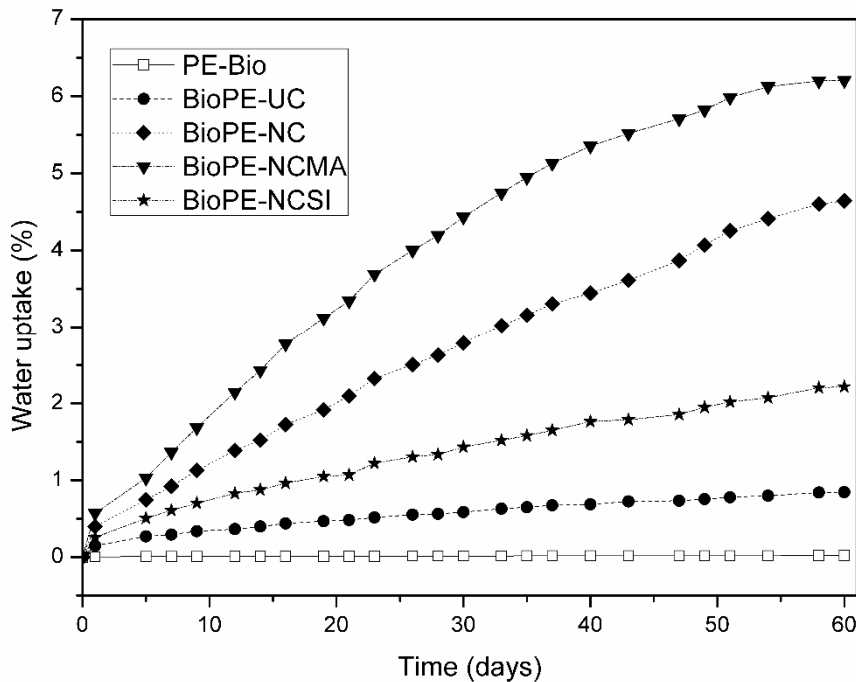


Figure II.4.10. Variation of the water uptake as a function of the treatment time for bio-HDPE/CS composites with different compatibilizing system.

The water uptake of the bio-HDPE/CS composites is a function of amount of fiber as shown in **Figure II.4.11**. Observed graphically as to lower fiber content, the amount of water uptake is low after 60 days of immersion. During this test time, the composite with 7.5 wt% and 15 wt% of fiber presents 0.384 wt% and 0.844 wt% of water, respectively. What is the same, with twice the amount of fiber, water uptake is almost twice. While high amounts of fiber (30 wt%) the composite behavior is different, showing high water uptake (5.35 wt%) to the same time test. This involves six times the sample of fiber 15 wt%, and 14 times for 7.5 wt% respectively. These results may be due to the low interfacial adhesion between the fiber and the matrix, which increase the rate of diffusion of water. So that the greater quantity of fiber in the composite, more water absorbency occurs because the voids formation on the fiber-matrix interface.

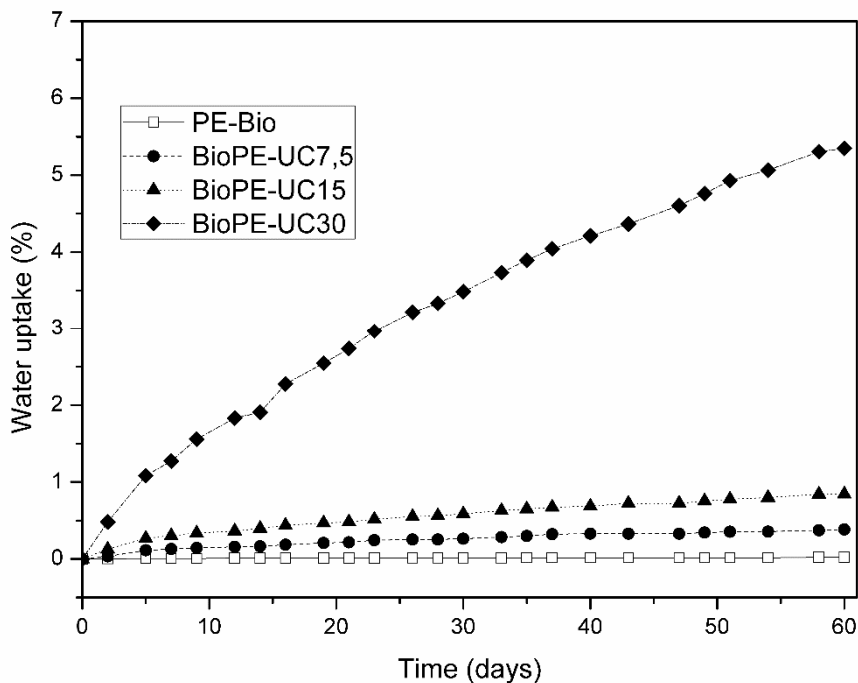


Figure II.4.11.- Variation of the water uptake as a function of the treatment time for bio-HDPE/CS composites with different *Cortaderia selloana* content.

II.4.4. Conclusions.

Addition of *Cortaderia selloana* short fiber to bio-based high density polyethylene leads to a remarkable increase in stiffness while strength (tensile and flexural) is not highly affected even with relatively high fiber load (30 wt.%). Elastic and flexural moduli for composites with 15-20 wt.% *Cortaderia selloana* are almost twice the values of unfilled HDPE, thus leading to stiff materials with potential use as wood substitute in applications in which structural properties are not required. The main advantage of bio-HDPE/CS composites is a high bio-based content provided by polyethylene from ethanol together with an agroforestral waste from *Cortaderia selloana*, natural intrinsic stabilization properties against thermo-oxidation due to *Cordateria selloana* natural antioxidants, low maintenance and a water uptake typical of other Wood Plastic Composites (WPC). The use of compatibilizing system based on alkali

treatment coupled to maleated copolymer or hydrophobic silane treatment do not provide better properties. It is important to remark that untreated *Cortaderia selloana* fibers have a feather-like structure which gives high surface area and this morphology is lost after a wet- treatment with silanes. Moreover, *Cortaderia selloana* it is an invasive species in Mediterranean Area. It forms dense populations which may exclude the presence of other plants. Diminishes the quality of pastures and increases the risk of fire. It has been suggested starting the plant as a preferred method of disposal and the use of herbicides (glyphosate) although it should evaluate potential impact on amphibian populations. importantly can influence the dynamics of river systems and control is essential to keep the channels in good condition. Authors consider that using *Cortaderia selloana* as filler a revaluation of cellulosic waste may be carried out, giving an economical and environmental solutions respect the elimination of this species.

Acknowledgements.

This work was funded by the Conselleria d'Educació, Cultura i Esport (Generalitat Valenciana) Ref: GV / 2014/008. The authors declare that they have no conflict of interest.

References.

- [1] G. Bogoeva-Gaceva, M. Avella, M. Malinconico, A. Buzarovska, A. Grozdanov, G. Gentile, M.E. Errico, "Natural fiber eco-composites", *Polymer Composites* (2007) **28**, 98-107.
- [2] D.U. Shah, "Developing plant fibre composites for structural applications by optimising composite parameters: a critical review", *Journal of Materials Science* (2013) **48**, 6083-6107.
- [3] L. Averous, "Biodegradable multiphase systems based on plasticized starch: A review", *Journal of Macromolecular Science-Polymer Reviews* (2004) **44**, 231-274.
- [4] F.S. Guner, Y. Yagci, A.T. Erciyes, "Polymers from triglyceride oils", *Progress in Polymer Science* (2006) **31**, 633-670.
- [5] D.P. Pfister, R.C. Larock, "Green composites from a conjugated linseed oil-based resin and wheat straw", *Composites Part a-Applied Science and Manufacturing* (2010) **41**, 1279-1288.
- [6] J.M. Raquez, M. Deleglise, M.F. Lacrampe, P. Krawczak, "Thermosetting (bio)materials derived from renewable resources: A critical review", *Progress in Polymer Science* (2010) **35**, 487-509.
- [7] M.I. Misnon, M.M. Islam, J.A. Epaarachchi, K.-t. Lau, "Potentiality of utilising natural textile materials for engineering composites applications", *Materials & Design* (2014) **59**, 359-368.
- [8] E. Bodros, I. Pillin, N. Montrelay, C. Baley, "Could biopolymers reinforced by randomly scattered flax fibre be used in structural applications?", *Composites Science and Technology* (2007) **67**, 462-470.
- [9] A. Kaymakci, N. Ayrilmis, F. Ozdemir, T. Gulec, "Utilization of Sunflower Stalk in Manufacture of Thermoplastic Composite", *Journal of Polymers and the Environment* (2013) **21**, 1135-1142.
- [10] S. Wong, R. Shanks, A. Hodzic, "Properties of poly(3-hydroxybutyric acid) composites with flax fibres modified by plasticiser absorption", *Macromolecular Materials and Engineering* (2002) **287**, 647-655.

II. Investigación previa.

- [11] S. Luo, A.N. Netravali, "Mechanical and thermal properties of environment-friendly "green" composites made from pineapple leaf fibers and poly(hydroxybutyrate-co-valerate) resin", *Polymer Composites* (1999) **20**, 367-378.
- [12] D.N. Saheb, J.P. Jog, "Natural fiber polymer composites: A review", *Advances in Polymer Technology* (1999) **18**, 351-363.
- [13] C. Alves, P.M.C. Ferrao, A.J. Silva, L.G. Reis, M. Freitas, L.B. Rodrigues, D.E. Alves, "Ecodesign of automotive components making use of natural jute fiber composites", *Journal of Cleaner Production* (2010) **18**, 313-327.
- [14] X. Zhou, Y. Yu, Q. Lin, L. Chen, "Effects of maleic anhydride-grafted polypropylene (MAPP) on the physico-mechanical properties and rheological behavior of bamboo powder-polypropylene foamed composites", *Bioresources* (2013) **8**, 6263-6279.
- [15] R. Khiari, Z. Marrakchi, M.N. Belgacem, E. Mauret, F. Mhenni, "New lignocellulosic fibres-reinforced composite materials: A stepforward in the valorisation of the Posidonia oceanica balls", *Composites Science and Technology* (2011) **71**, 1867-1872.
- [16] M. TabkhPaz, A.H. Behravesh, P. Shahi, A. Zolfaghari, "Procedure effect on the physical and mechanical properties of the extruded wood plastic composites", *Polymer Composites* (2013) **34**, 1349-1356.
- [17] M. Tasdemir, H. Biltekin, G.T. Caneba, "Preparation and characterization of LDPE and PP-wood fiber composites", *Journal of Applied Polymer Science* (2009) **112**, 3095-3102.
- [18] M. Zahedi, T. Tabarsa, A. Ashori, M. Madhoushi, A. Shakeri, "A comparative study on some properties of wood plastic composites using canola stalk, Paulownia, and nanoclay", *Journal of Applied Polymer Science* (2013) **129**, 1491-1498.
- [19] N. Petchwattana, S. Covavisaruch, S. Chanakul, "Mechanical properties, thermal degradation and natural weathering of high density polyethylene/rice hull composites compatibilized with maleic anhydride grafted polyethylene", *Journal of Polymer Research* (2012) **19**, 9921.

- [20] T. Boronat, V. Fombuena, D. Garcia-Sanoguera, L. Sanchez-Nacher, R. Balart, "*Development of a biocomposite based on green polyethylene biopolymer and eggshell*", Materials & Design (2015) **68**, 177-185.
- [21] H. Essabir, S. Nekhloui, M. Malha, M.O. Bensalah, F.Z. Arrakhiz, A. Qaiss, R. Bouhfid, "*Bio-composites based on polypropylene reinforced with Almond Shells particles: Mechanical and thermal properties*", Materials & Design (2013) **51**, 225-230.
- [22] D. Li, J. Li, X. Hu, L. Li, "*Effects of ethylene vinyl acetate content on physical and mechanical properties of wood-plastic composites*", Bioresources (2012) **7**, 2916-2932.
- [23] S.-K. Yeh, K.-J. Kim, R.K. Gupta, "*Synergistic effect of coupling agents on polypropylene-based wood-plastic composites*", Journal of Applied Polymer Science (2013) **127**, 1047-1053.
- [24] R. Khiari, M.F. Mhenni, M.N. Belgacem, E. Mauret, "*Chemical composition and pulping of date palm rachis and Posidonia oceanica - A comparison with other wood and non-wood fibre sources*", Bioresource Technology (2010) **101**, 775-780.
- [25] Q. Chen, X. Mao, H. Xue, Y. Deng, J. Lin, "*Preparation and characterization of bamboo fiber-graft-lauryl methacrylate and its composites with polypropylene*", Journal of Applied Polymer Science (2013) **130**, 2377-2382.
- [26] B. Ferrero, T. Boronat, R. Moriana, O. Fenollar, R. Balart, "Green composites based on wheat gluten matrix and posidonia oceanica waste fibers as reinforcements", Polymer Composites (2013) **34**, 1663-1669.
- [27] H.L. Ornaghi, Jr., M. Poletto, A.J. Zattera, S.C. Amico, "Correlation of the thermal stability and the decomposition kinetics of six different vegetal fibers", Cellulose (2014) **21**, 177-188.
- [28] E.C. Ramires, F. de Oliveira, E. Frollini, "Composites based on renewable materials: Polyurethane-type matrices from forest byproduct/vegetable oil and reinforced with lignocellulosic fibers", Journal of Applied Polymer Science (2013) **129**, 2224-2233.
- [29] P.E. Sanchez-Jimenez, L.A. Perez-Maqueda, A. Perejon, J.M. Criado, "Nanoclay nucleation effect in the thermal stabilization of a polymer nanocomposite: a kinetic mechanism change", Journal of Physical Chemistry C (2012) **116**, 11797-11807.

II. Investigación previa.

Composites Science and Technology 145 (2017) 1–9

Contents lists available at ScienceDirect
Composites Science and Technology
journal homepage: <http://www.elsevier.com/locate/compscitech>



Development and characterization of a new natural fiber reinforced thermoplastic (NFRP) with *Cortaderia selloana* (Pampa grass) short fibers

A. Jordá-Vilaplana ^{a,*}, A. Carbonell-Verdú ^a, M.D. Samper ^a, A. Pop ^b, D. Garcia-Sanoguera ^a

^a Instituto de Tecnología de Materiales, Universitat Politècnica de València, 03801, Alcoy, Spain

^b Department of Mechatronics, University of Oradea, 410087, Oradea, Romania

ARTICLE INFO

Article history:

Received 27 October 2016

Received in revised form

23 March 2017

Accepted 24 March 2017

Available online 27 March 2017

Keywords:

Cortaderia selloana

Natural fiber reinforced plastics (NFRP)

Bio-based polyethylene

Mechanical properties

ABSTRACT

In this work, fully bio-based thermoplastic composites are manufactured with bio-based polyethylene (from sugarcane) and short fibers coming from *Cortaderia selloana* (CS) wastes. These wastes are characterized by high cellulose content, which can provide high stiffness to the polymeric matrix. The effect of *Cortaderia selloana* short fibers on thermal properties has been evaluated by differential scanning calorimetry (DSC) and thermogravimetric analysis (TGA). The effect of the filler load on mechanical properties has also been evaluated by tensile and impact tests as well as the effects of different coupling agents. Fiber-matrix interactions have been studied by scanning electron microscopy (SEM). The addition of 15–30 wt% *Cortaderia selloana* short fiber leads to high elastic and flexural modulus without remarkable changes in thermal degradation of the polymer composite.

© 2017 Elsevier Ltd. All rights reserved.

Contents

1. Introduction	1
2. Experimental	2
2.1. Materials	2
2.2. Composites processing	2
2.3. Thermal characterization	3
2.4. Mechanical characterization	3
2.5. Fractography by scanning electron microscopy (SEM)	3
2.6. Water uptake characterization of bio-HDPE/CS composites	3
3. Results and discussion	3
3.1. Effect of compatibilizing system on the bio-HDPE/CS composite properties	3
3.2. Effect of <i>Cortaderia selloana</i> content on bio-HDPE/CS composite properties	5
3.3. Water uptake of bio-HDPE/ <i>Cortaderia</i> fibre composites	7
4. Conclusions	8
Acknowledgements	8
References	8

1. Introduction

In recent decades, society has raised awareness regarding the

need to preserve the environment. The way of life of modern societies based on consumption is responsible for the high production of wastes from both the manufacturer and the final consumer. This generates significant environmental and pollution problems. Governments in developed countries have the need to implement laws

* Corresponding author.

E-mail address: amjorvi@upv.es (A. Jordá-Vilaplana).



III. OBJETIVOS Y PLANIFICACIÓN



III.1. HIPÓTESIS Y OBJETIVOS.

Durante los últimos años el cada vez más cercano agotamiento del petróleo y el incesante y preocupante aumento de los niveles de contaminación han propiciado un cambio en nuestra sociedad. Una sociedad cada vez más concienciada en aspectos como la mejora del reciclaje y la necesidad de búsqueda de energías alternativas a las tradicionales que acaben con la actual dependencia a fuentes no renovables como el petróleo.

La problemática descrita ha favorecido la multiplicación de investigaciones y el desarrollo de nuevos materiales a partir de recursos renovables para su aplicación en sectores conquistados desde hace años por productos de origen petroquímico. Es el caso de las múltiples publicaciones científicas sobre el desarrollo de materiales poliméricos ecoeficientes o los esfuerzos para el desarrollo y validación de nuevos materiales con una huella de carbono inferior y, globalmente, con un mayor rendimiento medioambiental.

En el campo de los materiales poliméricos, los aceites vegetales representan una fuente renovable con atractivas posibilidades en la síntesis de polímeros u optimización de formulaciones de plásticos industriales.

A pesar de conocerse muchos tipos de bioplásticos, solamente algunos pueden competir con los polímeros tradicionales ya sea por sus propiedades o por su coste. Necesario resulta recordar el significado del término bioplásticos como aquellos materiales biodegradables o que provienen de una base biológica o bien que presentan ambas propiedades. Por lo tanto, que mejor manera de lograr polímeros a partir de los excedentes de aceite de un subproducto tan conocido y globalmente utilizado como el algodón.

La semilla del algodón, con una producción anual muy estable y sin grandes variaciones durante los últimos años, se situó en el año 2015 en 4,72 millones de toneladas. Esta cifra se encuentra, no obstante, muy por debajo del aceite de palma destinado, principalmente, al sector alimentario; un sector al que no se suele destinarse el aceite de semilla de algodón debido a la presencia de gisipol. Todo ello da lugar a la generación de excedentes de aceite de semilla de algodón que pueden ser aprovechados para otros usos industriales como el que se propone en la presente tesis. Asimismo, el

perfil lipídico del aceite de semilla de algodón indica que es un aceite con un 75 % aproximadamente de ácidos grasos insaturados y por lo tanto con altas posibilidades para su uso industrial.

Teniendo en cuenta las consideraciones citadas anteriormente, la principal hipótesis de trabajo que se plantea es la revalorización de un subproducto de la industria textil para la obtención de materiales con alto rendimiento medioambiental. Para lograr estructurar el documento y lograr dar la mayor salida al subproducto se divide el trabajo en tres bloques:

Bloque I.

“Utilización de aceites vegetales derivados de semilla de algodón para la obtención de materiales termoestables”.

Bloque II.

“Utilización de aceites vegetales derivados de semilla de algodón para la plastificación y flexibilización de polímeros termoplásticos”.

Bloque III.

“Utilización de aceites vegetales derivados de semilla de algodón para la mejora de propiedades de impacto de mezclas y compuestos derivados de ácido poli(láctico) - PLA”.

II.1.1. Objetivo general.

El objetivo general de este trabajo de investigación es el desarrollo y validación de nuevos materiales de origen renovable para la industria de los materiales poliméricos a partir del aceite de semilla de algodón sometido a procesos de epoxidación y maleinización con potencial uso como resinas epoxi o agentes plastificantes. Así como un uso integral derivado de la extracción del aceite, empleando y utilizando tanto el aceite extraído como el residuo generado durante su extracción.

II.1.2. Objetivos particulares.

Para alcanzar el objetivo general de esta tesis doctoral, se plantean los siguientes objetivos parciales:

[OP1] Definir, implementar y validar la metodología de epoxidación y maleinización del aceite de semilla de algodón a escala de laboratorio.

[OP2] Optimizar los parámetros de epoxidación de aceite de semilla de algodón en términos de ratios de componentes (aceite: ácido carboxílico: peróxido) así como la temperatura y tiempos de reacción.

[OP3] Optimizar los parámetros de maleinización del aceite de semilla de algodón en términos de exceso de anhídrido maleico, así como temperatura y tiempo de reacción.

[OP4] Desarrollar y validar materiales termoestables utilizando como resina base, resinas derivadas del aceite de semilla de algodón epoxidado (ECSO) entrecruzadas con anhídridos de origen petroquímico.

[OP5] Desarrollar y validar formulaciones de policloruro de vinilo (PVC) de alto rendimiento medioambiental con el empleo de plastificantes derivados de aceite de semilla de algodón epoxidado (ECSO).

[OP6] Desarrollar y validar formulaciones de ácido poliláctico (PLA) de origen bio y biodegradable con el empleo de plastificantes derivados de ECSO.

[OP7] Desarrollar y validar films de PLA con el empleo de aceite de semilla de algodón maleinizado (MCSO) y aceite de semilla de linaza maleinizado (MLO) como plastificante.

[OP8] Desarrollar y validar formulaciones de mezclas de polímeros biodegradables (PLA – PBAT) con ECSO y MCSO como compatibilizantes con el objetivo de comparar los resultados con los logrados al incorporar un oligómero de estireno acrílico comercial Joncryl.

[OP9] Desarrollar y validar formulaciones de PLA con el empleo de aceites de semilla de algodón modificados tanto mediante epoxidación como maleinización con la incorporación de cargas derivadas del residuo del proceso de obtención del CSO.

III.2. METODOLOGÍA Y PLANIFICACIÓN.

Para lograr los objetivos planteados previamente se plantea el siguiente programa de trabajo estructurado en fases, tareas y actividades (**Figura III.2.1**).

■ Bloque I. “Utilización de aceites vegetales derivados de semilla de algodón para la obtención de materiales termoestables”.

Capítulo 1. *“Development of Environmentally Friendly Composite Matrices from Epoxidized Cottonseed Oil”*

Tarea 1.1. Epoxidación del aceite de semilla de algodón.

- | | |
|------------------|---|
| Actividad 1.1.1. | Epoxidación del aceite de semilla de algodón. Optimización de los parámetros de epoxidación de aceite de semilla de algodón en términos de ratios de componentes (aceite: ácido carboxílico: peróxido) así como la temperatura y tiempos de reacción. |
| Actividad 1.1.2. | Realización de mediciones del índice de yodo y oxígeno oxirano cada 2 horas durante las 8 horas de la epoxidación. |

Tarea 1.2. Estudio de la cinética de curado del aceite de semilla de algodón con diferentes mezclas de anhídrido DDSA – MNA.

- Actividad 1.2.1. Realización del seguimiento de curado del aceite de semilla de algodón con diferentes mezclas de anhídrido DDSA – MNA
- Actividad 1.2.2. Obtención del tiempo de gel a 110 °C y 120 °C con diferentes mezclas de DDSA y MNA mediante reómetro oscilatorio plato-plato con la evolución del módulo de almacenamiento (G'), módulo de pérdidas (G'') y ángulo de fase (δ).
- Actividad 1.2.3. Obtención de los perfiles de curado con el uso de la técnica de calorimetría diferencial de barrido (DSC)

Tarea 1.3. Obtención de los materiales termoestables a partir de las condiciones logradas en la tarea anterior.

- Actividad 1.3. Curado de las distintas formulaciones propuestas con diferentes mezclas de anhídrido DDSA – MNA bajo las condiciones obtenidas como óptimas durante la caracterización llevada a cabo en la tarea 1.2 (3 horas a 110 °C). Obtención de probetas normalizadas para su posterior caracterización.

Tarea 1.3.1. Caracterización mecánica de los materiales termoestables.

- Actividad 1.3.1.1. Obtención de propiedades mecánicas mediante ensayos de flexión: módulo de flexión (E_t).

- Actividad 1.3.1.2. Obtención de las propiedades frente al impacto mediante el empleo del ensayo de impacto con péndulo Charpy.

Tarea 1.3.2. Caracterización de la morfología de los materiales termoestables.

- Actividad 1.3.2.1. Estudio de la morfología de fractura mediante el empleo de técnicas de microscopía electrónica (SEM).

Tarea 1.3.3. Caracterización termo-mecánica de los materiales termoestables.

- Actividad 1.3.3.1. Estudio de las propiedades mecánico-dinámicas mediante el empleo de análisis térmico mecánico-dinámico (DMTA). Evolución del módulo de almacenamiento (G') y del factor de pérdidas ($\tan \delta$) en función de la composición.

Tarea 1.4. Análisis y síntesis de resultados.

- Actividad 1.4.1. Análisis estadístico de los resultados obtenidos y síntesis de resultados en documento para su difusión/divulgación.

Bloque II. “Utilización de aceites vegetales derivados de semilla de algodón para la plastificación y flexibilización de polímeros termoplásticos”

Capítulo 2. *“A new biobased plasticizer for poly (vinyl chloride), PVC base on epoxidized cottonseed oil (ECSO)”*

Tarea 2.1 Fabricación de plastisoles de PVC – ECSO.

- Actividad 2.1.1. Selección de la formulación PVC - ECSO con las propiedades más equilibradas, tanto a nivel de propiedades mecánicas como de curado.
- Actividad 2.1.2. Realización de los plastisoles con un contenido de 70 phr de ECSO. Mezclado, eliminación del aire en cámara de vacío y curado en horno con temperaturas comprendidas entre 160 °C y 220 °C con tiempos de curado entre 7,5 y 17,5 min.

Tarea 2.2. Caracterización mecánica de los plastisoles PVC – ECSO.

- Actividad 2.2.1. Obtención de propiedades mecánicas mediante ensayo de tracción: alargamiento a la rotura ($\epsilon_b\%$), módulo de tracción (E_t) y tensión de rotura (σ_t).

Tarea 2.3. Caracterización de la morfología de fractura de plastisoles PVC –ECSO.

Actividad 2.3.1. Estudio de la morfología de fractura mediante el empleo de técnicas de microscopía electrónica (SEM).

Tarea 2.4. Caracterización de la migración de plastisoles de PVC –ECSO.

Actividad 2.4.1. Estudio de la migración con la utilización del disolvente n-hexano a temperaturas comprendidas entre 30 °C y 60 °C a diferentes tiempos: 2, 4, 6 y 8 horas.

Tarea 2.5. Caracterización térmica de plastisoles de PVC –ECSO.

Actividad 2.5.1. Determinación de las transiciones térmicas de los plastisoles mediante calorimetría diferencial de barrido (DSC)

Tarea 2.6. Medición de las coordenadas colorimétricas de los plastisoles de PVC –ECSO.

Actividad 2.6.1. Determinación de las coordenadas de color ($L^*a^*b^*$).

Tarea 2.7. Análisis y síntesis de resultados.

Actividad 2.7.1. Análisis estadístico de los resultados obtenidos y síntesis de resultados en documento para su difusión/divulgación.

Capítulo 3. “Plasticization effect of epoxidized cottonseed oil (ECSO) on poly(lactic acid)”

Tarea 3.1. Fabricación de formulaciones de PLA con aceite de semilla de algodón epoxidado (ECSO).

- Actividad 3.1.1. Extrusión de formulaciones de PLA con diferentes porcentajes de plastificante ECSO.
- Actividad 3.1.2. Inyección de formulaciones de PLA con diferentes porcentajes de ECSO en molde con probetas normalizadas para su caracterización.

Tarea 3.2. Caracterización mecánica de formulaciones de PLA – ECSO.

- Actividad 3.2.1. Obtención de las propiedades mecánicas mediante ensayos de tracción y flexión.
- Actividad 3.2.2. Ensayo impacto Charpy.

Tarea 3.3. Caracterización de la morfología de fractura de formulaciones de PLA – ECSO.

- Actividad 3.3.1. Estudio de la morfología de impacto de formulaciones de PLA con ECSO mediante técnicas de microscopía electrónica con emisión de campo (FESEM).

Tarea 3.4. Caracterización térmica y termo-mecánica de formulaciones de PLA - ECSO.

- Actividad 3.4.1. Determinación de las transiciones térmicas de las formulaciones de PLA con ECSO mediante calorimetría diferencial de barrido (DSC). Efecto de la composición en las transiciones térmicas del PLA: temperatura de transición vítrea (T_g), proceso de cristalización (T_{cc}) en frío y proceso de fusión (T_m).
- Actividad 3.4.2. Estudio de las propiedades mecánico-dinámicas mediante el empleo de análisis térmico mecánico-dinámico (DMTA). Evolución del módulo de almacenamiento (G') y del factor de pérdidas ($\tan \delta$) en función de la composición. Estimación de la T_g e influencia de la composición en las curvas DMTA.
- Actividad 3.4.3. Estudio del efecto de la temperatura en las propiedades mecánicas mediante ensayos de temperatura de reblandecimiento Vicat (VST) y de flexión térmica (HDT).

Tarea 3.5. Caracterización de los niveles de migración en las formulaciones de PLA-ECSO.

- Actividad 3.5.1. Estudio de la migración con la utilización del disolvente n-hexano a temperaturas comprendidas entre 30 °C y 60 °C manteniendo un tiempo constante de 8 horas.

Tarea 3.6. Análisis y síntesis de resultados.

- Actividad 3.6.1. Análisis estadístico de los resultados obtenidos y síntesis de resultados en documento para su difusión/divulgación.

Capítulo 4. “PLA films with improved flexibility properties by using maleinized cottonseed oil”

Tarea 4.1. Maleinización del aceite de semilla de algodón.

- Actividad IV.4.1.1. Maleinización del aceite de semilla de algodón. Optimización de los parámetros de maleinización del aceite de semilla de algodón en términos de exceso de anhídrido maleico, así como temperatura y tiempo de reacción.
- Actividad IV.4.1.2. Realización de mediciones del índice de acidez cada 30 min. durante las 2 primeras horas de la maleinización y finalmente durante la última hora del proceso las mediciones se llevaron a cabo cada 20 min.

Tarea 4.2. Fabricación de films de PLA con aceite de semilla de algodón maleinizado (MCSO) y aceite de semilla de linaza maleinizado (MLO) como plastificantes.

- Actividad 4.2.1. Extrusión de las formulaciones de PLA/MCSO/MLO con los diferentes porcentajes de aceites maleinizados propuestos para favorecer la homogeneización.
- Actividad 4.2.2. Extrusión de film de las mezclas homogeneizadas previamente de PLA/MCSO/MLO.

Tarea 4.2.1. Caracterización mecánica de los films de PLA plastificados con MCSO – MLO.

- Actividad 4.2.1.1. Obtención de las propiedades mecánicas mediante ensayo de tracción: alargamiento a la rotura ($\epsilon_b\%$), módulo de tracción (E_t) y tensión de rotura (σ_t).

Tarea 4.2.2. Caracterización de la morfología de fractura de los films de PLA plastificados con MCSO – MLO.

- Actividad 4.2.2.1. Estudio de la morfología de fractura mediante el empleo de técnicas de microscopía electrónica con emisión de campo (FESEM).

Tarea 4.2.3. Caracterización térmica de los films de PLA plastificados con MCSO – MLO.

- Actividad 4.2.3.1. Determinación de las transiciones térmicas los films de PLA/MCSO/MLO mediante calorimetría diferencial de barrido (DSC). Efecto de la composición en las transiciones térmicas de PLA: temperatura de transición vítrea (T_g), proceso de cristalización (T_{cc}) en frío y proceso de fusión (T_m).

- Actividad 4.2.3.2. Estudio de la estabilidad térmica frente a degradación de films de PLA/MCSO/MLO mediante análisis termogravimétrico (TGA). Estudio de las etapas de degradación y determinación de las temperaturas características del proceso de degradación: T_5 y T_{50} , correspondientes a la pérdida del 5 y 50 % de peso.

Tarea 4.2.4. Caracterización de las propiedades barrera de los films de PLA plastificados con MCSO – MLO.

Actividad 4.2.4.1. Determinación de la tasa de transmisión OTR de los films de PLA/MCSO/MLO en un analizador de permeabilidad de oxígeno.

Tarea 4.2.5. Medición del ángulo de contacto de los films de PLA plastificados con MCSO – MLO.

Actividad 4.2.5.1. Tras colocar la gota de agua la medición del ángulo de contacto se realizó a los 30 s y se obtuvo la humectabilidad de los materiales.

Tarea 4.2.6. Desintegración de los films de PLA plastificados con MCSO – MLO.

Actividad 4.2.6.1. Obtención de los resultados de la simulación de degradación bajo un ambiente de compostaje. A la vista de las imágenes obtenidas se refleja la desintegración y la influencia de los plastificantes.

Tarea 4.3. Análisis y síntesis de resultados.

Actividad 4.3.1. Análisis estadístico de los resultados obtenidos y síntesis de resultados en documento para su difusión/divulgación.

Bloque III. “Utilización de aceites vegetales derivados de semilla de algodón para la mejora de propiedades de impacto de mezclas y compuestos derivados de ácido poliláctico - PLA”

Capítulo 5. “*Manufacturing and compatibilization of PLA/PBAT binary blends by cottonseed oil-based derivatives*”

Tarea 5.1. Fabricación de mezclas binarias de PLA / PBAT compatibilizadas con ECSO/MCSO/Joncrys.

- Actividad 5.1.1. Extrusión de mezclas PLA/PBAT con diferentes compatibilizantes ECSO, MCSO y Joncrys.
- Actividad 5.1.2. Inyección de mezclas de PLA/PBAT con ECSO, MCSO y Joncrys en molde con probetas normalizadas para su caracterización.

Tarea 5.2. Caracterización mecánica de mezclas binarias de PLA / PBAT compatibilizadas con ECSO/MCSO/Joncrys.

- Actividad 5.2.1. Obtención de las propiedades mecánicas mediante ensayos de tracción: alargamiento a la rotura ($\epsilon_b\%$), módulo de tracción (E_t) y tensión de rotura (σ_t).

Tarea 5.3. Caracterización de la morfología de fractura de mezclas binarias de PLA / PBAT compatibilizadas con ECSO/MCSO/Joncrys.

Actividad 5.3.1. Estudio de la morfología de fractura mediante el empleo de técnicas de microscopía electrónica con emisión de campo (FESEM).

Tarea 5.4. Caracterización térmica y termomecánica de mezclas binarias de PLA / PBAT compatibilizadas con ECSO/MCSO/Joncrys

Actividad 5.4.1. Determinación de las transiciones térmicas de los films de PLA/PBAT con ECSO/MCSO/Joncrys mediante calorimetría diferencial de barrido (DSC). (T_g), (T_{cc}), (T_m) y ($\chi_c\%$).

Actividad 5.4.2. Estudio de la estabilidad térmica frente a degradación de films de PLA/PBAT con ECSO/MCSO/Joncrys mediante análisis termogravimétrico (TGA). Estudio de las etapas de degradación y determinación de las temperaturas características del proceso de degradación: T_5 y T_{50} , correspondientes a la pérdida del 5 y 50 % de peso.

Actividad 5.4.3. Estudio de las propiedades mecánico-dinámicas mediante el empleo de análisis térmico mecánico-dinámico (DMTA). (G') ($\tan \delta$) (T_g).

Tarea 5.5. Caracterización superficial de mezclas binarias de PLA / PBAT compatibilizadas con ECSO/MCSO/Joncrys.

- Actividad 5.5.1. Determinación de las coordenadas de color y más concretamente de la luminancia (L^*) para evaluar los cambios de transparencia.
- Actividad 5.5.2. Medición del ángulo de contacto.

Tarea 5.6. Desintegración de mezclas binarias de PLA / PBAT compatibilizadas con ECSO/MCSO/Joncrys.

- Actividad 5.6.1. Obtención de los resultados de la simulación de degradación bajo un ambiente de compostaje. A la vista de las imágenes obtenidas se refleja la desintegración y la influencia de los compatibilizantes.

Tarea 5.7. Análisis y síntesis de resultados.

- Actividad 5.7.1. Análisis estadístico de los resultados obtenidos y síntesis de resultados en documento para su difusión/divulgación.

Capítulo 6. “Processing and characterization of environmentally friendly composites from poly(lactic acid) and cottonseed waste materials”

Tarea 6.1. Fabricación de formulaciones de PLA/ECSO/MCSO/Harina de semilla de algodón (CSF).

- | | |
|------------------|---|
| Actividad 6.1.1. | Preparación de la harina obtenida del proceso de extracción del aceite de semilla de algodón. |
| Actividad 6.1.2. | Extrusión de formulaciones de PLA con diferentes porcentajes de plastificante ECSO - MCSO - CSF |
| Actividad 6.1.3. | Inyección de formulaciones de PLA con diferentes porcentajes de ECSO - MCSO - CSF en molde con probetas normalizadas para su caracterización. |

Tarea 6.2. Caracterización mecánica de formulaciones de PLA/ECSO/MCSO/Harina de semilla de algodón.

- | | |
|------------------|--|
| Actividad 6.2.1. | Obtención propiedades mecánicas mediante ensayo de tracción y flexión. |
| Actividad 6.2.2. | Ensayo impacto Charpy. |
| Actividad 6.2.3. | Ensayo de dureza shore D |

Tarea 6.3. Caracterización de la morfología de fractura de formulaciones de PLA/ECSO/MCSO/Harina de semilla de algodón.

- Actividad 6.3.1. Estudio de la morfología de impacto de formulaciones de PLA/ECSO/MCSO/Harina de semilla de algodón mediante técnicas de microscopía electrónica con emisión de campo (FESEM).

Tarea 6.4. Caracterización térmica y termo-mecánica de formulaciones de PLA/ECSO/MCSO/Harina de semilla de algodón.

- Actividad 6.4.1. Determinación de las transiciones térmicas de las formulaciones de PLA con ECSO mediante calorimetría diferencial de barrido (DSC). Efecto de la composición en las transiciones térmicas (T_g), (T_{cc}), (T_m) y (χ_c).
- Actividad 6.4.2. Estudio de las propiedades mecánico-dinámicas mediante el empleo de análisis térmico mecánico-dinámico (DMTA). (G') (G' a 40 °C) (T_g)

Tarea 6.5. Análisis y síntesis de resultados.

- Actividad 6.5.1. Análisis estadístico de los resultados obtenidos y síntesis de resultados en documento para su difusión/divulgación.

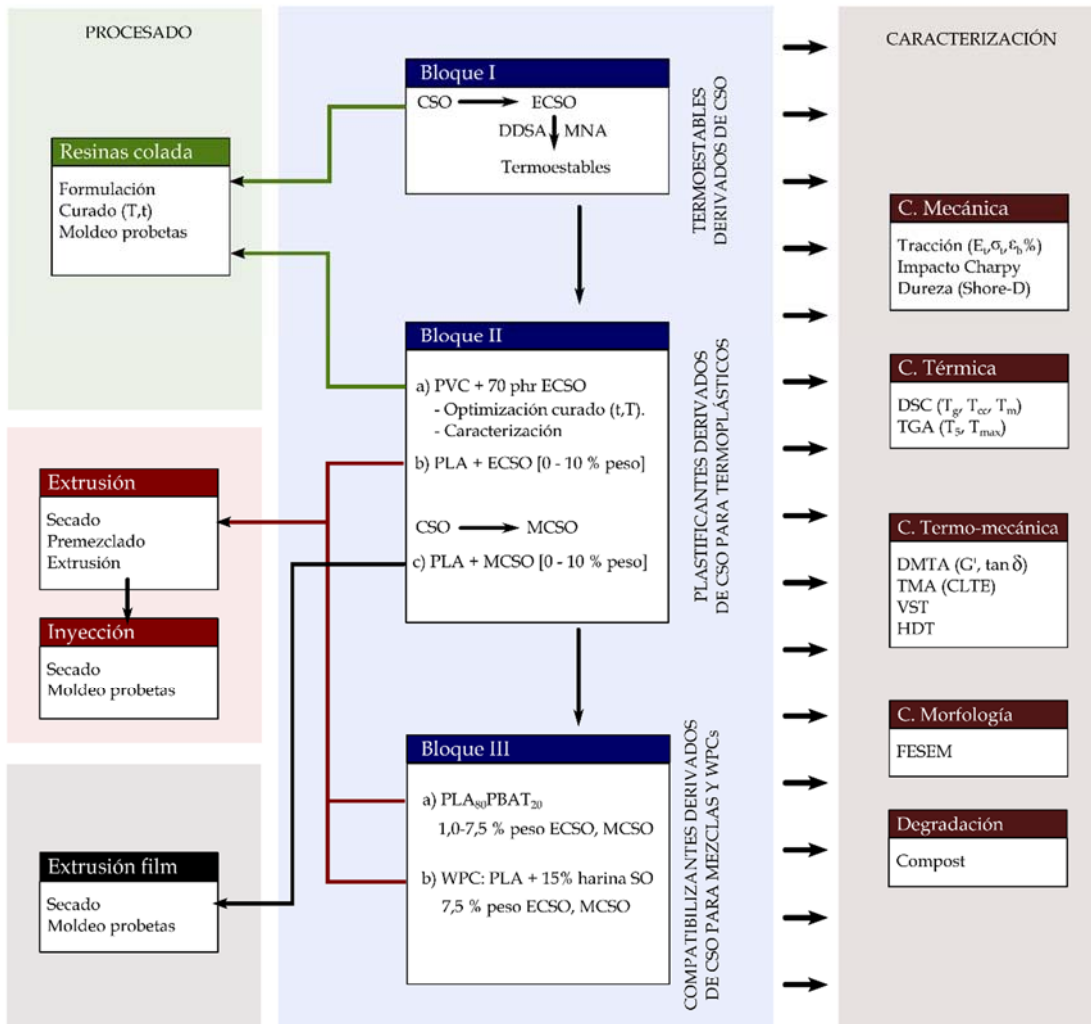
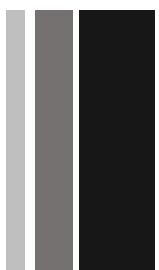


Figura III.2.1. Representación esquemática de la fase de investigación de la tesis doctoral centrada en el aprovechamiento de residuos de semilla de algodón.



IV. RESULTADOS Y DISCUSIÓN



RESUMEN.

Este capítulo muestra un resumen de los resultados de mayor relevancia que se han obtenido en este trabajo de investigación. Los resultados, se han clasificado en tres grandes bloques, cuyo contenido se describe a continuación:

Bloque I.

“Utilización de aceites vegetales derivados de semilla de algodón para la obtención de materiales termoestables”.

Este bloque contempla el desarrollo y optimización de los procesos de caracterización previa y modificación del aceite de semilla de algodón mediante procesos de epoxidación. Una vez optimizado dicho proceso, se procede a preparar resinas líquidas termoestables en combinación con diferentes agentes de entrecruzamiento líquidos y, finalmente, estas resinas líquidas se someten a procesos de entrecruzamiento a temperaturas altas con el empleo de diversos iniciadores y aceleradores. El resultado es un conjunto de resinas entrecruzadas con propiedades variables en función del agente de entrecruzamiento empleado (rígido o flexible), que amplían las posibilidades de los residuos de la semilla de algodón en el campo de los materiales termoestables. Se estudia el proceso de entrecruzamiento mediante técnicas de análisis térmico y, junto con esta caracterización del proceso de curado o entrecruzamiento, se lleva a cabo una completa caracterización mecánica, térmica y termomecánica de los materiales entrecruzados. Los aspectos más relevantes de esta investigación se resumen en el **Capítulo IV.1**.

Capítulo IV.1.

“Development of environmentally friendly composite matrices from epoxidized cottonseed oil”

Bloque II.

"Utilización de aceites vegetales derivados de semilla de algodón para la plastificación y flexibilización de polímeros termoplásticos".

Este bloque explora las posibilidades de los aceites vegetales derivados de la semilla de algodón, en la fabricación de aditivos plastificantes y agentes flexibilizantes para diversos polímeros termoplásticos como el poli(cloruro de vinilo) – PVC y el ácido poli(láctico) – PLA. En particular se desarrollan los procesos de epoxidación y maleinización y se lleva a cabo un completo estudio del efecto de la incorporación de estos plastificantes/modificadores de impacto en los diferentes polímeros. En relación al PVC se trabaja con formulaciones industriales y se lleva a cabo un estudio detallado del proceso de curado o gelificación de los plásticos vinílicos derivados de las resinas de PVC con los aceites de semilla de algodón epoxidados (ECSO). En relación al PLA, se estudia el efecto de plastificación, tanto del aceite de semilla de algodón epoxidado (ECSO) como el de aceite de semilla de algodón maleinizado (MCSO). Se trabaja en forma de pieza inyectada y en forma de film según las aplicaciones finales de los materiales y se lleva a cabo un estudio profundo del efecto de los diferentes derivados del aceite de semilla de algodón en las propiedades mecánicas, térmicas, termo-mecánicas, etc. Resultado de este bloque de investigación, se han obtenido 3 trabajos que se contemplan en los **Capítulos IV.2, IV.3 y IV.4.**

Capítulo IV.2.

"A new biobased plasticizer for poly (vinyl chloride), PVC base on epoxidized cottonseed oil (ECSO)"

Capítulo IV.3.

"Plasticization effect of epoxidized cottonseed oil (ECSO) on poly(lactic acid)"

Capítulo IV.4.

"PLA films with improved flexibility properties by using maleinized cottonseed oil"

Bloque III.

“Utilización de aceites vegetales derivados de semilla de algodón para la mejora de propiedades de impacto de mezclas y compuestos derivados de ácido poliláctico - PLA”.

Finalmente, este bloque se centra en el empleo de los derivados de la semilla de algodón para la mejora de diversas formulaciones industriales basadas en polímeros de alto rendimiento medioambiental. Partiendo de la fragilidad intrínseca del ácido poliláctico se definen diversas hipótesis de trabajo para solucionar o minimizar estos efectos. Por un lado, se aborda la mejora mediante la fabricación de mezclas binarias con un poliéster flexible, el poli(butilén adipato-co-tereftalato) – PBAT. En estas mezclas se valida el empleo de los aceites vegetales derivados de la semilla de algodón como plastificantes, extensores de cadena, compatibilizantes, etc. a través de las potenciales reacciones de los grupos funcionales de los aceites modificados (epoxi y anhídrido maleico) con los grupos hidroxilo de las cadenas terminales de ambos poliésteres. El segundo planteamiento, va más allá en el empleo de la semilla de algodón, ya que, por un lado, se emplea el aceite modificado según los procesos anteriores y, por otro lado, se emplean los residuos lignocelulósicos/proteicos obtenidos como subproducto en el proceso de extracción de los aceites por prensado en frío. Los resultados más interesantes de estas investigaciones se muestran resumidos en los **Capítulos IV.5 y IV.6**.

Capítulo IV.5.

“Manufacturing and compatibilization of PLA/PBAT binary blends by cottonseed oil-based derivatives”

Capítulo IV.6.

“Processing and characterization of environmentally friendly composites from poly(lactic acid) and cottonseed waste materials”

IV.1

IV.1. Development of Environmentally Friendly Composite Matrices from Epoxidized Cottonseed Oil.

A. Carbonell-Verdu¹, L. Bernardi², D. Garcia-Garcia¹, L. Sánchez-Nacher¹, R. Balart¹

¹ **Materials Technology Institute (ITM)**
Universitat Politècnica de València (UPV)
Plaza Ferrandiz y Carbonell 1, 03801, Alcoy, Alicante (Spain)

² **Centro de Tecnología (CT)**
Universidade Federal de Santa Maria (UFSM)
Santa Maria - RS, 97105-900, Brasil

"Development of Environmentally Friendly Composite Matrices from Epoxidized Cottonseed Oil"

Abstract

The continuous rise in oil prices has led to the use of other ways to obtain polymer materials. This paper proposes a methodology to obtain a thermosetting resin from cottonseed oil by epoxidation process. The cottonseed oil contains as most representative fatty acids: 52.5% of linoleic acid (C18: 2), 23.9% of palmitic acid (C16: 0) and 17.6% of oleic acid (C18: 1); the real iodine index, which is indicative of the number of double bonds, has a value of 107. Epoxidized cottonseed oil (ECSO) has been successfully obtained using conventional epoxidation process with hydrogen peroxide, acetic acid and sulfuric acid, maintaining a constant temperature of 70 °C with homogeneous magnetic stirring. Average oxirane oxygen content (OOC) of 5.32% can be obtained by conventional epoxidation process which represents a yield over 83%. The epoxidized oil has been crosslinked with mixtures of two cyclic anhydrides to tailor different properties on final crosslinked thermosetting resins: on the one hand, methyl nadic anhydride (MNA) which is characterized by a rigid molecular structure and on the other hand, dodecenylsuccinic anhydride (DDSA) with a long side chain that can confer flexibility. The crosslinking process has been followed by dynamic differential scanning calorimetry (DSC), ionic mobility and oscillatory rheometry (OR) as well as gel time determination. The effect of the hardener mixture (wt. % DDSA:MNA) on mechanical performance of cured materials has been followed by flexural and impact tests as well as the evolution of the storage modulus (G') by dynamic mechanical analysis (DMA) in torsion mode. By selecting the appropriate hardener mixture, it is possible to obtain crosslinked materials with different properties ranging from stiff matrices for ECSO crosslinked with MNA to flexible matrices for ECSO cured with DDSA. This has occurred with other thermosetting resins like epoxidized soy bean oil (ESBO) or epoxidized linseed oil (ELO).

Keywords

Cottonseed oil; Epoxidation; Dodecenylsuccinic anhydride; Biobased epoxy resin.

IV.1.1. Introduction.

The increasing concern about the environmental impact of polymer materials together with the problems related to petroleum depletion act as driving forces to replace petroleum-based polymer materials by others from renewable resources with a marked environmental efficiency and, in many cases, giving solution to industrial wastes. In the field of thermosetting resins, important advances have been obtained by using vegetable oils which can be converted into epoxy resins by different epoxidation methods. [1, 2] Currently some epoxidized oils are marketed industrially in large quantities such as soybean with a production of 200,000 t/year [3]. Vegetable oils with high content of unsaturated fatty acids such as oleic acid, linoleic acid and linolenic acid may be used to obtain epoxy groups [4] by using several epoxidation processes. [5-7] A schematic representation of the epoxidation process from cottonseed oil (CSO) is shown in **Figure IV.1.1.**

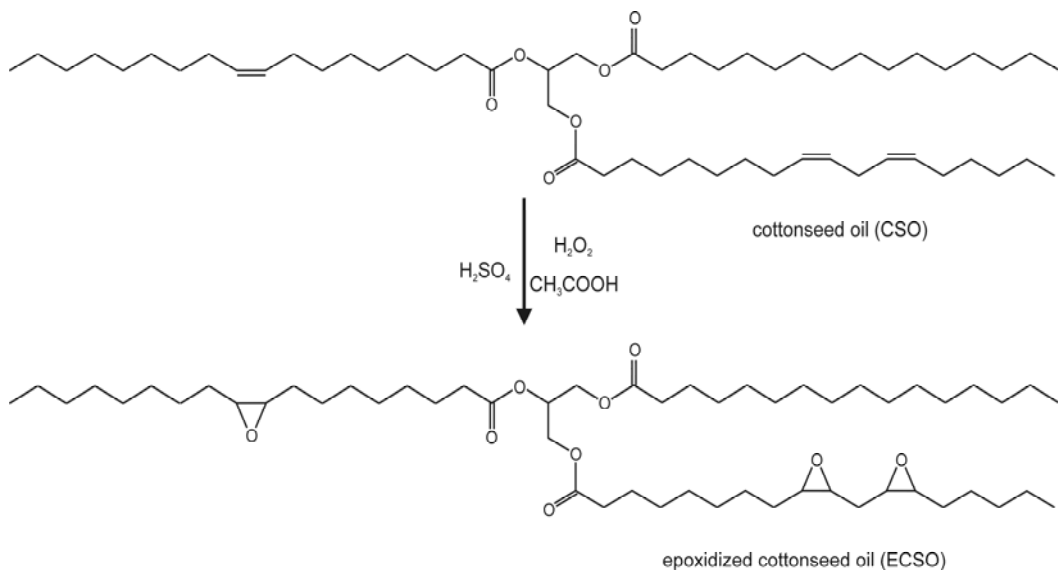


Figure IV.1.1. Schematic representation of the epoxidation process from cottonseed oil (CSO).

In the last decade, different epoxidation processes have been successfully used to obtain epoxidized vegetable oils (EVOs) being soybean oil (SBO) and linseed oil (LO) the most used with difference but it has been reported the use of sunflower oil [8, 9] wheat

oil [10] castor oil [11] or fish oil [12] with attracting uses as industrial plasticizers. The suitability of a vegetable oil to be subjected to an epoxidation process is directly related to the total content on unsaturated fatty acids being the iodine index a high representative value for the presence of unsaturations which can be converted into oxirane rings. The epoxidation of a fatty acid is a carbon-carbon double bond reaction with active oxygen, which results in the addition of an oxygen atom, which converts the original double bond into a three member ring (oxirane) [13]. The obtained epoxides may have several applications: they can be used as plasticizers for PVC [14], also as thermosetting resins for composites or as stabilizers for plastics and coatings [2].

Cottonseed oil can be considered as a co-product or by-product of the cotton industry and it finds some uses as edible oils [15] although there is some controversy on the potential health effects due to presence of some components such as gossypol [16, 17] and less strict control than all other plants whose main product is vegetable oil; cottonseed oil is also used for soap making, cosmetics and pharmaceuticals as well as a raw material in the manufacture of plastics, fungicides, paper, textiles, fuel, etc. [18, 19] Epoxidation is another way of using this oil since the global production was 5 million tons in 2011 [20] and its potential in the composites' industry is really promising.

Epoxidized vegetable oils can be crosslinked with different compounds. In contrast to terminal epoxides (typical of petroleum-based epoxies) that can be easily reacted with amines (even at room temperature) to give fully cured materials, the epoxy groups in epoxidized vegetable oils are not located in terminal positions so that, reaction with amines is difficult. [21] Reaction of non-terminal groups proceeds with carboxylic acids; so that, cyclic anhydrides derived from dicarboxylic acids have been proposed as attractive curing agents for EVOs. Maleic anhydride (MA) and phthalic anhydride (PA) have been used as hardeners for epoxy resins; nevertheless, as they have a melt point of 52.8 °C and 131.6 °C respectively, the formulation needs previous heating to homogenize mixture with the liquid resin. For this reason, low melting temperature cyclic anhydrides are preferable since they can be easily mixed with the EVO. Some cyclic anhydrides such as methyl hexahydrophthalic anhydride (MHHPA) and methyl tetrahydrophthalic anhydride (MTHPA) are liquids at room temperature and they are widely used as epoxy hardeners for high temperature thermosetting applications such as electric and electronic industry [22, 23]. In addition to these, other cyclic anhydrides such as alkenyl succinic anhydrides (ASA) have been proposed as curing agents for epoxy resins and the

effect of the side chain length on thermal and mechanical properties of crosslinked materials has been studied. [24-26] In general terms, it has been reported a decrease in tensile strength as the side chain length in ASA increases. The rigidity of the curing agent plays a key role on mechanical properties of cured materials. Although MHPA and MTHPA are quite rigid molecules, some derived structures offer more rigidity as it is the case of methyl nadic anhydride (MNA) characterized by the norbornene group which confers high rigidity [27] and this contributes to higher heat-distortion temperatures as well as higher stiffness on cured materials. [28]

The final stiffness of a cured epoxy not only depends on the rigidity of the curing agent molecule but also on the number of epoxy groups per triglyceride. The more epoxy groups, the higher number of crosslinking points can be achieved thus leading to more rigidity. The potential stiffness of a cured epoxide can be estimated by the equivalent epoxide weight (EEW) which represents the ratio between the molecular weight of the triglyceride and the average number of epoxide groups. Commercial epoxidized linseed oil (ELO) offers EEW in the 170-190 g equiv-1 range while epoxidized soybean oil (ESBO) is characterized by lower EEW values in the 230-240 g equiv-1 range (both values can vary depending on the purity on certain fatty acids such as linolenic and linoleic acids). In general terms, cured ELO epoxies are stiffer than ESBO cured materials. [29]

The main aim of this work is to evaluate the potential of cottonseed oil (CSO) as base material for obtaining epoxy-based thermosetting resins by epoxidation with in-situ generated peracetic acid obtained from hydrogen peroxide and acetic acid. The first part of the manuscript is focused on characterizing the epoxidation efficiency and the second part is focused on the study of the curing process of epoxidized cottonseed oil (ECSO) with mixtures of two cyclic anhydrides as well as the characterization of the final properties of the crosslinked materials. Anhydride mixtures were prepared with a flexible anhydride (DDSA- dodecenylsuccinic anhydride) and a highly rigid anhydride (MNA-methyl nadic anhydride) to tailor the desired properties on fully cured materials.

IV.1.2. Experimental.

Materials.

The PLA used in this work was a commercial grade IngeoTM Biopolymer 6201D.

The base vegetable oil for epoxidation was cottonseed oil (CSO) with a iodine value provided by the manufacturer between 109 and 120 with a density of 0.92 g cm⁻³.

The epoxidation process was carried out with *in situ* generated peracetic acid from acetic acid (99.7% from Sigma Aldrich) and hydrogen peroxide (30 % v/v supplied by Panreac Química) in acid media: sulfuric acid (96%) supplied by Panreac Química.

Formulations to crosslink epoxidized cottonseed oil were based on two different hardeners: on the one hand, a flexible cyclic anhydride namely dodecenylsuccinic anhydride (DDSA) with an anhydride equivalent weight (AEW) of 268.39 g equiv⁻¹ and on the other hand a rigid cyclic anhydride, methyl nadic anhydride (MNA) with an AEW of 178.2 g equiv⁻¹. Both curing agents were supplied by Sigma Aldrich. The EEW:AEW ratio was set to 1:1 and additional 1 wt. % glycerol (Sigma Aldrich) and 2 wt. % 1-methyl imidazole, 1-MI (Sigma Aldrich) were added as initiator and accelerator components respectively. **Figure IV.1.2** shows the chemical structures of the different components used to crosslink the epoxidized cottonseed oil.

For the characterization of the crosslinked resins, liquid resins were placed on a silicon mold with rectangular shapes (80 x 10 x 4 mm³) for mechanical characterization. The curing cycle consisted on isothermal curing process at 110 °C for 3 h.

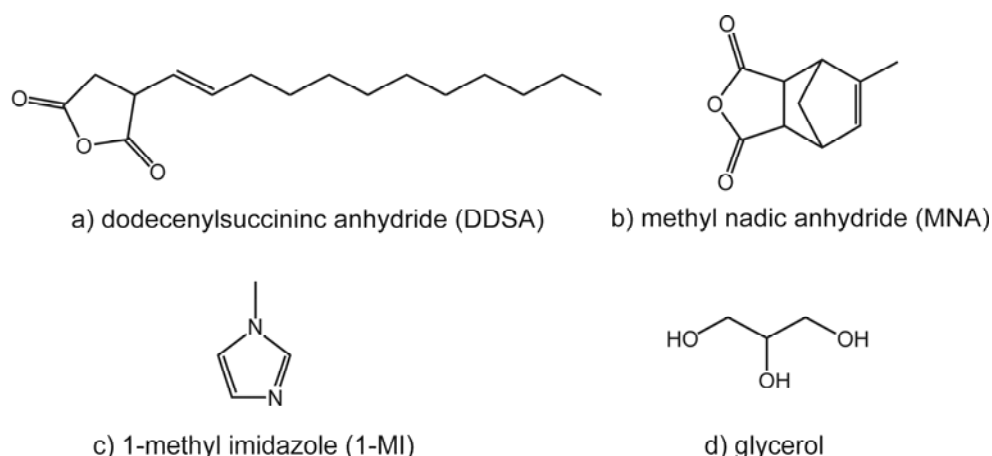


Figure IV.1.2. Schematic representation of different components used to crosslink epoxidized cottonseed oil.

Epoxidation process.

Epoxidation was carried out in a 500 mL three-neck round-bottom flask equipped with a heating mantle. A thermometer was connected to a neck to ensure constant temperature during reaction; the second neck was connected to a reflux condenser and the third neck was used to drop reactives and ensure inert atmosphere.

The procedure is summarized as follows: 188 g of cottonseed oil were added to the flask and magnetic stirring was maintained until a temperature of 55 °C was reached; then 19.7 mL of acetic acid was added. After 10 min at 55 °C, 192 mL (for a 3:1 ratio) hydrogen peroxide were added together with 1.52 mL of sulfuric acid. The mixture was added drop by drop in order to trigger the onset of the reaction using a dropping funnel over 30 min. The working temperature was 70 °C for 8 h; special attention was paid to reaction temperature after peroxide addition. Nitrogen atmosphere was used during peroxide addition to avoid an abrupt exothermic reaction. Samples were collected every two hours to analyze the iodine index according to Wij's method (ISO 3961:2009) [30] and oxirane oxygen (ASTM D1652-97) [31] with previous cleaning with distilled water and subsequent purification by centrifugation. Following the considerations of the ISO 3961:2009 the iodine value (W_I) has been calculated by the next formula:

$$W_t = 12.69 C (V_1 - V_2) / m$$

Equation IV.1.1

Where C is the concentration of the sodium thiosulphate (mol/mL), V_1 is the volume of standard sample sodium thiosulphate (mL), V_2 is the volume of sodium thiosulphate used in the determination (mL), and m is the mass of the analysis (g).

Characterization of the curing process of ECSO by oscillatory rheometry (OR). .

Evolution of the curing process was followed by plate-plate oscillatory rheometry in a AR-G2 rheometer (TA Instruments, New Castle, USA) with parallel plates ($D = 25$ mm). The smallest possible amount of mixture was prepared and placed between the two plates by setting the program to an isothermal curing at 110 °C and 120 °C for 4 hours because these are the minimum temperatures required for initiation of curing process. The controlled variables were a frequency of 1 Hz and at a constant deformation of 0.1%. Evolution of the storage modulus (G'), loss modulus (G'') and phase angle (δ) were obtained in terms of time. The last parameters have been calculated by the next formulae:

$$G' = \frac{\sigma_0 \cdot \cos(\delta)}{\varepsilon_0}$$

Equation IV.1.2

$$G'' = \frac{\sigma_0 \cdot \sin(\delta)}{\varepsilon_0}$$

Equation IV.1.3

$$\tan(\delta) = \frac{G''}{G'}$$

Equation IV.1.4

Where σ_0 is the stress and ε_0 is the strain.

In addition to this, gel time was also determined by following the guidelines of the DIN 16945 [32] in a TC-4 Gelnorm Geltimer (Gel Instrumente AG, Germany, Oberuzwill). Tests were conducted at 110 °C and 120 °C.

The evolution of the curing process was also followed by dielectric measurements with a Gelnorm DE (Gel Instrumente AG, Germany, Oberuzwill) in isothermal conditions according to DIN 16945 [32] equipped with a thermocouple sensor to ensure constant temperature. A small amount of the liquid formulation was placed on a hot plate 50 mm in diameter. The gold sensor sized 17x55x0.04 mm³ was embedded into the liquid resin to measure ionic conductivity by dielectric properties. Tests were carried out at 110 °C and 120 °C.

Additionally, the curing process was followed by dynamic differential scanning calorimetry (DSC) in a Mettler-Toledo DSC 821e (Mettler-Toledo S.A.E., Barcelona, Spain). 5-10 mg of the liquid formulations were placed inside standard 40 µL Al crucibles and subjected to a heating program from 30 °C to 350 °C at a heating rate of 10 °C min⁻¹ with a constant nitrogen flow rate of 40 mL min⁻¹.

Mechanical characterization of the crosslinked resins

The fracture toughness was evaluated using a Charpy pendulum from Metrotec (Metrotec SA, San Sebastian, Spain) with an energy of 6 J according to ISO 179 [33].

Flexural properties of the cured formulations were obtained in a universal test machine Ibertest 300 (Elib 30, E Ibertest S.A., Madrid, Spain) following the guidelines of the UNE-EN-ISO 178 [34]. All the tests were carried out at a speed of 5 mm min⁻¹. Each test was repeated at least five times and average values were used in data analysis.

Additionally, DMA characterization was carried out in a AR-G2 oscillatory rheometer (TA Instruments, New Castle, USA) equipped with DMA (shear-torsion mode) for solid samples. Samples 40x10x4 mm³ were subjected to a temperature sweep program from 30 to 140 °C at a heating rate of 5 °C min⁻¹ at a constant deformation (γ) of 0.1% and a frequency of 1 Hz.

Scanning electron microscopy (SEM) of fractured surfaces from impact tests were observed in a FEI, mod. Phenom (FEI Company, Eindhoven, The Netherlands) at a 5 kV accelerating voltage. Samples were covered with an ultrathin gold-palladium alloy with a sputter coater EMITECH mod. SC7620 (Quorum Technologies Ltd, East Sussex, UK).

IV.1.3. Results and discussion.

■ Optimization of the epoxidation conditions

Initially the cottonseed oil epoxidation was carried out with different equivalent molar ratio between peroxide and cottonseed oil, 1.5 and 3 to optimize the formulation for epoxidation. **Figure IV.1.3** shows a plot representation of the effect of the excess H₂O₂ on the efficiency of the epoxidation process. It can be clearly concluded that an excess molar ratio (peroxide:oil) of 3:1 gives higher values of oxirane oxygen for an epoxidation time of 8 h than the use of an excess molar ratio of 1.5:1.

The theoretical oxirane oxygen index calculated from the average values of fatty acid content in cottonseed oil is 6.4%. As we can see, the oxirane oxygen reaches values of about 5.32% after 8 h (for a peroxide:oil ratio of 3:1 which represents about 83% yield reaction by taking into account the oxirane oxygen criteria). Nevertheless, the initial iodine index (107) is reduced up to values of 1.79 after 8 h reaction time which indicates a 98.3% conversion of double bonds but it is important to take into account some parallel reactions which involve epoxy homopolymerization among others that do not contribute to an increase in the oxirane oxygen value but the conversion of double bonds and this fact leads to disparity in the conversion values by considering different criteria. The reaction proceeds quickly at the first two hours due to high availability of double bonds and almost no changes are observed over 8 h reaction time.

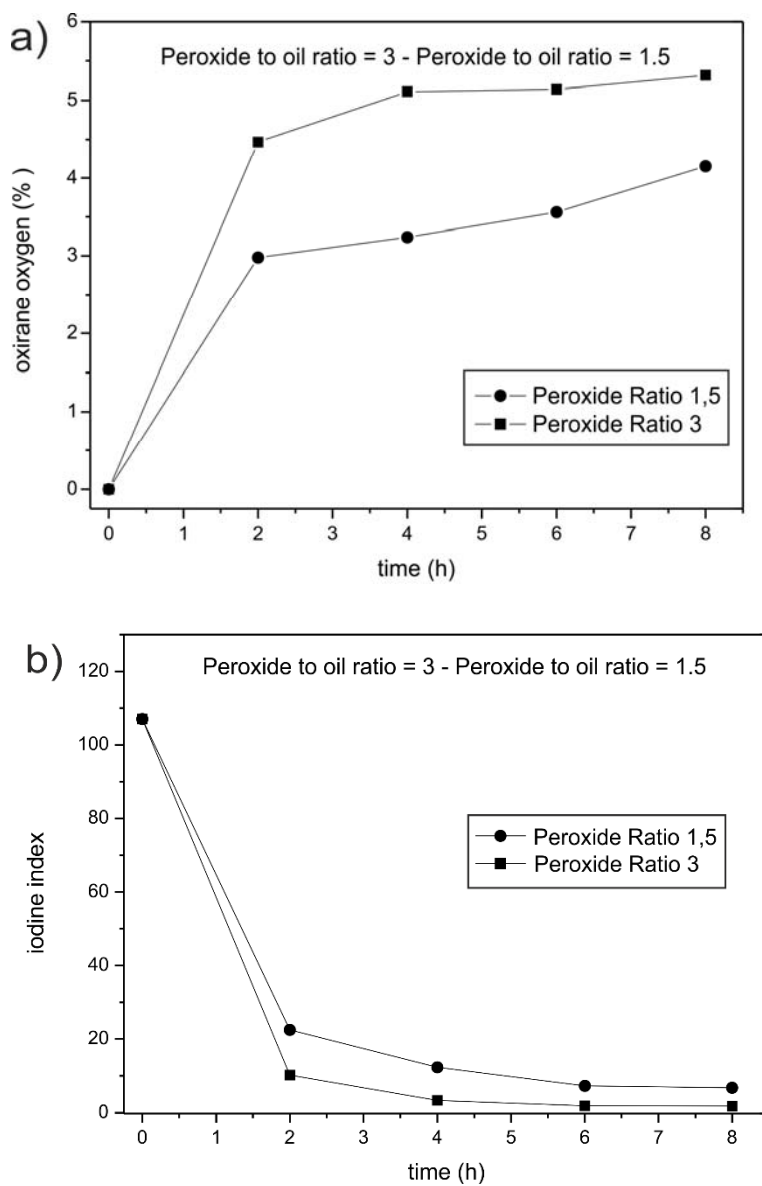


Figure IV.1.3. Influence of peroxide to oil ratio on a) oxirane oxygen change index during epoxidation of cottonseed oil and b) iodine index change during the epoxidation reaction.

Curing of epoxidized cottonseed oil with cyclic anhydrides.

As we have described previously, dodecenylsuccinic anhydride (DDSA) and methyl nadic anhydrides (MNA) can provide different properties to the crosslinked epoxidized cottonseed oil (ECSO) since DDSA could contribute to more flexible structures than those obtained with MNA due to differences in molecular rigidity. By combining these two cyclic anhydrides, it is possible to tailor a crosslinked material to the desired properties. For this reason, DDSA:MNA mixtures have been tested as crosslinking systems for epoxidized cottonseed oil.

Table IV.1.1 shows a summary of the gel time values for isothermal curing processes with different DDSA:MNA mixture hardener. The use of anhydride hardeners needs high curing temperatures in order to trigger the curing reaction and reach the gel time; so that, gel time at two different temperatures were compared. In addition, the curing rate is also related to the chemical structure of the cyclic anhydride which can contribute to accelerate or to delay the curing reaction, depending on chain length, chain mobility, etc. [35]

On the other hand, it is important to take into account the anhydride equivalent weight of each cyclic anhydride which can play an important role in the viscosity increase and, subsequently, decrease in gel time values. DDSA is characterized by a AEW of 268.39 g equiv⁻¹ while MNA possesses an equivalent weight of 178.2 g equiv⁻¹. Reaction of one epoxide group in ECSO with one DDSA molecule leads to higher molecular weight crosslinked structure than in the case of MNA and this is directly related to viscosity increase so that, viscosity increase occurs faster for the system cured with DDSA and this means lower gel time values.

Table IV.1.1. Gel time values at isothermal conditions for the crosslinking of epoxidized cottonseed oil (ECSO) with mixtures of dodecenylsuccinic anhydride (DDSA) and methyl nadic anhydride (MNA) at a constant EEW:AEW of 1.

DDSA (wt %)	MNA (wt %)	*Gel time (min) at 110 °C	*Gel time (min) at 120 °C
100	0	32	19
75	25	35	19
50	50	40	22
25	75	48	27
0	100	61	34

* Gel time values obtained as described in the DIN 16945 standard.

One interesting technique to follow up the curing of a thermosetting resin is by monitoring the evolution of the ionic mobility (obtained by dielectric measurements) with time. **Figure IV.1.4** shows the plot evolution of the ionic mobility *versus* time for different DDSA:MNA mixture hardeners. As time increases, the initial ionic mobility (expressed as percentage value, 100 %) decreases up to a constant value (asymptotic curve) which indicates fully curing of the epoxidized cottonseed oil. Initially, the liquid formulation allows the polar groups to rearrange as the electric field changes of polarity. As the crosslinking occurs, some polar groups are attached to higher molecular weight structures and steric restrictions can occur and this can block motions of polar groups thus making difficult to rearrange with the electric field change.

As expected, DDSA is a flexible molecule that enables ion mobility. As we can see in **Figure IV.1.4[a]** and **[b]**, the ionic mobility of ECSO cured with DDSA decreases in a great extent if compared with the curves corresponding to ECSO cured with MNA. Presence of a flexible (high chain mobility) hardener allows the ionic mobility to change from 100% up to values of about 57% after a curing time of about 150 min. In the case of the curing with rigid (low chain mobility) molecules such as MNA, the ionic mobility is highly restricted so that, it only changes from 100% up to values of 66%. [36, 37]

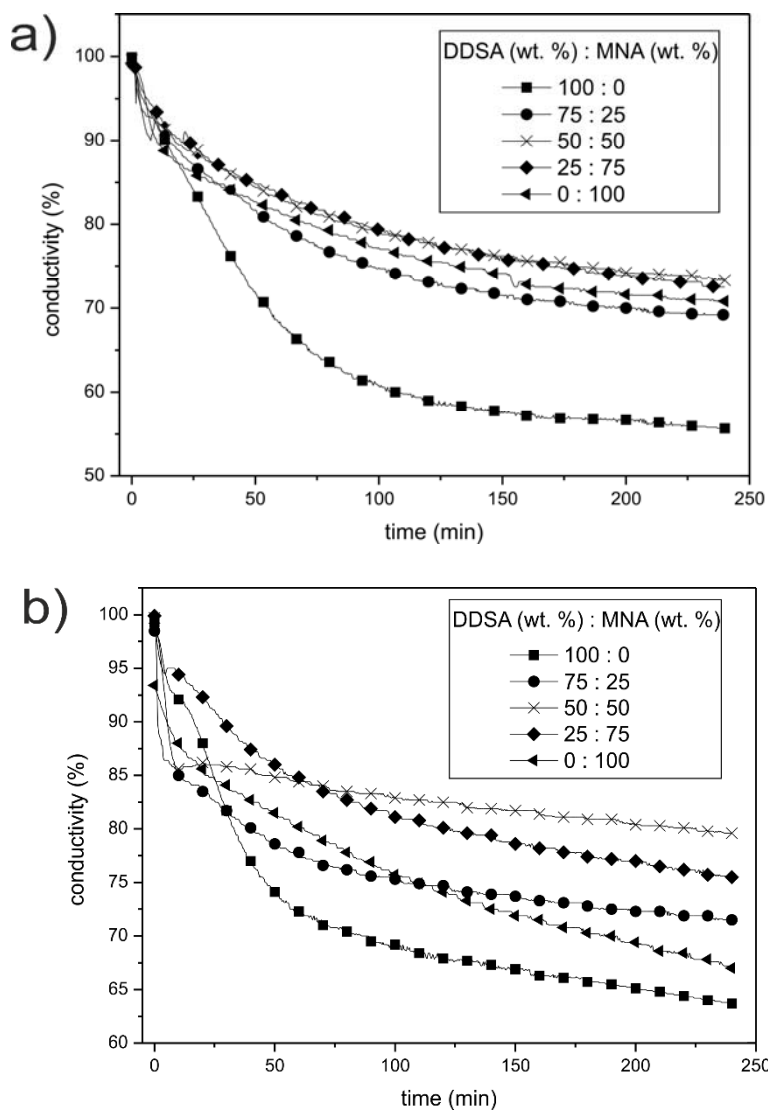


Figure IV.1.4. Plot evolution of the crosslinking of epoxidized cottonseed oil (ECSO) with mixtures of dodecenylsuccinic anhydride (DDSA) and methyl nadic anhydride (MNA) at a constant EEW:AEW of 1 in terms of the variation of the ionic mobility with time a) 110 °C and b) 120 °C.

The ability of each cyclic anhydride to react with epoxidized cottonseed oil can be also followed by dynamic differential scanning calorimetry (DSC). **Figure IV.1.5** shows a comparative plot of the DSC curing profiles of ECSO with different DDSA:MNA mixtures. It can be clearly observed that the peak temperature, which corresponds to the maximum reaction rate, is displaced up to higher values as the rigid anhydride content increases. The temperature peak for the system cured with DDSA is close to 179.2 °C and

this is increased up to values of 198.47 °C for the system cured with MNA. These results indicate that reaction of ECSO with DDSA occurs in a more easy way than using MNA and these results are consistent with those previously described about the gel time since we have observed that MNA leads to higher gel time values than DDSA.

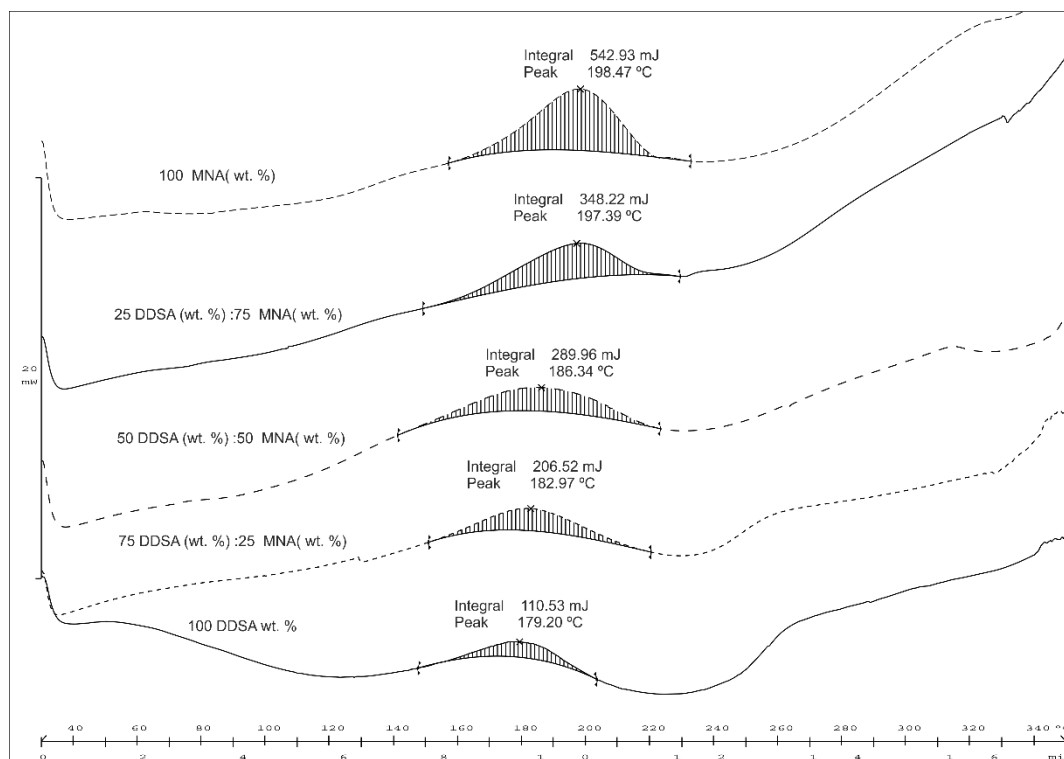


Figure IV.1.5. Comparative plot of the dynamic DSC curing curves of epoxidized cottonseed oil (ECSO) with mixtures of dodecenylsuccinic anhydride (DDSA) and methyl nadic anhydride (MNA) at a constant EEW:AЕW of 1.

Plate-plate oscillatory rheometry is highly useful to monitor the curing process by following the evolution of the storage modulus (G') or the phase angle (δ). At the early stages of the curing process, the liquid formulation is characterized by a high phase angle (close to 90 °C) and very low values of storage modulus (G'). As the crosslinking process occurs, the molecular weight of the cured material increases and, subsequently, the phase angle decreases; on the other hand, the storage modulus increases due to an increase in the elastic behavior of the material. This situation can be observed in **Figure IV.1.6** for the crosslinking reaction of epoxidized cottonseed oil with DDSA:MNA mixture hardeners for isothermal curing at 110 °C (**Figure IV.1.6[a]**) and 120 °C (**Figure**

IV.1.6[b]). As it has been described previously, reaction of epoxidized cottonseed oil with dodecenylsuccinic anhydride is faster than with methyl nadic anhydride. The gel time values are lower for the system cured with DDSA in comparison to MNA-cured ECSO. On the other hand, the temperature peak by dynamic DSC is lower for DDSA cured ECSO if compared to MNA cured ECSO.

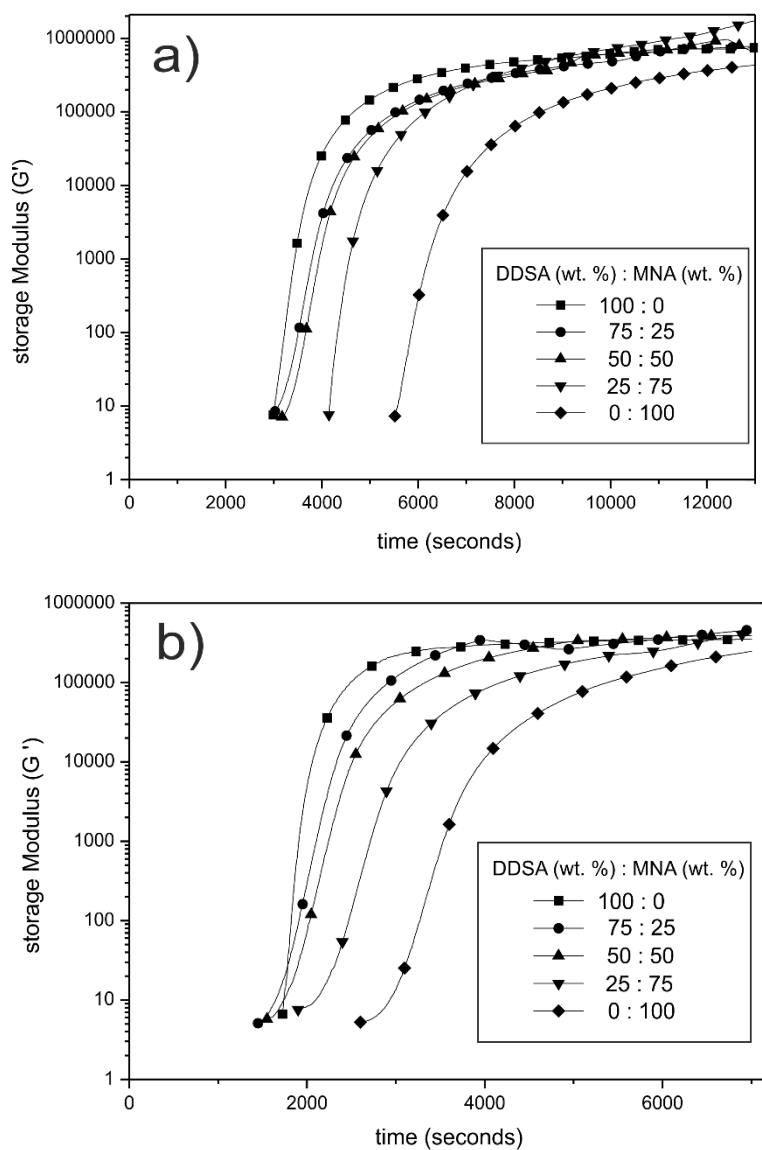


Figure IV.1.6. Comparative plot of the evolution of the storage modulus (G') for the curing of epoxidized cottonseed oil (ECSO) with mixtures of dodecenylsuccinic anhydride (DDSA) and methyl nadic anhydride (MNA) at a constant EEW:AEW of 1, obtained by plate-plate oscillatory rheometry at a constant temperature of a) 110 $^{\circ}\text{C}$ and b) 120 $^{\circ}\text{C}$.

This situation can also be observed by plate-plate oscillatory rheometry. The curing curve (G' vs time) for ECSO with DDSA is placed at the left while the cure curve for ECSO:MNA is remarkably displaced to longer times thus indicating that curing with DDSA occurs in a faster way. This is probably due to the fact that DDSA possesses higher anhydride equivalent weight and this leads to formation of high molecular weight crosslinked structures than in the case of MNA with a lower anhydride equivalent weight. This situation is repeated at both isothermal curing temperatures, 110 °C and 120 °C. Nevertheless, as the curing temperature increases, the curing profiles (G' vs time) move to lower times thus indicating more faster curing reactions. The use of DDSA:MNA mixture hardeners leads to intermediate curing profiles between the two extreme curves corresponding to DDSA and MNA-cured ECSO.

The phase angle (δ) follows similar tendency. Initially, the phase angle is close to 90° corresponding to typical newtonian liquid behaviour in which the response (elongation) is 90° delayed with regard to the applied dynamic stress. As the phase angle decreases, the crosslinking reaction occurs until δ reaches values close to 0° which are representative for typical elastic behaviour of solids in which the response (elongation) is not delayed (in-phase) with regard to the applied dynamic stress (immediate response). As we can see in **Figure IV.1.7** for two different isothermal curing conditions (110 °C and 120 °C), curing with DDSA starts at lower times if compared to curing with MNA. This is in accordance with the gel time values shown before as well as the evolution of the storage modulus (G'). The chemical structure of MNA and DDSA plays a key role in both curing reaction rate and mechanical properties of cured materials. In a first approach, DDSA structure allows reaction at lower temperatures than MNA; this fact is directly related to the structure since anhydride group in DDSA is more accessible than anhydride group in MNA due to molecular complexity. In general terms, DDSA possesses a flexible structure while MNA is characterized by a rigid structure.

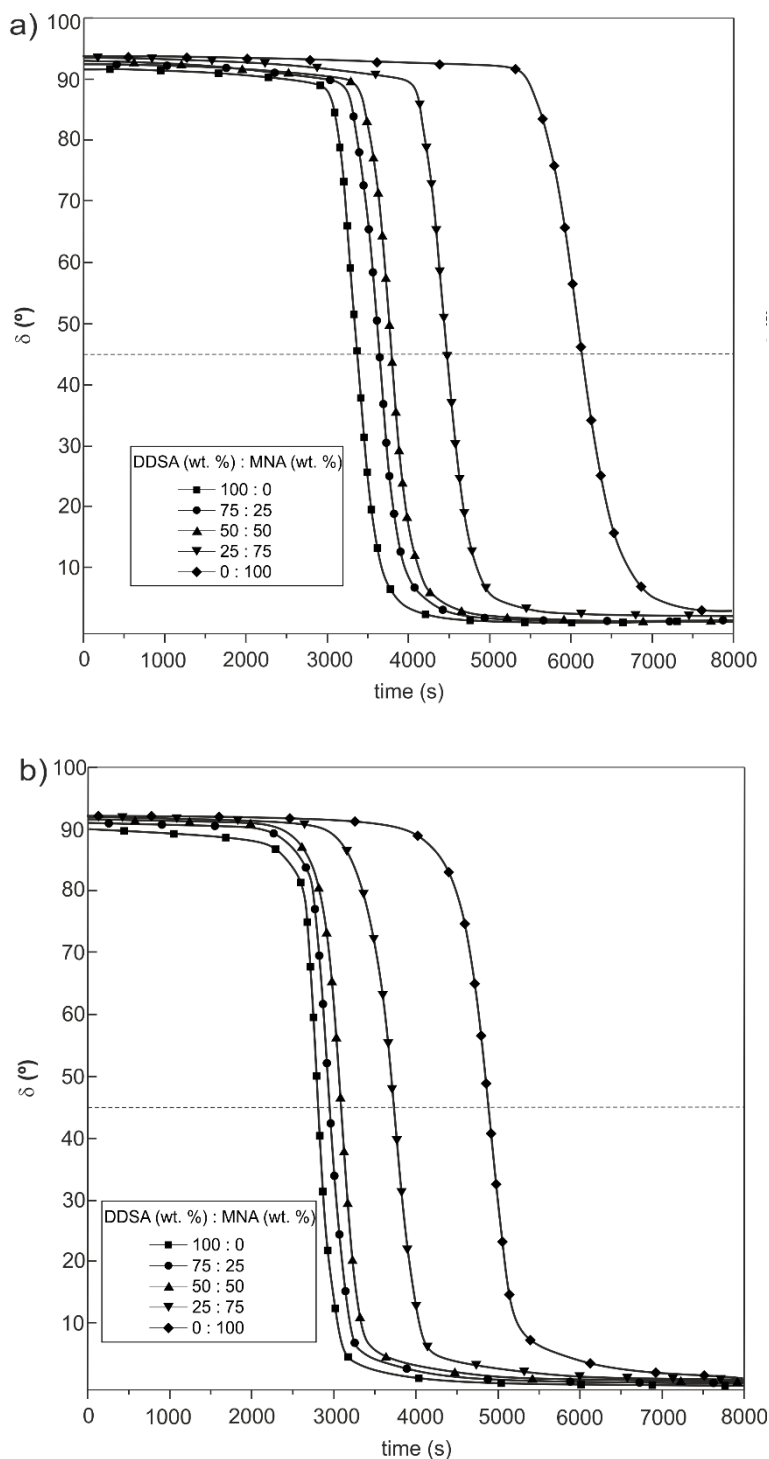


Figure IV.1.7. Comparative plot of the evolution of the phase angle (γ) for the curing of epoxidized cottonseed oil (ECSO) with mixtures of dodecenylsuccinic anhydride (DDSA) and methyl nadic anhydride (MNA) at a constant EEW:AEW of 1, obtained by plate-plate oscillatory rheometry at a constant temperature of a) 110 °C and b) 120 °C.

Characterization of the crosslinked resins.

The final properties of a thermosetting resin highly depend on several issues such as resin to hardener ratio, hardener structure, curing cycle, post curing, etc. The structure of the hardener not only influences the curing behavior of ECSO-based thermosetting resins but also the final properties of the fully cured materials. Table 2 summarizes some mechanical properties of fully cured ECSO-based thermosetting resins crosslinked with different DDSA-MNA mixtures using the same resin to hardener ratio (EEW:AEW = 1:1) and same curing cycle (3 h at 110 °C). So that it is possible to evaluate the influence of the hardener mixture on final properties of crosslinked materials. In a first approach, as DDSA is characterized by a flexible structure with a long side chain it could provide flexibility to crosslinked ECSO while the highly rigid molecule of MNA could restrict chain mobility thus providing stiffness.

Table IV.1.2. Results of mechanical properties of the ECSO cured resin during bending and impact tests.

DDSA (wt. %)	MNA (wt. %)	Flexural Modulus (MPa)	Max Flexural Strength (N)	Impact Resistance (kJ m⁻²)
100	0	38.95 ± 1.34	11.7 ± 1.84	3.32 ± 0.31
75	25	47.42 ± 1.46	14.5 ± 0.1	2.97 ± 0.52
50	50	92.43 ± 7.96	19.05 ± 3.89	2.55 ± 0.44
25	75	110.89 ± 7.04	23.15 ± 0.35	2.35 ± 0.29
0	100	151.19 ± 4.15	29.45 ± 0.21	1.92 ± 0.32

As we can see in **Table IV.1.2**, the flexural modulus of ECSO crosslinked with DDSA is 38.9 MPa, which is remarkably lower to the flexural modulus of ECSO cured with MNA with values of about 151.2 MPa. As expected, as the DDSA content in DDSA:MNA mixtures increases, we observe a clear increase in flexural modulus. Similar tendency can be observed in flexural strength. So, that MNA contributes to an increase in mechanical resistant properties. On the other hand, DDSA contributes to good ductile properties as observed in **Table IV.1.2** with impact resistance which changes from 1.92 kJ m⁻² (MNA-cured ECSO) up to twice values (DDSA-cured ECSO).

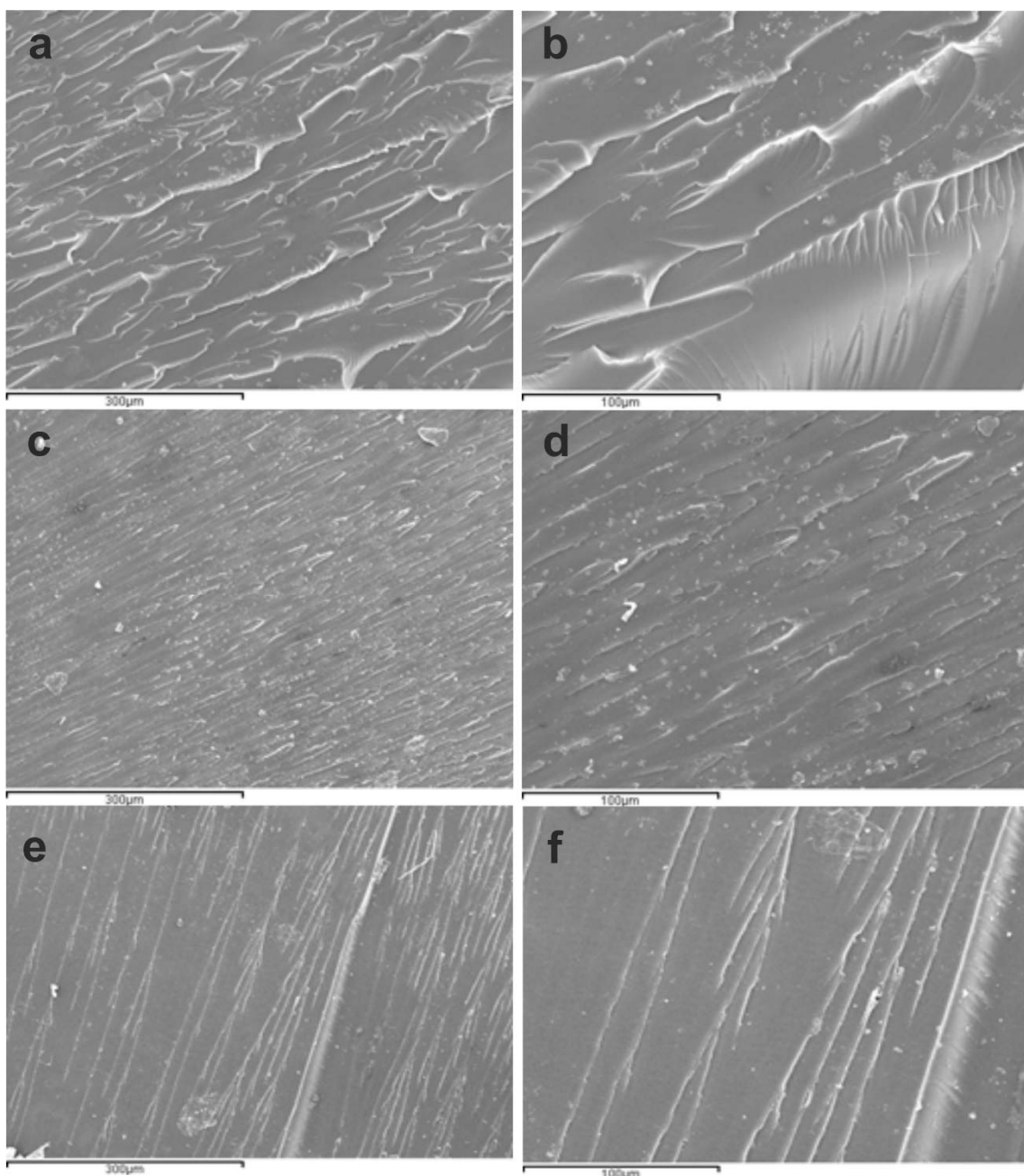


Figure IV.1.8. SEM images of the fractured surfaces from Charpy test corresponding with different DDSA:MNA mixture impact fracture of the curing with a) 100% DDSA, x200, b) 100% DDSA, x500, c) 50% DDSA:50% MNA, x200, d) 50% DDSA:50% MNA, x500, e) 100% MNA, x200, f) 100% MNA, x500.

Fracture surfaces of crosslinked ECSO show some differences in topographies between DDSA-cured ECSO (**Figure IV.1.8[a] & [b]**) and MNA-cured ECSO (**Figure IV.1.8[e] & [f]**) as it is shown in **Figure IV.1.8**. Fractured surface of DDSA-cured ECSO (**Figure IV.1.8[a] & [b]**) shows typical fracture of a rigid thermosetting material with quite smooth surface together with a fractal edge formation due to fracture mechanism with a main advancing front of a crack (longitudinal) and multiple microcracks growing perpendicular to this main axis and so on. With regard to the fractured surface of MNA-cured ECSO (**Figure IV.1.8[e] & [f]**) we also observe a fragile fracture surface but in this case, due to fragility, we do not observe the typical fractal formation. It is only observable the main advancing front of the crack. Intermediate compositions such as 50% DDSA:50% MNA (**Figure IV.1.8[c] & [d]**) offer a fracture surface topography intermediate between the two individual (DDSA and MNA) cured ECSO.

Figure IV.1.9 shows the dynamic behavior of ECSO-based cured materials subjected to a temperature ramp. The evolution of the storage modulus (G') is useful to compare the effect of the hardener composition on final properties. As we can see in **Figure IV.1.9**, G' shows a remarkable decrease in the 50-70 °C range which corresponds to the glass transition range. G' curve for DDSA-cured ECSO starts at values of about $3 \cdot 10^7$ Pa whilst the G' curve for MNA-cured ECSO starts at $1 \cdot 10^8$ Pa thus indicating that MNA-cured ECSO is stiffer than DDSA-cured ECSO as expected. These results are in total agreement with previous flexural properties. With regard to intermediate DDSA:MNA compositions as hardener, G' curve is placed between the two extreme curves corresponding to DDSA- and MNA-cured ECSO respectively. As we can see, all compositions overcome soft as T_g is reached but the difference in behavior after the glass transition temperature is not as remarked as prior to T_g . By taking the glass transition temperature as the $\tan \delta$ maximum, we can see the T_g value for the DDSA-cured ECSO is located at about 57 °C while the T_g value for MNA-cured ECSO is close to 65 °C which is slightly higher.

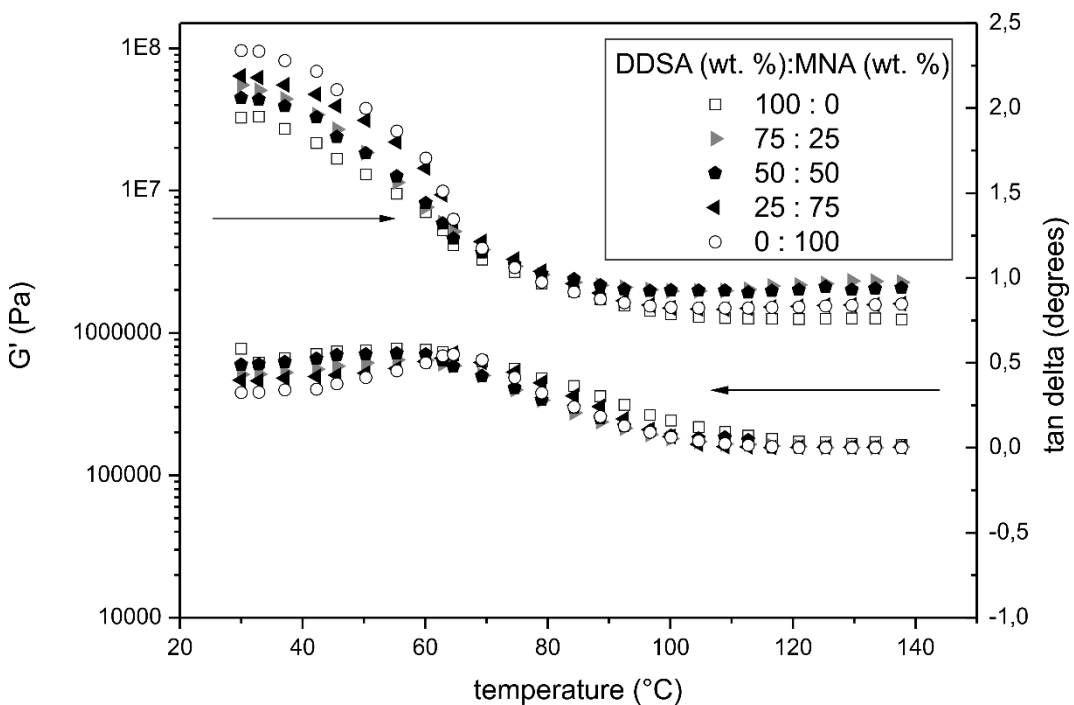


Figure IV.1.9. Plot evolution of the storage modulus (G') and $\tan \delta$ for solid ECSO-based thermosetting resins cured with different DDSA:MNA mixture hardeners in terms of temperature.

IV.1.4. Conclusions.

As the cotton industry demands high cotton plant productions, cottonseed oil (CSO) appears as a by-product of this industry and despite some applications in the food industry are addressed for this oil (with some controversy on its healthy benefits), new additional uses must be developed to absorb the high volume of cottonseed oil. This work reports the potential use of cottonseed oil as base material for obtaining bio-based epoxy resins for the composites' industry.

The resins resulting from the cottonseed oil epoxidation can offer attracting alternatives to some petroleum-derived epoxy resins. The epoxidation of cottonseed oil with peroxide increased the final yield with a peroxide:oil ratio of 3:1 with final oxirane oxygen number of 5.32% which is a slightly lower value if compared to conventional

epoxidized soybean oil (ESBO); so that, epoxidized cottonseed oil (ECSO) can compete with ESBO for similar applications (flexible thermosetting resin, plasticizer, additive for high rigidity epoxies, etc.).

Interesting thermosetting solid resins can be obtained by curing ECSO with cyclic anhydrides. In particular, by combining a flexible anhydride (dodecenylsuccinic anhydride, DDSA) and a rigid anhydride (methyl nadic anhydride, MNA) it is possible to tailor the desired properties on final cured materials as DDSA confers some flexibility whilst MNA leads to more rigid materials.

Acknowledgements.

Authors thank Conselleria d'Educació, Cultura i Esport (Generalitat Valenciana) Ref: GV/2014/008 for financial support.

References.

- [1] J.D. Espinoza-Perez, B.A. Nerenz, D.M. Haagenson, Z. Chen, C.A. Ulven, D.P. Wiesenborn "*Comparison of Curing Agents for Epoxidized Vegetable Oils Applied to Composites*", Polymer Composites (2011) **32**, 1806-1816.
- [2] V.V. Goud, S. Dinda, A.V. Patwardhan, N.C. Pradhan "*Epoxidation of Jatropha (Jatropha curcas) oil by peroxyacids*", Asia-Pacific Journal of Chemical Engineering (2010) **5**, 346-354.
- [3] C.S. Cai, H.G. Dai, R.S. Chen, C.X. Su, X.Y. Xu, S. Zhang, L.T. Yang "*Studies on the kinetics of in situ epoxidation of vegetable oils*", European Journal of Lipid Science and Technology (2008) **110**, 341-346.
- [4] V.V. Goud, N.C. Pradhan, A.V. Patwardhan "*Epoxidation of karanja (Pongamia glabra) oil by H₂O₂*", Journal of the American Oil Chemists Society (2006) **83**, 635-640.
- [5] R. Turco, R. Vitiello, V. Russo, R. Tesser, E. Santacesaria, M. Di Serio "*Selective epoxidation of soybean oil with performic acid catalyzed by acidic ionic exchange resins*", Green Processing and Synthesis (2013) **2**, 427-434.
- [6] S. Sun, P. Li, Y. Bi, F. Xiao "*Enzymatic epoxidation of soybean oil using ionic liquid as reaction media*", Journal of Oleo Science (2014) **63**, 383-390.
- [7] O. Fenollar, D. Garcia-Sanoguera, L. Sanchez-Nacher, T. Boronat, J. Lopez, R. Balart "*Mechanical and thermal properties of polyvinyl chloride plasticized with natural fatty acid esters*", Polymer-Plastics Technology and Engineering (2013) **52**, 761-767.
- [8] M.T. Benaniba, N. Belhaneche-Bensemra, G. Gelbard "*Epoxidation of sunflower oil with peroxyacetic acid in presence of ion exchange resin by various processes*", Energy Education Science and Technology (2008) **21**, 71-82.
- [9] R.d.C.S. Schneider, L.R.S. Lara, T.B. Bitencourt, M.d.G. Nascimento, M.R. dos Santos Nunes "*Chemo-enzymatic epoxidation of sunflower oil methyl esters*", Journal of the Brazilian Chemical Society (2009) **20**, 1473-1477.

- [10] L.A. Boyaca, A.A. Beltran "*Soybean epoxide production with in situ peracetic acid using homogeneous catalysis*", Ingenieria e Investigacion (2010) **30**, 136-140.
- [11] S. Sinadinovic-Fiser, M. Jankovic, O. Borota "*Epoxidation of castor oil with peracetic acid formed in situ in the presence of an ion exchange resin*", Chemical Engineering and Processing (2012) **62**, 106-113.
- [12] D.W. Marks, R.C. Larock "*The conjugation and epoxidation of fish oil*", Journal of the American Oil Chemists Society (2002) **79**, 65-68.
- [13] P.K. Gamage, M. O'Brien, L. Karunananayake "*Epoxidation of some vegetable oils and their hydrolysed products with peroxyformic acid - optimised to industrial scale*", Journal of the National Science Foundation of Sri Lanka (2009) **37**, 229-240.
- [14] O. Fenollar, D. Garcia, L. Sanchez, J. Lopez, R. Balart "*Optimization of the curing conditions of PVC plastisols based on the use of an epoxidized fatty acid ester plasticizer*", European Polymer Journal (2009) **45**, 2674-2684.
- [15] R.D. O'Brien, P.J. Wan, *Cottonseed oil: Processing and utilization*. Proceedings of the World Conference on Oilseed Processing and Utilization, ed. R.F. Wilson. 2001. 90-140.
- [16] P. Amato, R.A. Quercia "*A historical perspective and review of the safety of lipid emulsion in pregnancy*", Nutrition in clinical practice: official publication of the American Society for Parenteral and Enteral Nutrition (1991) **6**, 189-92.
- [17] I.C.N. Gadelha, N.B.S. Fonseca, S.C.S. Oloris, M.M. Melo, B. Soto-Blanco "*Gossypol toxicity from cottonseed products*", Scientific World Journal (2014) 231635.
- [18] N. Hoda "*Optimization of biodiesel production from cottonseed oil by transesterification using NaOH and methanol*", Energy Sources Part a-Recovery Utilization and Environmental Effects (2010) **32**, 434-441.
- [19] W.W. Song, K.B. He, J.X. Wang, X.T. Wang, X.Y. Shi, C. Yu, W.M. Chen, L. Zheng "*Emissions of EC, OC, and PAHs from cottonseed oil biodiesel in a heavy-duty diesel engine*", Environmental Science & Technology (2011) **45**, 6683-6689.
- [20] Monografía semilla de algodón. 2011.

- [21] N. Boquillon, G. Elbez, U. Schonfeld "Properties of wheat straw particleboards bonded with different types of resin", Journal of Wood Science (2004) **50**, 230- 235.
- [22] T. Koreeda, J. Matos "Thermal characterization of mica-epoxy composite used as insulation material for high voltage machines", Journal of Thermal Analysis and Calorimetry (2011) **106**, 619-623.
- [23] Z.W. Zhou, M.M. Yu, R.C. Bai, A.J. Li, J.L. Sun, M.S. Ren "Thermal analysis of a novel tetrafunctional epoxy resin cured with anhydride", Polymers & Polymer Composites (2014) **22**, 45-49.
- [24] F.-L. Jin, M. Han, S.-J. Park "Effect of side-chain length of succinic anhydride on coefficient of thermal expansion behavior of epoxy resins", Polymer International (2006) **55**, 1289-1295.
- [25] J.C. Jung, S.K. Lee, K.S. Lee, K.Y. Choi "Chain-length effect of alkenyl succinic anhydride on thermal and mechanical-properties of the cured epoxy-resins", Angewandte Makromolekulare Chemie (1991) **185**, 129-136.
- [26] H. Miyagawa, A.K. Mohanty, M. Misra, L.T. Drzal "Thermo-physical and impact properties of epoxy containing epoxidized linseed oil, 1 - Anhydride-cured epoxy", Macromolecular Materials and Engineering (2004) **289**, 629-635.
- [27] C.A. May, *Epoxy Resins*. 1988. 1244.
- [28] F. Kolar, J. Svitilova "Kinetics and mechanism of curing epoxy/anhydride systems", Acta Geodynamica Et Geomaterialia (2007) **4**, 85-92.
- [29] M.D. Samper, V. Fombuena, T. Boronat, D. Garcia-Sanoguera, R. Balart "Thermal and mechanical characterization of epoxy resins (ELO and ESO) cured with anhydrides", Journal of the American Oil Chemists Society (2012) **89**, 1521-1528.
- [30] ISO 178. "Plastics - Determination of flexural properties",
- [31] M. Yu, Z. Zhou, H. Lu, A. Li, R. Bai, J. Sun, M. Ren, H. Hu "Curing kinetics and thermal properties of aromatic multifunctional epoxy resins", Polymers & Polymer Composites (2014) **22**, 1-11.

- [32] K. Friedrich, J. Ulanski, G. Boiteux, G. Seytre "*Isothermal curing of epoxy resins as seen by direct current and rheological measurements*", Polimery (2006) **51**, 264-269.
- [33] G. Kortaberria, P. Arruti, N. Gabilondo, I. Mondragon "*Curing of an epoxy resin modified with poly(methylmethacrylate) monitored by simultaneous dielectric/near infrared spectroscopies*", European Polymer Journal (2004) **40**, 129-136.



Development of environmentally friendly composite matrices from epoxidized cottonseed oil



A. Carbonell-Verdu ^{a,*}, L. Bernardi ^b, D. Garcia-Garcia ^a, L. Sanchez-Nacher ^a, R. Balart ^a

^a Instituto de Tecnología de Materiales (ITM), Universitat Politècnica de València (UPV), Plaza Ferrandiz y Carbonell 1, 03801 Alcoy, Alicante, Spain

^b Centro de Tecnología (CT), Universidad Federal de Santa María (UFSM), Santa María, RS 97105-900, Brazil

ARTICLE INFO

Article history:

Received 6 October 2014

Received in revised form 24 November 2014

Accepted 28 November 2014

Available online 5 December 2014

Keywords:

Cottonseed oil

Epoxidation

Dodecenyldsuccinic anhydride

Methyl nadic anhydride

Biobased epoxy resin

ABSTRACT

The continuous rise in oil prices has led to the use of other ways to obtain polymer materials. This paper proposes a methodology to obtain a thermosetting resin from cottonseed oil by epoxidation process. The cottonseed oil contains as most representative fatty acids: 52.5% of linoleic acid (C18: 2), 23.9% of palmitic acid (C16: 0) and 17.6% of oleic acid (C18: 1); the real iodine index, which is indicative of the number of double bonds, has a value of 107. Epoxidized cottonseed oil (ECSO) has been successfully obtained using conventional epoxidation process with hydrogen peroxide, acetic acid and sulfuric acid, maintaining a constant temperature of 70 °C with homogeneous magnetic stirring. Average oxirane oxygen content (OOC) of 5.32% can be obtained by conventional epoxidation process which represents a yield over 83%. The epoxidized oil has been crosslinked with mixtures of two cyclic anhydrides to tailor different properties on final crosslinked thermosetting resins: on the one hand, methyl nadic anhydride (MNA) which is characterized by a rigid molecular structure and on the other hand, dodecenyldsuccinic anhydride (DDSA) with a long side chain that can confer flexibility. The crosslinking process has been followed by dynamic differential scanning calorimetry (DSC), ionic mobility and oscillatory rheometry (OR) as well as gel time determination. The effect of the hardener mixture (wt.% DDSA:MNA) on mechanical performance of cured materials has been followed by flexural and impact tests as well as the evolution of the storage modulus (G') by dynamic mechanical analysis (DMA) in torsion mode. By selecting the appropriate hardener mixture, it is possible to obtain crosslinked materials with different properties ranging from stiff matrices for ECSO crosslinked with MNA to flexible matrices for ECSO cured with DDSA. This has occurred with other thermosetting resins like epoxidized soybean oil (ESBO) or epoxidized linseed oil (ELO).

© 2014 Elsevier Ltd. All rights reserved.

1. Introduction

The increasing concern about the environmental impact of polymer materials together with the problems related to petroleum depletion act as driving forces to replace petroleum-based polymer materials by others from renewable resources with a marked environmental efficiency and, in

many cases, giving solution to industrial wastes. In the field of thermosetting resins, important advances have been obtained by using vegetable oils which can be converted into epoxy resins by different epoxidation methods [1,2]. Currently some epoxidized oils are marketed industrially in large quantities such as soybean with a production of 200,000 t/year [3]. Vegetable oils with high content of unsaturated fatty acids such as oleic acid, linoleic acid and linolenic acid may be used to obtain epoxy groups [4] by using several epoxidation processes [5–7].

* Corresponding author. Tel./fax: +34 96 652 84 33.
E-mail address: alcarve1@epsa.upv.es (A. Carbonell-Verdu).

IV.2

IV.2. A new biobased plasticizer for poly (vinyl chloride), PVC base on epoxidized cottonseed oil (ECSO).

A. Carbonell-Verdu¹, D. García-Sanoguera¹, A. Jordá-Vilaplana², L. Sánchez-Nacher¹, R. Balart¹

¹ Materials Technology Institute (ITM)
Universitat Politècnica de València (UPV)
Plaza Ferrandiz y Carbonell 1, 03801, Alcoy, Alicante (Spain)

² Departamento de Expresión Gráfica en la Ingeniería
Universitat Politècnica de València (UPV)
Plaza Ferrandiz y Carbonell 1, 03801, Alcoy, Alicante (Spain)

**"A new biobased plasticizer for poly (vinyl chloride),
PVC base on epoxidized cottonseed oil (ECSO)"**

Abstract

The use of epoxidized cottonseed oil (ECSO) as plasticizer for poly(vinyl chloride), PVC was studied. The plasticizer content was set to 70 phr and the optimum isothermal curing conditions were studied in the temperature range comprised between 160 °C and 220 °C with varying curing times in the 7.5 - 17.5 min range. The influence of the curing conditions on overall performance of cured plastisols was followed by the evolution of mechanical properties (tensile tests with measurements of tensile strength, elongation at break and modulus), change in colour, surface changes of fractured samples by scanning electron microscopy (SEM), thermal transitions by differential scanning calorimetry (DSC) and migration in *n*-hexane. The optimum mechanical features of cured plastisols are obtained for curing temperatures in the 190-220 °C range. For these curing conditions, fractography analysis by SEM gives evidences of full curing process as no PVC particles and free plasticizer can be found.

Keywords

Epoxidized cottonseed oil (ECSO); poly (vinyl chloride), PVC; plastisols; mechanical properties; isothermal curing.

IV.2.1. Introduction.

Poly(vinyl chloride), PVC is one of the most widely used commodity plastics [1]. It can be manufactured by conventional techniques such as rotational molding, extrusion, injection molding, blow molding and calendaring, among others, depending on the final product [2, 3]. PVC can be easily plasticized to give flexible materials (P-PVC) with tailored properties which find a wide variety of applications such as blood bags, films and coatings, flexible toys, insulation for electrical wires and soles due to the high versatility, easy processing and low cost [4-8]. Plastisols, or PVC pastes, are obtained by mixing a PVC resin with a liquid plasticizer to form a dispersion of resin particles in plasticizer. With heating, plasticizer diffuses into the resin particle solvating the non-crystalline parts of the polymer chain and causing the resin particles to swell. With further heating the plasticizer can solvate (fuse) the crystalline sections of the polymer, some of which effectively crosslink the resin, allowing polymer molecules originally found in different resin particles to interact. This paste can be converted into a flexible solid material by a curing process which involves heating the paste to a certain temperature for a given time [9]. Vinyl plastisols are characterized by high wear and corrosion resistance, as well as excellent electric insulation. By varying the plasticizer content it is possible to tailor the final properties of the cured plastisols [10].

Phthalates, citrates, adipates and carboxylates, among others, have been traditionally used as PVC plasticizers being phthalates the main group due to low cost and excellent overall properties [11]. Nevertheless, the use of phthalate-based plasticizers is being reconsidered due to toxicity problems and plasticizer migration [5, 12]. For this reason, new environmentally friendly plasticizers are being demanded by the PVC industry to fulfil the increasingly rigorous requirements of some industrial sectors. Epoxidized vegetable oils offer interesting possibilities in PVC plasticization. Their use as main plasticizer or, more often as secondary plasticizers is continually increasing; it is possible to find recent works based on the use of epoxidized vegetable oils derived from linseed oil, castor oil, soybean oil, sunflower oil, rubber seed oil, etc. as plasticizers for vinyl plastisols formulations [13-15].

In this study epoxidized cotton seed oil is used due to the surplus produced in the industry and also because it is a by-product of the cotton industry, with about 5.12 million

tons production in 2014/15 [16] being China and India the major producers with 1.396 and 1.320 million tons respectively. Other reasons for its use is the relatively high oxirane oxygen index achieved after epoxidation process (5.32%). This value is slightly lower than other readily available epoxidized vegetable oil such as epoxidized soybean oil (ESBO). ESBO is widely used as secondary plasticizer for PVC, thermal stabilizer for plastic formulations and base material for polymer synthesis. For this reason, as epoxidized cottonseed oil (ECSO) has a similar oxirane oxygen index to that of an epoxidized soybean oil, it is reasonable to expect similar performance although their respective lipid profiles and other contained chemical compounds are different.

The main concern about the use of phthalate-based plasticizers such as DBP (di-n-butyl phthalate), DIBP (diisobutyl phthalate), BBP (butyl benzyl phthalate), DEHP (bis(2-ethylhexyl) phthalate) and DIOP (diisoctyl phthalate) is their volatility and also their migration promoted by their relatively low molecular weight [17-20] which is also responsible for good mixing with PVC particles [21]. Typical molecular weight of phthalate-based plasticizers is lower than 400 g mol⁻¹ as it is the case of bis(2-ethylhexyl) phthalate with a molecular weight of 390.56 g mol⁻¹ or di-n-butyl phthalate with a molecular weight of 278.3 g mol⁻¹. On the other hand, the typical molecular weight of epoxidized vegetable oils is around 900-950 g mol⁻¹, which has a positive effect on migration restriction. Today, some high molecular weight phthalate-based plasticizers such as di-isobutyl phthalate (DINP), di-isodecyl phthalate (DIDP) and di-2-propylheptylphthalate (DPHP) are permitted as common plasticizers in such applications that require low migration [8, 22, 23].

The final mechanical features of the cured plastisols will depend on the curing cycle in terms of temperature and time. After mixing PVC resin with the plasticizer, the gelation process begins. This process can be divided into three different stages. Initially, the plastisol consists of PVC resin fine particles dispersed in a liquid plasticizer. With heating, the first stage in the gelation process begins. Plasticizer diffuses into the resin particles solvating the non-crystalline parts of the polymer, swelling the particles and causing a dramatic rise in the PVC paste viscosity. Plasticizer interacts with the somewhat polar PVC resin through electrostatic interactions including dipole-dipole and van der Waals forces [24]. This stage continues until all of the plasticizer has been absorbed into the resin particles [25]. With continued heating, the second stage of the plastisol gelation/fusion process begins. At these higher temperatures plasticizer can

solvate (fuse or melt) the crystalline parts of the PVC resin causing the PVC paste viscosity to drop and allowing polymer molecules to flow more freely and interact with polymer molecules from other resin particles. Upon cooling, the final stage in the gelation/fusion process begins. Crystallites form again effectively crosslinking polymer molecules. Physical entanglement of the processed flexible PVC polymer chains as well as crystalline crosslinks between polymer molecules provides its mechanical strength to the finished product. Plasticizer solvates the non-crystalline parts of the PVC polymer giving the finished product its particular flexibility [22, 26].

In commercial practice, P-PVC curing conditions affect efficient production and finished product properties. A low processing temperature profile leads to under-curing, which leads to poor mechanical performance. On the other hand, a high temperature profile promotes PVC degradation and, subsequently, a remarkable loss in mechanical properties [27].

This research work is a preliminary study about the possibilities of epoxidized cottonseed oil (ECSO) as biobased and environmentally friendly plasticizer for PVC plastisol formulations with potential use as substitute for conventional phthalates. PVC plastiols with constant plasticizer content (70 phr) were subjected to different curing cycles in terms of temperature and time; the effect of the curing parameters on mechanical performance, change in color, thermal transitions, and migration of PVC plastiols was evaluated to assess optimum curing conditions for this system.

IV.2.2. Experimental.

■ Materials.

PVC plastiols were obtained with a commercial suspension PVC (Lacovyl PB 1172 H) with K-value 67, supplied by Atofina (Atofina UK, Ltd, Midlands, United Kingdom). The base vegetable oil for plasticizer synthesis was cottonseed oil supplied by Sigma Aldrich (Sigma Aldrich España, Madrid, Spain). This vegetable oil is characterized

by an iodine value in the 109-120 range and a density of 0.92 g cm^{-3} which makes it suitable for epoxidation. In a previous research work the influence of different epoxidation process parameters were optimized [28].

■ Plastisol preparation.

PVC pastes with constant plasticizer content (70 parts per hundred parts of resin) were prepared in a mixing bowl of 1500 cm^3 by mixing the appropriate amounts of each component (85.72 gr PVC and 60 gr ECSO) at 23°C for 10 min at 200 rpm in a rotational mixer KAPL mod. 5KPMS (KAPL, Michigan, USA). Once homogeneous pastes were obtained, pastes were subjected to degassing in the same container for 1 h in a vacuum chamber MCP oo/LC (HEK-GmbH, Lubeck, Germany) to remove all entrapped air bubbles. After that, the liquid plastisols were placed into an aluminum mold with rectangular shape to obtain sheets sizing $190 \times 135 \times 4 \text{ mm}^3$. As other authors have reported previously, an aluminum mold with a low thickness (less than 1 mm) has been used due to low heat dissipation [27]. The curing process was carried out at different temperatures comprised in the $160 - 220^\circ\text{C}$ range with varying times in the 7.5-17.5 min in an air circulating oven mod. Selecta 2001245 (JP Selecta S.A., Barcelona, Spain). Standard samples for the different tests were obtained with a hot press mod. MEGA KCK-15A (Melchor Gabilondo SA, Vizcaya, Spain) using an appropriate die.

■ Mechanical characterization of cured PVC plastisols.

Mechanical properties of cured PVC plastisols subjected to different curing cycles were obtained in a universal test machine Ibertest ELIB 30 (Ibertest S.A.E., Madrid, Spain) following the guidelines of the ISO 527. The size of the samples for tensile tests was obtained as recommended by the previous standard. The specific dimensions used to calculate the cross section of each sample were 10 mm of width and 4 mm of thickness $\pm 0.2 \text{ mm}$. Tensile tests were carried out at a crosshead speed of 20 mm min^{-1} at 23°C .

Five different samples were tested and average values of tensile strength, elongation at break and modulus were calculated.

■ Surface characterization by scanning electron microscopy (SEM).

Before observation, the surface of fractured samples from the tensile test was subjected to a sputtering process in a Sputter Coater EMITECH mod. SC7620 (Quorum Technologies Ltd, East Sussex, UK) and subsequently, samples were observed in a scanning electron microscope FEI mod. PHENOM (FEI Company, Eindhoven, The Netherlands) at an accelerating voltage of 5 kV.

■ Solvent extraction test.

The solvent extraction test was carried out in n-hexane and the global migration was estimated by gravimetric measurements. Circular samples (25 mm diameter) were immersed in *n*-hexane and periodically removed to measure weight loss/gain. The solvent extraction test was carried out at different temperatures between 30 °C and 60 °C and the global migration was obtained for different migration times: 2, 4, 6 and 8 h.

■ Thermal characterization of cured plastisols.

Thermal characterization of cured plastisols was carried out by using differential scanning calorimetry (DSC) in a DSC 821e (Metler-Toledo S.A.E., Barcelona, Spain). Samples with an average weight of 6-7.5 mg were subjected to a heating program from -50 °C up to 60 °C in air atmosphere at a heating rate of 5 °C min⁻¹.

Measurements of colorimetric coordinates of cured plastisols.

Color coordinates were measured on cured samples subjected to different curing conditions using a Hunter Mod. CFLX-DIF-2 colorimeter (Hunterlab, Murnau, Germany). This equipment provides different colour scales but the selected coordinates were ($L^*a^*b^*$). This colorimeter also provides spectral data from 400 to 700 nm so that it is useful for opaque and translucent materials as it is the case of plastisols cured in different conditions.

IV.2.3. Results and discussion.

Influence of curing time and isothermal curing temperature on mechanical properties of cured PVC plastisols

The curing cycle of a liquid plastisol is defined in terms of the isothermal curing temperature and the necessary time to reach optimum mechanical properties on cured plastisols. **Figure IV.2.1[a]** shows the plot evolution of the tensile strength as a function of the curing time for different curing temperatures in the 160-220 °C range. The tensile strength of plastisols cured at the lowest considered temperature (160 °C) is lower than 3 MPa which is representative of very poor mechanical properties. The curing process has not been completed and that is why mechanical performance is very poor and the cured plastisol behaves as a wax. For this plastisol series it was impossible to test the material subjected to a curing time of 7.5 min as it collapses easily even with very low loads (typical of a waxy consistence). This behavior is typical of not fully cured plastisols. The plasticizer has promoted swelling of individual PVC particles but the temperature has not been high enough to completely melt the PVC [27]. All PVC plastisols, except the

one cured at 220 °C, provide increasing tensile strength values as the curing time increases. Tensile strength values of about 11.6 MPa can be obtained with curing conditions of 205 °C and a curing time of 17.5 min. Plastisols cured at 220 °C show a different behavior as initially (for low curing times) the tensile strength increases as observed with lower curing temperatures; nevertheless, when a certain curing time is reached, we observe a clear decrease in tensile strength values. This is directly related to thermal degradation of the PVC and important plasticizer loss as a consequence of the exposure of a liquid PVC paste to high temperatures and long times. For this reason, the material becomes brittle and a slight decrease in tensile strength is observed. As it can be observed in **Figure IV.2.1[a]**, it is possible to reach a particular tensile strength value by combining different curing temperatures and times; so that, even accounting standard deviations, plastisols cured at 205 °C for 15 min offer the same tensile strength than plastisols cured at 220 °C for 10 min. This could be interesting from industrial point of view as a reduction in the curing cycle could represent a reduction in manufacturing cycles; despite this, the use of high curing temperatures is dangerous as slight changes in the curing time could lead to a noticeable change in mechanical properties as observed in **Figure IV.2.1[a]**. Nevertheless, as PVC is highly sensitive to thermal degradation and this phenomenon has a negative effect on mechanical performance, even more conservative curing conditions at 205 °C for 15 min could be considered as appropriate.

With regard to elongation at break (**Figure IV.2.1[b]**) we observe an increase as both temperature and curing time increases. Again, the lowest elongation at break values are obtained for plastisols cured at 160 °C and this is representative for under-curing conditions and, consequently, the typical flexibility of well-cured plastisols is not achieved. Curing at 190 °C provides the highest slope in elongation at break; this increases by 625% with a change in curing time from 7.5 min to 12.5 min; after this remarkable increase, it remains almost constant with values between 130% and 140%. As indicated previously, the evolution of the elongation at break for plastisols cured at 220 °C offers two clear zones: for low curing times, we observe an increasing tendency up to curing times of about 12.5 min. Once this curing time is reached, a clear decrease in flexibility can be detected by a dramatic decrease in elongation at break values up to 30% (for a curing time of 17.5 min). As expected, the combination of high curing temperatures and long times define over-curing conditions. A clear evidence of over-curing state is the decrease in both tensile strength and elongation at break. A similar situation can be observed for plastisols cured at 205 °C.

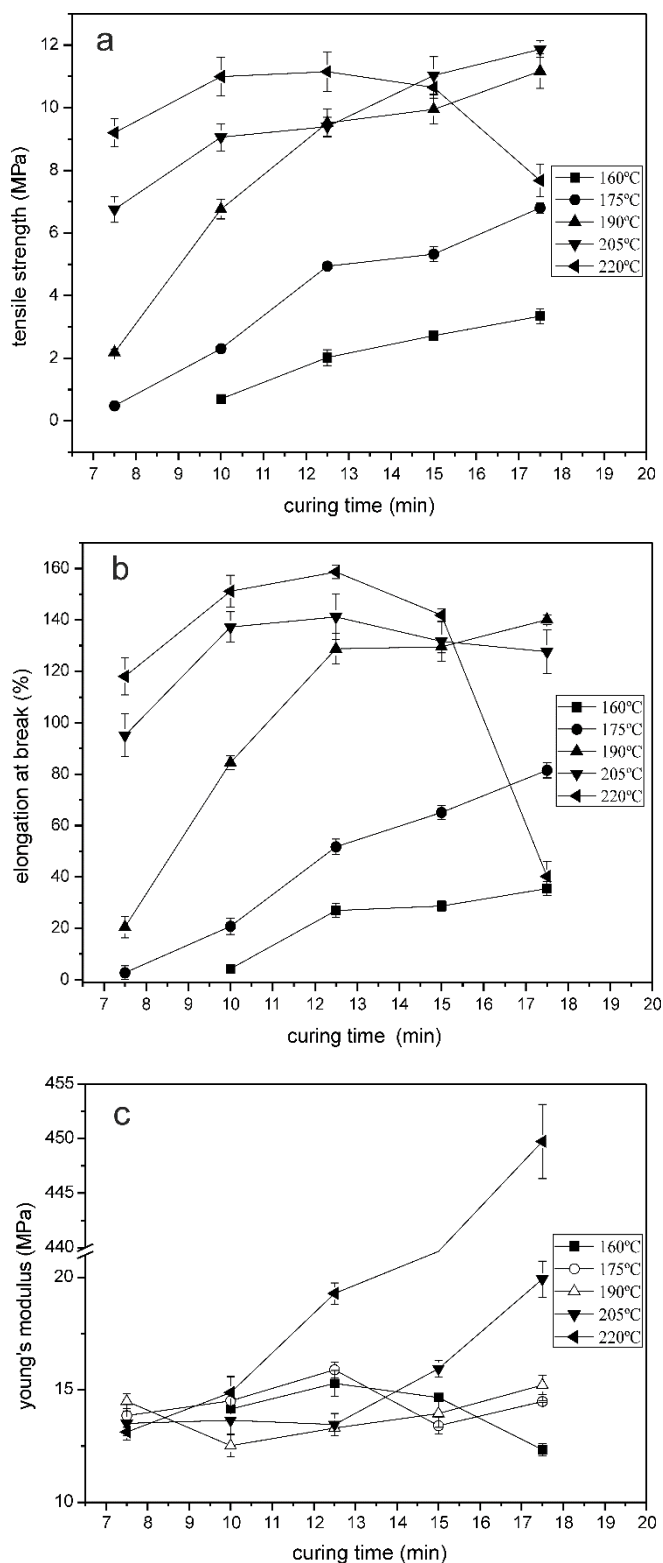


Figure IV.2.1. Mechanical properties of PVC plastisols plasticized with epoxidized cottonseed oil (ECSO) in terms of the curing time for different isothermal curing temperatures a) tensile strength, b) elongation at break, c) Young's modulus.

Regarding to the Young's modulus (**Figure IV.2.1[c]**), no significant changes are observed by curing with low temperatures profiles ($T < 190$ °C). Nevertheless, for curing temperatures over 205 °C, we observed a clear increasing tendency in the Young's modulus as the curing time increases. Thus, plastisols cured at 220 °C for 17.5 min offer a Young's modulus close to 450 MPa which is in the typical range of these type of materials.

By taking into account tensile strength and elongation at break values, it can be concluded that under our test conditions, curing the plastisols at a temperature of 220 °C for 10 min provides cured plastisols with optimum-balanced properties. These results are in total agreement with previous studies as reported by Fenollar *et al.* [29] An interesting combination of maximum elongation at break (near 160 %) and high tensile strength values (over 11 MPa) has been obtained. Nevertheless, it is critical not to exceed the curing time, as a remarkable decrease in mechanical performance will occur.

Table IV.2.1 shows a comparison of the main parameters (amount of plasticizer, curing conditions, sheet size and mechanical properties) of ECSO and different epoxidized vegetable oils and several commercially available phthalates in plasticized PVC formulations. Results of tensile strength and elongation at break show similar values of ECSO providing an overview of the potential use of this biobased plasticizer.

Table IV.2.1. Comparison of the mechanical properties of cured PVC plastisols with different plasticizers: epoxidized cottonseed oil (ECSO), epoxidized linseed oil (ELO), epoxidized soybean oil (ESBO), diisononyl phthalate (DINP), bis(2-ethylhexyl) phthalate (DEHP) and dioctyl phthalate (DOP).

Plasticizer	Content (phr)	Size (mm)	Curing temperature (°C)	Curing time (min)	Tensile strength (MPa)	Elongation at break (%)
ECSO	70	190 x 135 x 4	220	10	11	150
ELO [13]	70	190 x 125 x 5	220	8	11	205
ESBO [6]	50	60 x 100 x 3.4	170	8	-	-
ESBO [30]	50	-	180	10	18	100
DINP [22]	70	thickness of 2	187	-	16	--
DEHP [17]	70	-	155	10	5	166
DOP [26]	70	thickness of 3	180	15	11	-

ECSO-epoxidized cottonseed oil; ELO-epoxidized linseed oil; ESBO-epoxidized soybean oil; DINP-diisononyl phthalate; DEHP-diethylhexyl phthalate; DOP-dioctyl phthalate.

Influence of the curing conditions on plastisol structure.

Analysis of surface morphology of fractured samples from tensile tests is a useful technique to check the optimum curing conditions. As described previously, the plastisol gelation is a process in which a liquid PVC-plasticizer dispersion is converted into a flexible solid. To achieve optimum mechanical performance, gelation has to complete several stages that require combination of high temperatures and times [26]. **Figure IV.2. 2** and **Figure IV.2.3** show SEM images of the surfaces of fractured samples from tensile tests for the lowest (7.5 min) and the highest (17.5 min) curing times respectively. For short curing times and relatively low temperature profiles ($T < 200^{\circ}\text{C}$) (**Figure IV.2[a], [b] & [c]**), we observe the presence of spherical shapes which can be attributable to swollen PVC particles with the epoxidized cottonseed oil (ECSO) plasticizer but a homogeneous-continuous polymer matrix cannot be identified. This is representative of incomplete curing (under-cured plastisol). Individual swollen PVC particles can be detected; nevertheless, as the curing time and/or temperature increases, no spherical shapes are observed thus indicating that the curing process has been complete and a homogeneous matrix can be obtained so that, the plasticizer has been fully absorbed. For a particular curing cycle of 190°C and 7.5 min (**Figure IV.2.2[c]**) slight presence of spherical shapes on the fractured surface can be observed. The effect of curing time is evident if we compare this structure with the sample corresponding to a curing cycle of 190°C for 17.5 min (**Figure IV.2.3[c]**), which is characterized by a clear homogeneous surface without spherical shapes; this fact is indicative of optimum gelation-curing process and, consequently, good mechanical properties as described before [30]. For curing temperatures over 205°C (**Figure IV.2.2[g] & [e]** and **Figure IV.2.3[d] & [e]**), the fractured surfaces do not show presence of free plasticizer and spherical shapes thus indicating that the gelation is complete [31]. The degradation effects because of exposure to high temperature-time profiles can be observed in **Figure IV.2.3[e]** in which, dark regions can be observed due to plasticizer remove and/or thermal degradation of PVC subjected to high temperature.

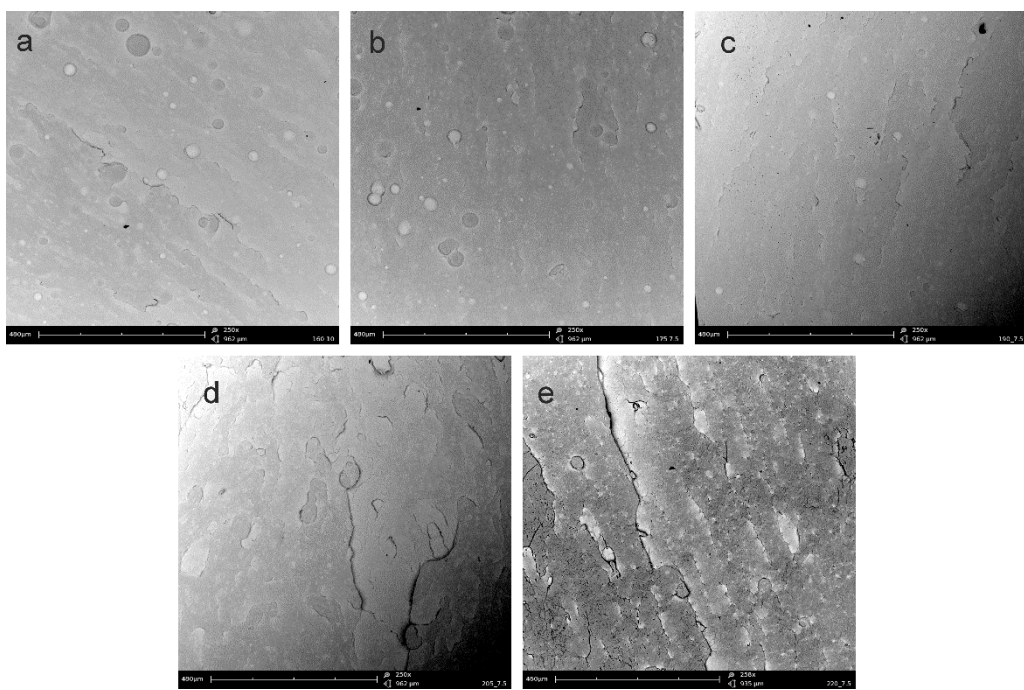


Figure IV.2.2. SEM images (250x) of surfaces of fractured samples from tensile tests of cured PVC plastisols subjected to curing cycles of 7.5 min and temperatures of a) 160 °C, b) 175 °C, c) 190 °C, d) 205 °C and e) 220 °C.

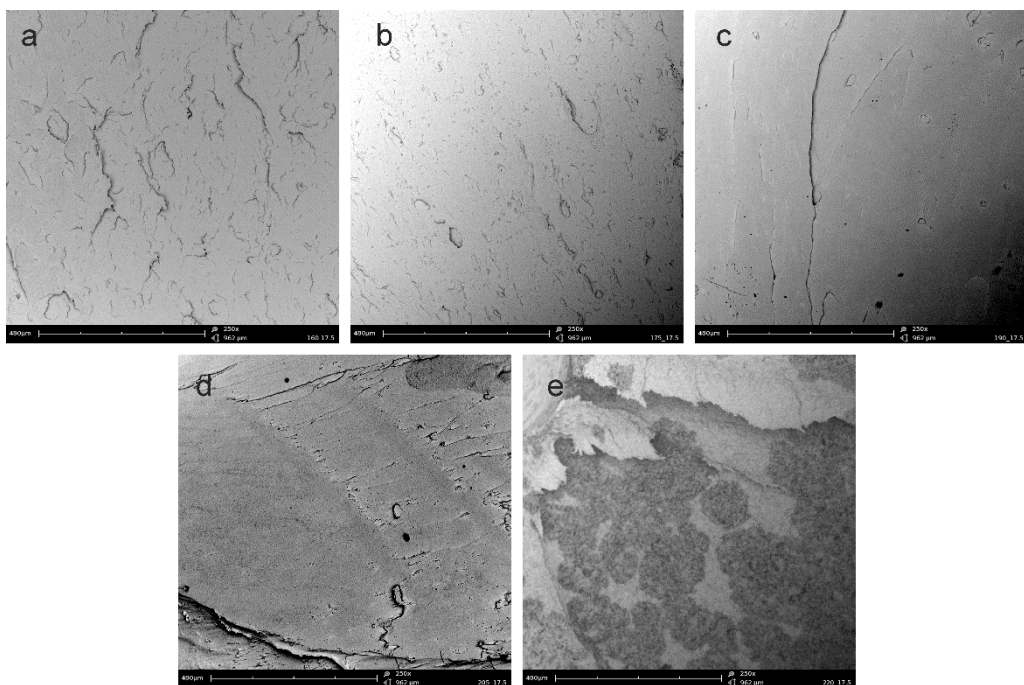


Figure IV.2.3. SEM images (250x) of surfaces of fractured samples from tensile tests of cured PVC plastisols subjected to curing cycles of 17.5 min and temperatures of a) 160 °C, b) 175 °C, c) 190 °C, d) 205 °C and e) 220 °C.

Optimum curing conditions can also be assessed by the solvent extraction test. A fully cured material is characterized by low migration in comparison to under-cured plastisol. **Figure IV.2.4** shows different plots of the migration evolution in terms of the curing time and isothermal curing temperatures for different migration times. As one can see the maximum migration levels are observed for PVC plastisols subjected to mild curing conditions ($160\text{ }^{\circ}\text{C}$ -7.5 min or $175\text{ }^{\circ}\text{C}$ -7.5 min). **Figure Iv.2.4[a]** shows the evolution of the migration levels at $30\text{ }^{\circ}\text{C}$ in terms of the curing times for the curing temperatures comprised between $160\text{ }^{\circ}\text{C}$ and $220\text{ }^{\circ}\text{C}$. The highest migration values at 2 h are close to 7.6% and correspond to a curing profile of $160\text{ }^{\circ}\text{C}$ and a curing time of 7.5 min. For this particular curing conditions, migration increases as the migration time increases thus leading to a remarkable migration level of 17.64% at 8 h. With regard to cured plastisols subjected to a curing profile of $175\text{ }^{\circ}\text{C}$ for 7.5 min, the migration levels are 3.03% and 11.53% for migration times of 2 and 8 h respectively. By comparing these migration values with the abovementioned migration values corresponding to curing cycles of $160\text{ }^{\circ}\text{C}$ -7.5 min, we see a clear decrease in the migrated plasticizer.

A negative migration (swelling) was observed for plastisols cured at temperatures over $190\text{ }^{\circ}\text{C}$ or at slower curing temperatures for curing times above $12.5\text{ }^{\circ}\text{C}$. The percentage weight gain due to swelling is low, no more than 2.5% for plastisols cured at $160\text{ }^{\circ}\text{C}$ for 17.5 min and did not undergo migration. It is difficult to ensure that there is not free plasticizer for these particular curing conditions as the overall effect is swelling but actually two competing phenomena occur simultaneously. On the one hand, plasticizer extraction by the solvent action and on the other hand, plastisol swelling due to the entrance of some solvent inside the plastisol structure. The overall effect of these two competing processes is a very slight weight gain. Finally, swelling shows similar tendency for plastisols subjected to more aggressive migration cycles as observed in **Figure IV.2.4[b], [c] & [d]**.

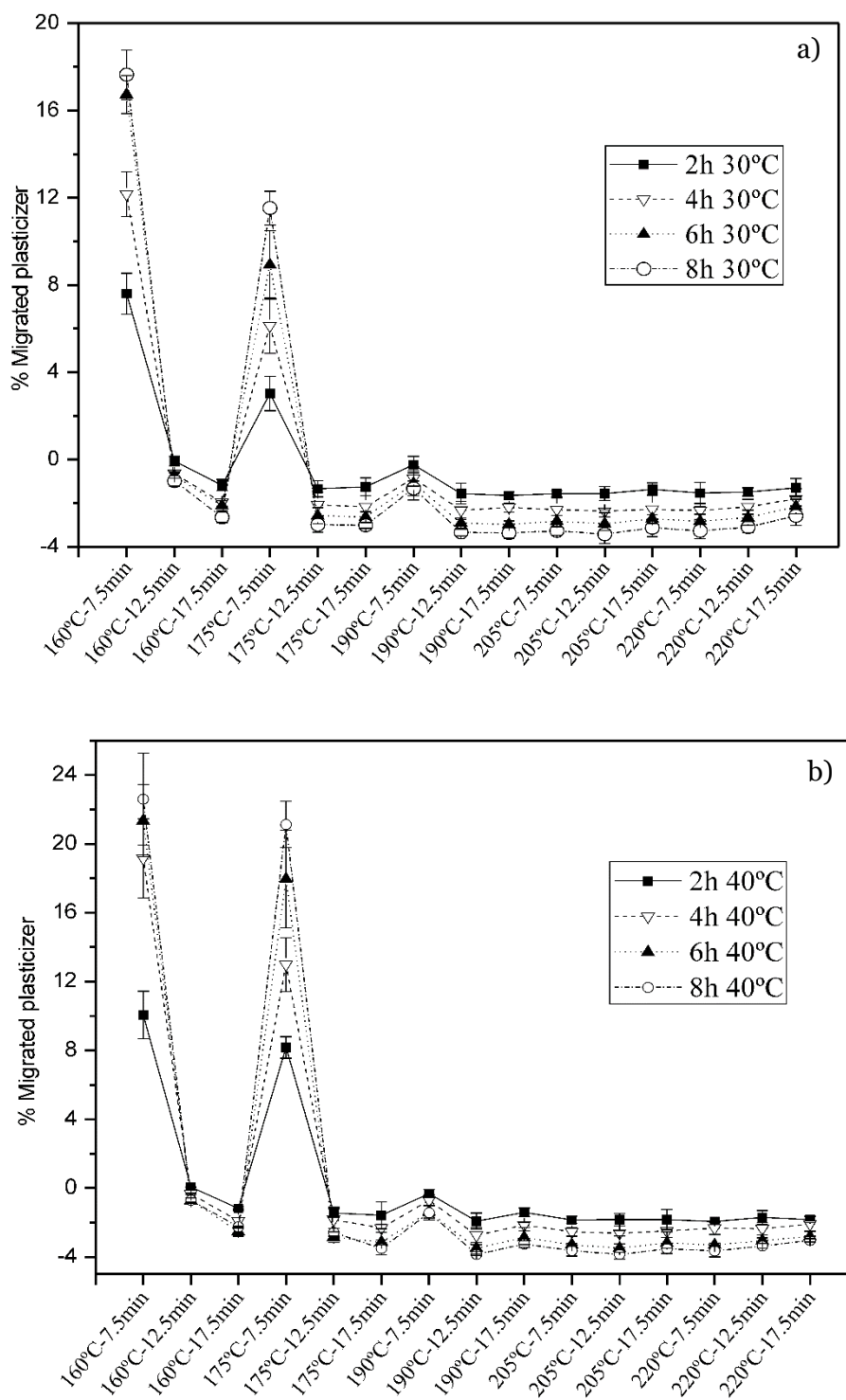


Figure IV.2.4. (1/2) Migration levels (weight percentage gain) of cured PVC plastisols with ECSO plasticizer subjected to different curing cycles at different migration temperatures a) 30 °C and b) 40 °C.

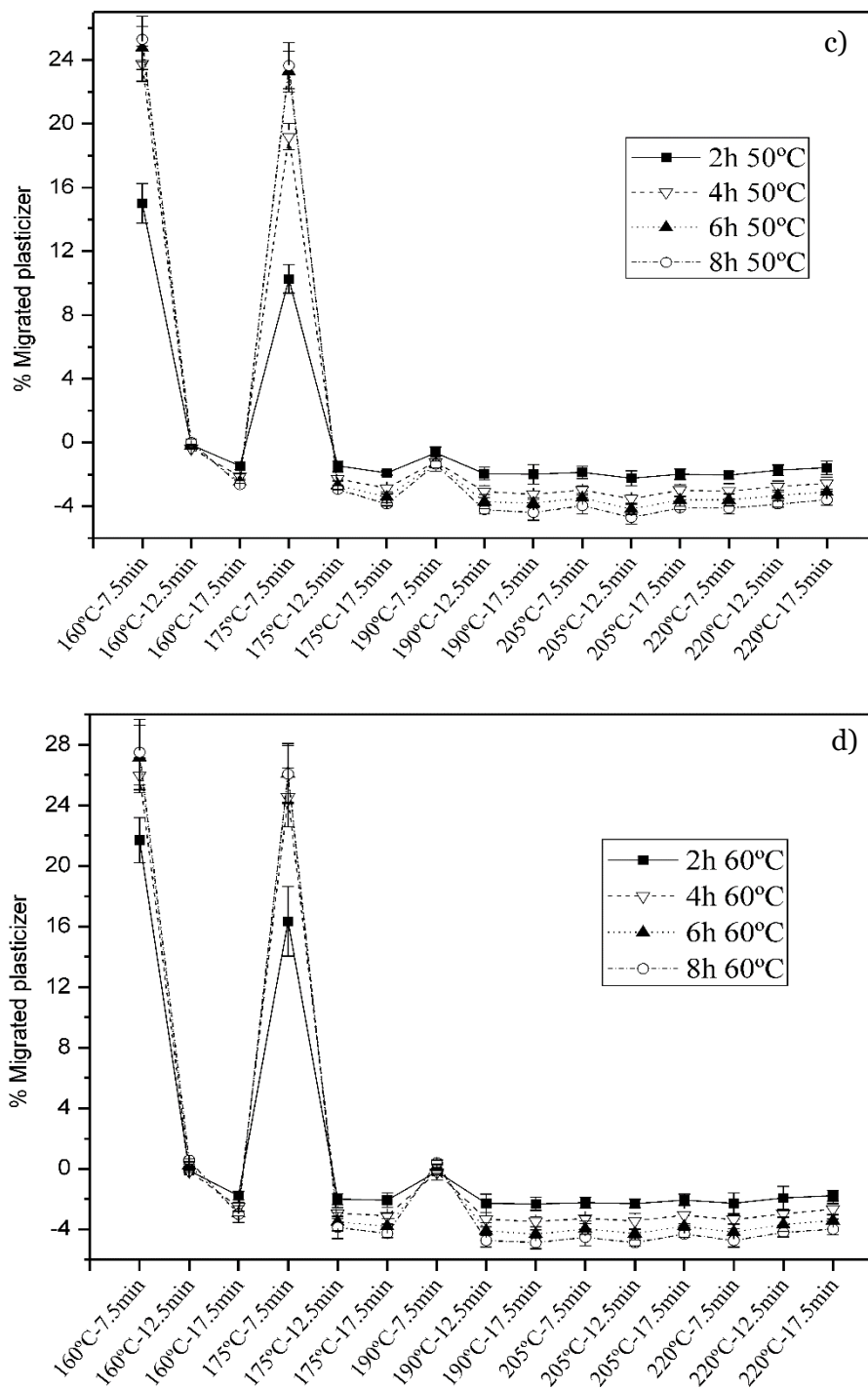
Cont.

Figure IV.2.4. (2/2) Migration levels (weight percentage gain) of cured PVC plastisols with ECSO plasticizer subjected to different curing cycles at different migration temperatures, c) 50 °C and d) 60 °C.

Temperature is another important factor to be considered for plasticizer extraction results. As the temperature for the solvent extraction tests increases, we observe a clear increase in the total extracted plasticizer (**Table IV.2.2**). To see migration values in detail curing profiles of 160 °C and 175 °C for 7.5 min were selected as they give clear evidence of the effect of both temperature and curing time on overall migrated mass weight.

Table IV.2.2[a]. Percentage plasticizer migration for PVC cured plastisols subjected to different a curing cycle of 7.5 min at 160 °C, in terms of the solvent extraction test with *n*-hexane in terms of migration time and temperature.

Tempearture of the migration test (°C)	Migration time (h) for PVC plastisols cured at 160 °C/7.5 min			
	2	4	6	8
30	7.60 ± 0.94	12.17 ± 1.02	16.73 ± 0.87	17.64 ± 1.14
40	10.05 ± 0.03	19.16 ± 2.3	21.34 ± 2.1	22.60 ± 2.67
50	15 ± 1.24	23.77 ± 1.11	24.75 ± 1.35	25.29 ± 1.43
60	21.71 ± 1.49	25.99 ± 1.14	27.17 ± 2.14	27.51 ± 2.17

Table IV.2.2[b]. Percentage plasticizer migration for PVC cured plastisols subjected to different a curing cycle of 7.5 min at 175 °C, in terms of the solvent extraction test with *n*-hexane in terms of migration time and temperature.

Tempearture of the migration test (°C)	Migration time (h) for PVC plastisols cured at 160 °C/7.5 min			
	2	4	6	8
30	3.03 ± 0.79	6.14 ± 1.27	8.92 ± 1.57	11.53 ± 0.77
40	8.18 ± 0.63	12.99 ± 1.57	17.95 ± 2.84	21.13 ± 1.34
50	10.25 ± 0.89	19.19 ± 0.83	23.28 ± 1.27	23.64 ± 1.44
60	16.35 ± 2.3	24.52 ± 1.94	26.10 ± 1.98	26.14 ± 1.87

For example, for plastisols cured at 160 °C for 7.5 min, the solvent extraction test at different temperatures gives the following results. For a solvent extraction test at 30 °C, the initial extracted plasticizer amount is 7.60% and this value is remarkably increased up to values of 21.71% for a testing temperature of 60 °C thus indicating the effect of temperature on plasticizer extraction which could be an important issue from a technical point of view as not fully cured plastisols are more sensitive to extraction and potential migration and this effect is even more accentuated by temperature. As describe

before, extraction of plastisols cured at 175 °C is lower than that observed for plastisols cured at 160 °C. Nevertheless, we observe the same tendency with a clear increase in extraction levels as the testing temperature increases. Obviously, as the extraction time increases, the total extracted plasticizer also increases as it can be seen in **Table IV.2.2** for extraction times of 2, 4, 6 and 8 h.

As we have described previously, incomplete curing of a plastisol leads to presence of free plasticizer. This can be observed by thermal analysis of cured materials. **Figure IV.2.5** shows a comparative plot of different DSC thermograms for cured plastisols subjected to different curing cycles. The endothermic peak located between -5 and 5 °C is attributable to the melt peak of free plasticizer as observed by other authors [29]. As the curing conditions reach the optimum, a decrease in the peak area is detected thus indicating less free plasticizer. For the mildest curing conditions used in this study (160 °C - 7.5 min) we see a peak at 2.4 °C which is representative for free epoxidized cottonseed oil (ECSO) plasticizer which has not participated in the swelling process of individual PVC particles, so that it remains as free plasticizer. Nevertheless, for more aggressive conditions, we do not see the peak located at 2 °C so that, it is indicating that the plasticizer has been fully absorbed by the individual PVC particles to form a gel structure.

With regard to the glass transition temperature, the T_g for unplasticized PVC, which is typically of 87 °C [22] is decreased up to values below room temperature thus giving highly flexible materials. For longer curing times (17.5 min), an enhance in the T_g was observed which was related to an improvement of the mechanical properties. As described previously, short curing times and low temperatures (7.5 min-160 °C) offered the worst mechanical properties and the highest migration values. The partially cured plastisol has similar behavior to that of a wax with poor consistency. It can be concluded that T_g lower than -22 °C indicates poor mechanical properties and higher migration values due to high amounts of free plasticizer that does not interact with PVC polymer chains; on the other hand, a T_g above -15 indicates absence of free plasticizer and is representative for fully cured PVC plastisols.

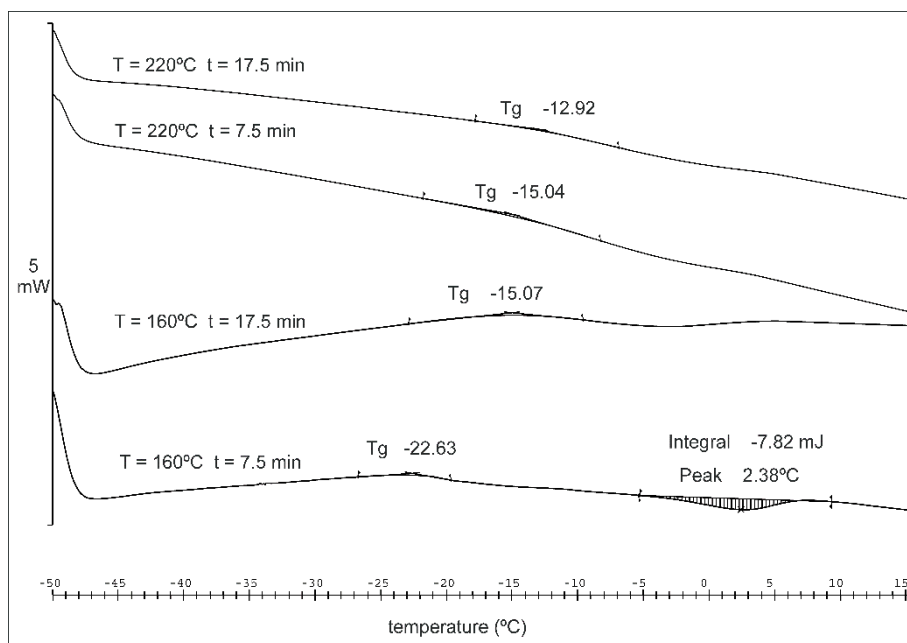


Figure IV.2.5. Comparative DSC curves of cured PVC plastisols plasticized with ECSO subjected to different curing cycles.

I nfluence of the curing time and temperature on final color of cured PVC plastisols.

PVC is highly sensitive to thermal degradation. One of the most evident signs of this degradation is yellowing and browning. Obviously, the curing conditions govern the physical and chemical changes during the curing process but they also can affect the final appearance of the cured plastisol due to changes in color because of the exposure to more aggressive thermal conditions (high temperature during short time periods or moderate temperatures with long exposure times). **Figure IV.2.6** shows a matrix representation of the color appearance of the cured plastisols subjected to different curing cycles in terms of isothermal curing temperature and time. As we can see, mild curing conditions ($160\text{ }^{\circ}\text{C}$ and $175\text{ }^{\circ}\text{C}$ and short curing times of 7.5 and 10 min) lead to an intense white color (fully opaque) but these conditions provide cured plastisols without good mechanical properties as described previously.



Figure IV.2.6. Optical photographs of cured PVC plastisols with ECSO plasticizer subjected to different curing conditions in terms of the isothermal curing temperature and curing time.

In fact, some of these cured plastisols could not be tested because they broke immediately, even with small pre-load application. As temperature and time increases, cured plastisols become translucent with a slight yellow color due to the intrinsic color of the plasticizer.

This appearance indicates that the curing process has been completed. For aggressive curing conditions ($205\text{ }^{\circ}\text{C}$ - 15 min or $220\text{ }^{\circ}\text{C}$ - 12.5 min) we observe a clear brownish color on cured plastisols which is indicative of thermal degradation. In addition to this change in color, a reduction of mechanical performance is detected because of plasticizer removal and PVC degradation. The cured plastisol subjected to the most aggressive conditions of this work ($220\text{ }^{\circ}\text{C}$ - 17.5 min) is completely dark brown and opaque. So that, the color of the cured plastisol together with its translucency can be useful from quality control since a simple observation of the final color could indicate the potential degradation during the curing cycle.

By comparing the luminance values of the cured PVC plastisols, which describes the amount of light that is able to pass across the plastisol, it is possible to evaluate the curing state: under-cured, fully cured and not degraded and cured and degraded (over-cured).

As the curing time increases, the luminance (L^*) values decrease thus leading to more transparent materials. For cured PVC plastisols subjected to a curing temperature of $160\text{ }^{\circ}\text{C}$ the luminance changes from 80% to 45% for curing times of 7.5 min and 17.5 min respectively. PVC plastisols cured at $175\text{ }^{\circ}\text{C}$ offer a change in luminance from 72% (7.5 min) up to 42% (17.5 min) and this range is still narrower for PVC plastisols cured at $190\text{ }^{\circ}\text{C}$ which suffers a decrease in luminance from 55% (7.5 min) to 40% (17.5 min). By taking into account the mechanical performance described previously, we can correlate the luminance values with the curing degree. So that, luminance values around 40 are representative for fully cured plastisols and not degraded.

Luminance values over 50 units indicate partially cured plastisols (under cured material) while luminance values under 30 are representative for thermal degradation of cured plastisol (**Figure IV.2.7**).

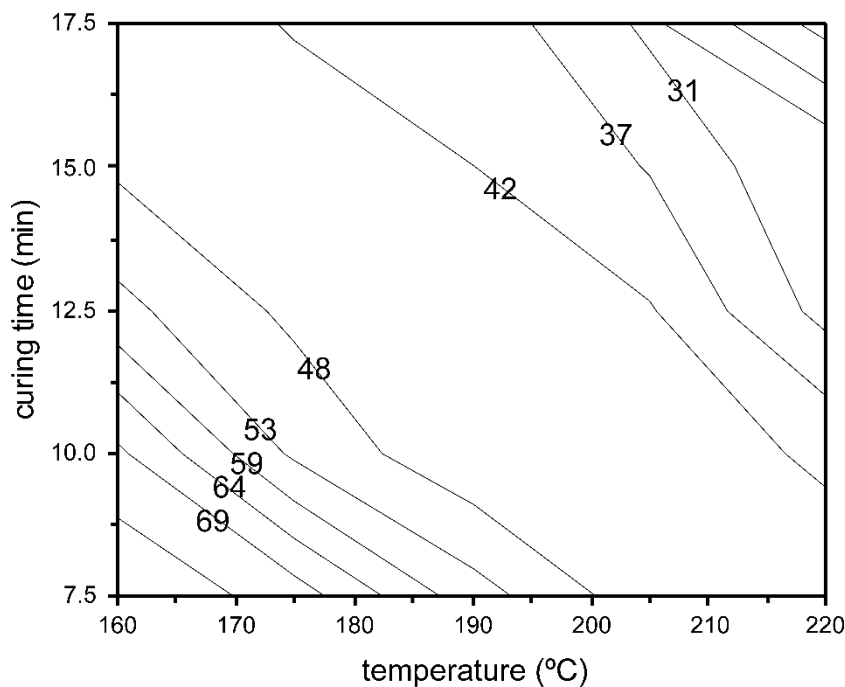


Figure IV.2.7. Contour plot of the luminance of cured PVC plastisols with ECSO plasticizer in terms of the isothermal curing temperature and curing time.

Additionally, the color coordinates a^* and b^* can be useful for quality control as it is possible to determine the curing degree of the PVC plastisol by relating these color coordinates with the previous mechanical results. These color coordinates change from red (positive a^* values) to green (negative a^* values) and from yellow (positive b^* values) to blue (negative b^* values). **Figure IV.2.8** shows a plot representation of the a^*b^* color space; this graph can be useful for quality control of cured plastisols as it is possible to identify different curing degrees as established before. By taking into account the mechanical performance of cured plastisols, SEM analysis and solvent extraction tests, the area corresponding to partially cured (under-cured) plastisols is characterized by a^* values comprised in the -4 to 0 and b^* values in the 2-11 range. Fully cured plastisols (and not degraded) are characterized by a^* values between 1 and 9 and an increase in b^* up to 20 (this area considers all the curing conditions corresponding to cured plastisols with the best performance). Over-cured plastisols (thermally degraded) are characterized by a^* values in the 6-13 range and low b^* values comprised between 2 and 10. This technique is very useful as it has been described in previous works with commercial epoxidized vegetable oils such as linseed oil [27, 29].

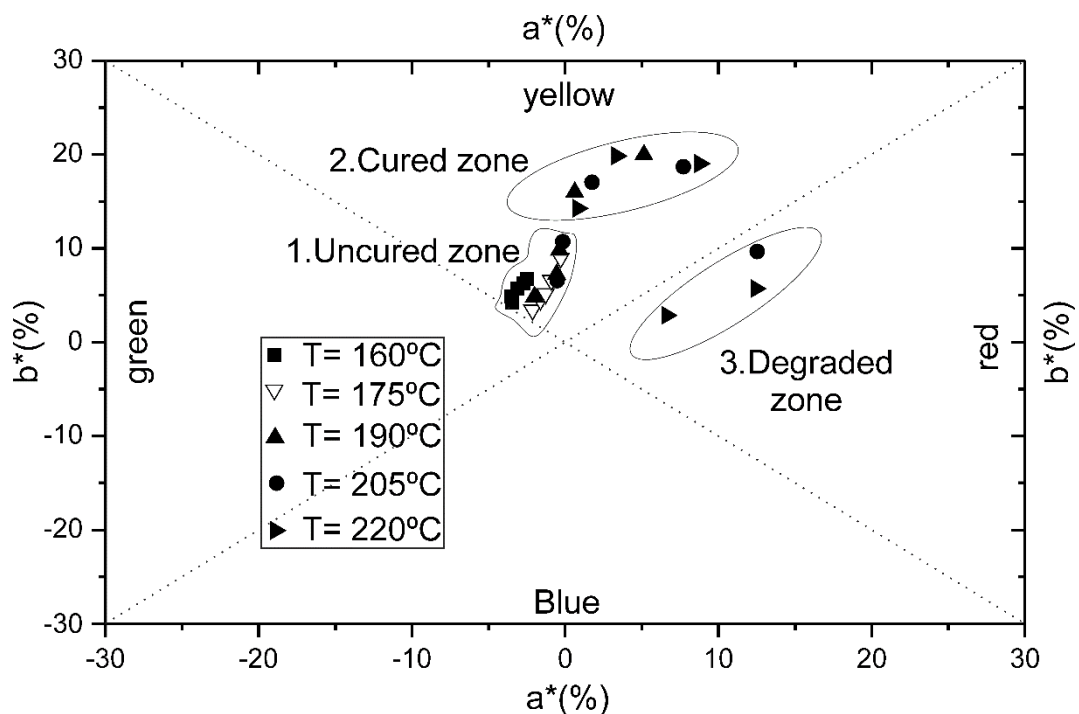


Figure IV.2.8. Variation of the color coordinates a^*b^* of cured PVC plastisols with ECSO plasticizer subjected to different curing conditions.

IV.2.4. Conclusions.

Epoxidized cottonseed oil (ECSO) can be used as plasticizer to give partially biobased PVC plastisols. The curing conditions play a critical role on final performance of cured plastisols. A curing profile of 220 °C and 10 min seems to be the optimum in terms of the best mechanical performance; nevertheless, as PVC is highly sensitive to thermal degradation, the use of lower temperature and higher curing times such as 205 °C for 15 min could be an interesting solution as the curing conditions are not as aggressive. It is possible to obtain cured PVC plastisols with high elongation at break values (over 150%) which can compete with other plasticized PVC materials. From a quality control point of view, a simple study of the color coordinates gives enough information about the curing degree of plastisols cured at different conditions. Solvent extraction tests are also useful to assess the optimum conditions since partially cured

plastisols are characterized by presence of free plasticizer that can easily migrate. In general terms, it is possible to obtain high environmentally low migration PVC plastisols by using epoxidized cottonseed oil as plasticizer.

Acknowledgements.

R. Balart wants to thank the Ministry of Economy and Competitiveness – MINECO (Ref: MAT2014-59242-C2-1-R) for funding support.

L. Sanchez-Nacher wants to thank the "Conselleria d'Educació, Cultura i Esport - Generalitat Valenciana" (reference number: GV/2014/008).

Carbonell-Verdu wants to thank the Polytechnic University of Valencia for their financial support through an FPI grant.

References.

- [1] M. Ali, T. Ueki, T. Hirai, T. Sato, T. Sato, "Dielectric and electromechanical studies of plasticized poly(vinyl chloride) fabricated from plastisol", *Polymer International* (2013) **62**, 501-506.
- [2] F. Wang, W.-g. Yao, C.-d. Qiao, Y.-x. Jia, "Finite element analysis of the physical gelation process of PVC plastisol during rotational molding", *Acta Polymerica Sinica* (2012) **12**, 1035-1041.
- [3] A. Marcilla, J.C. Garcia, R. Ruiz, S. Sanchez, C. Vargas, L. Pita, M.I. Beltran, "Rotational moulding of PVC plastisol", *International Polymer Processing* (2005) **20**, 47-54.
- [4] C.V. Prowse, D. de Korte, J.R. Hess, P.F. van der Meer, T. Biomed Excellence Safer, "Commercially available blood storage containers", *Vox Sanguinis* (2014) **106**, 1-13.
- [5] L. Coltro, J.B. Pitta, P.A. da Costa, M.A. Favaro Perez, V.A. de Araujo, R. Rodrigues, "Migration of conventional and new plasticizers from PVC films into food simulants: A comparative study", *Food Control* (2014) **44**, 118-129.
- [6] C. Bueno-Ferrer, M.C. Garrigos, A. Jimenez, "Characterization and thermal stability of poly(vinyl chloride) plasticized with epoxidized soybean oil for food packaging", *Polymer Degradation and Stability* (2010) **95**, 2207-2212.
- [7] F. Chiellini, M. Ferri, A. Morelli, L. Dipaola, G. Latini, "Perspectives on alternatives to phthalate plasticized poly(vinyl chloride) in medical devices applications", *Progress in Polymer Science* (2013) **38**, 1067-1088.
- [8] L. Coltro, J.B. Pitta, E. Madaleno, "Performance evaluation of new plasticizers for stretch PVC films", *Polymer Testing* (2013) **32**, 272-278.
- [9] A. Zoller, A. Marcilla, "Soft PVC foams: study of the gelation, fusion, and foaming processes. I. Phthalate ester plasticizers", *Journal of Applied Polymer Science* (2011) **121**, 1495-1505.

- [10] B. Bouchoul, M.T. Benaniba, V. Massardier, "Effect of biobased plasticizers on thermal, mechanical, and permanence properties of poly(vinyl chloride)", *Journal of Vinyl & Additive Technology* (2014) **20**, 260-267.
- [11] P. Veiga-Santos, L.M. Oliveira, M.P. Cereda, A.J. Alves, A.R.P. Scamparini, "Mechanical properties, hydrophilicity and water activity of starch-gum film: effect of additives and deacetylated xanthan gum", *Food Hydrocolloids* (2005) **19**, 341-349.
- [12] A. Marcilla, S. Garcia, J.C. Garcia-Quesada, "Migrability of PVC plasticizers", *Polymer Testing* (2008) **27**, 221-233.
- [13] O. Fenollar, D. Garcia-Sanoguera, L. Sanchez-Nacher, J. Lopez, R. Balart, "Effect of the epoxidized linseed oil concentration as natural plasticizer in vinyl plastisols", *Journal of Materials Science* (2010) **45**, 4406-4413.
- [14] N. Ghiou, M.T. Benaniba, "The effect of epoxidized sunflower oil on the miscibility of plasticized PVC/NBR blends", *International Journal of Polymeric Materials* (2010) **59**, 463-474.
- [15] B. Mehta, M. Kathalewar, A. Sabnis, "Benzyl ester of dehydrated castor oil fatty acid as plasticizer for poly(vinyl chloride)", *Polymer International* (2014) **63**, 1456-1464.
- [16] Oil World Annual 2014.
- [17] A. Jimenez, J. Lopez, A. Iannoni, J.M. Kenny, "Formulation and mechanical characterization of PVC plastisols based on low-toxicity additives", *Journal of Applied Polymer Science* (2001) **81**, 1881-1890.
- [18] J.L. Fugit, J.L. Taverdet, J.Y. Gauvrit, P. Lanteri, "Treatment of plasticized PVC to reduce plasticizer/solvent migration: optimization with an experimental design", *Polymer International* (2003) **52**, 670-675.
- [19] L.B. Manfredi, A. Jimenez, A. Vazquez, "Characterization of resol resins modified by the addition of PVC plastisols", *Polymer International* (2005) **54**, 576-580.
- [20] G. Leng, H.M. Koch, W. Gries, A. Schuetze, A. Langsch, T. Bruening, R. Otter, "Urinary metabolite excretion after oral dosage of bis(2-propylheptyl) phthalate (DPHP) to five male

volunteers - Characterization of suitable biomarkers for human biomonitoring", Toxicology Letters (2014) **231**, 282-288.

- [21] A. Lindstrom, M. Hakkarainen, "Environmentally friendly plasticizers for poly(vinyl chloride) - Improved mechanical properties and compatibility by using branched poly(butylene adipate) as a polymeric plasticizer", Journal of Applied Polymer Science (2006) **100**, 2180-2188.
- [22] B.Y. Yu, A.R. Lee, S.-Y. Kwak, "Gelation/fusion behavior of PVC plastisol with a cyclodextrin derivative and an anti-migration plasticizer in flexible PVC", European Polymer Journal (2012) **48**, 885-895.
- [23] H.M. Koch, J. Muller, J. Angerer, "Determination of secondary, oxidised di-iso-nonylphthalate (DINP) metabolites in human urine representative for the exposure to commercial DINP plasticizers", Journal of Chromatography B-Analytical Technologies in the Biomedical and Life Sciences (2007) **847**, 114-125.
- [24] P.H. Daniels, "A brief overview of theories of PVC plasticization and methods used to evaluate PVC-plasticizer interaction", Journal of Vinyl & Additive Technology (2009) **15**, 219-223.
- [25] J. Verdu, A. Zoller, A. Marcilla, "Plastisol gelation and fusion rheological aspects", Journal of Applied Polymer Science (2013) **129**, 2840-2847.
- [26] J. Lopez, R. Balart, A. Jimenez, "Influence of crystallinity in the curing mechanism of PVC plastisols", Journal of Applied Polymer Science (2004) **91**, 538-544.
- [27] O. Fenollar, D. Garcia, L. Sanchez, J. Lopez, R. Balart, "Optimization of the curing conditions of PVC plastisols based on the use of an epoxidized fatty acid ester plasticizer", European Polymer Journal (2009) **45**, 2674-2684.
- [28] A. Carbonell-Verdu, L. Bernardi, D. Garcia-Garcia, L. Sanchez-Nacher, R. Balart, "Development of environmentally friendly composite matrices from epoxidized cottonseed oil", European Polymer Journal (2015) **63**, 1-10.
- [29] O. Fenollar, L. Sanchez-Nacher, D. Garcia-Sanoguera, J. Lopez, R. Balart, "The effect of the curing time and temperature on final properties of flexible PVC with an epoxidized fatty acid ester as natural-based plasticizer", Journal of Materials Science (2009) **44**, 3702-3711.

- [30] A. Zoller, A. Marcilla, "DSC Study of foamable poly (vinyl chloride-co-vinyl acetate) plastisols of different commercial plasticizers", Journal of Applied Polymer Science (2011) **121**, 3314-3321.
- [31] S.Y. Kwak, "Structural-changes of pvc plastisols in progress of gelation and fusion as investigated with temperature-dependent viscoelasticity, morphology, and light-scattering", Journal of Applied Polymer Science (1995) **55**, 1683-1690.

A new biobased plasticizer for poly(vinyl chloride) based on epoxidized cottonseed oil**Alfredo Carbonell-Verdu,¹ David García-Sanoguera,¹ Amparo Jordá-Vilaplana,²
Lourdes Sanchez-Nacher,¹ Rafael Balart¹**¹Instituto de Tecnología de Materiales (ITM), Universitat Politècnica de València (UPV), Plaza Ferrández y Carbonell 1, Alcoy, Alicante 03801, Spain²Departamento de Expresión Gráfica en la Ingeniería, Universitat Politècnica de València (UPV), Plaza Ferrández y Carbonell 1, Alcoy, Alicante 03801, Spain

Correspondence to: A. Carbonell-Verdu (E-mail: alcarve1@epsa.upv.es)

ABSTRACT: The use of epoxidized cottonseed oil as plasticizer for poly(vinyl chloride) was studied. The plasticizer content was set to 70 phr and the optimum isothermal curing conditions were studied in the temperature range comprised between 160 and 220 °C with varying curing times in the 7.5–17.5 min range. The influence of the curing conditions on overall performance of cured plastisols was followed by the evolution of mechanical properties (tensile tests with measurements of tensile strength, elongation at break, and modulus), change in color, surface changes of fractured samples by scanning electron microscopy (SEM), thermal transitions by differential scanning calorimetry, and migration in *n*-hexane. The optimum mechanical features of cured plastisols are obtained for curing temperatures in the 190–220 °C range. For these curing conditions, fractography analysis by SEM gives evidences of full curing process as no PVC particles and free plasticizer can be found. © 2016 Wiley Periodicals, Inc. *J. Appl. Polym. Sci.* 2016, 133, 43642.

KEYWORDS: mechanical properties; plasticizer; poly(vinyl chloride)

Received 13 November 2015; accepted 14 March 2016

DOI: 10.1002/app.43642

INTRODUCTION

Poly(vinyl chloride), PVC is one of the most widely used commodity plastics.¹ It can be manufactured by conventional techniques such as rotational molding, extrusion, injection molding, blow molding, and calendaring, among others, depending on the final product.^{2,3} PVC can be easily plasticized to give flexible materials (P-PVC) with tailored properties which find a wide variety of applications such as blood bags, films and coatings, flexible toys, insulation for electrical wires, and soles due to the high versatility, easy processing, and low cost.^{4–8} Plastisols, or PVC pastes, are obtained by mixing a PVC resin with a liquid plasticizer to form a dispersion of resin particles in plasticizer. With heating, plasticizer diffuses into the resin particle solvating the noncrystalline parts of the polymer chain and causing the resin particles to swell. With further heating, the plasticizer can solvate (fuse) the crystalline sections of the polymer, some of which effectively cross-link the resin, allowing polymer molecules originally found in different resin particles to interact. This paste can be converted into a flexible solid material by a curing process which involves heating the paste to a certain temperature for a given time.⁹ Vinyl plastisols are characterized by high wear and corrosion resistance, as well as excellent elec-

tric insulation. By varying the plasticizer content, it is possible to tailor the final properties of the cured plastisols.¹⁰

Phthalates, citrates, adipates, and carboxylates—among others—have been traditionally used as PVC plasticizers being phthalates the main group due to low cost and excellent overall properties.¹¹ Nevertheless, the use of phthalate-based plasticizers is being reconsidered due to toxicity problems and plasticizer migration.^{5,12} For this reason, new environmentally friendly plasticizers are being demanded by the PVC industry to fulfil the increasingly rigorous requirements of some industrial sectors. Epoxidized vegetable oils offer interesting possibilities in PVC plasticization. Their use as main plasticizer or, more often as secondary plasticizers is continually increasing; it is possible to find recent works based on the use of epoxidized vegetable oils derived from linseed oil, castor oil, soybean oil, sunflower oil, rubber seed oil, and so on, as plasticizers for vinyl plastisols formulations.^{13–15}

In this study, epoxidized cotton seed oil (ECSO) is used due to the surplus produced in the industry and also because it is a by-product of the cotton industry, with about 5.12 million tons production in 2014/2015¹⁶ being China and India, the major producers with 1.396 and 1.320 million tons, respectively. Other

© 2016 Wiley Periodicals, Inc.

IV.3

IV.3. Plasticization effect of epoxidized cottonseed oil (ECSO) on poly(lactic acid).

A. Carbonell-Verdu¹, M. Dolores Samper¹, D. García-García¹, L. Sánchez-Nacher¹, R. Balart¹

¹ **Materials Technology Institute (ITM)**
Universitat Politècnica de València (UPV)
Plaza Ferrandiz y Carbonell 1, 03801, Alcoy, Alicante (Spain)

"Plasticization effect of epoxidized cottonseed oil (ECSO) on poly(lactic acid)"

Abstract

In this work, the use of an environmentally friendly plasticizer derived epoxidized cottonseed oil (ECSO) for poly(lactic acid) (PLA) is proposed. Melt extrusion was used to plasticize PLA formulations with different ECSO contents in the 0 - 10 wt.%. PLA formulation with 10 wt.% shows a remarkable increase in mechanical ductile properties with a percentage increase in elongation at break of more than 1100% and a noticeable increase in the impact absorbed energy. Differential scanning calorimetry (DSC) and dynamic mechanical thermal analysis (DMTA) revealed a clear decrease in the glass transition temperature of neat PLA as the ECSO content increased. Field emission scanning electron microscopy (FESEM) of fractured surfaces from impact tests showed an improvement of ductility with typical rough and porous topographies. Migration tests in n-hexane at different temperatures revealed very low migration properties thus leading to new interesting plasticizers for improved PLA industrial formulations

Keywords

Poly(lactic acid)-PLA; epoxidized cottonseed oil (ECSO); mechanical properties; thermal properties; migration.

IV.3.1. Introduction.

One of the most promising biopolymers as alternative to conventional petroleum-based polymers is poly(lactic acid)-PLA with an annual production of more than 140,000 tons [1]. PLA is an aliphatic polyester obtained by polymerization of lactic acid (hydroxyl propionic acid) obtained from renewable and sustainable starch rich materials such as corn and sugarcane [2-4].

In the last years PLA has become an industrial alternative to some petroleum-based polymers because of its relatively low price [5] and overall balanced mechanical properties such as high tensile strength and Young's modulus with similar values of those of poly(ethylene terephthalate), PET [6] which is widely used in plastic bottle manufacturing due to its excellent barrier properties. PLA possesses acceptable barrier properties, and additionally it can be transparent due to the low crystallization rate [6]. It is also shiny and offers low flammability; all these features, together with a relatively easy processing conditions, similar to many commodities, make PLA a good candidate for a wide variety of products in the packaging industry, automotive parts, textile fibers, prostheses and medical devices, etc. among others [7, 8]. Nevertheless, PLA is characterized by high fragility, which is drawback for some technical applications in which some flexibility is required [9].

For these reasons, different approaches have been explored to overcome this high intrinsic fragility by increasing ductile properties such as elongation at break, impact resistance, etc. while maintaining its environmentally friendly nature. A typical approach has been blending PLA with other ductile polymers. In this field, PLA was blended with chitosan, which is able to form films but the mixtures resulted in immiscible blends due to their different polarity and poly(vinyl alcohol), PVA was necessary to provide somewhat compatibility [1]. Thermoplastic starch (TPS) also showed immiscibility with PLA and several compatibilizers such as maleic anhydride and methylene diphenyl diisocyanate (MDI) were needed to improve the overall properties [10-12]. Blends with poly(hydroxybutyrate), PHB gave an interesting improvement on barrier properties of neat PLA but resulting blends were characterized by high fragility so that, different plasticizers such as acetyl(tributyl citrate), ATBC [13] and poly(ethylene glycol), PEG [14] were needed to overcome this drawback. PLA has also been blended with biodegradable

petroleum-based polymers to give fully biodegradable blends. Among these petroleum-based polymers interesting results have been obtained with poly(caprolactone)-PCL biodegradable polyester. Although both PLA and PCL are polyester-type polymers, they show restricted miscibility but the high flexibility of PCL is enough to reduce the intrinsic fragility of PLA [15-17]. Other petroleum-based polymers such as poly(butylene succinate)-PBS [18], poly(butylene succinate-co-adipate)-PBSA [19], poly(butyl acrylate)-PBA [20] and poly(butylene adipate-co-terephthalate)-PBAT [21, 22] have been successfully blended with PLA with remarkable increase in flexibility.

Another way to improve the flexibility of neat PLA is by using plasticizers. Among the wide variety of commercial plasticizers, most of them derived from petroleum, epoxidized vegetable oils (EVOs) represent an interesting alternative as they are cost-effective materials with high performance as plasticizers and are obtained from renewable resources, mainly from vegetable oils with non-food purposes. Epoxidized oils are used in the PVC industry as secondary plasticizers and thermal stabilizers due to their free radical scavenging properties [23-25].

In the last years, the potential of different epoxidized vegetable oils has been explored. Some epoxidized oils such as epoxidized soybean oil (ESBO) and epoxidized linseed oil (ELO) are commercially available at a relatively low cost and, consequently, they can be readily employed in industrial applications. Epoxidized soybean oil (ESBO) contains an oxirane oxygen content comprised in the 6.5 – 8% range and it has been reported as an interesting plasticizer for PLA. The study developed by Yu-Qiong Xu *et al.* revealed that addition of 6 wt.% ESBO to PLA increased the elongation at break from 3.98% for neat PLA to values of 6.50%. Similar findings were reported by Shalini Vijayarajan *et al.* They evaluated the influence of ESBO content (up to 20 wt.%) on ductility, measured as the ratio between the failure to yield strain. They found the best overall ductile properties for ESBO contents in the 5-10 wt.% range [26, 27]. With regard to epoxidized linseed oil (ELO), which contains more average number of oxirane groups per triglyceride than ESBO, Javed Alam *et al.* reported the plasticizing effect provided by ELO with a remarkable increase in elongation at break and a subsequent decrease in tensile strength. Addition of carbon nanotubes contributed to balanced mechanical ductile and resistant properties [28]. Interesting results with low oxirane oxygen content epoxidized oils have also been reported. Buong Woei Chieng *et al.* reported the potential of epoxidized palm oil (EPO) with an oxirane oxygen content of 3.23% and a mixture of

epoxidized palm oil and epoxidized soybean oil with an average oxirane oxygen content of 3.58%, showing that 5 wt.% of the epoxidized oil leads to a remarkable increase in ductile properties. Furthermore, the mixture with higher oxirane oxygen content led to the highest elongation at break values [6].

Cottonseed oil (CSO) is considered a by-product of the cotton industry with a total production around 5.12 million tons in 2014/15 [29], being China and India the major world producers with 1.396 and 1.320 million tons respectively. Although some uses in the food industry are common, its generalized use is restricted because of some drawbacks: on the one hand, it is worth to note that the main product of the cotton industry is cotton fiber so that, cotton crops are not subjected to the severe controls and regulations regarding the use of pesticides and other chemicals. On the other hand, cottonseed oil contains high amounts of free gossypol which has been reported as a potentially toxic substance [30]. The particular lipid profile of cotton seed oil, with approximately 75% of unsaturated fatty acids makes this oil an interesting candidate for chemical modification such as epoxidation [31]. The oxirane oxygen content of epoxidized cottonseed oil (ECSO) is located between low values typical of epoxidized palm oil (EPO) and high values typical of epoxidized soybean oil (ESBO) and epoxidized linseed oil (ELO). For this reason, this work aims to study the potential of epoxidized cottonseed oil (ECSO) with an intermediate oxirane oxygen content as environmentally friendly plasticizer for poly(lactic acid), PLA. The effect of the epoxidized oil content on mechanical, thermal and migration properties of PLA were tested.

IV.3.2. Experimental.

Materials.

Poly(lactic acid), PLA commercial grade Ingeo TM Biopolymer 6201D was supplied by NatureWorks LLC (Minnetonka, USA) in pellet form with a density of 1.24 g cm⁻³. Its melt flow index is in the 15-30 g/10 min range measured at a temperature of 210 °C. The base oil for plasticizer synthesis was cottonseed oil (CSO). This was supplied by Sigma Aldrich (Sigma Aldrich, Madrid, Spain). This oil is characterized by a density 0.92

g cm^{-3} at $25\text{ }^{\circ}\text{C}$ and an iodine number of 107. This vegetable oil was subjected to an epoxidation process as indicated elsewhere with hydrogen peroxide and acetic acid [31]. After epoxidation, the oxirane number of the synthesized epoxidized cottonseed oil was 5.32% and its iodine number was 1.79. **Figure IV.3.1** shows an schematic representation of the chemical structures of poly(lactic acid) and epoxidized cottonseed oil.

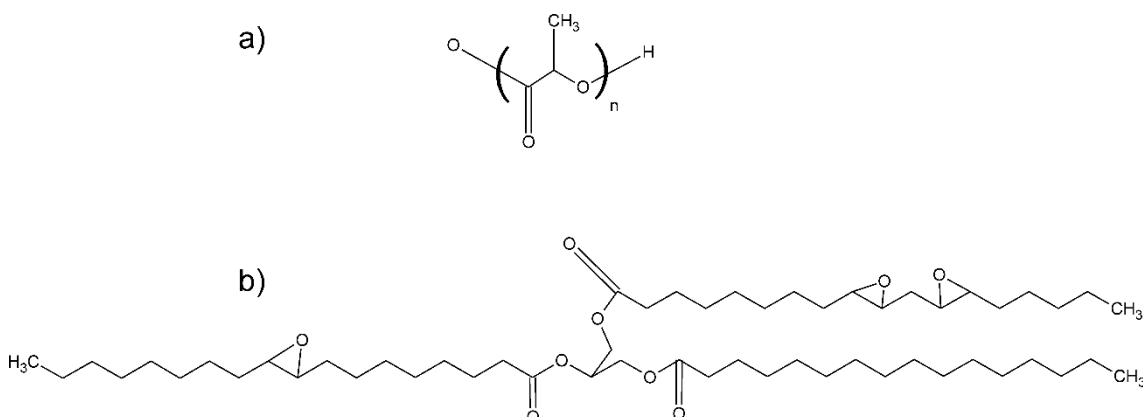


Figure IV.3.1. Schematic representation of the chemical structure of a) poly(lactic acid)-PLA and b) epoxidized cottonseed oil (ECSO).

■ Manufacturing of plasticized poly(lactic acid).

Firstly, PLA pellets were dried at $60\text{ }^{\circ}\text{C}$ for 24 h. PLA pellets and the corresponding amounts of the liquid plasticizer (see **Table IV.3.1**) were mechanically mixed in a zip bag until homogenization.

Table IV.3.1. Composition of ECSO plasticized PLA materials and labelling.

Reference	PLA (wt.%)	ECSO (wt.%)
PLA	100	0
PLA – 2.5 % ECSO	97.5	2.5
PLA – 5 % ECSO	95.0	5.0
PLA – 7.5 % ECSO	92.5	7.5
PLA – 10 % ECSO	90.0	10.0

After this stage, the mixtures were extruded in a twin screw extruder at a constant speed of 40 rpm. The temperature profile ranged from 170 °C (feeding zone) to 180 °C (die). Then the extrudate was pelletized and subsequently shaped into standard samples in an injection molding machine Meteor 270/75 (Mateu & Solé, Barcelona, Spain) at an injection temperature of 180 °C.

Mechanical characterization of ECSO plasticized PLA.

Mechanical characterization was conducted with standard tensile, flexural and impact tests. Tensile and flexural characterization was carried out in a universal test machine Ibertest Elib 30 (Ibertest S.A.E., Madrid, Spain). A minimum of five different samples were tested using a 5 kN load cell. Tensile tests were carried out at a crosshead speed of 10 mm min⁻¹ as recommended by the ISO 527 standard. An axial extensometer from Ibertest was used to give accurate values of the Young's modulus. Regarding the flexural test, the crosshead speed was set to 5 mm min⁻¹ as suggested by the ISO 178. The impact absorbed energy was measured in a 6 J Charpy's pendulum (Metrotect S.A., San Sebastián, Spain) following the guidelines of the ISO 197:1993.

Morphology of ECSO plasticized PLA.

Fractured surfaces from impact tests were observed by field emission scanning electron microscopy (FESEM) in a Zeiss Ultra microscope 55 (Oxford Instruments, Oxfordshire, United Kingdom) with an accelerating voltage of 2 kV. Fractured surfaces were previously coated with a thin platinum layer in a sputter coater EM MED020 (Leica Microsystems).

Thermomechanical characterization of ECSO plasticized PLA.

Thermomechanical characterization was conducted by measuring the Vicat softening temperature (VST), heat deflection temperature (HDT). VST and HDT values were determined in a DEFLEX 687-A2 station (Metrotect S.A., San Sebastián, Spain). VST was measured according to ISO 306 (B method) at a constant heating rate of 50 °C h⁻¹ and a load of 50 N. Regarding HDT values, they were obtained as recommended by the ISO 75 (A method) at a fixed heating rate of 120 °C h⁻¹ and a constant load of 1.8 MPa. Additionally, dynamic mechanical thermal analysis (DMTA) was used to evaluate changes in storage modulus (G') and damping factor. Samples sizing 40x40x4 mm³ were tested in torsion mode in an oscillatory rheometer AR G2 (TA Instruments, New Castle, USA) equipped with an accessory clamp for solid samples. Samples were subjected to a thermal program from 25 °C to 130 °C at a heating rate of 2 °C min⁻¹. The frequency was set to 1 Hz and the maximum deformation (γ) was 0.1%.

Thermal characterization of ECSO plasticized PLA.

Thermal behavior of ECSO plasticized PLA samples was tested by differential scanning calorimetry (DSC) and thermogravimetric analysis (TGA). Differential scanning calorimetry tests were carried out in a Mettler-Toledo calorimeter 821e (Mettler-Toledo Inc., Schwerzenbach, Switzerland). Samples with an average weight in the 7-8 mg range were subjected to the following thermal program: initial heating from 30 °C to 210 °C at a heating rate of 10 °C min⁻¹ in nitrogen atmosphere with a nitrogen flux of 66 mL min⁻¹. The glass transition temperature (T_g), cold crystallization peak (T_{cc}) and the melt peak temperature (T_m) were obtained for each plasticized PLA formulation. The degree of crystallinity (X_c %) was calculated by Equation IV.3.1.

$$X_c (\%) = 100 \times \frac{|\Delta H_{cc} + \Delta H_m|}{\Delta H_m(100\%)} \times \frac{1}{W_{PLA}}$$
Equation IV.3.1

Where ΔH_{cc} is the cold crystallization enthalpy, ΔH_m is the melt enthalpy, $\Delta H_m(100\%)$ is the theoretical melt enthalpy for a fully crystalline PLA structure (93 J g^{-1}) [32] and WPLA is the PLA weight fraction.

The initial heating step was applied to remove the previous thermal history of the materials.

Thermogravimetric analysis was carried out in a TGA/SDTA 851 thermobalance from Mettler-Toledo (Mettler-Toledo Inc., Schwerzenbach, Switzerland). Samples with an average weight of 10 mg were subjected to a heating program from 30°C to 700°C at a heating rate of $20^\circ\text{C min}^{-1}$ and constant nitrogen flux (66 mL min^{-1}).

■ Plasticizer migration by the solvent extraction test.

Plasticizer migration was studied by solvent extraction with n-hexane. Samples were immersed in *n*-hexane and placed in an air circulating oven mod. Selecta 2001245 (JP Selecta S.A., Barcelona, Spain) working at different temperatures, between 30°C and 60°C during 8 hours. Finally, the samples were removed from n-hexane to measure weight loss.

IV.3.3. Results and discussion.

■ Mechanical properties of ECSO plasticized PLA formulations.

The study of the effect of the epoxidized cottonseed oil (ECSO) on mechanical properties of PLA-based formulations is a good method to assess the plasticization that ECSO provides. PLA is a brittle polymer with relatively high tensile and flexural strength

values, high modulus and very low elongation at break. **Table IV.3.2** summarizes the main results obtained by tensile and flexural tests.

Table IV.3.2. Summary of mechanical properties from tensile and flexural tests of plasticized PLA formulations with different weight % of epoxidized cottonseed oil (ECSO).

wt.% ECSO plasticizer	Tensile strength (MPa)	Young's modulus (MPa)	Elongation at break (%)	Flexural Modulus (MPa)	Flexural Strength (MPa)
0	63.7 ± 2.41	3592 ± 130	9.06 ± 0.12	3296 ± 78.7	116.3 ± 1.11
2.5	58.5 ± 1.08	3346 ± 136	13.5 ± 2.11	3233 ± 14.4	83.7 ± 2.05
5	56.6 ± 0.32	3390 ± 165	34.9 ± 4.45	3369 ± 5.70	78.6 ± 2.97
7.5	52.3 ± 0.34	3334 ± 143	74.8 ± 7.92	3317 ± 142	64.6 ± 3.48
10	49.5 ± 0.87	3399 ± 145	110.5 ± 13.73	3361 ± 73.8	53.3 ± 4.41

Neat PLA possesses a tensile strength of 63.7 MPa with very low elongation at break values around 9%. As the elastic modulus is defined by the ratio strength to elongation in the linear region, high strength with very low elongation give high modulus of 3.6 GPa. The plasticization effect is evident by observing the changes in both mechanical resistant and ductile properties. Plasticized PLA with 2.5 wt.% ECSO is characterized by slightly higher elongation at break values of 13.5% and a subsequent decrease in both tensile strength and Young's modulus with values of 58.5 MPa and 3.3 GPa respectively. As the total plasticizer content in PLA formulations increases it is clearly detectable a remarkable improvement in ductile properties by a dramatic change in elongation at break up to values of 110.5% for PLA formulations containing 10 wt.% ECSO which is approximately eleven times higher than the elongation at break of unplasticized PLA (9%). This represents an overall percentage increase of around 1128% regarding to neat PLA, calculated as the percentage ratio of the variation in elongation at break (110.5% - 9%) to the elongation at break of neat PLA (9%).

These results are in accordance with previous works regarding PLA plasticization with epoxidized vegetable oils. Buong Woei Chieng *et al.* reported a percentage increase in elongation at break of more than 2000% with the only addition of 5 wt.% epoxidized palm oil (EPO) to PLA formulations. In fact, the elongation at break changed from 5.3% (neat PLA) up to 114.4% for the corresponding EPO-plasticized formulation. Even better results were obtained in PLA formulations plasticized with a mixture of epoxidized palm

and soybean oil (EPSO) with an elongation at break of 220.5%. They also reported a noticeable drop on tensile strength values from values close to 60 MPa for neat PLA up to values of 35 MPa for plasticized PLA formulations with an epoxidized palm oil (EPO) content between 5 – 10 wt.%. This dramatic drop in tensile strength is directly related to polymer-plasticizer interactions.

The epoxy groups contained in the epoxidized vegetable oil can interact with the hydroxyl groups located in the end chains of PLA. As they suggest, these interactions are stronger as the oxirane oxygen content increases [6]. Their findings are in total accordance with the plasticizing effect that epoxidized cottonseed oil (ECSO) provides. ECSO is characterized by a medium oxirane oxygen content (5.32%) compared to epoxidized palm oil (EPO) with low values (3.23%) and epoxidized linseed oil (ELO) with high values around 10%. As it can be observed in **Table IV.3.2**, the tensile strength of neat PLA (63.7 MPa) is reduced to values close to 50 MPa with the maximum ECSO content. This drop in tensile strength is lower than that observed by Buong Woei Chieng *et al.* with epoxidized palm oil (EPO). The higher oxirane oxygen content in ECSO can interact more strongly with PLA chains leading to intense polymer-plasticizer interactions that provide balanced tensile strength and elongation at break values. Regarding the Young's modulus, the initial value corresponding to unplasticized PLA is 3.6 GPa and this is slightly reduced up to values of 3.3 GPa for plasticized formulations with varying ECSO content.

Although the plasticization effect of ECSO and other epoxidized vegetable oils is evident through a remarkable increase in elongation at break values. It has been reported that once the optimum plasticizer content has reached, a plasticizer excess leads to lower elongation at break values due to a possible phase separation [33]. Although the values are not summarized in **Table IV.3.2**, a plasticized PLA formulation was also prepared with 15 wt.% ECSO. The elongation at break of this formulation was similar to that obtained for the plasticized PLA formulation with 5 wt.% thus giving a clear evidence of plasticizer saturation which has a negative effect on ductile properties due to phase separation.

Similar behaviour has been found for flexural tests. As it can be observed in **Table IV.3.2** the flexural strength of neat PLA (116.3 MPa) is progressively reduced up to values of 78.6 MPa and 53.3 MPa for plasticized PLA formulations containing 5 wt.% and 10 wt.% ECSO respectively. Although slight changes can be produced on flexural

modulus, these changes are in the typical error range so that, no clear tendency can be observed.

As above mentioned, the addition of ECSO provides a clear plasticizing effect on PLA with a remarkable increase in mechanical ductile properties such as elongation at break. Besides this, ECSO plasticized PLA formulations are remarkably toughened as it can be seen in **Figure IV.3.2**. The high intrinsic brittleness of neat PLA is reduced due to the toughening and elastomeric effect provided by the ECSO plasticizer. An increasing tendency of impact absorbed energy can be seen in **Figure IV.3.2**. Neat PLA possesses an impact energy of 30.8 kJ m⁻² and this is progressively increased up to values of 38.42 kJ m⁻² for the plasticized PLA formulation with 10 wt.% ECSO which represents a percentage increase of 25% regarding neat PLA. As shown by tensile and flexural tests, addition of ECSO promotes a remarkable increase in elongation and this has a positive effect on energy absorption.

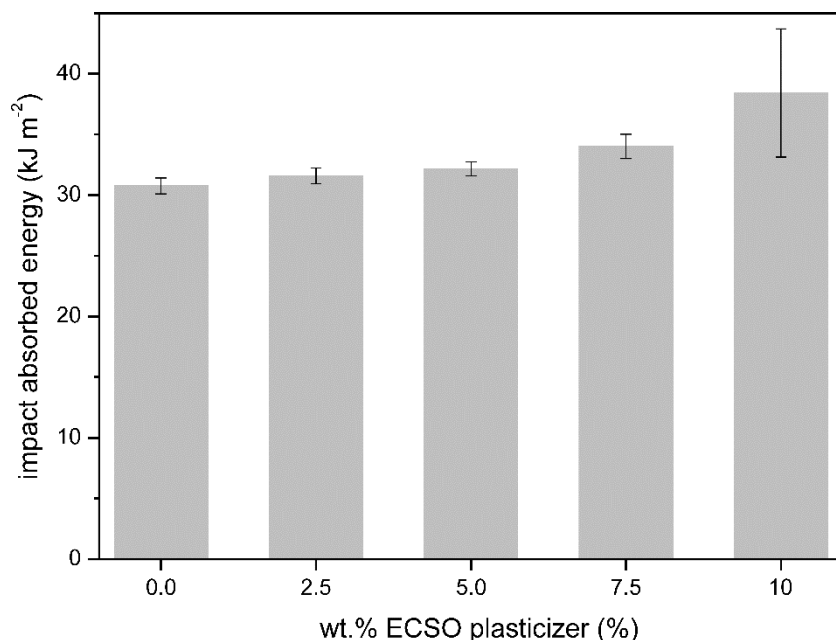


Figure IV.3.2. Plot evolution of the impact absorbed energy measured by the Charpy's test for plasticized PLA formulations with different weight % of epoxidized cottonseed oil (ECSO).

The effect of epoxidized cottonseed oil (ECSO) on the morphology of plasticized PLA formulations can be observed in **Figure IV.3.3** which shows FESEM images of

fractured surfaces from impact tests samples. **Figure IV.3.3[a]** shows the typical fracture surface of a brittle polymer with a flat and smooth surface and no evidence of plastic deformation.

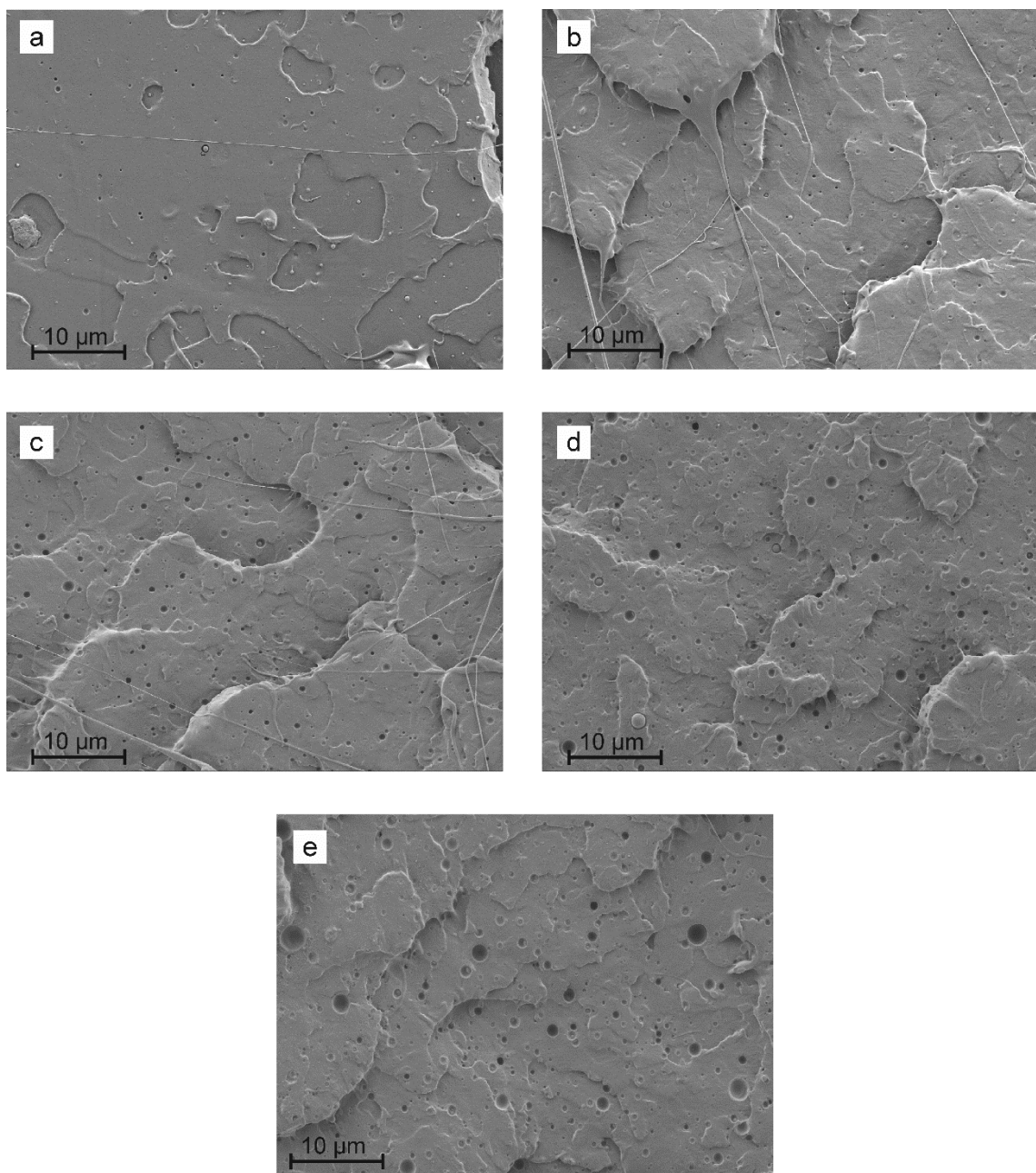


Figure IV.3.3. FESEM images of fractured surfaces from impact tests corresponding to plasticized PLA formulations with different weight % of epoxidized cottonseed oil (ECSO) at 2000x: a) neat PLA, b) 2.5 wt.% ECSO, c) 5.0 wt.% ECSO, d) 7.5 wt.% ECSO and e) 10 wt.% ECSO.

For low ECSO plasticizer content of 2.5 wt.% (**Figure IV.3.3[b]**) a homogeneous surface can be observed which is representative for good compatibility between PLA and ECSO plasticizer that is uniformly distributed in the PLA matrix. In addition to this, other plasticization signs can be detected in the form of fibrils resulting from plastic deformation during a sudden impact. This phenomenon is in total accordance with the previous mechanical properties.

Plasticized PLA formulations with very low amounts of ECSO plasticizer are characterized by a relative low increase in elongation at break. This fact could be related to strong interactions between PLA polymer chains and the epoxidized cottonseed oil. These strong interactions occur because no phase separation occurs as observed in **Figure IV.3.3[b]**. As the weight % of ECSO increases some spherical cavities/voids can be observed. These are produced by a cavitation process caused by debonding. The empty microvoids indicate presence of an epoxidized cottonseed oil rich phase dispersed in the PLA matrix that becomes more evident with increasing ECSO content. Presence of fibrils is less evident as the ECSO content increases. In general, FESEM reveals good miscibility between PLA and ECSO plasticizer for very low plasticizer content as observed by V. S. Giita Silverajah et al [34]. By increasing the plasticizer content, phase separation is more evident but elongation at break is highly improved until plasticizer saturation occurs. Over 10 wt.% ECSO, plasticizer saturation occurs and mechanical properties are not improved.

Thermal properties of ECSO plasticized PLA formulations.

Effective plasticization promotes important changes in thermal transitions, mainly the glass transition temperature (T_g) due to increased polymer chain mobility. **Figure IV.3.4** and **Figure IV.3.5** show the effect of the ECSO plasticizer on dynamic mechanical response of plasticized PLA formulations. As it can be seen in **Figure IV.3.4**, the storage modulus (G') shows a flat plot from room temperature up to 50 °C. Then the storage modulus undergoes a drops of nearby three orders of magnitude and tends to stabilize at about 70 °C. This abrupt drop is directly related to the glass transition temperature (T_g) [6]. As the temperature raises and reaches values comprised

in the 80 – 90 °C range, a new increase in storage modulus can be detected which is related to the cold crystallization process. Regarding samples with different loads of ECSO plasticizer, the storage modulus curves are identical in shape but the typical values are shifted to lower temperatures thus indicating a decrease in both the glass transition temperature and cold crystallization process. The storage modulus of neat PLA below the glass transition temperature is close to 1.4 GPa. All plasticized formulations show a slight decrease in the storage modulus in this initial stage with typical values of 1.1 GPa thus indicating a clear plasticization effect. Plasticizer increases chain mobility and this has a positive effect on lowering both glass transition temperature and cold crystallization. The cold crystallization represents the realignment of PLA chains to form a more packed structure. It is evident that the plasticizer enables this rearrangement as it increases polymer chain mobility. The cold crystallization temperature changes from 81.7 °C for neat PLA to values of 78 °C for ECSO plasticized PLA formulations.

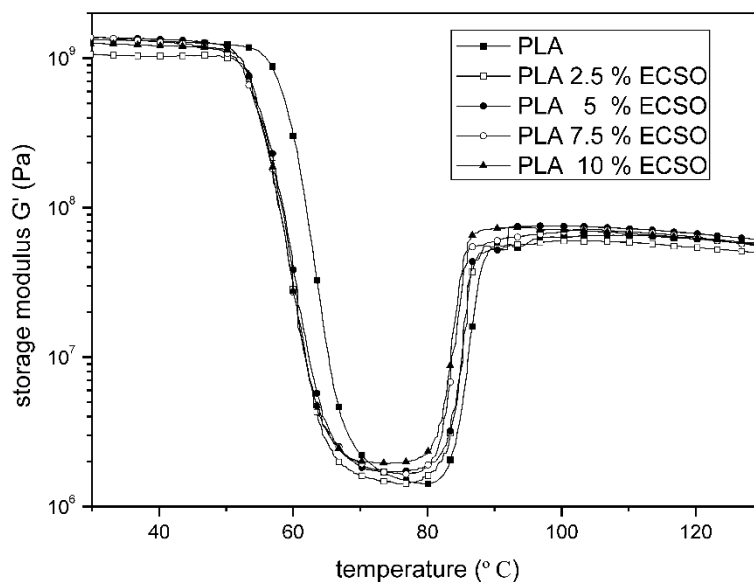


Figure IV.3.4. Plot evolution of the storage modulus (G') as function of temperature for plasticized PLA formulations with different weight % of epoxidized cottonseed oil (ECSO).

By observing the evolution of the damping factor ($\tan \delta$) it is possible to detect two relaxations located at 50-70 °C and 80-90 °C which are attributed to the glass

transition (T_g) and the cold crystallization (T_{cc}) temperatures respectively. The efficiency of the ECSO plasticizer can be assessed by measuring the changes in the glass transition temperature (T_g) [35]. Although the glass transition occurs in a temperature range, maximum values of the damping factor were taken as representative values (see **Figure IV.3.5**). The T_g of neat PLA is 66.2 °C. As the ECSO content increases, a decreasing tendency in T_g values can be observed up to values of 63.4 °C and 62.5 °C for plasticized PLA formulations with 2.5 wt.% and 10 wt.% ECSO respectively.

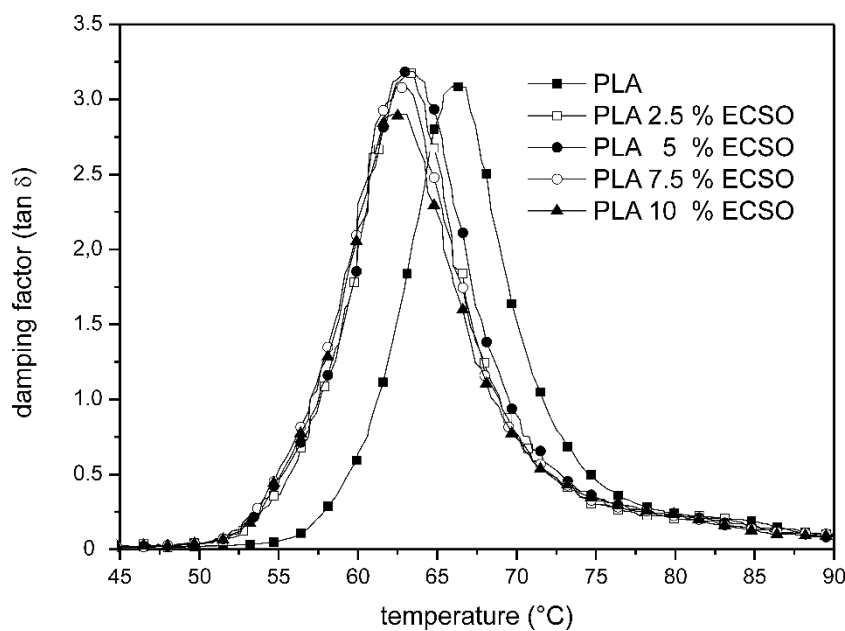


Figure IV.3.5. Plot evolution of the damping factor ($\tan \delta$) as function of temperature for plasticized PLA formulations with different weight % of epoxidized cottonseed oil (ECSO).

The plasticizing effect is also evident by observing the evolution of the Vicat softening temperature (VST) and heat deflection temperature (HDT) as seen in **Table IV.3.3**. Neat PLA is characterized by a HDT value of 47.6 °C and this is reduced up to values in the 43 - 44 °C range for all compositions. With regard to the Vicat softening temperature (VST) it changes from 52.8 °C for neat PLA up to values of 43 °C for the plasticized formulation with 10 wt.% ECSO thus indicating a clear plasticization effect related to increased polymer chain mobility.

Table IV.3.3. Summary of thermomechanical properties, Vicat softening temperature (VST) and heat deflection temperature (HDT) of plasticized PLA formulations with different weight % of epoxidized cottonseed oil (ECSO).

wt.% ECSO plasticizer	Heat deflection temperature, HDT (°C)	Vicat softening temperature, VST (°C)
0	47.6	52.8
2.5	43.6	47.6
5.0	43.4	43.4
7.5	43.2	43.4
10.0	44.2	43.0

As indicated previously, both the storage modulus (G') and the damping factor ($\tan \delta$) obtained by dynamic mechanical thermal analysis revealed a decrease in the glass transition temperature (T_g) of neat PLA with increasing the ECSO plasticizer content. Differential scanning calorimetry (DSC) is a powerful technique that provides information not only about the glass transition and cold crystallization processes but also about the melt process.

Figure IV.3.6 shows a comparative plot of the DSC heating thermograms of neat PLA and plasticized PLA formulations with different ECSO content. The glass transition temperature of neat PLA is 66.75 °C. The cold crystallization process is clearly evident as an exothermic peak located in the 86 °C – 114 °C range with a maximum crystallization rate located at 97 °C. Finally, the endothermic process between 156 °C – 177 °C corresponds to the melting of the crystalline phase in PLA. By observing the DSC heating thermograms of the plasticized PLA formulations with different weight % of ECSO plasticizer it is clearly evident a decrease in both the glass transition temperature (T_g) and the cold crystallization temperature range (and its representative temperature peak, T_{cc}). Thus, the plasticized formulation with low plasticizer content (2.5 wt.% ECSO) possesses a glass transition and cold crystallization temperatures of 63.8 °C and 91.2 °C respectively. These values are still lower for PLA plasticized formulations with higher plasticiser content. Therefore, PLA formulation with 10 wt.% ECSO is characterized by a glass transition temperature of 60.7 °C and a cold crystallization peak located at 86.95 °C. The decrease in the temperature range of the cold crystallization process is directly related to the plasticizing effect that ECSO provides. The plasticizer molecules, characterized by low molecular weight compared to polymer chains, diffuse inside the polymer matrix and are placed between polymer chains. This situation leads to an

increase in the free volume that allows polymer chain motions to occur at lower temperatures.

Additionally, the polymer-polymer interactions are less strong because the distance between polymer chains is increased by the plasticizer. Furthermore, in addition to the dilution effect that ECSO provides on the cold crystallization enthalpy (ΔH_{cc}), these values are lower because of the increased free volume that allows easy packing of the plasticized structure. Similar findings were reported by V. S. Giita Silverajah *et al.* with plasticized PLA with epoxidized palm oil (EPO). They concluded that good miscibility/compatibility between PLA and EPO was obtained for very low EPO content of 1 wt.%. They also reported a decrease in the glass transition of neat PLA for EPO contents of 5 wt.% but they observed clear phase separation for these formulations [34].

By taking into account the melt and cold crystallization enthalpies, it is possible to assume that PLA possesses a degree of crystallinity (X_c %) of 20.5%. The presence of plasticizer enables chain mobility and this has a positive effect on crystallization as polymer chains can move to a packed structure. The only addition of 2.5 wt.% ECSO leads to a degree of crystallinity of about 31.3% and similar values around 32.3% are obtained for plasticized PLA formulations with 10 wt.% ECSO. Similar findings were reported by Ferri *et al.* with plasticized PLA formulations with epoxidized fatty acid esters [33].

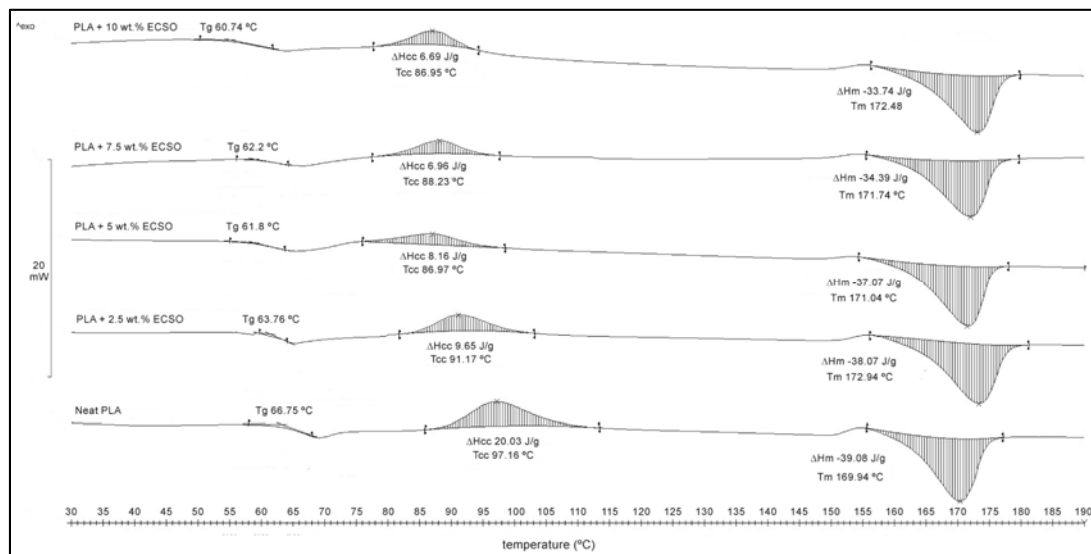


Figure IV.3.6. Comparative plot of the DSC heating thermograms of neat PLA and plasticized PLA formulations with different weight % of epoxidized cottonseed oil (ECSO).

Epoxidized vegetable oils also provide improved stability. The oxirane rings are able to scavenge acid groups by catalytic degradation and this has a positive effect on both thermal and light stabilization. In fact, one of the main commercial uses of epoxidized vegetable oils is as secondary plasticizers and thermal and light stabilizers [36].

Table IV.3.4 shows the typical degradation temperatures for neat PLA and plasticized PLA formulations with varying ECSO content. The onset degradation temperature has been assessed by the temperature with a wt.% loss of 5% ($T_{5\%}$). In addition, the temperature for a 50 wt.% loss has been assessed ($T_{50\%}$). The thermal stabilization effect that epoxidized cottonseed oil provides can be seen by observing the evolution of the onset degradation temperature. Neat PLA is characterized by a $T_{5\%}$ of 335.5 °C and this is upward shifted to almost 340 °C for PLA formulations containing 10 wt.% ECSO.

Table IV.3.4. Main degradation parameters obtained by thermogravimetric analysis (TGA) for plasticized PLA formulations with different weight % of epoxidized cottonseed oil (ECSO).

wt.% ECSO plasticizer	$T_{5\%}$ (°C)	$T_{50\%}$ (°C)
0	335.5	363.6
2.5	337.5	363.9
5.0	336.9	365.8
7.5	337.1	365.7
10.0	339.2	364.8

■ Plasticizer migration assessment on plasticized PLA formulations with ECSO.

The potential migrants from poly(lactic acid) include lactic acid, the cyclic dimer of lactic acid (lactide), the linear dimer of lactic acid (lactoyl lactic acid) and other oligomers. Several studies have assessed PLA as a safe substance for food-contact and lactic acid has been declared as a generally recognized as safe (GRAS) substance [37].

Nevertheless, most industrial PLA formulations include plasticizers and other additives to tailor properties.

For this reason, it is important to know the potential plasticizer migration levels as it can restrict some uses in the food packaging industry. The solvent extraction test is a quite aggressive test to measure total migrated plasticizer and gives interesting results about the potential use of plasticizers at industrial scale.

Figure IV.3.7 shows a comparative plot of the total plasticizer migrated in terms of increasing temperature (all migrated amounts are referred at a migration time of 8 h). As it can be observed, PLA does not show any relevant migration at 8 h in the temperature range comprised between 30 °C and 60 °C with weight % migration values less than 0.02%. Regarding PLA formulations with epoxidized cottonseed oil (ECSO) the lowest migration levels are obtained, as expected, at the lowest temperature considered in this study (30 °C) with typical values of 0.03% and 0.06% for PLA formulations with 2.5 wt.% and 10 wt.% ECSO respectively. As temperature increases, the total amount of migrated plasticizer increases as well but the maximum migration levels achieved are less than 0.12% which indicates a very low plasticizer migration. It is important to note that epoxidized vegetable oils are characterized by a molecular weight comprised between 850 g mol⁻¹ to 950 g mol⁻¹.

Although these values are extremely lower compared to poly(lactic acid) molecular weight, other monomeric plasticizers for PLA have lower molecular weight, *i.e.* acetyl tributyl citrate, ATBC (402.5 g mol⁻¹) [38], tributyl citrate, TBC (360.44 g mol⁻¹) [39], di-2-ethylhexyladipate, DOA (371 g mol⁻¹) [40].

For this reason, the migration levels with epoxidized vegetable oils is extremely low compared to other monomeric plasticizers. As expected, migrated plasticizer amounts increase with temperature with similar values for all plasticized PLA formulations. These relative low migration levels indicate good plasticizer compatibility as indicated previously. Interaction of epoxy groups present in epoxidized cottonseed oil (ECSO) with hydroxyl groups in poly(lactic acid) leads to a plasticization effect and potential chain extension phenomenon. These strong interactions positively contribute to low migration levels thus indicating the feasibility of using these plasticized formulations at industrial scale.

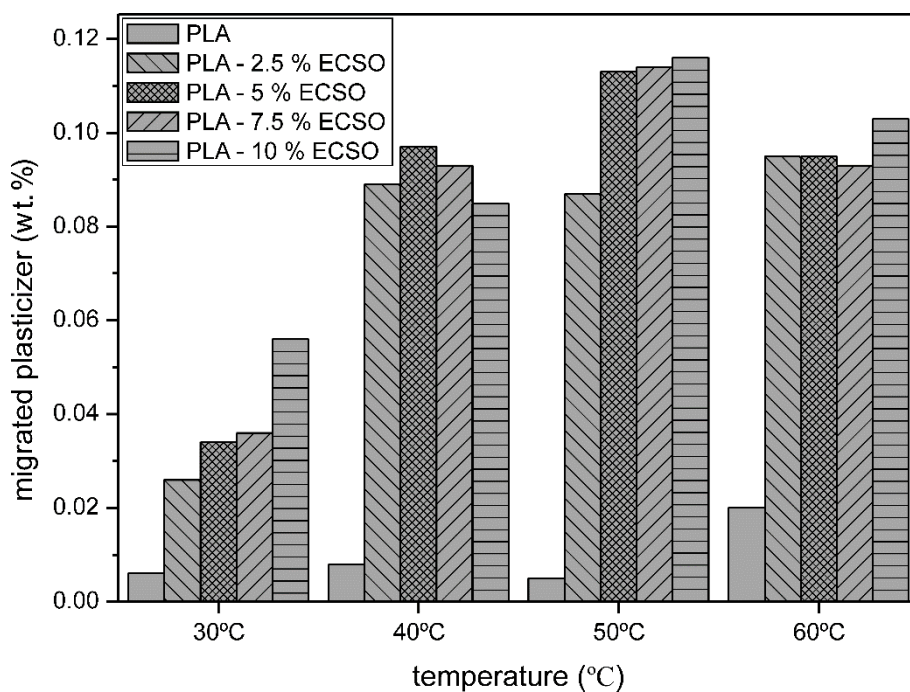


Figure IV.3.7. Plasticizer migration levels by the solvent extraction test on plasticized PLA formulations with different weight % of epoxidized cottonseed oil (ECSO).

IV.3.4. Conclusions.

New environmentally friendly plasticized PLA formulations were obtained with epoxidized cottonseed oil (ECSO). The low intrinsic elongation at break of PLA (9%) was improved up to values of 110.5% for plasticized formulations with 10 wt% ECSO. Field emission scanning microscopy (FESEM) revealed good miscibility at low ECSO concentrations (lower than 2.5 wt%) while slight phase separation occurred over this composition. Despite this, a remarkable increase in toughness was observed for compositions over 2.5 wt.% due to the particular morphology defined by a PLA matrix with finely dispersed spherical ECSO domains. The glass transition temperature was reduced by around 5-6 °C for plasticized formulations with 7.5 – 10.0 wt.% ECSO. This decrease in T_g gave evidences of increased free volume with a positive effect on chain mobility, so that both the glass transition and the cold crystallization temperature were

moved to lower values. Very low migration levels were assessed by the solvent extraction test with n-hexane with a maximum migration of 0.12% at 50-60 °C while very low plasticizer migration (<0.06%) was observed at 30 °C. The results obtained in this work suggest that high environmentally friendly toughened PLA formulations can be obtained by using epoxidized cottonseed oil (ECSO) in the 5 – 10 wt% range. Over 10 wt% ECSO, plasticizer saturation occurs and this has a negative effect on overall properties.

Acknowledgements.

This research was supported by the Ministry of Economy and Competitiveness - MINECO, Ref: MAT2014-59242-C2-1-R. Authors also thank to "Conselleria d'Educació, Cultura i Esport" - Generalitat Valenciana, Ref: GV/2014/008 for financial support. A. Carbonell-Verdu wants to thank Universitat Politècnica de València for financial support through an FPI grant. D. Garcia-Garcia wants to thanks the Spanish Ministry of Education, Culture and Sports for their financial support through an FPU grant (FPU13/06011).

References.

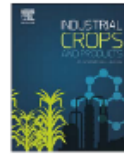
- [1] R. Grande, L.A. Pessan, A.J.F. Carvalho, "Ternary melt blends of poly(lactic acid)/poly(vinyl alcohol)-chitosan", *Industrial Crops and Products* (2015) **72**, 159-165.
- [2] E.A.J. Al-Mulla, A.H. Suhail, S.A. Aowda, "New biopolymer nanocomposites based on epoxidized soybean oil plasticized poly(lactic acid)/fatty nitrogen compounds modified clay: Preparation and characterization", *Industrial Crops and Products* (2011) **33**, 23-29.
- [3] L. Sansone, A. Aldi, P. Musto, E. Di Maio, E. Amendola, G. Mensitieri, "Assessing the suitability of polylactic acid flexible films for high pressure pasteurization and sterilization of packaged foodstuff", *Journal of Food Engineering* (2012) **111**, 34-45.
- [4] I. Blanco, V. Siracusa, "Kinetic study of the thermal and thermo-oxidative degradations of polylactide-modified films for food packaging", *Journal of Thermal Analysis and Calorimetry* (2013) **112**, 1171-1177.
- [5] O. Gordobil, R. Delucis, I. Eguees, J. Labidi, "Kraft lignin as filler in PLA to improve ductility and thermal properties", *Industrial Crops and Products* (2015) **72**, 46-53.
- [6] B.W. Chieng, N.A. Ibrahim, Y.Y. Then, Y.Y. Loo, "Epoxidized vegetable oils plasticized poly(lactic acid) biocomposites: mechanical, thermal and morphology properties", *Molecules* (2014) **19**, 16024-16038.
- [7] M. Murariu, A. Da Silva Ferreira, M. Pluta, L. Bonnaud, M. Alexandre, P. Dubois, "Polylactide (PLA)-CaSO₄ composites toughened with low molecular weight and polymeric ester-like plasticizers and related performances", *European Polymer Journal* (2008) **44**, 3842-3852.
- [8] C.L. Morelli, M. Mahrous, M.N. Belgacem, M.C. Branciforti, R.E.S. Bretas, J. Bras, "Natural copaiba oil as antibacterial agent for bio-based active packaging", *Industrial Crops and Products* (2015) **70**, 134-141.

- [9] Z.N. Wang, S. Xia, H. Chen, S. Wang, K.M. Nie, Z.B. Li, "Effects of poly(ethylene glycol) grafted silica nanoparticles on crystallization behavior of poly(D-lactide)", *Polymer International* (2015) **64**, 1066-1071.
- [10] S.H. Clasen, C.M.O. Mueller, A.T.N. Pires, "Maleic anhydride as a compatibilizer and plasticizer in TPS/PLA blends", *Journal of the Brazilian Chemical Society* (2015) **26**, 1583-1590.
- [11] V. Mittal, T. Akhtar, N. Matsko, "Mechanical, thermal, rheological and morphological properties of binary and ternary blends of PLA, TPS and PCL", *Macromolecular Materials and Engineering* (2015) **300**, 423-435.
- [12] Y. Yang, Z. Tang, Z. Xiong, J. Zhu, "Preparation and characterization of thermoplastic starches and their blends with poly(lactic acid)", *International Journal of Biological Macromolecules* (2015) **77**, 273-279.
- [13] M.P. Arrieta, J. López, D. López, J.M. Kenny, L. Peponi, "Development of flexible materials based on plasticized electrospun PLA-PHB blends: Structural, thermal, mechanical and disintegration properties", *European Polymer Journal* (2015) **73**, 433-446.
- [14] C. Courgneau, S. Domenek, A. Guinault, L. Averous, V. Ducruet, "Analysis of the structure-properties relationships of different multiphase systems based on plasticized poly(lactic acid)", *Journal of Polymers and the Environment* (2011) **19**, 362-371.
- [15] V.B. Carmona, A.C. Correa, J.M. Marconcini, L.H. Capparelli Mattoso, "Properties of a biodegradable ternary blend of thermoplastic starch (TPS), poly(epsilon-caprolactone) (PCL) and poly(lactic acid) (PLA)", *Journal of Polymers and the Environment* (2015) **23**, 83-89.
- [16] R.Y. Tabasi, Z. Najarzadeh, A. Ajji, "Development of high performance sealable films based on biodegradable/compostable blends", *Industrial Crops and Products* (2015) **72**, 206-213.
- [17] J.M. Ferri, O. Fenollar, A. Jorda-Vilaplana, D. Garcia-Sanoguera, R. Balart, "Effect of miscibility on mechanical and thermal properties of poly(lactic acid)/polycaprolactone blends", *Polymer International* (2016) **65**, 453-463.

- [18] Y. Deng, N.L. Thomas, "Blending poly(butylene succinate) with poly(lactic acid): Ductility and phase inversion effects", European Polymer Journal (2015) **71**, 534-546.
- [19] W. Pivsa-Art, S. Pivsa-Art, K. Fujii, K. Nomura, K. Ishimoto, Y. Aso, H. Yamane, H. Ohara, "Compression molding and melt-spinning of the blends of poly(lactic acid) and poly(butylene succinate-co-adipate)", Journal of Applied Polymer Science (2015) **132**, 41856.
- [20] B. Meng, J. Deng, Q. Liu, Z. Wu, W. Yang, "Transparent and ductile poly(lactic acid)/poly(butyl acrylate) (PBA) blends: Structure and properties", European Polymer Journal (2012) **48**, 127-135.
- [21] M. Kumar, S. Mohanty, S.K. Nayak, M. Rahail Parvaiz, "Effect of glycidyl methacrylate (GMA) on the thermal, mechanical and morphological property of biodegradable PLA/PBAT blend and its nanocomposites", Bioresource Technology (2010) **101**, 8406-8415.
- [22] L.C. Arruda, M. Magaton, R.E.S. Bretas, M.M. Ueki, "Influence of chain extender on mechanical, thermal and morphological properties of blown films of PLA/PBAT blends", Polymer Testing (2015) **43**, 27-37.
- [23] O. Fenollar, D. Garcia, L. Sanchez, J. Lopez, R. Balart, "Optimization of the curing conditions of PVC plastisols based on the use of an epoxidized fatty acid ester plasticizer", European Polymer Journal (2009) **45**, 2674-2684.
- [24] B. Mehta, M. Kathalewar, A. Sabnis, "Benzyl ester of dehydrated castor oil fatty acid as plasticizer for poly(vinyl chloride)", Polymer International (2014) **63**, 1456-1464.
- [25] A. Carbonell-Verdu, D. Garcia-Sanoguera, A. Jordá-Vilaplana, L. Sanchez-Nacher, R. Balart, "A new biobased plasticizer for poly(vinyl chloride) based on epoxidized cottonseed oil", Journal of Applied Polymer Science (2016) **133**, 43642.
- [26] Y.Q. Xu, J.P. Qu, "Mechanical and rheological properties of epoxidized soybean oil plasticized poly(lactic acid)", Journal of Applied Polymer Science (2009) **112**, 3185-3191.
- [27] S. Vijayarajan, S.E.M. Selke, L.M. Matuana, "Continuous blending approach in the manufacture of epoxidized soybean plasticized poly(lactic acid) sheets and films", Macromolecular Materials and Engineering (2014) **299**, 622-630.

- [28] J. Alam, M. Alam, M. Raja, Z. Abduljaleel, L.A. Dass, "MWCNTs-reinforced epoxidized linseed oil plasticized polylactic acid nanocomposite and its electroactive shape memory behaviour", International Journal of Molecular Sciences (2014) **15**, 19924-19937.
- [29] O.W.M.a. Trade, *Report from the United States Department of Agriculture, Foreign Agricultural Service*. March 2016.
- [30] I.C.N. Gadelha, N.B.S. Fonseca, S.C.S. Oloris, M.M. Melo, B. Soto-Blanco, "Gossypol toxicity from cottonseed products", The Scientific World Journal (2014), 231635.
- [31] A. Carbonell-Verdu, L. Bernardi, D. Garcia-Garcia, L. Sanchez-Nacher, R. Balart, "Development of environmentally friendly composite matrices from epoxidized cottonseed oil", European Polymer Journal (2015) **63**, 1-10.
- [32] M.P. Arrieta, M.D. Samper, J. Lopez, A. Jimenez, "Combined effect of poly(hydroxybutyrate) and plasticizers on polylactic acid properties for film intended for food packaging", Journal of Polymers and the Environment (2014) **22**, 460-470.
- [33] J.M. Ferri, M.D. Samper, D. García-Sanoguera, M.J. Reig, O. Fenollar, R. Balart, "Plasticizing effect of biobased epoxidized fatty acid esters on mechanical and thermal properties of poly(lactic acid)", Journal of Materials Science (2016) 1-11.
- [34] V.S. Giita Silverajah, N.A. Ibrahim, W.M.Z.W. Yunus, H.A. Hassan, C.B. Woei, "A comparative study on the mechanical, thermal and morphological characterization of poly(lactic acid)/epoxidized palm oil blend", International journal of molecular sciences (2012) **13**, 5878-98.
- [35] H. Liu, J. Zhang, "research progress in toughening modification of poly(lactic acid)", Journal of Polymer Science Part B-Polymer Physics (2011) **49**, 1051-1083.
- [36] F.S. Mohammed, M. Conley, S.R. Saunders, J. Switzer, R. Jha, J.M. Cogen, B.I. Chaudhary, P. Pollet, C.A. Eckert, C.L. Liotta, "Epoxidized linolenic acid salts as multifunctional additives for the thermal stability of plasticized PVC", Journal of Applied Polymer Science (2015) **132**, 41736.

- [37] R.E. Conn, J.J. Kolstad, J.F. Borzelleca, D.S. Dixler, L.J. Filer, B.N. Ladu, M.W. Pariza, "*Safety assessment of polylactide (PLA) for use as a food-contact polymer*", Food and Chemical Toxicology (1995) **33**, 273-283.
- [38] L. Dobircău, N. Delpouve, R. Herbinet, S. Domeneck, L. Le Pluart, L. Delbreilh, V. Ducruet, E. Dargent, "*Molecular mobility and physical ageing of plasticized poly(lactide)*", Polymer Engineering and Science (2015) **55**, 858-865.
- [39] V. Tanrattanakul, P. Bunkaew, "*Effect of different plasticizers on the properties of bio-based thermoplastic elastomer containing poly(lactic acid) and natural rubber*", Express Polymer Letters (2014) **8**, 387-396.
- [40] V.P. Martino, A. Jimenez, R.A. Ruseckaite, "*processing and characterization of poly(lactic acid) films plasticized with commercial adipates*", Journal of Applied Polymer Science (2009) **112**, 2010-2018.



Plasticization effect of epoxidized cottonseed oil (ECSO) on poly(lactic acid)

Alfredo Carbonell-Verdu^a, M. Dolores Samper, Daniel Garcia-Garcia, Lourdes Sanchez-Nacher,
 Rafael Balart

Instituto de Tecnología de Materiales (ITM), Universitat Politècnica de València (UPV), Plaza Ferrández y Carbonell s/n, 03801, Alcoy, Alicante, Spain



ARTICLE INFO

Keywords:
 Poly(lactic acid)-PLA
 Epoxidized cottonseed oil (ECSO)
 Mechanical properties
 Thermal properties
 Migration

ABSTRACT

In this work, the use of an environmentally friendly plasticizer derived epoxidized cottonseed oil (ECSO) for poly(lactic acid) (PLA) is proposed. Melt extrusion was used to plasticize PLA formulations with different ECSO contents in the 0–10 wt.%. PLA formulation with 10 wt.% shows a remarkable increase in mechanical ductile properties with a percentage increase in elongation at break of more than 1100% and a noticeable increase in the impact absorbed energy. Differential scanning calorimetry (DSC) and dynamic mechanical thermal analysis (DMTA) revealed a clear decrease in the glass transition temperature of neat PLA as the ECSO content increased. Field emission scanning electron microscopy (FESEM) of fractured surfaces from impact tests showed an improvement of ductility with typical rough and porous topographies. Migration tests in *n*-hexane at different temperatures revealed very low migration properties thus leading to new interesting plasticizers for improved PLA industrial formulations.

1. Introduction

One of the most promising biopolymers as alternative to conventional petroleum-based polymers is poly(lactic acid)-PLA with an annual production of more than 140,000 tons (Grande et al., 2015). PLA is an aliphatic polyester obtained by polymerization of lactic acid (hydroxyl propionic acid) obtained from renewable and sustainable starch rich materials such as corn and sugarcane (Al-Mulla et al., 2011; Blanca and Siracusa, 2013; Sansone et al., 2012). In the last years PLA has become an industrial alternative to some petroleum-based polymers because of its relatively low price (Gordobil et al., 2015) and overall balanced mechanical properties such as high tensile strength and Young's modulus with similar values of those of poly(ethylene terephthalate), PET (Chieng et al., 2014) which is widely used in plastic bottle manufacturing due to its excellent barrier properties. PLA possesses acceptable barrier properties, and additionally it can be transparent due to the low crystallization rate (Chieng et al., 2014). It is also shiny and offers low flammability; all these features, together with a relatively easy processing conditions, similar to many commodities, make PLA a good candidate for a wide variety of products in the packaging industry, automotive parts, textile fibers, prostheses and medical devices, etc. among others (Morelli et al., 2015; Murariu et al., 2008). Nevertheless, PLA is characterized by high fragility, which is drawback for some technical applications in which some flexibility is required (Wang et al., 2015). For these reasons, different approaches

have been explored to overcome this high intrinsic fragility by increasing ductile properties such as elongation at break, impact resistance, etc. while maintaining its environmentally friendly nature. A typical approach has been blending PLA with other ductile polymers. In this field, PLA was blended with chitosan, which is able to form films but the mixtures resulted in immiscible blends due to their different polarity and poly(vinyl alcohol), PVA was necessary to provide somewhat compatibility (Grande et al., 2015). Thermoplastic starch (TPS) also showed immiscibility with PLA and several compatibilizers such as maleic anhydride and methylene diphenyl diisocyanate (MDI) were needed to improve the overall properties (Clasen et al., 2015; Mittal et al., 2015; Yang et al., 2015). Blends with poly(hydroxybutyrate), PHB gave an interesting improvement on barrier properties of neat PLA but resulting blends were characterized by high fragility so that, different plasticizers such as acetyl(tributyl citrate), ATBC (Arrieta et al., 2015) and poly(ethylene glycol), PEG (Courgnau et al., 2011) were needed to overcome this drawback. PLA has also been blended with biodegradable petroleum-based polymers to give fully biodegradable blends. Among these petroleum-based polymers interesting results have been obtained with poly(caprolactone)-PCL biodegradable polyester. Although both PLA and PCL are polyester-type polymers, they show restricted miscibility but the high flexibility of PCL is enough to reduce the intrinsic fragility of PLA (Carmona et al., 2015; Ferri et al., 2016a; Tabasi et al., 2015). Other petroleum-based polymers such as poly(butylene succinate)-PBS (Deng and Thomas, 2015), poly(butylene

* Corresponding author.
 E-mail address: alcarvel@epsa.upv.es (A. Carbonell-Verdu).

<https://dx.doi.org/10.1016/j.indcrop.2017.04.050>
 Received 6 June 2016; Received in revised form 17 March 2017; Accepted 27 April 2017
 Available online 08 May 2017
 0926-6690/ © 2017 Elsevier B.V. All rights reserved.

IV.4

IV.4. PLA films with improved flexibility properties by using maleinized cottonseed oil.

**A. Carbonell-Verdu¹, D. García-García¹, F. Dominici², L. Torre², L. Sánchez-Nacher¹,
R. Balart¹**

¹ Materials Technology Institute (ITM)
Universitat Politècnica de València (UPV)
Plaza Ferrandiz y Carbonell 1, 03801, Alcoy, Alicante (Spain)

² Dipartimento di Ingegneria Civile e Ambientale
Università di Perugia
Loc. Pentima Bassa, 05100 Terni (Italy)

"PLA films with improved flexibility properties by using maleinized cottonseed oil"

Abstract

This work assesses the potential of maleinized cottonseed oil – MCSO as plasticizer in poly(lactic acid) – PLA films with improved ductile behaviour. The effects of MCSO are compared with commercially available maleinized oil, *i.e.* maleinized linseed oil – MLO in terms of mechanical, thermal and barrier properties, as well as morphology changes. Plasticized PLA formulations were obtained with a maleinized oil content in the 0 – 10 wt% range. Addition of both maleinized vegetable oils leads to a slight decrease in the glass transition temperature (T_g) of neat PLA from 63 °C to 60 – 61 °C. Nevertheless, MCSO provides better overall properties. Addition of 7.5 wt% MCSO increases the elongation at break by 292%. Regarding the barrier properties, both maleinized vegetable oils increase the oxygen transmission rate – OTR. Nevertheless, this increase is less pronounced in the case of MCSO thus indicating its higher efficiency compared to MLO. On the other hand, addition of both maleinized vegetable oils do not compromise the overall disintegration of the obtained PLA formulations, thus positioning these additives as environmentally friendly solutions to increase ductile properties in PLA-based films.

Keywords

Poly(lactic acid) – PLA; cottonseed oil; maleinization; mechanical properties; thermal properties; barrier properties.

IV.4.1. Introduction.

The growing awareness about the ongoing environmental pollution, together with the, still distant but increasingly close, problematics of petroleum depletion, are leading the research on obtaining materials from renewable resources and, potentially, biodegradable. This situation is particularly accentuated in the packaging industry due to the huge amounts of wastes that are generated worldwide. For these reasons, new polymers and industrial formulations are continuously being developed with the main aim of lowering their environmental impacts.

Today, a wide variety of polymers can be obtained from renewable resources. Polysaccharides are a promising source of polymers due to their worldwide abundance. Different starches *e.g.* maize, potato, rice, etc. can be converted into industrial plastic formulations by using appropriate plasticizers such as glycerol, water, sorbitol, etc. leading to the so called “thermoplastic starches” – TPS [1, 2]. A new range of materials have been successfully synthesised from chitin which is the Earth’s second most abundant polysaccharide, surpassed only by cellulose. Chitin can be found in the exoskeleton of crustaceans [3]. Proteins are another important source of polymers. It is worthy to note the use of vegetable proteins such as gluten or soy protein in the field of polymers and composites, as well as animal proteins such as collagen, casein, ovalbumin, etc. widely used in the food industry [4, 5].

Aliphatic polyesters represent a promising solution to environmentally friendly polymers. Although some of them are obtained from petroleum derivatives, *e.g.* poly(butylene succinate) – PBS, poly(ϵ -caprolactone) – PCL, poly(butylene succinate – co – adipate) – PBSA, etc. some polyesters can be obtained from renewable resource and could represent a full solution to both petroleum depletion and environmental impact as all these polyesters can be disintegrated in controlled soil [6, 7]. These high environmental efficiency polyesters include several bacterial polyesters (polyhydroxyalkanoates – PHAs) such as poly(hydroxybutyrate) – PHB, poly(hydroxybutyrate – co – hydroxyvalerate) – PHBV, among others [8, 9]. Although PHAs are very promising due to an excellent balance between mechanical, thermal and barrier properties, their cost is still high and their offer a very narrow processing window which limits a massive use in [10]. Other aliphatic polyester that has owned a privileged

position in the last years is poly(lactic acid) – PLA which can be synthesised from ring-opening polymerization (ROP) of lactic acid obtained from starch fermentation [11, 12]. In addition, PLA offers balanced mechanical and barrier properties, it is transparent, brilliant and shows excellent resistance to fats. All these features have led PLA to a wide variety of sectors such as medical, automotive, textile, packaging, etc. [13-16]. However, not all are advantages; PLA is quite fragile and this fact restricts its use in some industrial sectors [17]. To overcome this fragility, different strategies have been proposed. One interesting solution is blending PLA with flexible polymers such as thermoplastic starch – TPS, poly(ϵ -caprolactone) – PCL, poly(butylene succinate – co – adipate) – PBSA, or others, with a remarked increase in toughness and other ductile properties [18-22]. Although physical blending is a cost-effective solution to overcome this drawback, the lack of miscibility between the components restricts the improvement on toughness. For this reason, some authors have proposed the use of compatibilizer agents. Ferri *et al.* reported PLA/TPS blends with a clear phase separation due to immiscibility. They suggested the use of maleinized linseed oil – MLO as compatibilizer agent with a noticeable increase in the elongation at break [2].

Modified vegetable oils – MVOs represent an interesting alternative to petroleum-based plasticizers. In the last years, different modified vegetable oils (epoxidized, maleinized, acrylated, hydroxylated, etc.) have been successfully used as renewable plasticizers with a positive contribution on environmental efficiency. Some epoxidized vegetable oils are commercially available. This is the case of epoxidized soybean oil (ESBO) [23, 24] and epoxidized linseed oil (ELO) [25] which are widely used in the poly(vinyl chloride) – PVC industry as secondary plasticizers with additional thermal stabilization effects on PVC. Other research works have focused on the plasticization efficiency of other epoxidized vegetable oils derived from palm oil [26] and sunflower oil [27]. Mauck SC *et al.* reported the use of acrylated epoxidized soybean oil – AESO as plasticizer in toughened PLA formulations [28] and Ferri *et al.* reported the potential of maleinized linseed oil – MLO as plasticizer for PLA with a remarkable increase in the elongation at break higher than 1000% with addition of 20 phr MLO. They also reported a decrease of 6 °C in the glass transition temperature (Tg) [29].

Cottonseed oil – CSO has shown its potential in the polymer industry in several fields such as thermosetting resins [30], PVC plasticizer [31] and PLA plasticization, with promising results. Cottonseed oil can be considered a by-product of the cotton industry

whose main product is the cotton fiber. Approximately, 5.12 million tons cotton is produced annually worldwide and the main by-products are the oil and the cottonseed meal. Cottonseed oil can be converted into its corresponding maleinized oil by a conventional procedure [32]. This reaction can follow several paths, being the “ene” addition the most favourable path. Nevertheless, in some cases, when conjugated double bonds are present in the fatty acid chain, the Diels-Alder condensation can also take place as it is shown in **Figure IV.4.1**. Tarek *et al.* reported that over 200 °C, maleic anhydride is bonded to the triglyceride in an allylic position in the unsaturated fatty acid [33]. **Figure IV.4.1** shows a schematic representation of the maleinization process of cottonseed oil.

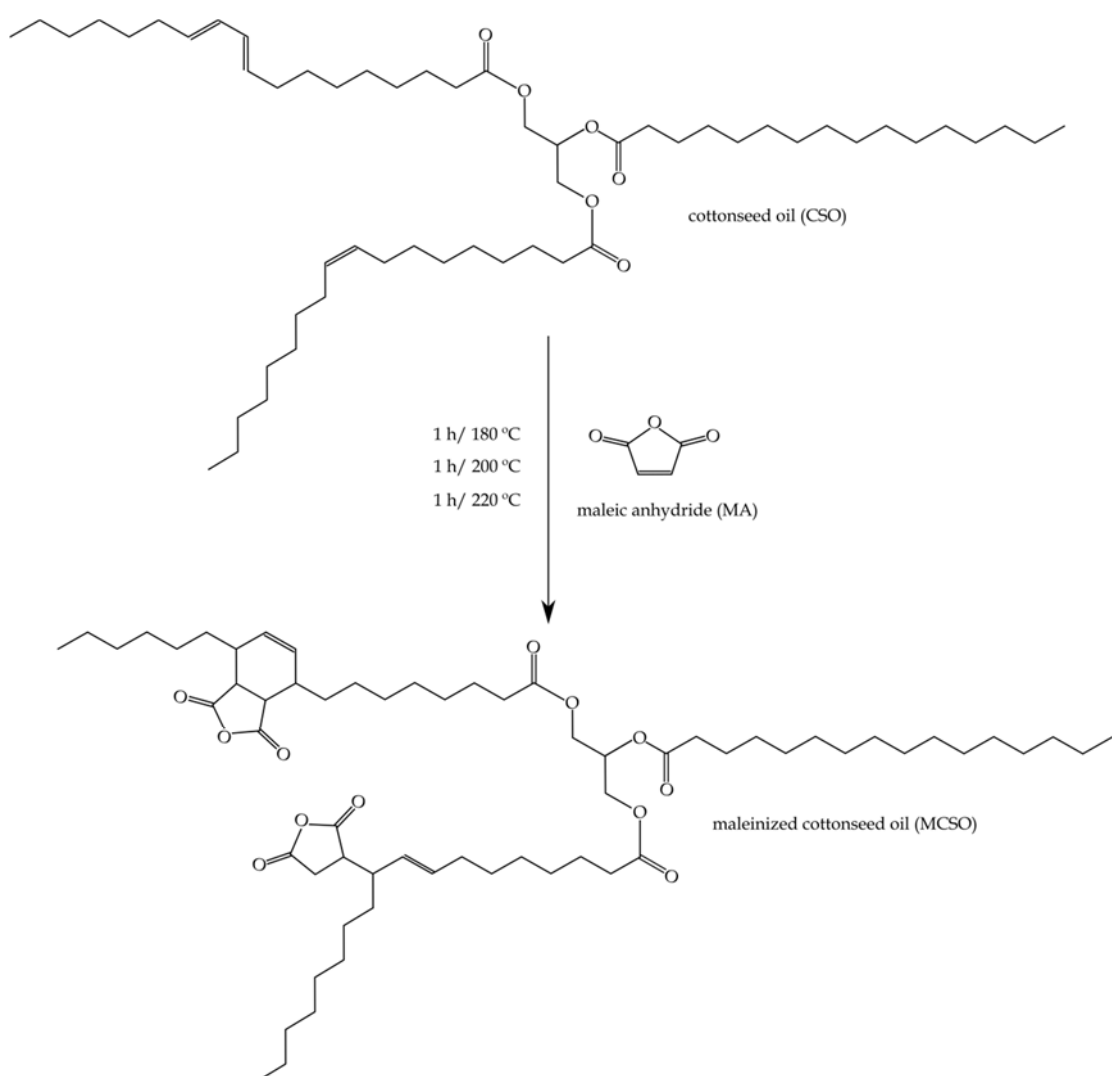


Figure IV.4.1. Schematic representation of the maleinization process of cottonseed oil.

This work assesses the potential of cottonseed oil as natural-based plasticizer for PLA films. Optimum maleinization process are described and the effect of maleinized cottonseed oil – MCSO on mechanical, thermal and barrier properties as well as morphology is evaluated and compared with a commercially available maleinized oil: maleinized linseed oil – MLO.

IV.4.2. Experimental.

■ Materials.

A PLA commercial grade Ingeo Biopolymer 6210D from NatureWorks LLC (Minnetonka, USA) was used in pellet form as base material for films. It shows a melt flow index of 15 – 30 g/(10 min) at 210 °C and a density of 1240 kg m⁻³. Cottonseed oil was purchased from Sigma Aldrich España (Madrid, Spain) and used without further purification. Its density is 920 kg m⁻³ and its iodine value is comprised in the 109 – 120 range. Its acid number is 0.25 mg KOH g⁻¹ as obtained following ISO 660:2009.

Maleinized linseed oil, commercial grade VEOMER LIN was purchased from Vandeputte (Mouscron, Belgium) with an average acid number of 105-130 mg KOH g⁻¹. Maleic anhydride (Purity>98) was supplied by Sigma Aldrich (Madrid, Spain).

■ Maleinization of cottonseed oil.

A three neck round flask with a capacity of 500 mL equipped with a heating mantle was used to synthesize maleinized cottonseed oil. A reflux condenser was placed in the central neck. A digital thermometer was connected to a second neck and was used to measure the temperature during the reaction. Finally, the third neck was used to add maleic anhydride, simple extraction for evaluation and provide an inert atmosphere with nitrogen gas. A typical batch production is summarized as follows: 300 g of cottonseed oil were placed in the round flask and subjected to magnetic stirring and heating until

the first temperature step was reached. The process was carried out in three temperature steps at 180 °C, 200 °C and 220 °C. At each temperature step, the same portion of maleic anhydride (9 g of maleic anhydride per 100 g cottonseed oil) was dropped into the flask and subjected to magnetic stirring while temperature was maintained constant for 1 additional hour. To evaluate the extent of the maleinization reaction, samples were extracted from the flask every 30 min (for the temperatures of 180 °C and 200 °C) and every 20 min for the maximum temperature step at 220 °C. Finally, the mixture was cooled down to room temperature and subjected to centrifugation at 4000 rpm to allow full separation.

The maleinization extent was followed through the measurement of the acid number as indicated in ISO 660:2009 with the following equation.

$$\text{Acid number} = \frac{56.1 \times V \times C}{m}$$

Equation IV.4.1

Where V stands for the volume of the KOH standard solution (mL), C represents the exact concentration of the KOH standard solution (mol L^{-1}) and m is the mass of the maleinized oil used in the analysis (g).

Manufacturing of PLA films with maleinized vegetable oils.

Table IV.4.1 summarizes the compositions and codes used for the different plasticized PLA formulations with maleinized cottonseed oil – MCSO and maleinized linseed oil – MLO. PLA was dried at 60 °C for 24 h. Initially, the appropriate amounts of PLA and the corresponding maleinized oil, were mechanically mixed in a zipper bag and subjected to a compounding process in a twin-screw co-rotating extruder ($D= 30 \text{ mm}$; $L/D = 20:1$) by DUPRA (Alicante, Spain), at a rotating speed of 60 rpm. The following temperature program was programmed: 167.5 °C (feeding), 170 °C, 172.5 °C, 175 °C (die). The obtained compounds were cooled down to room temperature, subsequently

pelletized and dried at 50 °C for 24 h. Films with an average thickness 100 µm were obtained in a cast-roll machine from Eurotech S.A.S. (San Marino in Riu, Italy). The extrusion rate was set to 55 rpm and the calendering process was 2 m min⁻¹.

Table IV.4.1. Composition and labelling of the plasticized PLA formulations with different maleinized vegetable oils.

Reference	wt% PLA	wt% MCSO	wt% MLO
PLA	100	-	-
2.5 % MCSO	97.5	2.5	-
5 % MCSO	95.0	5.0	-
7.5 % MCSO	92.5	7.5	-
10 % MCSO	90.0	10.0	-
2.5 % MLO	97.5	-	2.5
5 % MLO	95.0	-	5.0
7.5 % MLO	92.5	-	7.5
10 % MLO	90.0	-	10.0

■ Mechanical characterization.

Mechanical characterization of films was carried out by testing five different standard tensile samples (type 2) as indicated in ISO 527-3, with a total length of 160 mm, a width of 10 mm and a thickness of 100 µm. The different sample films were tested in a universal testing machine ELIB 30 from S.A.E. Ibertest (Madrid, Spain) using specific pneumatic clamps at a crosshead rate of 5 mm min⁻¹.

■ Morphology characterization.

The morphology of transversal cross sections of the obtained films was observed and characterized in a field emission scanning electron microscope – FESEM model ZEISS ULTRA from Oxford Instruments (Oxfordshire, United Kingdom) using an acceleration voltage of 2 kV. A sputtered metal coating with platinum was used to increase the electrical conductivity of the samples prior to observation as well as to work

with low acceleration voltage and avoid sample damage. The sputter-coater equipment was an EM MED020 from Leica Microsystems (Wetzlar, Germany).

■ Thermal characterization.

The main thermal transitions of plasticized PLA films were studied by differential scanning calorimetry – DSC in a 821e calorimeter from Mettler Toledo Inc. (Schwerzenbach, Switzerland) using a dynamic temperature program from 25 °C to 300 °C at a constant heating rate of 10 °C min⁻¹ in nitrogen atmosphere (66 mL min⁻¹). The degree of crystallinity (%X_c) was calculated by using Equation IV.4.2.

$$\%X_c = 100 \times \frac{\Delta H_m - \Delta H_{cc}}{\Delta H_m (100\%)} \times \frac{1}{w} \quad \text{Equation IV.4.1}$$

Where ΔH_m stands for the melt enthalpy, ΔH_{cc} represents the cold crystallization enthalpy, ΔH_m (100%) indicates the melt enthalpy of theoretically 100% crystalline PLA (93 J g⁻¹) [34] and w represents the weight fraction of PLA in plasticized formulations.

Degradation at high temperatures was followed by thermogravimetric analysis – TGA in a TGA/SDTA 851 thermobalance from Mettler-Toledo Inc. (Schwerzenbach, Switzerland). A dynamic thermal program from 25 °C up to 700 °C at a heating rate of 10 °C min⁻¹ in nitrogen atmosphere (66 mL min⁻¹).

■ Barrier properties.

The oxygen transmission rate – OTR was obtained in triplicate using an oxygen permeation analyser Systech model 8500 from Metrotec S.A. (San Sebastián, Spain) with pure oxygen (99.9%). Samples were cut in circular shapes with a diameter of 14 cm and average thickness of 100 µm. A Mitutoyo digimatic micrometer model 293-832 (Illinois,

USA) was used to calculate the average thickness – e of the samples all around their perimeter. The oxygen flow rate was monitored until a stationary state was reached. The product $OTR \cdot e$ for each film was calculated and compared.

Contact angle measurements.

The contact angle (θ) was obtained in a goniometer model FM140 from Krüss GmbH (Hamburg, Germany). Samples with an average thickness of 100 μm were dried at 40 °C for 24 h before testing. Five different water drops (~100 μl) were placed into the film surface and ten different measurements were obtained for each water drop and averaged. The static contact angle was measured after 30 s.

Disintegration in controlled compost soil.

The disintegration test in controlled compost conditions was carried out by following the guidelines of ISO 20200 in triplicate. Samples sizing 25x25 mm^2 with an average thickness of 100 μm were placed in a compost reactor (300x200x100 mm^3). Samples were dried at 40 °C for 24 h before they were dug into the synthetic compost soil. The synthetic soil was composed of sawdust, feed for rabbits, mature compost, corn starch, saccharose, corn oil and urea in the proportions indicated in the ISO 20200. All samples were initially weighed and immersed in water before placing them into the mixture. Samples were extracted from the reactor at 6, 8, 9, 10, 11 and 13 days, washed with distilled water and dried for 24 h before weighing. In addition, optical images of the samples were collected at these disintegration periods.

IV.4.3. Results and discussion.

Synthesis of maleinized cottonseed oil - MCSO.

Figure IV.4.2 shows the evolution of the acid number along the three temperature steps at 180 °C, 200 °C and 220 °C. At the beginning of the reaction, cottonseed oil shows an acid number of 0.25 mg KOH g⁻¹. After the first two hours, an important increase is detected thus indicating that maleinization has taken place. At the end of the second temperature step at 200 °C, the acid number reaches 16.9 mg KOH g⁻¹.

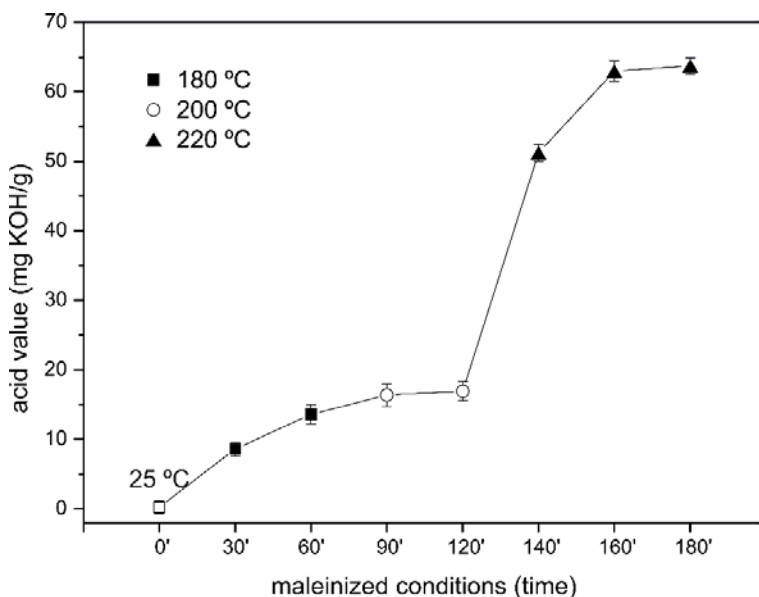


Figure IV.4.2. Effect of temperature and time on the efficiency of the maleinization process of cottonseed oil with maleic anhydride.

Nevertheless, it is in the third temperature step at 220 °C when the maleinization process takes place in a high extent. After 20 min at 220 °C, the acid number has reached 51.2 mg KOH g⁻¹ due to the high availability of maleic anhydride which can be readily attached to an allylic position in the unsaturated fatty acid which is specially favoured above 200 °C [33]. As the reaction time increases while maintaining the temperature at 220 °C, the acid number tends to stabilize at about 63.7 mg KOH g⁻¹. These results are in

total agreement with other reported maleinization processes. A.I. Aigbodion *et al.* maleinized rubber seed oil with similar conditions and obtained an acid number of 75.8 mg KOH g⁻¹ [35].

An important change in colour was also obtained as a consequence of the maleinization process. During the first temperature step at 180 °C, the colour was yellow as most of the vegetable oils. As the maleinization takes place, a change in colour from yellow to reddish was observed as it can be seen in **Figure IV.4.3**. Ernzen J.R *et al.*, reported a similar change in colour during the maleinization of soybean oil with an intense reddish colour at the end of the reaction [36].



Figure IV.4.3. Influence of the reaction temperature and time on the colour during maleinization process of cottonseed oil, a) 180 °C – 60 min, b) 200 °C – 60 min, c) 220 °C – 60 min.

Mechanical properties of plasticized PLA with MCSO.

The efficiency of MCSO as biobased plasticizer for PLA films was assessed by comparing with a commercial MLO. **Figure IV.4.4** shows the results obtained in the tensile test. Unplasticized PLA film shows the maximum tensile strength and Young's modulus with values of 46.8 MPa and 1.64 GPa respectively. Regarding the elongation at break, unplasticized PLA shows a remarkably low value close to 4% thus leading to a fragile behaviour. The plasticization effect that MCSO provides is evident by seeing the evolution of mechanical properties. The only addition of 2.5 wt% MCSO gives an

improvement on elongation at break up to values of 5.8% whilst the tensile strength and modulus decrease to 43.9 MPa and 1.18 GPa respectively. As the MCSO content increases, the elongation at break increases up to values of 12.9% and 15.7% for plasticized PLA films with 5.0 wt% and 7.5 wt% MCSO. These results are in total agreement with those reported by Sheli C. Mauck with similar elongation at break value on PLA plasticized with epoxidized soybean oil – ESBO [28]. Despite this increasing tendency, it seems that plasticizer saturation occurs at a relatively low MCSO content of 5.0-7.5 wt%. In fact, the elongation at break for the plasticized PLA film with 10 wt% MCSO decreases due to a phase separation process as reported by Balart JF *et al.* [37].

These results suggest a slight plasticizing effect of MCSO. As it has been reported, small amounts of modified vegetable oils have a positive effect on PLA ductile properties. Despite this, as Ferri JM *et al.* have also reported, plasticizer saturation occurs at relatively low oil content and phase saturation occurs over this threshold with a subsequent decrease in ductile properties [14]. The good performance of MCSO as plasticizer for PLA films is evident by comparing its effects with MLO. In this way, although addition of 2.5 wt% MLO to PLA leads to an elongation at break of 6.9%, which is slightly higher than the obtained with the same MCSO content, this is the maximum value that MLO can achieve. In fact, plasticized PLA films with 5.0 – 7.5 wt% give lower elongation at break values close to 5% and the plasticized formulation with 10 wt% MLO gives even lower elongation at break the unplasticized PLA films.

Regarding mechanical resistant properties, the decrease in tensile strength is more pronounced by using MLO as if can be seen in **Figure IV.4.4[b]** with values of 26.6 MPa for the plasticized PLA film with 10 wt% MLO. Buong Woei Chieng *et al.* also observed this dramatic decrease in tensile strength in formulations of PLA plasticized with epoxidized palm oil – EPO from 60 MPa (neat PLA) down to 30 MPa with addition of 10 wt% EPO [38].

With regard to the Young's modulus, MLO provides similar behaviour to MCSO as it can be seen in **Figure IV.4.4[c]**. In fact, the minimum value is 0.97 GPa and 0.86 GPa for plasticized PLA films with 10 wt% MLO and MCSO respectively. These results agree with some other works that use modified vegetable oils as plasticizers in polymers [23].

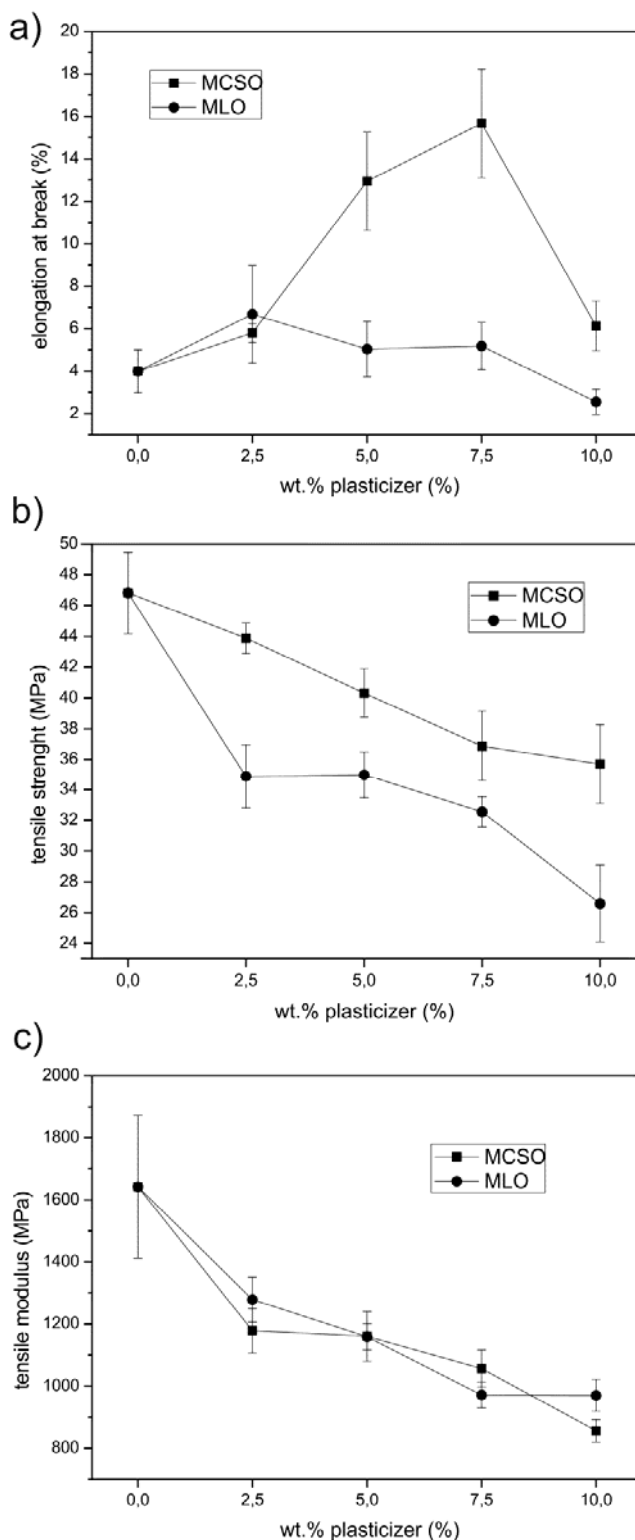


Figure IV.4.4. Plot evolution of mechanical properties of plasticized PLA films as a function of the wt% of MCSO and MLO, a) elongation at break, b) tensile strength and c) Young's modulus.

The plasticization effect can be seen by observing FESEM images in **Figure IV.4.5**. Although there are not pronounced differences between the FESEM images of PLA plasticized with MLO (**Figure IV.4.5[b] & [c]**) compared to unplasticized PLA, plasticized PLA films with MCSO (**Figure IV.4.5[d] & [e]**) show slightly higher differences.

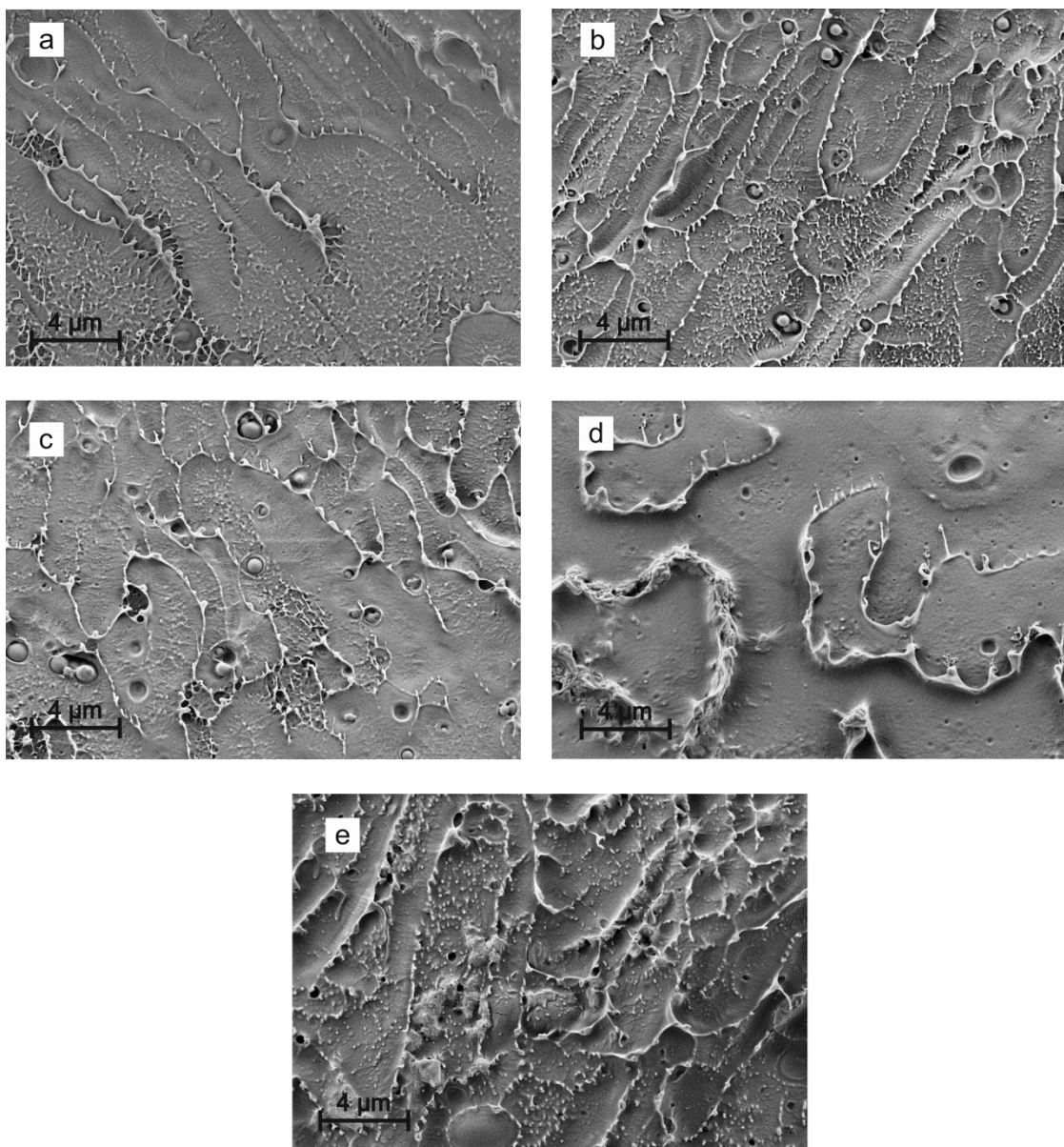


Figure IV.4.5. FESEM images (5000x) of the cross section of plasticized PLA films with different maleinized vegetable oils, a) unplasticized PLA, b) PLA with 5 wt% MLO, c) PLA with 7.5 wt% MLO, d) PLA with 5 wt% MCSO and e) PLA with 7.5 wt% MCSO.

Ferri *et al.* reported a restricted miscibility between PLA and MLO with a clear phase separation when plasticizer saturation occurred [29]. As it has been described previously, the results of mechanical properties, suggest better behaviour of MCSO compared to MLO. This could be related to slightly higher miscibility of MCSO with PLA than that of MLO. Unplasticized PLA film (**Figure IV.4.5[a]**) shows a cross section image typical of a fragile polymer with a smooth surface topography. The morphology of plasticized PLA films with MLO (**Figure IV.4.5[b] & [c]** with 5 wt% and 7.5 wt% MLO respectively) is similar, but small spherical shapes can be distinguished, which correspond to excess MLO. This is typical of a phase separation process and is responsible for low elongation at break values as previously seen. Conversely, the cross section of plasticized PLA films with MCSO shows more plastic deformation areas, which are in accordance with the abovementioned increased ductility. In a similar way, there is a direct relationship between the MCSO content and the presence of spherical shapes. Voids indicate a better dispersion of MCSO into the PLA matrix and this has a positive effect on elongation at break and other ductile properties.

Thermal properties of plasticized PLA with MCSO.

Both maleinized oils, MCSO and MLO, have a direct effect on thermal properties of plasticized PLA formulations as it can be seen in **Table IV.4.2**. The main thermal transition of unplasticized PLA are: the glass transition temperature (T_g) located at 63 °C, the cold crystallization temperature peak (T_{cc}) located at 117.3 °C and the melt temperature peak at 171.7 °C. Both plasticizers have a clear effect on the glass transition temperature and cold crystallization process, thus indicating a more or less intense plasticizing effect. In fact, both plasticizers, MCSO and MLO, give lower T_g and T_{cc} temperatures due to increased chain mobility [2]. The very low decrease in T_g obtained for both MCSO and MLO with values of 60 – 61 °C, indicates limited plasticizing effect due to restricted miscibility. Nevertheless, although the plasticization effects are not so high in terms of thermal properties, the particular morphology of plasticized PLA formulations with MCSO and, in a less extent, with MLO, is responsible for a toughening phenomenon on PLA with a positive effect on ductile properties, mainly with MCSO. Regarding the melt temperature peak, DSC thermograms do not show any additional

peak or a noticeable change in the peak shape. The melt temperature peak remains at values of 170 – 171 °C. Nevertheless, slight changes can be observed for the melt enthalpy and its components.

Table IV.4.2. Summary of the main thermal properties of neat PLA and plasticized PLA films with maleinized oils, obtained by differential scanning calorimetry – DSC and thermogravimetric analysis – TGA.

Sample code	DSC					TGA		
	T_g (°C)	T_{cc} (°C)	ΔH_{cc} (J g ⁻¹)	T_m (°C)	ΔH_m (J g ⁻¹)	X_c (%)	T_{5%} (°C)	T_{50%} (°C)
PLA	63.0	117.3	32.3	171.7	38.1	6.2	329.4	358.5
2.5 % MCSO	61.7	109.8	26.9	170.6	36.5	10.6	323.5	351.3
5 % MCSO	61.6	113.1	25.2	171.0	34.6	10.6	334.2	363.7
7.5 % MCSO	61.6	110.4	24.6	170.5	37.4	15.0	327.3	361.9
10 % MCSO	61.1	109.7	22.5	170.3	38.5	19.1	333.1	361.0
2.5 % MLO	61.7	108.9	23.3	171.6	35.1	13.0	322.4	355.5
5 % MLO	60.9	104.5	22.6	170.3	36.2	15.4	329.6	359.1
7.5 % MLO	60.4	105.5	23.8	170.5	34.6	12.5	329.7	361.6
10 % MLO	60.6	106.2	23.1	170.7	32.8	11.6	320.7	356.9

The melt enthalpy is directly related to two crystal fractions: one obtained after cooling after injection moulding and a second one achieved during the cold crystallization process. The degree of crystallinity (%X_c) is representative for the crystal fraction obtained during processing while the second crystal fraction is obtained during the cold crystallization.

The most relevant changes can be observed for the cold crystallization enthalpy (important decrease) whilst the melt enthalpy does not change in a remarkable way. This indicates that MCSO contributes to increase the degree of crystallinity after injection moulding due to increased chain mobility. For this reason, the cold crystallization enthalpy decreases in a greater extent than the melt enthalpy. With regard to the cold crystallization temperature range, once again both maleinized vegetable oils, lead to a remarkable decrease in the characteristic temperature peak. In the case of MCSO, T_{cc} falls down to values around 110 °C while the decrease is still higher for MLO with T_{cc} values located at about 105 °C. This decrease is directly related to the plasticization effect that both maleinized oils provide. Modified triglyceride molecules are placed between PLA polymer chains with a subsequent increase in the free volume. This phenomenon

allows PLA chains to arrange towards a packed/ordered structure at lower temperatures [39]. In agreement with this, the degree of crystallinity (%Xc) also increases with both maleinized plasticizers. Unplasticized PLA offers a crystallinity of 6.2%. By using MCSO in plasticized PLA films, the crystallinity increases up to 10.6% for MCSO contents of 2.5-5.0 wt%. It is important to remark that plasticized PLA films with 10 wt% MCSO show 19% crystallinity. Similar findings can be observed by using MLO, while it is true that the maximum crystallinity is close to 15%. These results give support to the mechanical properties as PLA films with MCSO showed higher tensile strength values than those obtained with MLO. This phenomenon could be related to the higher crystallinity that MCSO provides *versus* MLO. As it has been shown, plasticizer saturation with MLO occurs at lower concentrations regarding MCSO and this can also affect the crystallinity [37].

Table IV.4.2 also summarizes the influence of MCSO on the thermal degradation of plasticized PLA films. In particular, the temperatures at which a weight loss of 5% and 50% are given ($T_{5\%}$ and $T_{50\%}$ respectively). As per the results, it is worth to note that the thermal stability of PLA is not remarkably affected by MCSO. Maleinized vegetable oils seem to provide lower thermal stabilization than epoxidized vegetable oils which have been widely used as thermal stabilizers in poly(vinyl chloride) – PVC formulations as well as in other polymer based formulations. Chieng *et al.* reported a remarkable increase in the thermal stability of PLA by using modified vegetable oils, *e.g.* epoxidized palm oil (EPO) and a mixture of epoxidized palm oil and soybean oil (EPSO). Specifically, the onset degradation temperature changed from 274.26 °C (neat PLA) up to values of 313.54 °C and 330.40 °C for plasticized PLA formulations with 5 wt % EPO and EPSO respectively [38]. Maleinized vegetable oils still contain unsaturations; for this reason, they show lower thermal stabilization effects than the epoxidized counterpart oils. Ferri *et al.* reported negligible effects of MLO on the thermal stability of PLA formulations with MLO content comprised in the 5 – 20 phr range. In fact they report a decrease in the $T_{5\%}$ from 336.9 °C (neat PLA) down to 331.8 °C for the plasticized formulation with 10 phr MLO [29]. The obtained results suggest that MCSO does not increase in a remarkable way the thermal stability of PLA which remains unaffected by MCSO content.

█ Barrier properties and surface wetting properties of plasticized PLA with MCSO.

Barrier properties are directly related to the free volume, therefore, it is not expectable an improvement on the barrier properties, since thermal analysis has suggested an increase in the free volume due to a slight plasticization effect. PLA is characterized by moderate barrier properties. In fact, PLA has high OTR compared to ethylene-vinyl alcohol copolymer (EVOH) but it offers lower OTR values than highly oxygen permeable polymer such as LDPE [40-42]. As reported by Auras *et al.* the OTR of oriented PLA is ten times lower than oriented poly(styrene) – PS but six times higher than poly(ethylene terephthalate) – PET, which is widely used due to its excellent barrier properties against oxygen [43].

Table IV.4.3 summarizes the product $OTR \cdot e$ to compare the effects of both MCSO and MLO, at different concentrations, in plasticized PLA films. As it was expected, both plasticizers offer worse barrier properties than unplasticized PLA. The $OTR \cdot e$ value for unplasticized PLA is close to $19 \text{ cm}^3 \text{ mm m}^{-2} \text{ day}^{-1}$; the plasticized formulation with 5 wt% MCSO increases this up to $20.63 \text{ cm}^3 \text{ mm m}^{-2} \text{ day}^{-1}$ which represents a percentage increase of 8.23%. In the case of MLO, addition of 5 wt% to PLA leads to an $OTR \cdot e$ value of $26.67 \text{ cm}^3 \text{ mm m}^{-2} \text{ day}^{-1}$ which represents almost a 40% increase. Obviously, the $OTR \cdot e$ product is still increased as the plasticizer content increased due to its effects on the global free volume. These results were observed by Burgos N. *et al.* in PLA formulations plasticized with oligomeric lactic acid – OLA. They reported a clear increasing tendency in the $OTR \cdot e$ parameter with increasing the plasticizer content. Specifically, the $OTR \cdot e$ value increased from $33 \text{ cm}^3 \text{ mm m}^{-2} \text{ day}^{-1}$ up to values over $70 \text{ cm}^3 \text{ mm m}^{-2} \text{ day}^{-1}$ for plasticized formulations with 25 wt% OLA [39]. Martino VP *et al.* also reported the same phenomenon in plasticized PLA formulations with di-2-ethylhexyladipate – DEHA or DOA, with a percentage increase in the $OTR \cdot e$ parameter of 54.58% with regard to neat PLA films. In particular, the $OTR \cdot e$ rate increased from $29.5 \text{ cm}^3 \text{ mm m}^{-2} \text{ day}^{-1}$ (neat PLA) up to $66.4 \text{ cm}^3 \text{ mm m}^{-2} \text{ day}^{-1}$ for PLA formulations with 20 wt% DOA [44]. Armentano *et al.* reported similar results with PLA/PHB blends plasticized with 20 wt% OLA. They observed that the $OTR \cdot e$ for neat PLA ($22.9 \text{ cm}^3 \cdot \text{mm} \cdot \text{m}^{-2} \cdot \text{day}^{-1}$) increased up to $25.5 \text{ cm}^3 \cdot \text{mm} \cdot \text{m}^{-2} \cdot \text{day}^{-1}$ by the addition of 20 wt% OLA plasticizer [13].

Table IV.4.3. Barrier properties against oxygen measured as the product between the oxygen transmission rate – OTR and the average thickness ($OTR \cdot e$) and water contact angle (θ_{water}) measurements for plasticized PLA formulations with maleinized oils.

Sample code	$OTR \cdot e$ (cm ³ mm m ⁻² day ⁻¹)	Water contact angle, WCA (°)
PLA	19.06±0.99	63.5±3.6
5 % MCSO	20.63±0.09	74.1±1.5
7.5 % MCSO	23.39±0.52	74.5±2.7
5 % MLO	26.67±0.92	77.8±0.8
7.5 % MLO	28.57±0.76	77.6±1.4

Maleinized oils also have an effect on the surface properties of plasticized PLA films as it can be seen in **Table IV.4.3**. Unplasticized PLA film shows a θ_{water} of 63.5°C which is lower than other highly hydrophobic polymer films such as polyolefins. Both maleinized oils provide increased hydrophobicity which could possibly be related to the increase in crystallinity as Arrieta MP *et al.* have suggested [11] and the intrinsic nature of hydrophobic fatty acid segments. The θ_{water} increases up to values of 74° and 77° for plasticized PLA films with MCSO and MLO respectively which could have a positive effect on restricting of water permeation. Darie-Nita *et al.* evaluated the influence of several plasticizers, *e.g.* ESBO, OLA and PEG on the water contact angle of plasticized PLA formulations. They observed a decrease in the water contact angle for all three plasticizers thus giving evidences of increased hydrophilicity with a positive effect on biocompatibility but negative effects on water barrier properties. The plasticizer with the strongest effects on surface hydrophilicity was PEG [45]. Ljungberg *et al.* evaluated the effect of the storage time on the water contact angle on plasticized PLA films. They observed an initial increase in the water contact angle by adding triacetine – TAc (15 wt%) as plasticizer but this decreased after 45 days due to migration thus indicating that although some hydrophobic properties can be obtained initially with some plasticizers, migration with time could lead to increased hydrophilicity [46].

■ Disintegration of plasticized PLA films with MCSO in controlled compost soil.

Figure IV.4.6 gathers different images corresponding to different disintegration times of unplasticized PLA and plasticized PLA films with 5 wt% and 7.5 wt% MCSO and MLO.

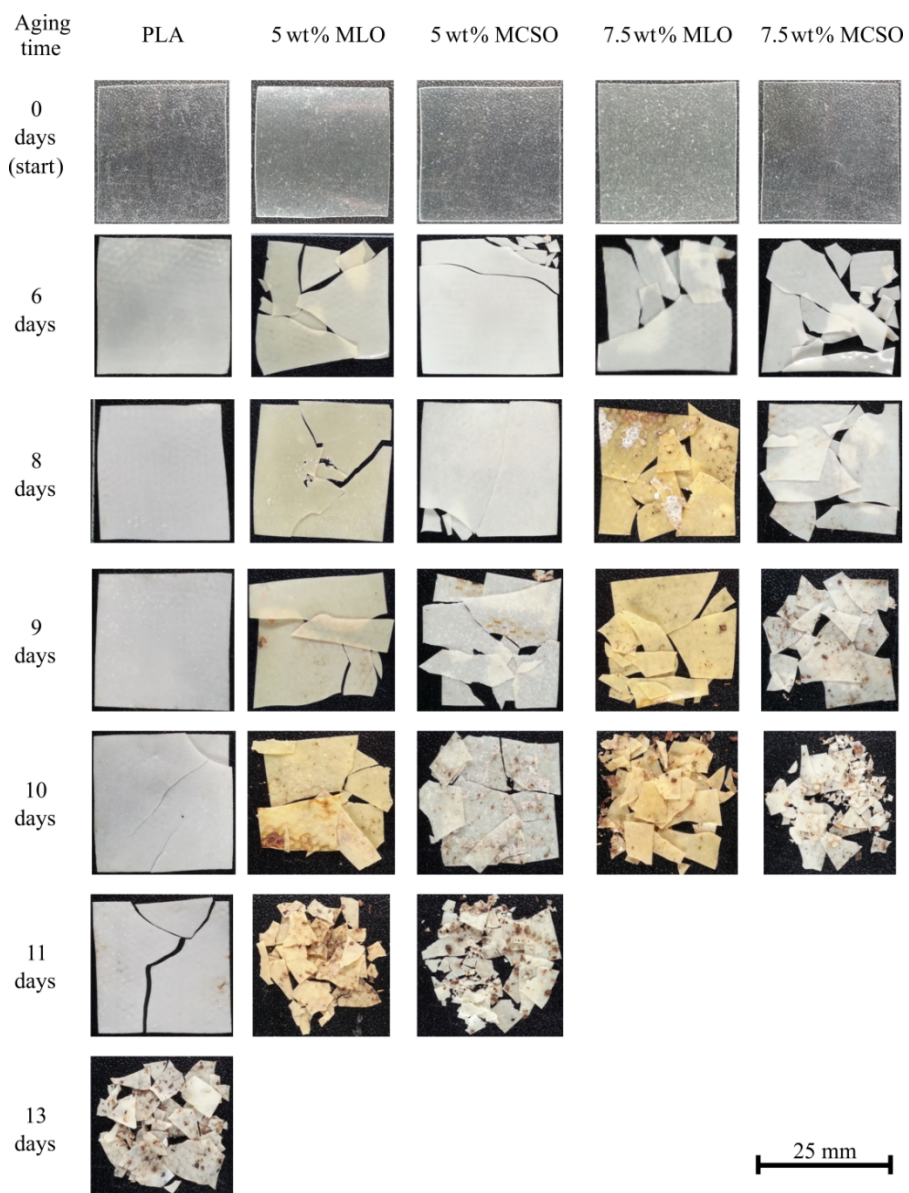


Figure IV.4.6. Visual aspect of plasticized PLA films with maleinized oils in terms of the oil content and disintegration time (the initial size of all films was 25 x 25 mm²).

With only a disintegration time of 6 days, the effects are clearly detectable. In fact, all films become translucent and opaque due to the increase in crystallinity during the initial stages of the degradation which are particularly favoured by moisture and temperature inside the compost reactor [6].

Nevertheless, unplasticized PLA shows different behaviour than that observed for all plasticized formulations. As a matter of fact, PLA does not become fragile until 10 days which is evidenced by the appearance of cracks. Nevertheless, plasticized PLA films with MCSO and MLO become highly fragile for an aging time of 6 days and this fragility is much more evident with increasing the aging time. As suggested by these images, plasticized PLA formulations with both MCSO and MLO seem to accelerate the disintegration process in controlled compost soil. In fact, while PLA requires almost 14 days to disintegrate, plasticized films with 5 wt% of both MCSO or MLO, need only 11 days to achieve the same disintegration level and plasticized films with 7.5 wt% of MCSO or MLO reach the same disintegration level after an aging period of 10 days. Similar findings have been reported by Arrieta MP *et al.* with plasticized PLA and PLA/PHB blends with acetyl tri-n-butyl citrate – ATBC [11].

IV.4.4. Conclusions.

This research work assesses the usefulness of maleinized cottonseed oil – MCSO as plasticizer for PLA films. In addition, a comparison of the potential of the synthesised MCSO and a commercially available maleinized vegetable oil, maleinized linseed oil – MLO, shows better performance of MCSO *versus* MLO. A slight plasticization effect was observed by differential scanning calorimetry, with an associated decrease in the glass transition temperature – T_g of 2 °C. In a similar way, the cold crystallization process was advanced by 7 °C for MCSO and 10 °C for MLO, thus indicating increased chain mobility with the subsequent increase in PLA crystallinity. This phenomenon is much more pronounced in the case of plasticized PLA films with MCSO and this has a positive effect on their mechanical properties. Although the plasticizing effect of MCSO is poor, mechanical ductile properties are remarkably improved. The very low elongation at

break of neat PLA (around 4%) is increased up to almost 16% in formulations containing 7.5 wt% MCSO. FESEM analysis revealed a particular morphology on plasticized PLA films, which is composed of micro-spherical oil particles dispersed in the PLA matrix, which could positively contribute to increase ductile properties. Although the barrier properties are not improved with MCSO addition, the OTR·e changes from $19.06 \text{ cm}^3 \text{ mm m}^{-2} \text{ day}^{-1}$ for neat PLA up to $20.63 \text{ cm}^3 \text{ mm m}^{-2} \text{ day}^{-1}$ in plasticized films with 5 wt% MCSO, thus showing good enough barrier properties. The results with MLO were worse. Finally, MCSO does not compromise the disintegration; as the MCSO increases, the disintegration process is noticeably accelerated. It is possible to conclude that MCSO is a highly efficient plasticizer for PLA films with high interest from both technical and environmental standpoints.

Acknowledgements.

This research was supported by the Ministry of Economy and Competitiveness - MINECO, Ref: MAT2014-59242-C2-1-R. A. Carbonell-Verdu wants to thank Universitat Politècnica de València for financial support through an FPI grant. D. Garcia-Garcia wants to thanks the Spanish Ministry of Education, Culture and Sports for their financial support through an FPU grant (FPU13/06011).

References.

- [1] V. Mittal, T. Akhtar, N. Matsko, "Mechanical, thermal, rheological and morphological properties of binary and ternary blends of PLA, TPS and PCL", Macromolecular Materials and Engineering (2015) **300**, 423-435.
- [2] J.M. Ferri, D. Garcia-Garcia, L. Sanchez-Nacher, O. Fenollar, R. Balart, "The effect of maleinized linseed oil (MLO) on mechanical performance of poly(lactic acid)-thermoplastic starch (PLA-TPS) blends", Carbohydrate Polymers (2016) **147**, 60-68.
- [3] M.L. Skoric, I. Terzic, N. Milosavljevic, M. Radetic, Z. Saponjic, M. Radoicic, M.K. Krusic, "Chitosan-based microparticles for immobilization of TiO₂ nanoparticles and their application for photodegradation of textile dyes", European Polymer Journal (2016) **82**, 57-70.
- [4] T. Garrido, I. Leceta, S. Cabezudo, P. Guerrero, K. de la Caba, "Tailoring soy protein film properties by selecting casting or compression as processing methods", European Polymer Journal (2016) **85**, 499-507.
- [5] V. Fombuena, L. Sanchez-Nacher, M.D. Samper, D. Juarez, R. Balart, "Study of the properties of thermoset materials derived from epoxidized soybean oil and protein fillers", Journal of the American Oil Chemists Society (2013) **90**, 449-457.
- [6] F. Luzi, E. Fortunati, A. Jiménez, D. Puglia, D. Pezzolla, G. Gigliotti, J.M. Kenny, A. Chiralt, L. Torre, "Production and characterization of PLA_PBS biodegradable blends reinforced with cellulose nanocrystals extracted from hemp fibres", Industrial Crops and Products (2016) **93**, 276-289.
- [7] J.A. Simao, C.F. Bellani, M.C. Branciforti, "Thermal properties and crystallinity of PCL/PBSA/cellulose nanocrystals grafted with PCL chains", Journal of Applied Polymer Science (2017) **134**, 44493.
- [8] I. Armentano, E. Fortunati, N. Burgos, F. Dominici, F. Luzi, S. Fiori, A. Jiménez, K. Yoon, J. Ahn, S. Kang, J.M. Kenny, "Bio-based PLA_PHB plasticized blend films: Processing and structural characterization", LWT - Food Science and Technology (2015) **64**, 980-988.

- [9] D. Garcia-Garcia, J.M. Ferri, N. Montanes, J. Lopez-Martinez, R. Balart, "Plasticization effects of epoxidized vegetable oils on mechanical properties of poly(3-hydroxybutyrate)", *Polymer International* (2016) **65**, 1157-1164.
- [10] M.P. Arrieta, J. López, D. López, J.M. Kenny, L. Peponi, "Biodegradable electrospun bionanocomposite fibers based on plasticized PLA-PHB blends reinforced with cellulose nanocrystals", *Industrial Crops and Products* (2016) **93**, 290-301.
- [11] M.P. Arrieta, J. López, D. López, J.M. Kenny, L. Peponi, "Development of flexible materials based on plasticized electrospun PLA-PHB blends: Structural, thermal, mechanical and disintegration properties", *European Polymer Journal* (2015) **73**, 433-446.
- [12] M.L. Sanyang, S.M. Sapuan, M. Jawaid, M.R. Ishak, J. Sahari, "Development and characterization of sugar palm starch and poly(lactic acid) bilayer films", *Carbohydrate Polymers* (2016) **146**, 36-45.
- [13] I. Armentano, E. Fortunati, N. Burgos, F. Dominici, F. Luzi, S. Fiori, A. Jimenez, K. Yoon, J. Ahn, S. Kang, J.M. Kenny, "Processing and characterization of plasticized PLA/PHB blends for biodegradable multiphase systems", *Express Polymer Letters* (2015) **9**, 583-596.
- [14] J.M. Ferri, M.D. Samper, D. Garcia-Sanoguera, M.J. Reig, O. Fenollar, R. Balart, "Plasticizing effect of biobased epoxidized fatty acid esters on mechanical and thermal properties of poly(lactic acid)", *Journal of Materials Science* (2016) **51**, 5356-5366.
- [15] M. Rapa, A.C. Mitelut, E.E. Tanase, E. Grosu, P. Popescu, M.E. Popa, J.T. Rosnes, M. Sivertsvik, R.N. Darie-Nita, C. Vasile, "Influence of chitosan on mechanical, thermal, barrier and antimicrobial properties of PLA-biocomposites for food packaging", *Composites Part B-Engineering* (2016) **102**, 112-121.
- [16] A. Ruellan, V. Ducruet, A. Gratia, L.S. Jimenez, A. Guinault, C. Sollogoub, G. Chollet, S. Domenek, "Palm oil deodorizer distillate as toughening agent in polylactide packaging films", *Polymer International* (2016) **65**, 683-690.
- [17] F. Hassouma, I. Mihai, L. Fetzer, T. Fouquet, J.M. Raquez, A. Laachachi, H. Ibn Al Ahrach, P. Dubois, "Design of new cardanol derivative: synthesis and application as potential biobased

- plasticizer for poly(lactide)", Macromolecular Materials and Engineering (2016) 301, 1267-1278.*
- [18] M. Akrami, I. Ghasemi, H. Azizi, M. Karrabi, M. Seyedabadi, "A new approach in compatibilization of the poly(lactic acid)/thermoplastic starch (PLA/TPS) blends", Carbohydrate Polymers (2016) 144, 254-262.
- [19] P. Müller, J. Bere, E. Fekete, J. Móczó, B. Nagy, M. Kállay, B. Gyarmati, B. Pukánszky, "Interactions, structure and properties in PLA/plasticized starch blends", Polymer (2016) 103, 9-18.
- [20] T. Malwela, S.S. Ray, "Enzymatic degradation behavior of nanoclay reinforced biodegradable PLA/PBSA blend composites", International Journal of Biological Macromolecules (2015) 77, 131-142.
- [21] R. Al-Ittry, K. Lamnawar, A. Maazouz, N. Billon, C. Combeaud, "Effect of the simultaneous biaxial stretching on the structural and mechanical properties of PLA, PBAT and their blends at rubbery state", European Polymer Journal (2015) 68, 288-301.
- [22] M. Forouharshad, L. Gardella, D. Furfaro, M. Galimberti, O. Monticelli, "A low-environmental-impact approach for novel biocomposites based on PLLA/PCL blends and high surface area graphite", European Polymer Journal (2015) 70, 28-36.
- [23] S. Vijayarajan, S.E.M. Selke, L.M. Matuana, "Continuous blending approach in the manufacture of epoxidized soybeanplasticized poly(lactic acid) sheets and films", Macromolecular Materials and Engineering (2014) 299, 622-630.
- [24] C. Xing, L.M. Matuana, "Epoxidized soybean oil-plasticized poly(lactic acid) films performance as impacted by storage", Journal of Applied Polymer Science (2016) 133, 43201.
- [25] J. Alam, M. Alam, M. Raja, Z. Abduljaleel, L.A. Dass, "MWCNTs-reinforced epoxidized linseed oil plasticized polylactic acid nanocomposite and its electroactive shape memory behaviour", International Journal of Molecular Sciences (2014) 15, 19924-19937.

- [26] Y.B. Tee, R.A. Talib, K. Abdan, N.L. Chin, R.K. Basha, K.F.M. Yunos, "Comparative study of chemical, mechanical, thermal, and barrier properties of poly(lactic acid) plasticized with epoxidized soybean oil and epoxidized palm oil", *Bioresources* (2016) **11**, 1518-1540.
- [27] M.M. Wadhi, R. Weliam, "Effect of epoxidized sunflower oil on polylactic acid properties", *Research on Chemical Intermediates* (2014) **40**, 399-406.
- [28] S.C. Mauck, S. Wang, W.Y. Ding, B.J. Rohde, C.K. Fortune, G.Z. Yang, S.K. Ahn, M.L. Robertson, "Biorenewable tough blends of polylactide and acrylated epoxidized soybean oil compatibilized by a polylactide star polymer", *Macromolecules* (2016) **49**, 1605-1615.
- [29] J.M. Ferri, D. Garcia-Garcia, N. Montanes, O. Fenollar, R. Balart, "The effect of maleinized linseed oil as biobased plasticizer in poly(lactic acid)-based formulations", *Polymer International* (2017) **66**, 882-891.
- [30] A. Carbonell-Verdu, L. Bernardi, D. Garcia-Garcia, L. Sanchez-Nacher, R. Balart, "Development of environmentally friendly composite matrices from epoxidized cottonseed oil", *European Polymer Journal* (2015) **63**, 1-10.
- [31] A. Carbonell-Verdu, D. Garcia-Sanoguera, A. Jorda-Vilaplana, L. Sanchez-Nacher, R. Balart, "A new biobased plasticizer for poly(vinyl chloride) based on epoxidized cottonseed oil", *Journal of Applied Polymer Science* (2016) **133**, 43642.
- [32] C. Liu, Z. Liu, B.H. Tisserat, R. Wang, T.P. Schuman, Y. Zhou, L. Hu, "Microwave-assisted maleation of tung oil for bio-based products with versatile applications", *Industrial Crops and Products* (2015) **71**, 185-196.
- [33] T. Eren, S.H. Kusefoglu, R. Wool, "Polymerization of maleic anhydride-modified plant oils with polyols", *Journal of Applied Polymer Science* (2003) **90**, 197-202.
- [34] C.R. Li, H. Liu, B.H. Luo, W. Wen, L.M. He, M.X. Liu, C.R. Zhou, "Nanocomposites of poly(L-lactide) and surface-modified chitin whiskers with improved mechanical properties and cytocompatibility", *European Polymer Journal* (2016) **81**, 266-283.

- [35] A.I. Aigbodion, F.E. Okieimen, E.O. Obazee, I.O. Bakare, "Utilisation of maleinized rubber seed oil and its alkyd resin as binders in water-borne coatings", Progress in Organic Coatings (2003) **46**, 28-31.
- [36] J.R. Ernzen, F. Bondan, C. Luvison, C.H. Wanke, J.D. Martins, R. Fiorio, O. Bianchi, "Structure and properties relationship of melt reacted polyamide 6/maleinized soybean oil", Journal of Applied Polymer Science (2016) **133**, 10.
- [37] J.F. Balart, V. Fombuena, O. Fenollar, T. Boronat, L. Sanchez-Nacher, "Processing and characterization of high environmental efficiency composites based on PLA and hazelnut shell flour (HSF) with biobased plasticizers derived from epoxidized linseed oil (ELO)", Composites Part B-Engineering (2016) **86**, 168-177.
- [38] B.W. Chieng, N.A. Ibrahim, Y.Y. Then, Y.Y. Loo, "Epoxidized vegetable oils plasticized poly(lactic acid) biocomposites: mechanical, thermal and morphology properties", Molecules (2014) **19**, 16024-16038.
- [39] N. Burgos, V.P. Martino, A. Jimenez, "Characterization and ageing study of poly(lactic acid) films plasticized with oligomeric lactic acid", Polymer Degradation and Stability (2013) **98**, 651-658.
- [40] H. Kwon, D. Kim, J. Seo, "Thermal and barrier properties of EVOH/EFG nanocomposite films for packaging applications: effect of the mixing method", Polymer Composites (2016) **37**, 1744-1753.
- [41] K. Shahverdi-Shahraki, T. Ghosh, K. Mahajan, A. Ajji, P.J. Carreau, "Polyethylene terephthalate/calcined kaolin composites: effect of uniaxial stretching on the properties", Polymer Engineering and Science (2015) **55**, 1767-1775.
- [42] M. Vishnuvarthan, N. Rajeswari, "Effect of mechanical, barrier and adhesion properties on oxygen plasma surface modified PP", Innovative Food Science & Emerging Technologies (2015) **30**, 119-126.
- [43] R.A. Auras, S.P. Singh, J.J. Singh, "Evaluation of oriented poly(lactide) polymers vs. existing PET and oriented PS for fresh food service containers", Packaging Technology and Science (2005) **18**, 207-216.

- [44] V.P. Martino, A. Jimenez, R.A. Ruseckaite, "*Processing and characterization of poly(lactic acid) films plasticized with commercial adipates*", Journal of Applied Polymer Science (2009) **112**, 2010-2018.
- [45] R.N. Darie-Nita, C. Vasile, A. Irimia, R. Lipsa, M. Rapa, "*Evaluation of some eco-friendly plasticizers for PLA films processing*", Journal of Applied Polymer Science (2016) **133**, 43223.
- [46] N. Ljungberg, T. Andersson, B. Wesslen, "*Film extrusion and film weldability of poly(lactic acid) plasticized with triacetine and tributyl citrate*", Journal of Applied Polymer Science (2003) **88**, 3239-3247.



Contents lists available at ScienceDirect

European Polymer Journal

journal homepage: www.elsevier.com/locate/europolj

PLA films with improved flexibility properties by using maleinized cottonseed oil



Alfredo Carbonell-Verdu^{a,*}, Daniel Garcia-Garcia^a, Franco Dominici^b, Luigi Torre^b, Lourdes Sanchez-Nacher^a, Rafael Balart^a

^a Instituto de Tecnología de Materiales (ITM), Universidad Politécnica de Valencia (UPV), Plaza Ferrández y Carbonell s/n, 03801 Alcoy, Alicante, Spain

^b Dipartimento di Ingegneria Civile e Ambientale, Università di Perugia, Italy

ARTICLE INFO

Keywords:
 poly(lactic acid) – PLA
 Cottonseed oil
 Maleinization
 Mechanical properties
 Thermal properties
 Barrier properties

ABSTRACT

This work assesses the potential of maleinized cottonseed oil – MCSO as plasticizer in poly(lactic acid) – PLA films with improved ductile behaviour. The effects of MCSO are compared with commercially available maleinized oil, i.e. maleinized linseed oil – MLO in terms of mechanical, thermal and barrier properties, as well as morphology changes. Plasticized PLA formulations were obtained with a maleinized oil content in the 0–10 wt% range. Addition of both maleinized vegetable oils leads to a slight decrease in the glass transition temperature (T_g) of neat PLA from 63 °C to 60–61 °C. Nevertheless, MCSO provides better overall properties. Addition of 7.5 wt% MCSO increases the elongation at break by 292%. Regarding the barrier properties, both maleinized vegetable oils increase the oxygen transmission rate – OTR. Nevertheless, this increase is less pronounced in the case of MCSO thus indicating its higher efficiency compared to MLO. On the other hand, addition of both maleinized vegetable oils do not compromise the overall disintegration of the obtained PLA formulations, thus positioning these additives as environmentally friendly solutions to increase ductile properties in PLA-based films.

1. Introduction

The growing awareness about the ongoing environmental pollution, together with the, still distant but increasingly close, problematics of petroleum depletion, are leading the research on obtaining materials from renewable resources and, potentially, biodegradable. This situation is particularly accentuated in the packaging industry due to the huge amounts of wastes that are generated worldwide. For these reasons, new polymers and industrial formulations are continuously being developed with the main aim of lowering their environmental impacts. Today, a wide variety of polymers can be obtained from renewable resources. Polysaccharides are a promising source of polymers due to their worldwide abundance. Different starches e.g. maize, potato, rice, etc. can be converted into industrial plastic formulations by using appropriate plasticizers such as glycerol, water, sorbitol, etc. leading to the so called “thermoplastic starches” – TPS [1,2]. A new range of materials have been successfully synthesised from chitin which is the Earth’s second most abundant polysaccharide, surpassed only by cellulose. Chitin can be found in the exoskeleton of crustaceans [3]. Proteins are another important source of polymers. It is worthy to note the use of vegetable proteins such as gluten or soy protein in the field of polymers and composites, as well as animal proteins such as collagen, casein, ovalbumin, etc. widely used in the food industry [4,5]. Aliphatic polyesters represent a promising solution to environmentally friendly polymers. Although some of them are

* Corresponding author.
 E-mail address: alcarvel@epsa.upv.es (A. Carbonell-Verdu).

<http://dx.doi.org/10.1016/j.eurpolymj.2017.04.013>
 Received 10 February 2017; Received in revised form 30 March 2017; Accepted 11 April 2017
 Available online 12 April 2017
 0014-3057/© 2017 Elsevier Ltd. All rights reserved.

IV.5

IV.5. Manufacturing and compatibilization of PLA/PBAT binary blends by cottonseed oil-based derivatives.

A. Carbonell-Verdu¹, J.M. Ferri¹, F. Dominici², T. Boronat¹, L. Sánchez-Nacher¹, R. Balart¹ L. Torre²

¹ Materials Technology Institute (ITM)
Universitat Politècnica de València (UPV)
Plaza Ferrandiz y Carbonell 1, 03801, Alcoy, Alicante (Spain)

² Dipartimento di Ingegneria Civile e Ambientale
Università di Perugia
Strada di Pentima 4, 05100 Terni (Italy)

“Manufacturing and compatibilization of PLA/PBAT binary blends by cottonseed oil-based derivatives”

Abstract

This research work aims to the compatibilization of poly(lactic acid)/poly(butylene adipate-co-terephthalate), PLA/PBAT binary blends by using cottonseed oil derivatives, *i.e.* epoxidized (ECSO) and maleinized (MCSO) cottonseed oil. The potential of these vegetable oil-based compatibilizers are compared *versus* the effects of a conventional styrene-acrylic oligomer. The base PLA/PBAT binary blend composition was 80 wt% PLA/20 wt% PBAT and the amount of compatibilizer was set to 1 wt% and 7.5 wt%. The effects of the different compatibilizers were evaluated on PLA/PBAT films in terms of mechanical and thermal properties as well as blend's morphology by field emission scanning electron microscopy (FESEM). Complementary, biodisintegration tests in controlled compost soil and surface properties were evaluated to assess the effects of the compatibilizers. Addition of 1 wt% ECSO and MCSO led to a remarkable increase in the elongation at break up to values over 100% with regard to neat PLA. Despite this, maximum elongation at break was obtained for the compatibilized PLA/PBAT blend with 7.5 wt% MCSO, reaching values of about 321.2% respect neat PLA keeping mechanical resistant properties, such as Young's modulus and tensile strength, at high levels. Therefore, vegetable oil-derived compatibilizers stand out as environmentally friendly additives for PLA/PBAT binary blends with improved properties.

Keywords

Biopolymers; biocomposites; poly(lactic acid) PLA; cotton seed oil; maleinization; epoxidation.

IV.5.1. Introduction.

Poly(lactic acid), PLA is currently considered one of the most promising polymers from renewable resources, due to an excellent balance between mechanical properties and a competitive price day by day [1]. Nevertheless, it is intrinsically quite brittle, its chemical barrier behavior is not optimum compared to other widely used polymers, its thermal stability is also restricted and its resistance to external agents (UV radiation, moisture, etc.) are issues to overcome. For this reason, industrial PLA and other polymer formulations usually contain several additives with different purposes thus widening its use in sectors such as agriculture [2], packaging [3, 4], medical devices [5], 3D printing, textile fibers [6]. With the aim of a sustainable development and a low environmental impact, biobased additives are been searched, *i.e.* antioxidants, plasticizers, fillers, etc. [7-10]. With the increasing development of nanotechnology, many research works have been focused of using nanostructures to improve the properties of PLA-based materials [11-13] and interactions.

Typical PLA materials are characterized by low toughness and this is one of the main drawbacks in a massive use of this biopolyester. A broad range of approaches has been observed in the last decade to minimize this effect Xu *et al.* [14] reported a new injection molding technology (oscillating shear) to improve all properties of PLA, including its toughness. One of the easiest methods to overcome the intrinsic brittleness of PLA is by physical blends with ductile polymers [15]. A wide variety of binary and ternary blends with PLA have been proposed as a technical solution to improve toughness. Among others, it is worthy to note some interesting PLA-based blends with poly(ϵ -caprolactone)(PCL) [16], thermoplastic starch (TPS) [17], poly(butylene succinate) (PBS) [18], poly(butylene succinate-co-adipate) (PBSA) [19], poly(glycolic acid) (PGA) [20], poly(hydroxybutyrate) (PHB) [21], poly(hydroxybutyrate-co-valerate) (PHBV) [22], poly(butylene adipate-co-terephthalate) (PBAT) [23], etc. Ternary blends allow obtaining tailored properties in PLA-based blends [24, 25]. Despite some increase in mechanical ductile properties are achieved with these blends, most of PLA-based blends show partial or total immiscibility, being this an important drawback to obtain synergistic effects. To improve compatibility between immiscible of partially miscible polymers, different approaches have been proposed. Reactive extrusion stands out as a cost effective alternative to copolymerization [26]. Reactive extrusion with PLA

considers chemical reactions with some additives such as triphenyl phosphite, adimides (*e.g.* Bioadimide®), epoxy-based styrene-acrylic oligomers (*e.g.* Joncryl®), glycidyl copolymers [27], etc. with the hydroxyl terminal groups present in PLA and other biobased polyesters. This allows chain extension and/or branching with a positive effect on compatibilization of both polymers in the blend with a subsequent improvement in toughness. Ojijo *et al.* [28] developed PLA/PBSA blends with 2% triphenyl phosphite (TPP). They reported an increase in elongation at break of 37% and the energy absorption changed from 6.76 kJ m⁻² (neat PLA) up to 16.4 kJ m⁻² for the PLA blend with 10% PBSA and 2% TPP. Over 2% TPP, over-crosslinking occurs and properties are not improved. Al-Ittry *et al.* [29] studied the effect of Joncryl ADR-4368 (an epoxidized styrene-acrylic oligomer) on PLA/PBAT blends. In fact, they reported a percentage increase in the elongation at break of 900% with regard to neat PLA. In addition, the other mechanical properties were not affected to a great extent, since the effect of this oligomer is not only chain extension, but also branching and/or crosslinking as reported by Torres-Giner *et al.* [30].

Similar results have been reported with reactive extrusion by generating free radicals during the extrusion process, which can be achieved by using organic peroxides. This leads to a combination of chain extension, branching and crosslinking. Bureepukdee *et al.* [31] compared the compatibilizing effect of di(tert-butylperoxy isopropyl) benzene (DTBP) and 2, 5-dimethyl-2, 5-(t-butylperoxy) hexane (DTBH). They reported a continuous phase by using 0.1 phr DTBP on a binary PLA blend with 40% PBSA with a remarkable increase in ductility.

With the aim of obtaining high environmentally friendly PLA formulations, the use of vegetable-oil (VO)-derived additives is increasing as vegetable oils can be chemically modified to tailor some particular functionalities which can react with PLA and other biopolymers. Currently, epoxidized vegetable oils (EVOs) are widely used in the new generation of environmentally friendly plasticized PVC formulations [32, 33] and thermosetting resins [34]. Their use in the packaging industry is attracting due to low migration rates towards the food [35]. A new generation of biobased poly(urethanes) has been developed by using vegetable oil-derived polyols [36]. Modified vegetable oils could potentially act as compatibilizers in binary and ternary blends. Some vegetable oils (those with unsaturated fatty acids such as oleic, linoleic, linolenic, etc.) can be subjected to a wide variety of chemical modifications such as epoxidation, acrylation,

hydroxylation, maleinization, etc. among others. With these processes, oxirane rings, acrylic groups, hydroxyl groups and maleic anhydride, and other functional groups can be added to the vegetable oil structure thus increasing their reactivity towards terminal hydroxyl groups in PLA and other biopolymers.

In previous works, cotton seed oil (CSO) was chemically modified by conventional epoxidation process [35] to obtain epoxidized cotton seed oil (ECSO). Moreover, CSO was subjected to a maleinization process with maleic anhydride [37] to give maleinized cotton seed oil (MCSO). Both CSO-derivatives showed a clear plasticization effect on PLA. Specifically, the addition of 10 wt% ECSO led to a noticeable increase in elongation at break up to values of 110% of PLA, characterized by an elongation at break close to 9%. Similar findings were obtained with MCSO. Ferri *et al.* [38, 39] studied the effect of maleinized linseed oil (MLO) as compatibilizer in PLA/TPS blends. Two different phenomena were attributed to MLO: on one hand, a clear plasticization effect was observed but on the other hand, MLO also acted as a compatibilizer with a remarkable improvement on miscibility on such binary blends. Furthermore, MLO contributed to improve the processing of PLA/TPS blends.

The main aim of this research work is to assess the potential of cottonseed oil derivatives, *i.e.* epoxidized cottonseed oil (ECSO) and maleinized cottonseed oil (MCSO) as compatibilizers in PLA/PBAT binary blends. The effect of these two vegetable oil-derived compatibilizers is compared with a conventional epoxy styrene-acrylic oligomer in terms of mechanical properties, thermal stability, thermomechanical properties and blend's morphology. The novelty of this work is the assessment of cottonseed oil as potential base material for blend compatibilization with comparable features to other commercially available modified-vegetable oils. This widens the use of cottonseed wastes in industrial applications and contributes to high biobased content materials.

IV.5.2. Experimental.

Materials.

The PLA grade used was IngeoTM Biopolymer 2003 D supplied by NatureWorks LLC (Minnetonka, USA) in pellet form with a density of 1.24 g cm^{-3} and a melt flow index of $6 \text{ g}/(10 \text{ min})$ measured at 210°C . A PBAT commercial grade Biocosafe™ 2003 F was supplied by Xinfu Pharmaceutical Co. Ltd. (Zhejiang, China) and it is characterized by a density of 1.25 g cm^{-3} and a melt flow index $<6 \text{ g}/(10 \text{ min})$ at 190°C . PBAT has been selected because of its flexibility (an average tensile strength of 14 MPa and an elongation at break of 525%) which can contribute to improve toughness of PLA.

Two cottonseed oil derivatives, *i.e.* epoxidized cottonseed oil (ECSO) and maleinized cottonseed oil (MCSO) were used as compatibilizers, and compared with an epoxy styrene-acrylic oligomer, *i.e.* Joncryl®. The cottonseed oil (CSO) was supplied by Sigma Aldrich Spain (Madrid, Spain). Its main properties are a density of 0.92 g cm^{-3} and an iodine index comprised in the $109 - 120$ range, which allows chemical modification. Joncryl® ADR-4368 was supplied by BASF S.A (Barcelona, Spain) and is characterized by a T_g of 54°C , an epoxy equivalent weight of 285 g mol^{-1} and a molecular weight, M_w of 6800 g mol^{-1} . The cottonseed oil was subjected to epoxidation [40] and maleinization as reported in previous works [37]. The most relevant parameters obtained after the corresponding chemical processes are as follows. With regard to ECSO, the oxirane oxygen index was 5.32 after 8 h. Regarding MCSO an acid value of $63.72 \text{ mg KOH g}^{-1}$ was obtained after 3 h reaction. **Figure IV.5.1** shows a schematic representation of the base polymers and the compatibilizer additives.

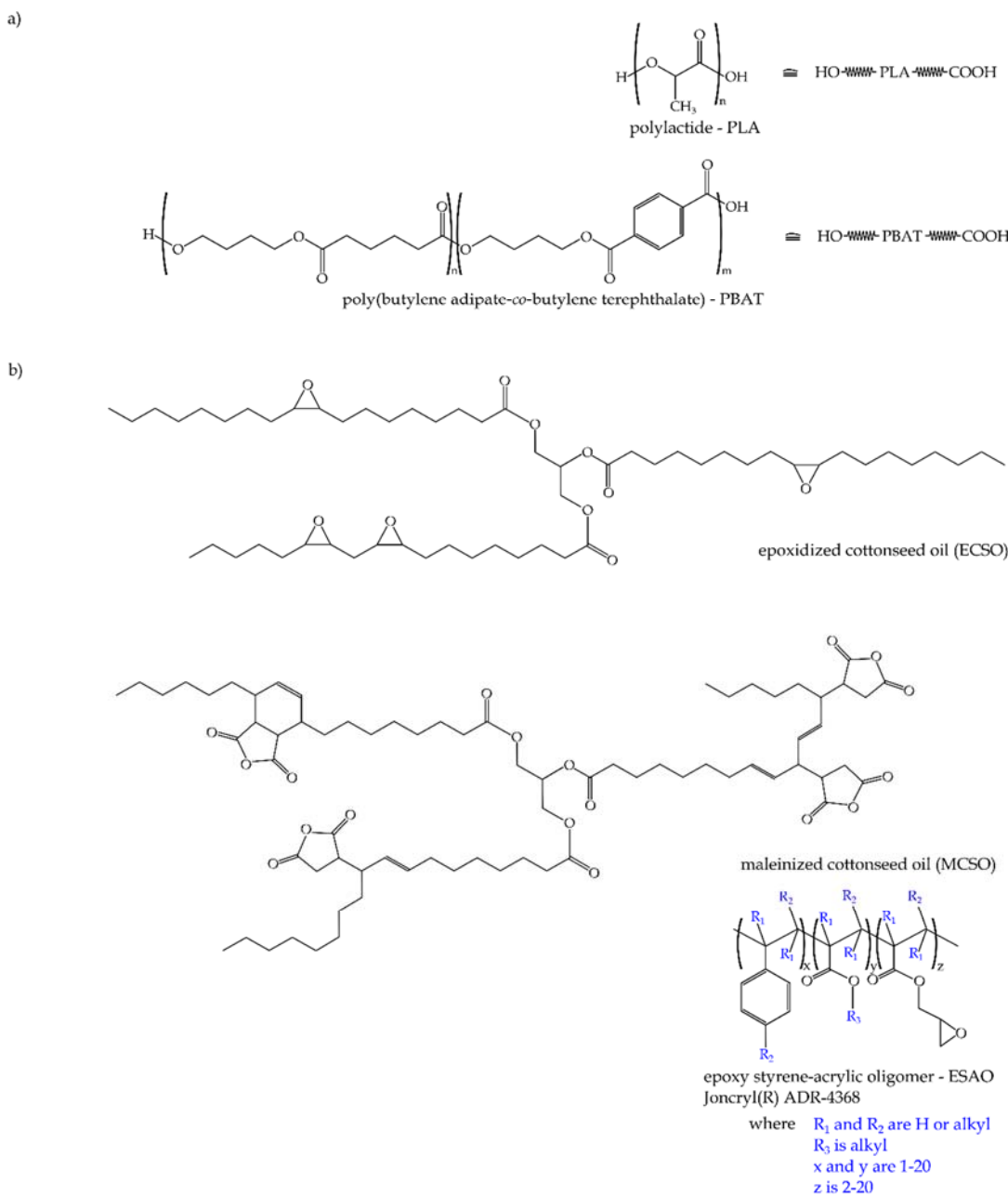


Figure IV.5.1. Schematic representation of the chemical structure of a) base polymers, *i.e.* poly(lactic acid) – PLA and poly(butylene adipate – co – terephthalate) – PBAT and b) epoxidized cottonseed oil – ECSO, maleinized cottonseed oil – MCSO and epoxy styrene-acrylic oligomer Joncryl® (generic structure).

Manufacturing of PLA/PBAT films.

PLA/PBAT blends were manufactured with different compositions as summarized in **Table IV.5.1**. The amount of Joncrys® was set to 1 wt% as the manufacturer recommends an additive load comprised between 0.25 – 2 wt%. With regard to the cottonseed oil derivatives, two different loads were used, *i.e.* 1 and 7.5 wt% as previous results have suggested [35, 37].

Table IV.5.1. Composition and coding of PLA/PBAT binary blends compatibilized with cottonseed oil derivatives.

Code	PLA wt%	PBAT wt%	Joncrys® wt%	ECSO wt%	MCSO wt%
PLA	100	-	-	-	-
PBAT	-	100	-	-	-
PLA/PBAT	80	20	-	-	-
PLA/PBAT/1 ECSO	79.2	19.8	-	1.0	-
PLA/PBAT/7.5 ECSO	74.0	18.5	-	7.5	-
PLA/PBAT/1 MCSO	79.2	19.8	-	-	1.0
PLA/PBAT/7.5 MCSO	74.0	18.5	-	-	7.5
PLA/PBAT/1 Joncrys®	79.2	19.8	1.0	-	-

PLA was dried for 24 h at 60 °C while PBAT was dried overnight at 40 °C. All materials were processed by extrusion in a DSM Xplore MC 15 micro compounder at 180 °C. The pre-mixing time inside the plasticization chamber was set to 3 min at a rotating speed of 100 rpm. After this time, the compounded material was forced to exit the plasticization chamber and extruded through a nozzle connected to a chill-roll system to obtain a continuous film, 30 mm width and 30 µm thick films at 15 rpm and a controlled force of 700 N.

Mechanical characterization.

Mechanical characterization was carried out as indicated in ISO 527-3 in a universal test machine LLOYD 30 K (Hampshire, England). Samples (type 2) were tested at a crosshead speed rate of 5 mm min⁻¹ with a load cell of 500 N. The samples sized 160 mm in length, 20 mm width and an average thickness of 30 µm. Special grips for thin films supplied by LLOYD (TG series) were used to appropriate characterize films avoiding premature fracture due to the clamp force. These grips are used for tensile testing of thin materials such as paper, rubber, thin plastic films, woven and non-woven textiles. At least five different samples were tested at room temperature and average values of the main parameters were calculated.

Morphological characterization.

The fracture surface obtained by cryofracture (longitudinal to the extrusion direction) was observed in a field emission scanning electron microscope, FESEM Zeiss Ultra from Oxford Instruments at an acceleration voltage of 2 kV. An ultrathin metallic layer of platinum was sputtered on the fractured films in a sputter coater EM MED020 from Leica Microsystems.

Thermal and thermomechanical characterization of PLA/PBAT films.

The most relevant thermal transitions were obtained by differential scanning calorimetry (DSC) in a Mettler–Toledo DSC mod. 821 (Schwerzenbach, Switzerland). The DSC runs were programmed into three stages: first a heating from -25 °C to 200 °C; then a cooling process down to -25 °C and a final heating stage up to 200 °C again. All three stages used the same heating rate of 10 °C min⁻¹ and were run under nitrogen

atmosphere (66 mL min⁻¹). The degree of crystallinity ($\chi_c\%$) was calculated from the second DSC heating runs using the equation.

$$\chi_c (\%) = 100 \times \frac{\Delta H_m - \Delta H_{cc}}{\Delta H_m (100\%)} \times \frac{1}{W_{PLA}} \quad \text{Equation IV.5.1}$$

Where ΔH_m and ΔH_{cc} stand for the melt and cold crystallization enthalpies respectively (J g⁻¹). On the other hand, ΔH_m (100%) represents the melt enthalpy of a theoretical fully crystalline PLA (93 J g⁻¹) [21] and W_{PLA} is the wt% PLA in the blend. With regard to the glass transition temperature, ISO 11357-2:2015 was used. Among all methods described in this standard, the inflection point was considered as the T_g value of all developed materials. In this method, the T_g value is assigned to the maximum of the derivative DSC curve or the temperature with the maximum slope in the glass transition area.

Thermal degradation at high temperatures was followed by thermogravimetric (TGA) analysis. Samples with an average weight of about 5-7 mg were placed in standard alumina pans and subjected to a heating program from 30 °C up to 660 °C at a heating rate of 20 °C min⁻¹ in a Mettler-Toledo TGA/SDTA851e/SF/1100 thermobalance in nitrogen atmosphere. In addition to the TGA thermograms, two representative temperatures, were calculated: $T_{5\%}$ and $T_{50\%}$ which correspond to temperatures at which a 5 wt% and a 50 wt% loss occurs, respectively.

Thermomechanical characterization of PLA/PBAT films was carried out in an oscillatory rheometer AR G2 from TA Instruments equipped with a special clamp system for solid samples working in a combined shear-torsion mode. Samples sizing 10 x 20 mm² with an average thickness of 30 µm, were subjected to a temperature sweep from -40 °C up to 100 °C at a heating rate of 2 °C min⁻¹. The selected frequency was 1 Hz and the normal force was 0.02 N while the maximum deformation was maintained at 1% (% γ).

■ Surface characterization of PLA/PBAT films.

The wetting properties of the developed blends were obtained by contact angle measurements in a Krüss goniometer model FM140 from KRÜSS GmbH (Hamburg, Germany). Five different water droplets were deposited onto the film surface and the corresponding contact angle was measured after 30 s to obtain stabilized values. Prior to contact angle characterization, sample films were dried at 40 °C for 24 h.

In addition, the color properties of the developed films were characterized in a Hunter Mod. CFLX-DIF-2 colorimeter from Hunterlab (Murnau, Germany). Although the apparatus can provide different measurements, only the luminance (L^*) was measured to evaluate the change in transparency.

■ Disintegration in controlled compost soil of PLA/PBAT films.

Disintegration tests were conducted on squared samples ($25 \times 25 \text{ mm}^2$) with an average thickness of 30 μm under the recommendations of the ISO 20200. Samples were placed into an aerobic reactor with a synthetic waste manufactured as indicated in ISO20200. Before placing samples into the reactor, all films were dried at 40 °C for 24 h. Then, the films were buried into the compost soil and extracted at 6, 8, 9, 10, 11, 14, 16, 21 and 23 days, washed with distilled water and dried at 40 °C for a day. Finally, optical images were taken to follow the disintegration process.

IV.5.3. Results and discussion.

Effect of compatibilizers on mechanical properties of PLA/PBAT films of maleinized cottonseed oil - MCSO.

Figure IV.5.2 shows the main results obtained with the herein-developed PLA/PBAT blends. As it can be seen, neat PLA is quite brittle with a modulus of 3145 MPa and a tensile strength of 54.5 MPa. Regarding its ductility, its elongation at break is close to 29.2% (in film form).

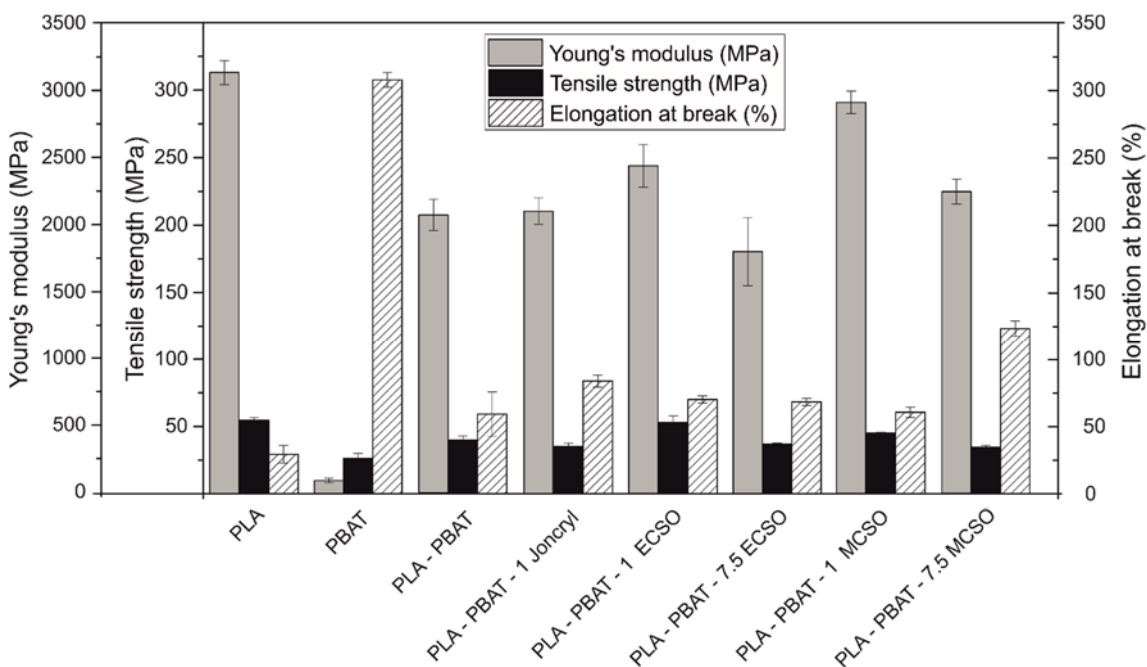


Figure IV.5.2. Comparative bar plot of tensile properties, *i.e.* Young's modulus, tensile strength and elongation at break, of neat PLA, neat PBAT and PLA/PBAT blends with and without compatibilizers.

These features limit the use of PLA in the packaging industry in which flexible films are required. On the other hand, PBAT is an extremely ductile polymer with a modulus of 96.4 MPa and a tensile strength of 26.2 MPa. In contrast, its elongation at

break reaches values of 307.6% thus giving clear evidences of its flexibility. For this reason, blends of PLA with PBAT are expected to be more flexible. As it can be seen in the above-mentioned figures, the uncompatibilized PLA/PBAT blend containing 20 wt% PBAT shows an increased elongation at break of 59.0% with interesting mechanical resistant properties, *i.e.* a Young modulus of 2079 MPa and a tensile strength of 39.9 MPa. The addition of 1 wt% Joncrys® gives similar mechanical resistant properties (modulus and tensile strength) while the elongation at break is remarkably improved up to 83.7% compared to the uncompatibilized blend.

These results give clear evidences of the compatibilization effects that Joncrys® can provide to polyesters. Specifically, the compatibilization is achieved by the reaction of the epoxy groups in Joncrys® oligomers and the hydroxyl terminal groups in polyesters (See **Figure IV.5.3[a]**) leading to chain extension and potential crosslinking. Racha Al-Ittry *et al.* [29] reported similar results with a PLA/PBAT blend with an elongation at break of 50% which was increased up to 135% with the addition of 0.5 wt% Joncrys®. Addition of 1 wt% of both ECSO and MCSO leads to an increase in elongation at break with values of 70.0% and 60.5% respectively but this increase is not as high as that observed with Joncrys®.

Nevertheless, it is worthy to note that both 1 wt% ECSO and MCSO provide improved mechanical resistant properties with tensile strength values of 52.9 MPa and 45.0 MPa respectively which are noticeable higher than those of Joncrys® (39.9 MPa). This suggests that both ECSO and MCSO (even at very low concentrations) provide a plasticizing effect but due to the triglyceride structure, not only chain extension but also branching and somewhat crosslinking, can occur as shown in **Figure IV.5.3[b]**. It has been reported that small amounts of modified vegetable oils can slightly plasticize PLA and other polyesters. Nevertheless, the efficiency of vegetable oil-based plasticizers is very poor as, in general, a very slight decrease on the glass transition temperature is achieved. Nevertheless, the highly reactive groups in modified vegetable oils (mainly epoxy, acrylate, maleic anhydride groups, among others) can react with hydroxyl groups present in the end chains of polyesters thus leading to additional reactions that could lead to chain extension, branching and crosslinking simultaneously as reported by Quiles-Carrillo *et al.* [41-43] in several works.

With regard to Joncrys®, typical amounts of 1 wt% are recommended by suppliers to avoid gel formation by crosslinking. So that, it is expectable a more intense

overlapping of chain extension, branching and crosslinking when using ECSO and MCSO than in the case of Joncrys®. A FTIR study carried out by Quiles-Carrillo *et al.* [43] on poly(lactic acid) with lignocellulosic fillers demonstrated the reaction between maleinized linseed oil (MLO) and hydroxyl groups in PLA end chains and cellulose particles therefore giving clear evidences of reactive extrusion.

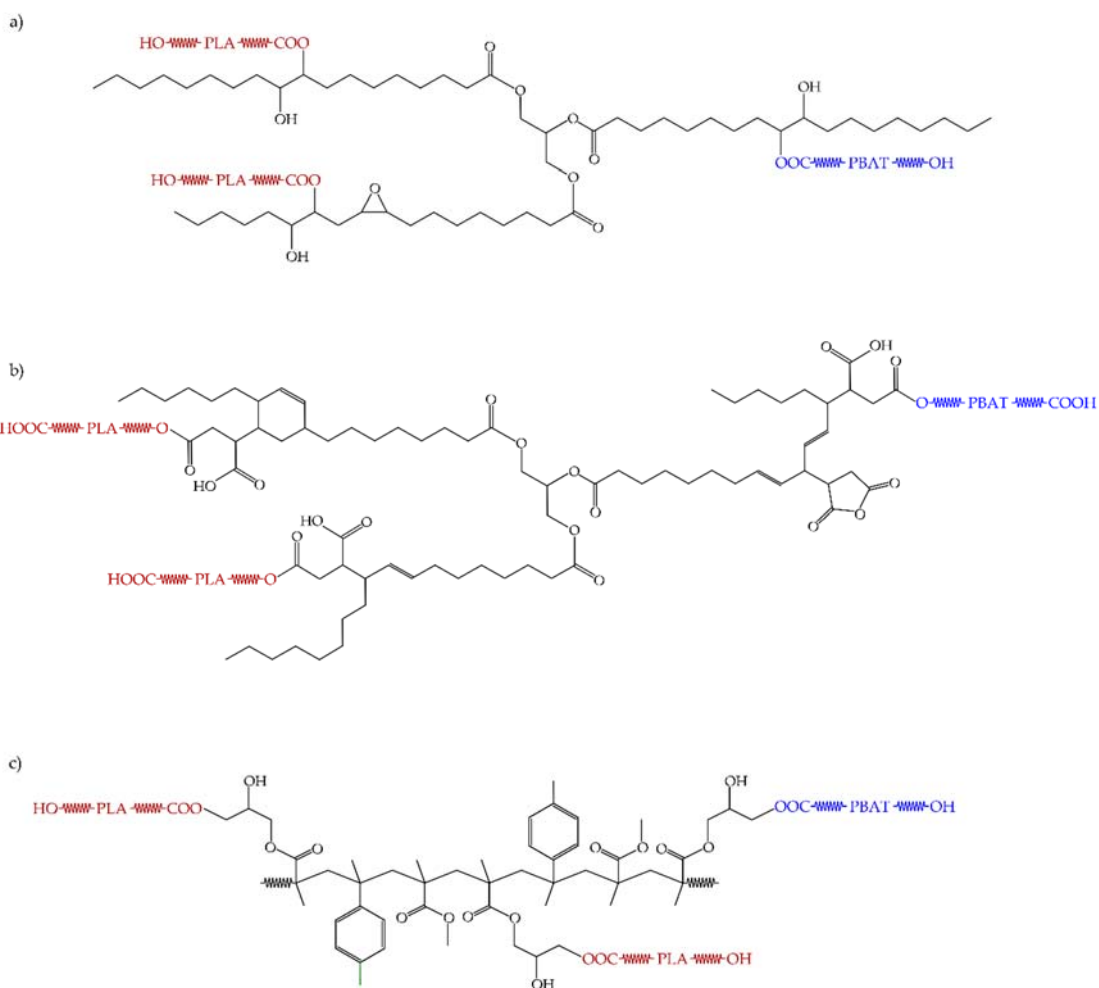


Figure IV.5.3. Schematic representation of a) ECSO compatibilized PLA/PBAT blend, b) MCSO compatibilized PLA/PBAT blend and c) Joncrys®-compatibilized PLA/PBAT blend.

Effect of compatibilizers on morphology of PLA/PBAT films.

The addition of 7.5 wt% ECSO does not provide any improvement on mechanical ductile nor mechanical resistant properties. Nevertheless, PLA/PBAT blend compatibilized with 7.5 wt% MCSO offers the maximum elongation at break of all developed formulations, reaching values of 123.0% without compromising in a remarkable way other mechanical resistant properties such as modulus and tensile strength. **Figure IV.5.4** shows some evidences of the compatibilizing effect of the different additives used in this study. It has been reported that PLA/PBAT system can show miscibility, partial miscibility or even, immiscibility [44] with 20 wt% PBAT.

As it can be observed in **Figure IV.5.4[b]**, PLA/PBAT does not show the typical droplet-like structure of immiscible polymer blends but DSC and DMA results suggest poor miscibility as it will be discussed later. It is possible to expect that PBAT-rich domains are very small. On the other hand, neat PLA (**Figure IV.5.4[a]**) shows a smooth surface typical of a brittle fracture. Addition of 1 wt% of the different compatibilizers provides some differences. The PLA/PBAT blend compatibilized with 1 wt% ECSO (**Figure IV.5.4[d]**) shows a smooth fracture surface similar to that of the PLA/PBAT blend and some small spherical domains can be detected, while PLA/PBAT blends compatibilized with Joncryl® or MCSO show presence of cavities/voids and filaments in the longitudinal (extrusion) direction. Phase separation has been reported for vegetable oil-derived additives over 5 wt% as small spherical domains due to excess plasticizer/compatibilizer [45].

Nevertheless, the PLA/PBAT system shows a heterogeneous fracture surface, even for the ECSO- and MCSO-compatibilized blends with 7.5 wt% compatibilizer (**Figure IV.5.4[f] & [g]**) which suggests phase separation as well. Despite this, the fracture surface of the ECSO-compatibilized PLA/PBAT blend (**Figure IV.5.4[f]**) shows high heterogeneity which can be related to phase separation while the MCSO-compatibilized blend (**Figure IV.5.4[g]**), offers a more homogeneous fracture surface which could be responsible for the maximum elongation at break achieved.

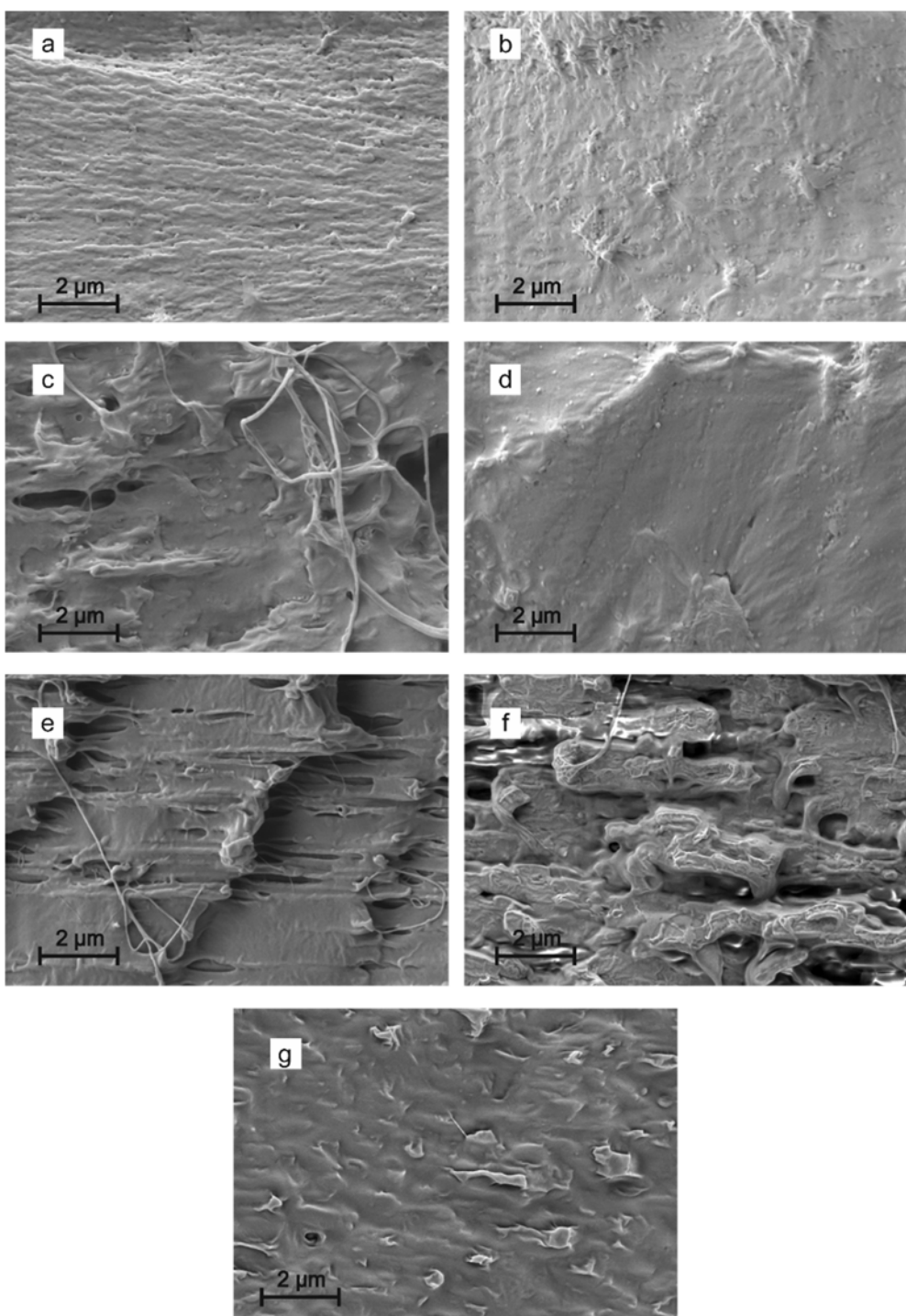


Figure IV.5.4. FESEM images of the cryofractured films at 10000x, a) neat PLA b) uncompatibilized PLA/PBAT c) PLA/PBAT (80/20 wt/wt) compatibilized with 1 wt% Joncryl®, d) PLA/PBAT (80/20 wt/wt) compatibilized with 1 wt% ECSO e) PLA/PBAT (80/20 wt/wt) compatibilized with 1 wt% MCSO, f) PLA/PBAT (80/20 wt/wt) compatibilized with 7.5 wt% ECSO and g) PLA/PBAT (80/20 wt/wt) compatibilized with 7.5 wt% MCSO.

Effect of compatibilizers on thermal properties of PLA/PBAT films.

Figure IV.5.5 shows the DSC profiles of the neat polymers, namely PLA and PBAT during the second heating stage, while **Figure IV.5.6** gathers the comparative DSC thermograms of PLA/PBAT blends without and with several compatibilizers.

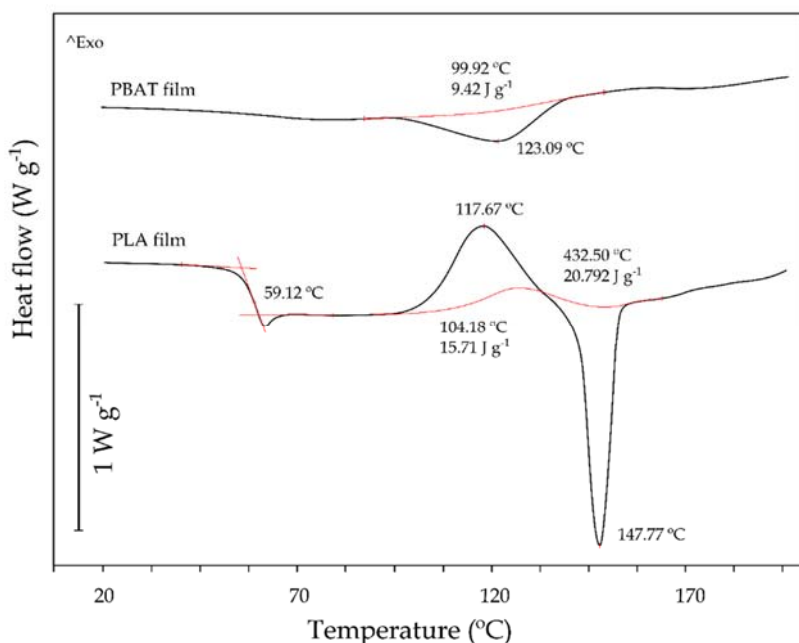


Figure IV.5.5. Differential scanning calorimetry (DSC) thermograms for neat PLA and PBAT.

The glass transition temperature (T_g) of neat PLA can be clearly observed in **Figure IV.5.5** as a step in the base line located at 59.1 °C. The glass transition temperature of PBAT cannot be observed in the temperature range covered by the DSC temperature program as it is located below room temperature. With regard to the melt peak temperature, PLA and PBAT melt at 147.8 °C and 123.1 °C respectively. In addition, PLA shows a cold crystallization (endothermic peak) between the T_g and the melt process, with a peak temperature (T_{cc}) located at 117.7 °C. The glass transition temperature for PBAT was determined by DMA and was -22.9 °C.

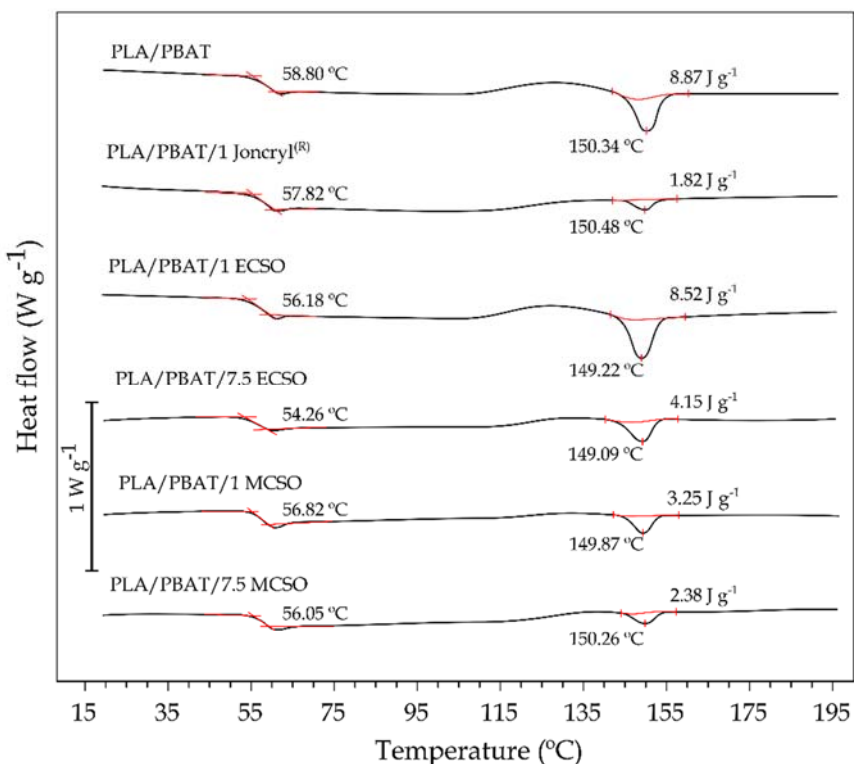


Figure IV.5.6. Comparative plot of the DSC thermograms of uncompatibilized PLA/PBAT blend (80/20 wt/wt) and the same blend compatibilized with different amounts of Joncrys®, ECSO and MCSO.

Some miscibility between PLA and PBAT polymer chains can be expected as the T_g for the uncompatibilized blend is slightly lower (58.8 °C). In a similar way, the study by Mohamed A. Abdelwahab *et al.* revealed poor miscibility between these two polymers as indicated by DSC characterization. In particular, they only observed a decrease in the T_g of neat PLA of 0.25 °C for a PLA/PBAT blend containing 30 wt% PBAT [46]. The addition of all three compatibilizers, whatever their amount, led to an additional decrease in T_g . In the case of Joncrys®, addition of 1 wt% to the PLA/PBAT blend led to a decrease of almost 1.3 °C as obtained by DSC. Mohamed A. Abdelwahab *et al.* reported negligible changes in T_g in PLA/PBAT blends with 20 wt% organosolv lignin (OL) and different Joncrys® loading [46].

With regard to the vegetable oil-derived compatibilizers, it has been proved that their plasticization effects are not as pronounced as typical primary plasticizers. Nevertheless, vegetable-oil derived compatibilizers exert a dual function: on one hand, they promote chain extension due to reaction of epoxide rings or maleic anhydride groups with hydroxyl terminal groups in both PLA and PBAT polyesters. On the other hand, they contribute to compatibilization as they can react with both PLA and PBAT polymeric chains, acting as a bridge between the two immiscible (or low miscibility) polymers. Vegetable oil derivatives, with the triglyceride structure, provide increased free volume and this has a positive effect on chain mobility [35, 37]. It is, in fact, the PLA/PBAT blend with 7.5 wt% MCSO which reaches the lowest T_g values among all the formulations in this study (56.1 °C). The main advantage of vegetable oil-derived compatibilizers/plasticizers is that the elongation at break is remarkably increased but, in contrast, other mechanical resistant properties are not reduced in a great extent.

With regard to the crystallinity, it is worthy to note that neat PLA possesses a $\chi_c\%$ of 5.46%. Although it seems that the cold crystallization process decreases in the blend, it is important to remark that both the cold crystallization of PLA and the melt process of PBAT occur in a similar temperature range (see **Figure IV.5.5**). As these two energetically opposite processes are overlapped, it is not appropriate to calculate the degree of crystallinity of PLA in the uncompatibilized and compatibilized blends. It could be possible to separate these processes by using modulated signal

PLA/PBAT films were also characterized by dynamic mechanical thermal analysis (DMA). This is a more sensitive technique to obtain the T_g values and measure mechanical properties, *i.e.* storage modulus – G' and damping factor – tan δ in dynamic conditions. **Figure IV.5.7** gathers the DMA of neat PLA, PBAT and their blend (80/20 wt/wt) without and with different compatibilizers. As it can be seen, the uncompatibilized PLA/PBAT blend shows a slight decrease in T_g from 66.3 °C (neat PLA) down to 65.0 °C. This is representative for very low miscibility between the two blend components. Al-Ittry *et al.* revealed similar decrease in T_g when 20 wt% PBAT was added to PLA. Specifically, the T_g was reduced by 1 °C with regard to unblended PLA [47]. Addition of 1 wt% of the three compatibilizers used in this study led to a slight decrease in T_g of about 2 °C which indicates some compatibilizing/plasticization behavior but these two phenomena are overlapped. Once again, the highest reduction in the T_g is obtained with high vegetable oil-derived compatibilizer.

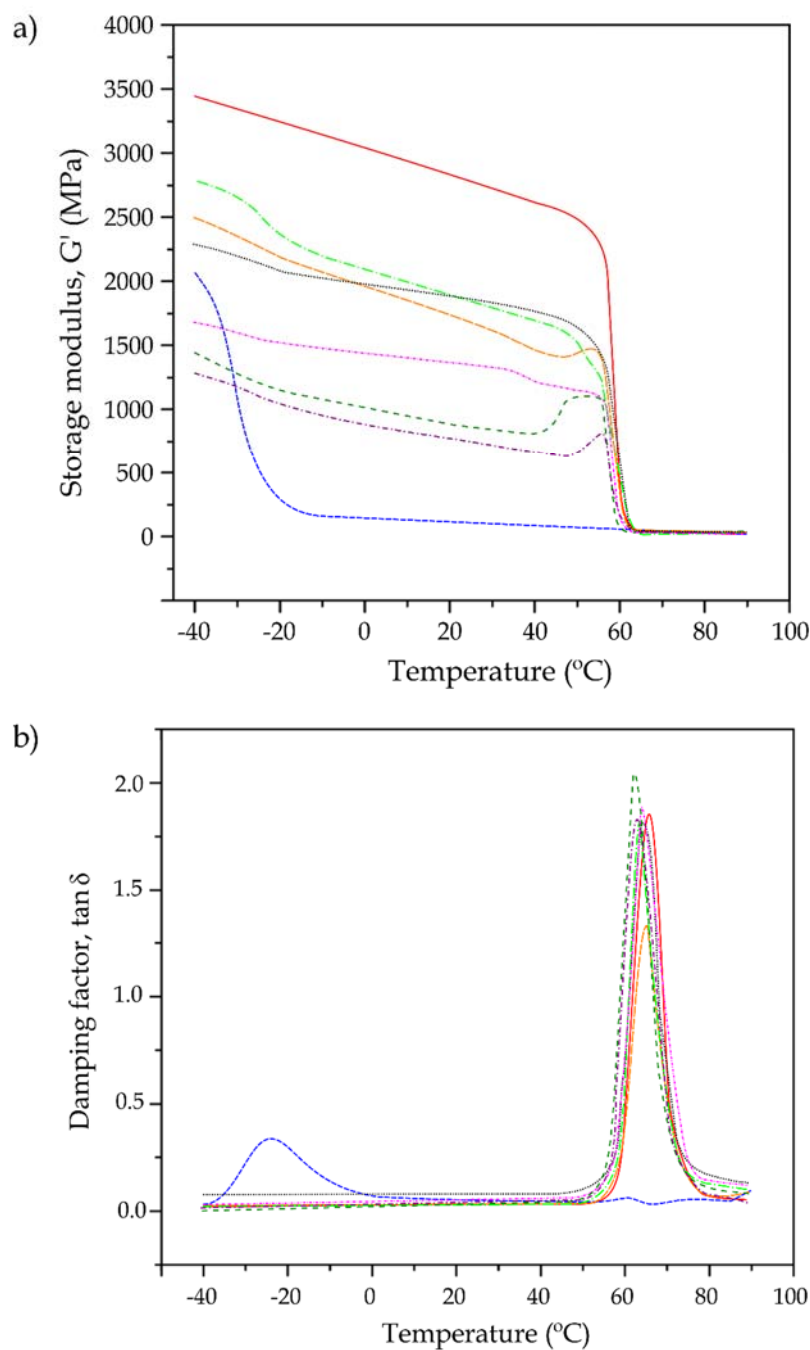


Figure IV.5.7. Plot comparison of a) storage modulus, G' and b) damping factor, $\tan \delta$ of neat PLA, PBAT and PLA/PBAT blend (80/20 wt/wt) without and with different compatibilizers. — PLA; - - - PBAT; - - - - PLA/PBAT; - · - · PLA/PBAT/1 Joncryl®; - - - - PLA/PBAT/1 ECSO; - · - · PLA/PBAT/1 MCSO; - - - - - PLA/PBAT/7.5 ECSO; - - - - - - PLA/PBAT/7.5 MCSO.

In particular, the T_g decreases down to 62.2 °C and 62.6 °C in blends with 7.5 wt% ECSO and MCSO respectively. Nevertheless, the most relevant information regarding the effect of all used compatibilizers can be observed by following the evolution of the storage modulus, G' . Neat PLA is the stiffer material with a G' value of about 2500 MPa. Obviously, neat PBAT is an extremely flexible polymer with a very low G' value at 30 °C of about 100 MPa.

With regard to the uncompatibilized PLA/PBAT blend, the G' at 30 °C is close to 1650 MPa thus showing the flexibilization effect of PBAT on PLA/PBAT blends. ECSO seems to be more reactive as the corresponding compatibilized blend with 1 wt% ECSO shows a G' value of 1750 MPa at 30 °C which is similar to the Joncrys-compatibilized blend (1800 MPa). MCSO seems to give more flexible materials with G' values at 30 °C of 1300 MPa and 950 MPa for 1 wt% and 7.5 wt% MCSO content in PLA/PBAT blends.

All these results are in total agreement with the previous mechanical properties. Although G' suggests the T_g of the PBAT rich phase (decrease in G' at about -20 °C), the corresponding damping factor peaks are not detectable. It is important to take into account that G' is plotted in a decimal scale (not logarithmic) and this change is less pronounced in a logarithmic scale.

One important issue to take into account in these formulations is their thermal stability. As it can be seen in **Figure IV.5.8**, both vegetable oil-derived additives contribute to an improvement on overall thermal stability while Joncrys® does not provide any relevant increase in thermal stability.

This could be related to the particular thermal stability of vegetable oils and the flexibility they provide to the compatibilized structure. In fact, one of the main uses of modified vegetable oils, is as secondary plasticizers in poly(vinyl chloride) – PVC industrial formulations as these can act as free radical scavengers thus leading to increased thermal stability. In fact, PVC is extremely sensitive to thermal degradation and presence of modified vegetable oils leads to improved thermal stability [8]. As suggested by TGA analysis, Joncrys seems to slightly decrease the thermal stability as it probably, cannot act as a free radical scavenger.

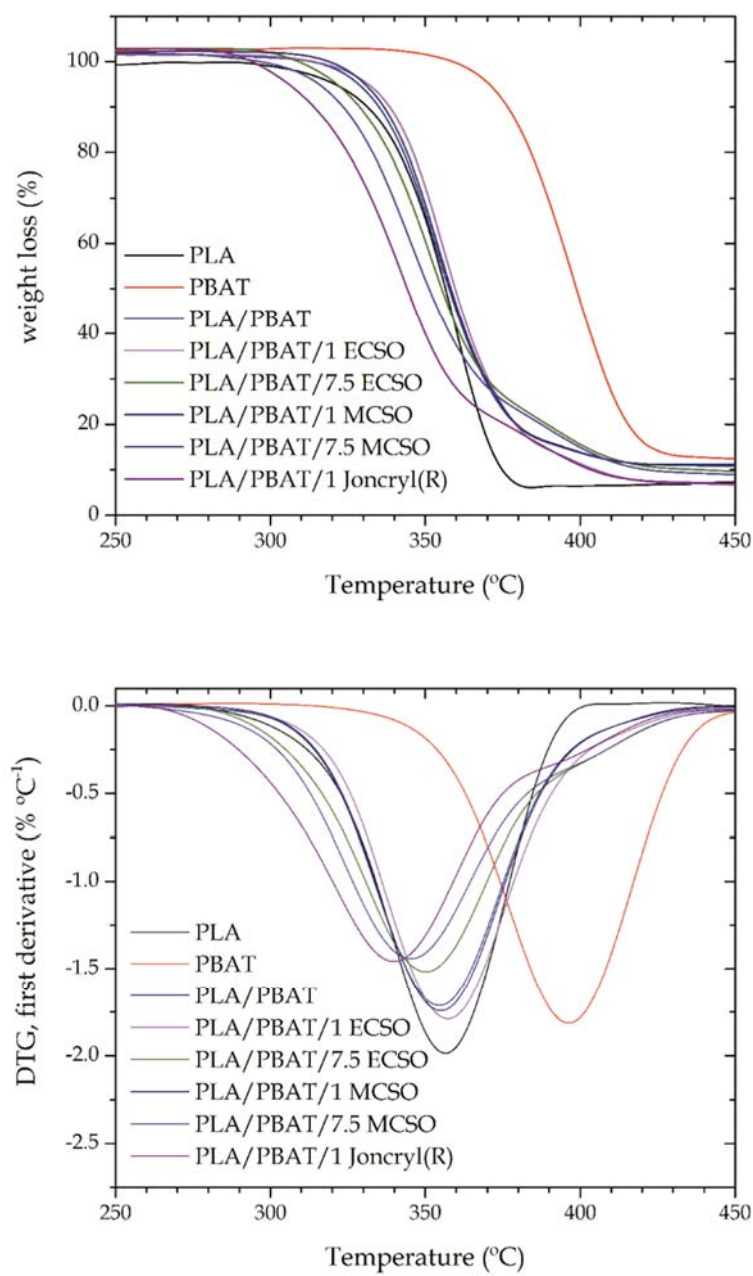


Figure IV.5.8. Comparative plot of the TGA thermograms of neat PLA, PBAT and PLA/PBAT blend (80/20 wt/wt) without and with different compatibilizers, a) TGA and b) first derivative DTG.

The main parameters obtained by TGA analysis are summarized in **Table IV.5.2** with the temperature values corresponding to 5 wt% and 50 wt% loss, $T_{5\%}$ and $T_{50\%}$ respectively.

Table IV.5.2. Summary of the main results of the thermal degradation of neat PLA, PBAT and PLA/PBAT blend (80/20 wt/wt) without and with different compatibilizers.

Code	TGA	
	T_{5%} (°C)	T_{50%} (°C)
PLA	321.2	356.6
PBAT	370.9	398.7
PLA/PBAT	328.2	357.8
PLA/PBAT/1 ECSO	331.7	359.8
PLA/PBAT/7.5 ECSO	321.5	355.3
PLA/PBAT/1 MCSO	330.5	358.3
PLA/PBAT/7.5 MCSO	315.7	351.3
PLA/PBAT/1 Joncrys	305.9	344.1

As it can be seen, the simple addition of PBAT in the uncompatibilized blend, gives increased thermal stability. The onset degradation temperature, measured at 5 wt% loss, changes from 321.2 °C up to 328.2 °C. Similar findings were reported by Xiang Lu *et al.* that observed an increase of 11.2 °C in thermal stability of PLA with addition of 30 wt% PBAT [48]. It is also worthy to note the additional stabilization that ECSO and MCSO provides with T_{5%} values over 330 °C – 331 °C with 1 wt% ECSO or MCSO while higher ECSO or MCSO content leads to a small decrease in thermal stability, probably due to a plasticizer excess. This behavior has been reported previously with other vegetable oil-derived compatibilizers/plasticizers [49, 50]. Similar trend can be seen for T_{50%}. With regard to Joncrys®, it leads to small decrease in thermal stability.

Effect of compatibilizers on surface and disintegration properties of PLA/PBAT films.

The wetting properties of the herein developed materials was determined by contact angle measurements. **Table IV.5.3** shows the water contact angle obtained on PLA, PBAT and their compatibilized and uncompatibilized blend. PLA shows an average contact angle of 66.4° which is lower than typical polyolefins, *i.e.* poly(ethylene) – PE, poly(propylene) – PP, with contact angles close to 90° [51, 52]. With regard to PBAT, due to its chemical structure, its water contact angle is located at 53.9°. Addition of all three compatibilizers at a fixed composition of 1 wt%, provides increased hydrophobicity

as the water contact angle increases up to values of about 71° for Joncrys® and 75° for ECSO and MCSO. Hydrophobicity is an interesting property in films so that, all three compatibilizers at 1 wt% give good results. Nevertheless, blends with 7.5 wt% of both ECSO and MCSO show a decrease in hydrophobicity (lower water contact angle values of about 63° and 56° respectively). This could be related to phase separation at high vegetable oil content. Finely dispersed droplets of ECSO and MCSO could play an important role in reducing hydrophobicity due to their functionality [53]. **Table IV.5.3** also summarizes the luminance (L^*) which is a direct measurement of the transparency. Neat PLA film shows the highest transparency, with a L^* of 99.4%. All the developed formulations show high luminance, thus indicating very low effects on transparency.

Table IV.5.3. Summary of some surface properties, *i.e.* water contact angle and luminance (L^*) for neat PLA, PBAT and PLA/PBAT blend (80/20 wt/wt) without and with different compatibilizers.

Code	Water contact angle, θ_w (°)	Luminance (L^*)
PLA	66.4 ± 1.6	99.4 ± 0.1
PBAT	53.9 ± 1.1	98.7 ± 0.1
PLA/PBAT	66.2 ± 3.4	98.0 ± 0.3
PLA/PBAT/1 ECSO	75.6 ± 2.6	98.1 ± 0.1
PLA/PBAT/7.5 ECSO	62.7 ± 1.4	98.9 ± 0.1
PLA/PBAT/1 MCSO	74.2 ± 2.8	98.3 ± 0.2
PLA/PBAT/7.5 MCSO	56.3 ± 4.0	97.9 ± 0.1
PLA/PBAT/1 Joncrys	71.6 ± 4.1	99.1 ± 0.1

Disintegration in controlled compost soil gives interesting information about the effect of the different compatibilizers on the biodisintegration process. **Figure IV.5.9** shows in a qualitative way the evolution of the disintegration process of neat PLA, PBAT and their uncompatibilized and compatibilized blend (1 wt% Joncrys®, ECSO, MCSO). After an induction period of 11 days, relevant changes appear. Very smooth changes take place during this induction period. First changes are related to a change in PLA crystallinity due to hydrolysis as reported by Xu *et al.* [54] The luminance is directly related to the transparency. Neat PLA film shows the highest transparency while the uncompatibilized PLA/PBAT shows decreased transparency (and decreased luminance as seen in **Table IV.5.3**).

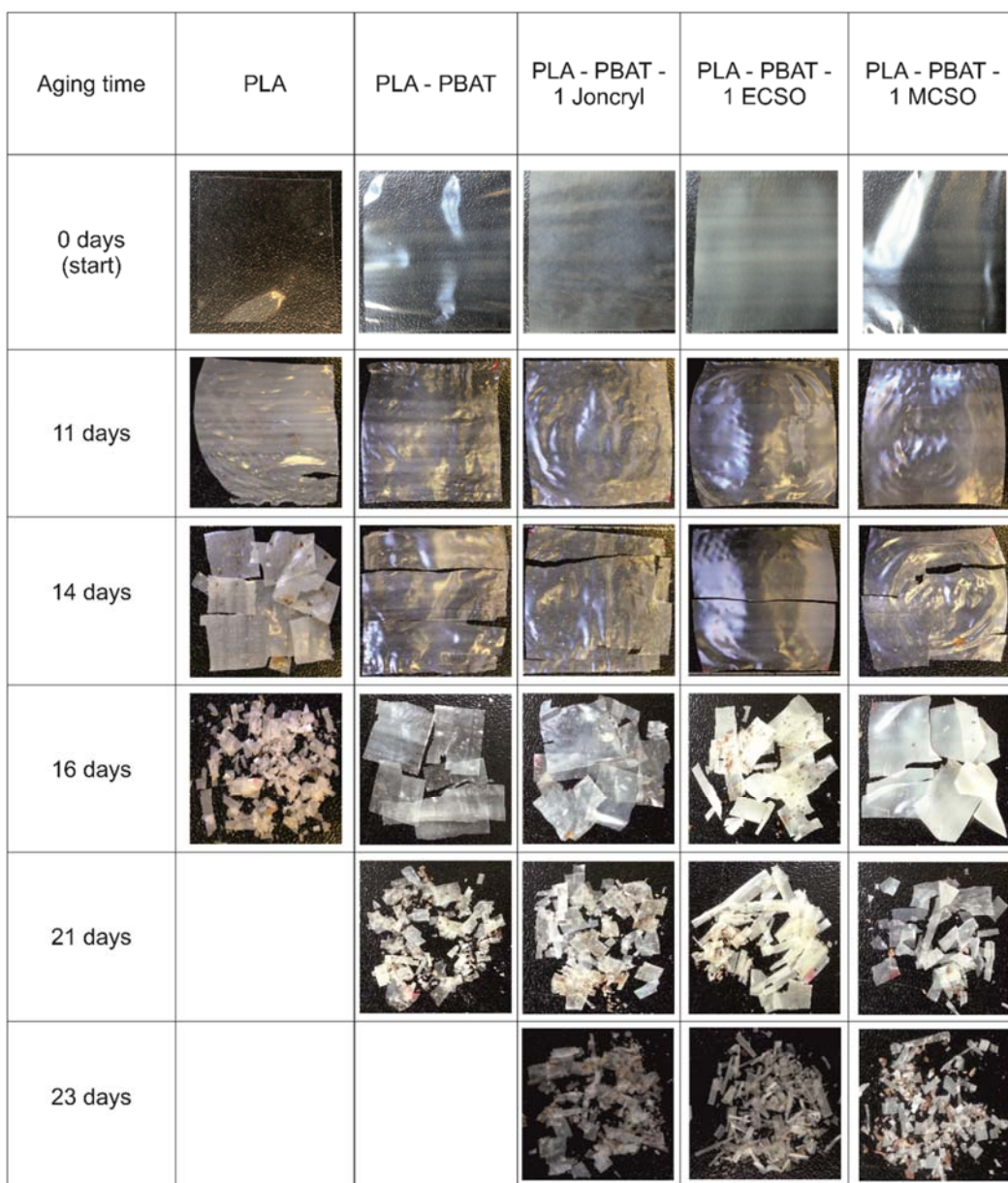


Figure IV.5.9. Qualitative assessment of the disintegration in controlled compost soil of neat PLA, PBAT and PLA/PBAT blend (80/20 wt/wt) without and with 1 wt% different compatibilizers.

Both ECSO and MCSO contribute to slightly lower transparency and, consequently, the change in luminance is very small. Although Joncryl compatibilized film could seem to be less transparent than ECSO and MCSO compatibilized blend films, it is important to remark that luminance values were obtained as average values of a

series of measurements in different parts while images in **Figure IV.5.9** are individual pictures.

It can be seen that PBAT delays the disintegration process since first signs of disintegration appears at 14 days whilst neat PLA is highly degraded at the same period. PBAT degradation rate is much higher than that of PLA. Ramin *et al.* reported an incubation time of 45 days on PBAT films which is noticeably higher than that of PLA [55]. It is worthy to note that PLA is almost disintegrated at 16 days and all other formulations (uncompatibilized and compatibilized PLA/PBAT blends) degrade at 26 days. Although it has been reported that MCSO can lead to a reduction of the induction time in neat PLA [37], the herein developed blends show higher induction time due to presence of PBAT and a combination of different reactions with the compatibilizers, *i.e.* chain extension, branching and crosslinking, all those having an effect on delaying the disintegration time.

IV.5.4. Conclusions.

This work assesses the potential of vegetable oil-derived additives as compatibilizers in PLA/PBAT blends containing 20 wt% PBAT. The only addition of PBAT to PLA gives increased elongation at break due to the high flexibility of PBAT. Nevertheless, poor miscibility between PLA and PBAT was observed by FESEM and confirmed by a very low decrease in the glass transition temperature of neat PLA. Compatibilization with epoxidized cottonseed oil (ECSO) and maleinized cottonseed oil (MCSO), gave a remarkable increase in elongation at break without compromising other mechanical resistant properties. In fact, the compatibilized blend with 7.5 wt% MCSO gives the best results in terms of balanced mechanical ductile and resistant properties, even better than those provided by an epoxy styrene-acrylic oligomer (Joncryl®) widely used as chain extender and/or compatibilizer. The plasticization effect of the different compatibilizers is restricted as the glass transition temperature, T_g , is not reduced in a great extent. Besides, the transparency of the films is not highly affected by the presence of the different additives. With regard to the disintegration process, PBAT delays the overall disintegration period due to its low disintegration rate. Both ECSO and MCSO do

not have a relevant effect on overall disintegration but they contribute positively to improve the thermal stability as revealed by thermogravimetry. Use of vegetable oil-derived compatibilizers (epoxidized and maleinized vegetable oils) stands out as an environmentally friendly solution to improve miscibility of polyester-type blends with excellent balance on mechanical and thermal properties.

Acknowledgements.

This work was supported by the Ministry of Economy and Competitiveness (MINECO) (grant number MAT2017-84909-C2-2-R). A. Carbonell-Verdu wants to thank Universitat Politècnica de València for financial support through an FPI grant.

References.

- [1] n.-I. GmbH, *Market study and database on bio-based polymers in the world: capacities, production and applications: Status quo and trends towards 2020*. <http://bio-based.eu/top-downloads/>.
- [2] E. Castro-Aguirre, F. Iñiguez-Franco, H. Samsudin, X. Fang, R. Auras, "Poly(lactic acid)-mass production, processing, industrial applications, and end of life", Advanced Drug Delivery Reviews (2016) **107**, 333-366.
- [3] M.P. Arrieta, E. Fortunati, F. Dominici, E. Rayon, J. Lopez, J.M. Kenny, "PLA-PHB/cellulose based films: Mechanical, barrier and disintegration properties", Polymer Degradation and Stability (2014) **107**, 139-149.
- [4] W. Yang, E. Fortunati, F. Dominici, G. Giovanale, A. Mazzaglia, G.M. Balestra, J.M. Kenny, D. Puglia, "Synergic effect of cellulose and lignin nanostructures in PLA based systems for food antibacterial packaging", European Polymer Journal (2016) **79**, 1 - 12.
- [5] E. Aydin, J.A. Planell, V. Hasirci, "Hydroxyapatite nanorod-reinforced biodegradable poly(l-lactic acid) composites for bone plate applications", Journal of Materials Science: Materials in Medicine (2011) **22**, 2413-2427.
- [6] G.A. Baig, C.M. Carr, "Surface and structural damage to PLA fibres during textile pretreatments", Fibres & Textiles in Eastern Europe (2016) **24**, 52-58.
- [7] M.D. Samper, E. Fages, O. Fenollar, T. Boronat, R. Balart, "The potential of flavonoids as natural antioxidants and UV light stabilizers for polypropylene", Journal of Applied Polymer Science (2013) **129**, 1707-1716.
- [8] O. Fenollar, D. Garcia-Sanoguera, L. Sanchez-Nacher, J. Lopez, R. Balart, "Effect of the epoxidized linseed oil concentration as natural plasticizer in vinyl plastisols", Journal of Materials Science (2010) **45**, 4406-4413.

- [9] J.M. Ferri, M.D. Samper, D. García-Sanoguera, M.J. Reig, O. Fenollar, R. Balart, "Plasticizing effect of biobased epoxidized fatty acid esters on mechanical and thermal properties of poly(lactic acid)", Journal of Materials Science (2016) **51**, 5356-5366.
- [10] V. Fombuena, L. Sanchez-Nacher, M.D. Samper, D. Juarez, R. Balart, "Study of the properties of thermoset materials derived from epoxidized soybean oil and protein fillers", Journal of the American Oil Chemists Society (2013) **90**, 449-457.
- [11] H. Xu, K.H. Adolfsson, L. Xie, S. Hassanzadeh, T. Pettersson, M. Hakkarainen, "Zero-dimensional and highly oxygenated graphene oxide for multifunctional poly(lactic acid) bionanocomposites", Acs Sustainable Chemistry & Engineering (2016) **4**, 5618-5631.
- [12] H. Xu, Y. Bai, L. Xie, J. Li, M. Hakkarainen, "Heat-resistant and microwaveable poly(actic acid) by quantum-dot promoted stereocomplexation", Acs Sustainable Chemistry & Engineering (2017) **5**, 11607-11617.
- [13] H. Xu, L. Xie, J. Li, M. Hakkarainen, "Coffee grounds to multifunctional quantum dots: extreme nanoenhancers of polymer biocomposites", Acs Applied Materials & Interfaces (2017) **9**, 27972-27983.
- [14] H. Xu, G.-J. Zhong, Q. Fu, J. Lei, W. Jiang, B.S. Hsiao, Z.-M. Li, "Formation of shish-kebabs in injection-molded poly(l-lactic acid) by application of an intense flow field", Acs Applied Materials & Interfaces (2012) **4**, 6773-6783.
- [15] L.T. Lim, R. Auras, M. Rubino, "Processing technologies for poly(lactic acid)", Progress in Polymer Science (2008) **33**, 820-852.
- [16] J.M. Ferri, O. Fenollar, A. Jordà-Vilaplana, D. García-Sanoguera, R. Balart, "Effect of miscibility on mechanical and thermal properties of poly(lactic acid)/ polycaprolactone blends", Polymer International (2016) **65**, 453-463.
- [17] E.d.M. Teixeira, A.A.S. Curvelo, A.C. Correa, J.M. Marconcini, G.M. Glenn, L.H.C. Mattoso, "Properties of thermoplastic starch from cassava bagasse and cassava starch and their blends with poly (lactic acid)", Industrial Crops and Products (2012) **37**, 61-68.

- [18] T. Yokohara, M. Yamaguchi, "Structure and properties for biomass-based polyester blends of PLA and PBS", European Polymer Journal (2008) **44**, 677- 685.
- [19] L. Jiang, M.P. Wolcott, J.W. Zhang, "Study of biodegradable polyactide/poly(butylene adipate-co-terephthalate) blends", Biomacromolecules (2006) **7**, 199-207.
- [20] T. Takayama, Y. Daigaku, H. Ito, H. Takamori, "Mechanical properties of bio-absorbable PLA/PGA fiber-reinforced composites", Journal of Mechanical Science and Technology (2014) **28**, 4151-4154.
- [21] M.P. Arrieta, M.D. Samper, J. Lopez, A. Jimenez, "Combined effect of poly(hydroxybutyrate) and plasticizers on polylactic acid properties for film intended for food packaging", Journal of Polymers and the Environment (2014) **22**, 460-470.
- [22] S. Muniyasamy, O. Ofosu, M.J. John, R.D. Anandjiwala, "Mineralization of poly(lactic acid) (PLA), poly(3-hydroxybutyrate-co-valerate) (PHBV) and PLA/PHBV blend in compost and soil environments", Journal of Renewable Materials (2016) **4**, 133-145.
- [23] E. Quero, A.J. Müller, F. Signori, M.-B. Coltell, S. Bronco, "Isothermal cold-crystallization of PLA/PBAT blends with and without the addition of acetyl tributyl citrate", Macromolecular Chemistry and Physics (2012) **213**, 36-48.
- [24] V. Mittal, T. Akhtar, N. Matsko, "Mechanical, thermal, rheological and morphological properties of binary and ternary blends of PLA, TPS and PCL", Macromolecular Materials and Engineering (2015) **300**, 423-435.
- [25] M.J. Garcia-Campo, L. Quiles-Carrillo, J. Masia, M.J. Reig-Perez, N. Montanes, R. Balart, "Environmentally friendly compatibilizers from soybean oil for ternary blends of poly(lactic acid)-PLA, poly(epsilon-caprolactone)-PCL and poly(3-hydroxybutyrate)-PHB", Materials (2017) **10**, 1339.
- [26] G. Kfouri, F. Hassouna, J.M. Raquez, V. Tonazzo, D. Ruch, P. Dubois, "Tunable and durable toughening of polylactide materials via reactive extrusion", Macromolecular Materials and Engineering (2014) **299**, 583-595.

- [27] Y. Yuryev, A.K. Mohanty, M. Misra, "A new approach to supertough poly(lactic acid): a high temperature reactive blending", *Macromolecular Materials and Engineering* (2016) **301**, 1443-1453.
- [28] V. Ojijo, S. Sinha Ray, R. Sadiku, "Toughening of biodegradable polylactide/poly(butylene succinate-co-adipate) blends via *in situ* reactive compatibilization", *ACS Applied Materials & Interfaces* (2013) **5**, 4266-4276.
- [29] R. Al-Ittry, K. Lamnawar, A. Maazouz, "Rheological, morphological, and interfacial properties of compatibilized PLA/PBAT blends", *Rheologica Acta* (2014) **53**, 501-517.
- [30] S. Torres-Giner, N. Montanes, T. Boronat, L. Quiles-Carrillo, R. Balart, "Melt grafting of sepiolite nanoclay onto poly(3-hydroxybutyrate-co-4-hydroxybutyrate) by reactive extrusion with multi-functional epoxy-based styrene-acrylic oligomer", *European Polymer Journal* (2016) **84**, 693-707.
- [31] C. Bureepukdee, S. Suttiruengwong, M. Seadan, *A study on reactive blending of poly (lactic acid) and poly(butylene succinate-co-adipate)*, in Global Conference on Polymer and Composite Materials. 2015, IOP Publishing.
- [32] G. Lligadas, J.C. Ronda, M. Galià, V. Cádiz, "Renewable polymeric materials from vegetable oils: a perspective", *Materials Today* (2013) **16**, 337-343.
- [33] A. Carbonell-Verdu, D. Garcia-Sanoguera, A. Jordá-Vilaplana, L. Sanchez-Nacher, R. Balart, "A new biobased plasticizer for poly(vinyl chloride) based on epoxidized cottonseed oil", *Journal of Applied Polymer Science* (2016) **133**, 43642.
- [34] J.M. Espana, M.D. Samper, E. Fages, L. Sanchez-Nacher, R. Balart, "Investigation of the effect of different silane coupling agents on mechanical performance of basalt fiber composite laminates with biobased epoxy matrices", *Polymer Composites* (2013) **34**, 376-381.
- [35] A. Carbonell-Verdu, M.D. Samper, D. Garcia-Garcia, L. Sanchez-Nacher, R. Balart, "Plasticization effect of epoxidized cottonseed oil (ECSO) on poly(lactic acid)", *Industrial Crops and Products* (2017) **104**, 278-286.

- [36] T.F. Garrison, Z.Y. Zhang, H.J. Kim, D. Mitra, Y. Xia, D.P. Pfister, B.F. Brehm-Stecher, R.C. Larock, M.R. Kessler, "Thermo-mechanical and antibacterial properties of soybean oil-based cationic polyurethane coatings: effects of amine ratio and degree of crosslinking", *Macromolecular Materials and Engineering* (2014) **299**, 1042-1051.
- [37] A. Carbonell-Verdu, D. Garcia-Garcia, F. Dominici, L. Torre, L. Sanchez-Nacher, R. Balart, "PLA films with improved flexibility properties by using maleinized cottonseed oil", *European Polymer Journal* (2017) **91**, 248-259.
- [38] J.M. Ferri, D. Garcia-Garcia, N. Montanes, O. Fenollar, R. Balart, "The effect of maleinized linseed oil as biobased plasticizer in poly(lactic acid)-based formulations", *Polymer International* (2017) **66**, 882-891.
- [39] J.M. Ferri, D. Garcia-Garcia, L. Sánchez-Nacher, O. Fenollar, R. Balart, "The effect of maleinized linseed oil (MLO) on mechanical performance of poly(lactic acid)-thermoplastic starch (PLA-TPS) blends", *Carbohydrate Polymers* (2016) **147**, 60-68.
- [40] A. Carbonell-Verdu, L. Bernardi, D. Garcia-Garcia, L. Sanchez-Nacher, R. Balart, "Development of environmentally friendly composite matrices from epoxidized cottonseed oil", *European Polymer Journal* (2015) **63**, 1-10.
- [41] L. Quiles-Carrillo, M.M. Blanes-Martinez, N. Montanes, O. Fenollar, S. Torres-Giner, R. Balart, "Reactive toughening of injection-molded polylactide pieces using maleinized hemp seed oil", *European Polymer Journal* (2018) **98**, 402-410.
- [42] L. Quiles-Carrillo, S. Duart, N. Montanes, S. Torres-Giner, R. Balart, "Enhancement of the mechanical and thermal properties of injection-molded polylactide parts by the addition of acrylated epoxidized soybean oil", *Materials & Design* (2018) **140**, 54-63.
- [43] L. Quiles-Carrillo, N. Montanes, C. Sammon, R. Balart, S. Torres-Giner, "Compatibilization of highly sustainable polylactide/almond shell flour composites by reactive extrusion with maleinized linseed oil", *Industrial Crops and Products* (2018) **111**, 878-888.
- [44] E.J. Dil, P.J. Carreau, B.D. Favis, "Morphology, miscibility and continuity development in poly(lactic acid)/poly(butylene adipate-co-terephthalate) blends", *Polymer* (2015) **68**, 202-212.

- [45] D. Garcia-Garcia, O. Fenollar, V. Fombuena, J. Lopez-Martinez, R. Balart, "Improvement of mechanical ductile properties of poly(3-hydroxybutyrate) by using vegetable oil derivatives", Macromolecular Materials and Engineering (2017) **302**, 1600330.
- [46] M.A. Abdelwahab, S. Taylor, M. Misra, A.K. Mohanty, "Thermo-mechanical characterization of bioblends from polylactide and poly(butylene adipate-co-terephthalate) and lignin", Macromolecular Materials and Engineering (2015) **300**, 299-311.
- [47] R. Al-Ittry, K. Lamnawar, A. Maazouz, N. Billon, C. Combeaud, "Effect of the simultaneous biaxial stretching on the structural and mechanical properties of PLA, PBAT and their blends at rubbery state", European Polymer Journal (2015) **68**, 288-301.
- [48] X. Lu, J.Q. Zhao, X.Y. Yang, P. Xiao, "Morphology and properties of biodegradable poly (lactic acid)/poly (butylene adipate-co-terephthalate) blends with different viscosity ratio", Polymer Testing (2017) **60**, 58-67.
- [49] D. Garcia-Garcia, J.M. Ferri, N. Montanes, J. Lopez-Martinez, R. Balart, "Plasticization effects of epoxidized vegetable oils on mechanical properties of poly(3-hydroxybutyrate)", Polymer International (2016) **65**, 1157-1164.
- [50] J.F. Balart, V. Fombuena, O. Fenollar, T. Boronat, L. Sanchez-Nacher, "Processing and characterization of high environmental efficiency composites based on PLA and hazelnut shell flour (HSF) with biobased plasticizers derived from epoxidized linseed oil (ELO)", Composites Part B-Engineering (2016) **86**, 168-177.
- [51] V. Fombuena, J. Balart, T. Boronat, L. Sanchez-Nacher, D. Garcia-Sanoguera, "Improving mechanical performance of thermoplastic adhesion joints by atmospheric plasma", Materials & Design (2013) **47**, 49-56.
- [52] K.N. Pandiyaraj, R.R. Deshmukh, A. Arunkumar, M.C. Ramkumar, I. Ruzybayev, S.I. Shah, P.G. Su, M.H. Periyah, A.S. Halim, "Evaluation of mechanism of non-thermal plasma effect on the surface of polypropylene films for enhancement of adhesive and hemo compatible properties", Applied Surface Science (2015) **347**, 336-346.
- [53] A.M. Zolali, B.D. Favis, "Partial to complete wetting transitions in immiscible ternary blends with PLA: the influence of interfacial confinement", Soft Matter (2017) **13**, 2844-2856.

- [54] H. Xu, X. Yang, L. Xie, M. Hakkarainen, "Conformational footprint in hydrolysis-induced nanofibrillation and crystallization of poly(lactic acid)", *Biomacromolecules* (2016) **17**, 985-995.
- [55] R.Y. Tabasi, A. Ajji, "Selective degradation of biodegradable blends in simulated laboratory composting", *Polymer Degradation and Stability* (2015) **120**, 435-442.

Manufacturing and compatibilization of PLA/PBAT binary blends by cottonseed oil-based derivatives

A. Carbonell-Verdu¹, J. M. Ferri¹, F. Dominici², T. Boronat^{1*}, L. Sanchez-Nacher¹, R. Balart¹, L. Torre²

¹Technological Institute of Materials (ITM), Universitat Politècnica de València (UPV), Plaza Ferrández y Carbonell 1, 03801 Alcoy, Alicante, Spain

²Dipartimento di Ingegneria Civile e Ambientale, Università di Perugia, Strada di Pentima, 4, 05100, Temi, Italy

Received 5 February 2018; accepted in revised form 1 May 2018

Abstract. This research work aims at the compatibilization of poly(lactic acid)/poly(butylene adipate-co-terephthalate), PLA/PBAT binary blends by using cottonseed oil derivatives, *i.e.* epoxidized (ECSO) and maleinized (MCSO) cottonseed oil. The potential of these vegetable oil-based compatibilizers are compared versus the effects of a conventional styrene-acrylic oligomer. The base PLA/PBAT binary blend composition was 80 wt% PLA/20 wt% PBAT and the amount of compatibilizer was set to 1 and 7.5 wt%. The effects of the different compatibilizers were evaluated on PLA/PBAT films in terms of mechanical and thermal properties as well as blend's morphology by field emission scanning electron microscopy (FESEM). Complementary, biodisintegration tests in controlled compost soil and surface properties were evaluated to assess the effects of the compatibilizers. Addition of 1 wt% ECSO and MCSO led to a remarkable increase in the elongation at break up to values over 100% with regard to neat PLA. Despite this, maximum elongation at break was obtained for the compatibilized PLA/PBAT blend with 7.5 wt% MCSO, reaching values of about 321.2% respect neat PLA keeping mechanical resistant properties, such as Young's modulus and tensile strength, at high levels. Therefore, vegetable oil-derived compatibilizers stand out as environmentally friendly additives for PLA/PBAT binary blends with improved properties.

Keywords: biopolymers, biocomposites, poly(lactic acid), cotton seed oil, maleinization

1. Introduction

Poly(lactic acid), PLA is currently considered as one of the most promising polymers from renewable resources, due to an excellent balance between mechanical properties and a competitive price day by day [1]. Nevertheless, it is intrinsically quite brittle, its chemical barrier behavior is not optimum compared to other widely used polymers, its thermal stability is also restricted and its resistance to external agents (UV radiation, moisture, etc.) are issues to overcome. For this reason, industrial PLA and other polymer formulations usually contain several additives with different purposes thus widening its use in sectors such as agriculture [2], packaging [3, 4],

medical devices [5], 3D printing, textile fibers [6]. With the aim of a sustainable development and a low environmental impact, biobased additives are been searched, *i.e.* antioxidants, plasticizers, fillers, etc. [7–10]. With the increasing development of nanotechnology, many research works have been focused of using nanostructures to improve the properties of PLA-based materials [11–13] and interactions.

Typical PLA materials are characterized by low toughness and this is one of the main drawbacks in a massive use of this biopolyester. A broad range of approaches has been observed in the last decade to minimize this effect Xu *et al.* [14] reported a new

*Corresponding author, e-mail: tboronat@dmrm.upv.es
 © BME-PT

IV.6

IV.6. Processing and characterization of environmentally friendly composites from poly(lactic acid) and cottonseed waste materials.

A. Carbonell-Verdu¹, F. Dominici², L. Torre², T. Boronat¹, L. Sánchez-Nacher¹, O. Fenollar¹

¹ **Materials Technology Institute (ITM)**
Universitat Politècnica de València (UPV)
Plaza Ferrandiz y Carbonell 1, 03801, Alcoy, Alicante (Spain)

² **Dipartimento di Ingegneria Civile e Ambientale**
Università di Perugia
Loc. Pentima Bassa, 05100 Terni (Italy)

Polymer Testing – **Submitted, July 2018**

"Processing and characterization of environmentally friendly composites from poly(lactic acid) and cottonseed waste materials"

Abstract

Environmentally friendly composites from poly(lactic acid) (PLA) and cottonseed-derived materials were successfully manufactured by extrusion, followed by injection molding. Cottonseed flour (CSF) was used as reinforcement filler and modified cottonseed oil (epoxidized and maleinized cottonseed oil, ECSO and MCSO respectively) were used to improve polymer-filler interactions. Mechanical characterization was carried out by standard tensile, flexural, impact and hardness tests while morphological characterization of the fractured surfaces was conducted by field emission scanning electron microscopy (FESEM). The main thermal transitions were obtained by differential scanning calorimetry (DSC) and the effect of both cottonseed flour and chemically-modified cottonseed oil was evaluated on dynamic mechanical behavior of the obtained composites. Unlike typical lignocellulosic fillers, 15 wt.% cottonseed flour does not lead to more brittle materials due to stress concentration phenomena. In fact, cottonseed flour provides improved elongation at break and toughness with regard to neat PLA without any other compatibilizer. Addition of both epoxidized and maleinized cottonseed (7.5 wt.%) oil positively contributes to improve ductile properties thus leading to high environmental efficiency materials with balanced mechanical properties. Specifically, the impact strength is remarkably improved which is a key factor in PLA-based composites due to the intrinsic brittleness of neat PLA.

Keywords

Poly(lactic acid); cottonseed oil; cottonseed meal; natural fillers.

IV.6.1. Introduction.

Currently, cotton industry has important economic effects in different countries. World cotton production reached 23 million tons in 2016-17 according to the data provided by the International Cotton Advisory Committee (ICAC), being China, India, USA and Pakistan the main producers, although it is grown in more than 100 countries. Obtaining cotton fiber from the raw cotton plants generates a large volume of by-products, among which, cottonseed stands out. The fiber represents between 38 – 40 wt% of the raw cotton plant, while the seeds could represent more than 60 wt%. Only less than 1 wt% of these seeds is intended for sowing, while the rest is used without any other processing for animal feeding or subjected to an oil extraction process. The oil contained in the cotton seed represents around 16 wt% while cottonseed meal stands for a 45 wt%. The rest are husk, waste and other residues. With these data it is possible to say that almost 5 million tons of cotton seed oil are produced annually [1].

Cottonseed oil is characterized by containing about 52% polyunsaturated fatty acids, mainly linoleic acid, 17% of monounsaturated fatty acids (oleic acid) and some saturated fatty acids (22% palmitic acid and 2.5% stearic acid) as well. In some countries, cottonseed oil is used for human consumption as other vegetable oils; nevertheless, several studies have revealed the potential toxicity of some of its components as it is the case of gossypol. Gossypol is a toxic compound that is present in all parts of the plant due to its efficiency against insects, as it is a natural pesticide. Thus, it is possible to find about 0.3 – 20 g gossypol per kilogram cottonseed and a part of this gossypol can be present in the extracted oil [2]. Cottonseed oil is also used in cosmetics (soaps, creams, shampoos, masks, and so on) and as insecticide and biofuel as well [3, 4]. In the recent years, the polymer industry is facing new challenges to give environmentally friendly materials. Among other, poly(lactic acid) (PLA) is, with difference, one of the most used environmentally friendly plastics. PLA can be obtained from fermentation processes of corn starch or sugar cane, for example [5-9]. It is a brittle thermoplastic polyester with good mechanical resistance and similar properties to poly(styrene) (PS). The worldwide production of PLA has increased in a remarkable way in the last few years. Today, PLA is widely used in medical devices, packaging industry, textile, agriculture, automotive, 3D printing, among others [10-14]. Several studies have reported its potential to compete with other commodity plastics but with the additional advantages of being

biodegradables (disintegrable in controlled compost soil), biocompatible and bio-sourced. To overcome its intrinsic brittleness, plasticization is an interesting approach. The most recent trends in plasticization include the use of vegetable oil-derived plasticizers with optimized interactions obtained by epoxidation, maleinization, acrylation and hydroxylation [15-20].

Epoxidized linseed oil (ELO) and epoxidized soybean oil (ESBO) have demonstrated their efficiency in plasticizing commodity plastics such as poly(vinyl chloride) (PVC) [21, 22], and biopolymers such as PLA as well [23-25]. Addition of 5 – 10 wt% ESBO to PLA lead to a remarkable increase in the elongation at break, thus giving improved toughness. In a similar way, addition of ELO promoted a slight decrease in the glass transition temperature (T_g) and provided increased toughness as well [16]. Chieng *et al.* successfully used epoxidized palm oil (EPO) as PLA plasticizer with noticeable increase in elongation at break. Al-Mulla *et al.* showed that 20% EPO addition to PLA provides an elongation at break of 210%. In addition they reported good somewhat miscibility between PLA and the modified oil [18, 19, 26]. Some other studies revealed the potential of epoxidized sunflower oil as plasticizer for PLA and thermal stabilization, with similar features to ESBO [17]. The results obtained in these investigations show that the main difference in terms of plasticization effectiveness lies in the number of oxirane rings contained in the triglyceride structure [16, 19, 23, 27]. Regarding this issue, it is worthy to note that ELO possesses around 6 epoxy rings per triglyceride molecule while ESBO and ECSO show similar oxirane oxygen content with about 4 epoxy rings per triglyceride molecule.

Epoxy modification is not the only one to give plasticization properties. Maleinization is an alternative chemical modification which can provide modified oils with interesting plasticizing effects. Maleinized linseed oil (MLO) has been successfully used to toughen P3HB which is an extremely brittle polymer. Addition of 5 phr MLO to P3HB led to an increase of 28% in elongation at break and the impact resistance was increased by 71% [28]. Ferri *et al.* reported good plasticizing effects of MLO on PLA with MLO contents in the 15 – 20 phr range, leading to an increase in elongation at break of about 80% [29, 30]. In addition to a plasticizing effect, MLO could provide a compatibilizing effect as well, as reported wood plastic composites, binary blends and other polymer systems with modified vegetable oils [31]. In a previous work, MCSO (7.5

wt%) was successfully used to toughen PLA with a noticeable increase in elongation at break of 292% without compromising the disintegration in controlled compost soil [32].

One interesting approach to upgrade lignocellulosic wastes (from agroforestry or from food industry). In the last years, wood plastic composites (WPC) and natural fiber reinforces plastics (NFRP) have become a green alternative to give high environmental efficiency materials. WPC and NFRP consist on a polymer matrix with a lignocellulosic reinforcement filler such as natural fibers (flax, hemp, flax, kenaf, among others), wood flour or lignocellulosic wastes from different industries [7, 33-37]. Currently, cottonseed flour is used as protein supply for animal feeding but its lignocellulosic nature converts into a valuable filler for green composites [38-40].

The aim of this work is to compare the effects of two cottonseed oil-derivatives, namely epoxidized linseed oil (ELO) and maleinized cottonseed oil (MCSO) on mechanical, thermal and thermomechanical properties of PLA filled with cottonseed flour to give high environmentally friendly composite materials. In this way, in addition to cotton fiber, which is the main product of the cotton industry, new interesting uses are given to seeds to obtain modified vegetable oils and lignocellulosic fillers, thus leading to sustainable materials.

IV.6.2. Experimental.

■ Materials.

The base polymer for composites was a PLA commercial grade Ingeo Biopolymer 6201D from Nature Works LLC (Minnetonka, USA). This grade is suitable for injection molding as its melt flow index is comprised between 15 – 30 g/10 min (measured at 210 °C). Its density is 1.24 g cm⁻³.

Cottonseed meal was obtained as a waste during oil extraction. The oil extraction process was carried out in a Rinaldini Oil Press (Perugia, Italy) with a maximum power of 5 kW, by mechanical methods and the obtained solid residue was dried, grinded in a Bosch MKM-6000 and, subsequently, sieved to a maximum particle size of 100 µm (see **Figure IV.6.1**).

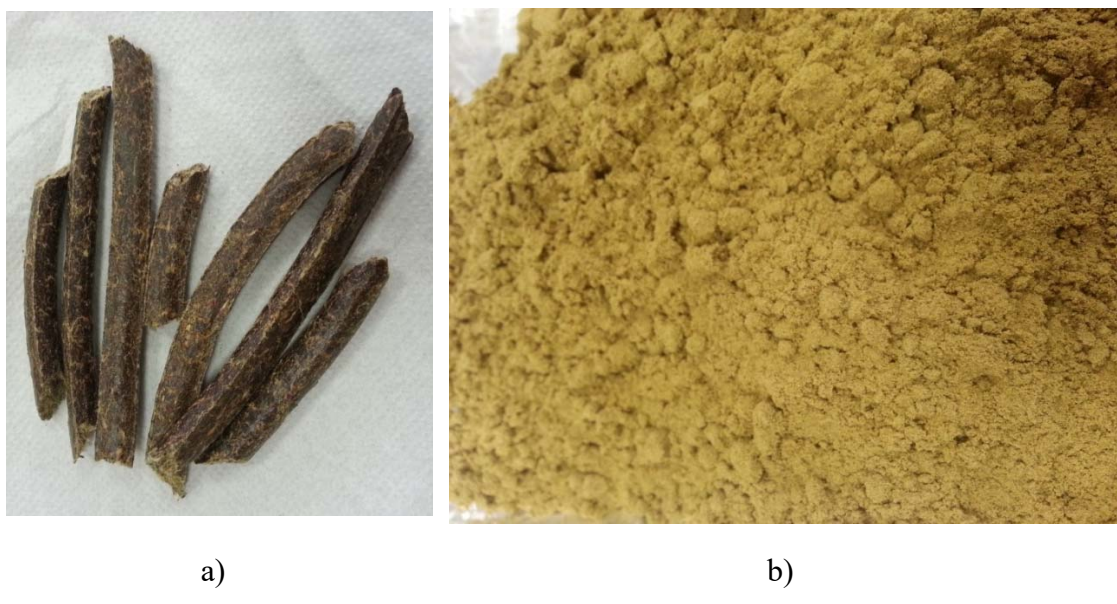


Figure IV.6.1. Images of a) the waste generated during the cold press extraction of cottonseeds and b) micronized cottonseed waste after milling and sieving.

Cottonseed oil (CO) was purchased from Sigma Aldrich (Madrid, Spain) and was used as the base vegetable oil for two different chemical modifications, *i.e.* epoxidation and maleinization. This oil possesses an iodine index between 109 – 120 and a density of 0.92 g cm⁻³. Cottonseed oil was subjected to epoxidation with hydrogen peroxide and acetic acid as reported previously, reaching an oxirane oxygen index of 5 after 8 h epoxidation process [32]. With regard to maleinization process, it was carried out on raw cottonseed oil and maleic anhydride as reported previously. The acid number after the maleinization was 63.7 mg KOH g⁻¹ [41].

Figure IV.6.2 shows a schematic representation of the chemical structures of both epoxidized and maleinized cottonseed oil.



Figure IV.6.2. Schematic plot of the chemical structure of epoxidized and maleinized cottonseed oil, ECSO and MCSO respectively.

■ Sample preparation.

The cottonseed flour (CSF) was dried at 60 °C for 24 h and an additional heating at 160 °C for 15 min was applied to remove the residual moisture. PLA was dried at 50 °C for 24 h. **Table IV.6.1** summarizes the compositions and coding of the developed formulations. Premixing was carried out in a twin-screw DSC Research micro 15 equipped with three heating zones programmed at 175 °C, 175 °C and 190 °C. The formulations were subjected to a mixing cycle at 180 rpm during 3 min. After this time, the material was discharged into the mold cavity placed in a microinjection machine IM 5.5 mL from Xplore. Thus, standardized samples for characterization were obtained.

Table IV.6.1. Composition of the PLA-cottonseed composites with different loads of cottonseed oil (epoxidized-ECSO or maleinized-MCSO), and cottonseed flour (CSF).

Code	PLA (wt.%)	ECSO (wt.%)	MCSO (wt.%)	CSF (wt.%)
PLA	100	-	-	-
PLA-7.5E	92.5	7.5	-	-
PLA-7.5M	92.5	-	7.5	-
PLA-15CSF	85	-	-	15
PLA-7.5E-15CSF	77.5	7.5	-	15
PLA-7.5M-15CSF	77.5	-	7.5	15

■ Mechanical characterization.

Mechanical properties (tensile and flexural) were obtained in a universal test machine Ibertest ELIB 30 from S.A.E. Ibertest (Madrid, Spain) using a 5 kN load cell. At least five different samples were tested and the most relevant properties were averaged. Regarding tensile tests, the Young modulus (E), tensile strength (σ_t) and the elongation at break (ϵ_b) were obtained as indicated in ISO 527 at a constant crosshead speed of 5 mm min $^{-1}$. To obtain accurate values of the Young modulus, an axial extensometer from S.A.E. Ibertest was used. With regard to the flexural test, the flexural modulus (E_f) and strength (σ_f) were obtained following ISO 178 at a crosshead speed of 5 mm min $^{-1}$.

The impact strength was obtained using a 6 J Charpy's pendulum from Metrotect (San Sebastian, Spain) on un-notched and notched ("V" type notch with a radius of 0.25 mm) samples, following the guidelines of ISO197:1993.

■ Morphology characterization.

To elucidate the morphology of the developed materials, the surface of fractured samples from impact tests was observed by field emission scanning electron microscopy (FESEM) in a ZEISS ULTRA 55 microscope from Oxford Instruments (Oxfordshire, United Kingdom) at different magnifications. Prior to observation, all samples were

subjected to a sputtering process with platinum in a high vacuum EM MED020 sputter coater from Leica Microsystems (Wetzlar, Germany)

Thermal and thermomechanical characterization.

Thermal characterization of PLA-CSF composites with ECSO or MCSO was carried out by differential scanning calorimetry (DSC) in a Mettler-Toledo DSC mod. 821 (Schwerzenbach, Switzerland). A dynamic temperature program with the following sequence was used to evaluate all thermal transitions: 1st - heating cycle from 25 °C to 250 °C at 10 °C min⁻¹; 2nd – cooling cycle from 250 °C to 25 °C at -10 °C min⁻¹ and 3rd – heating cycle from 25 °C to 250 °C at 10 °C min⁻¹. All thermal cycles were performed in presence of a nitrogen atmosphere with a flow rate of 66 mL min⁻¹.

Dynamic Mechanical Analysis, DMA, in torsion mode was carried out in an oscillatory rheometer AR-G2 (TA Instruments, New Castle, EEUU) equipped with an environmental test chamber (ETC) and a special clamp system for solid samples working in torsion/shear mode. Samples sizing 40x10x4 mm³ were subjected to a temperature sweep from 30 °C to 140 °C at a heating rate of 2 °C min⁻¹, at a frequency of 1 Hz and a maximum shear deformation percentage ($\gamma\%$) of 0.1%.

IV.6.3. Results and discussion.

Mechanical properties of PLA with cottonseed derivatives

Table IV.6.2 shows a summary of the main parameters obtained by the tensile test on PLA and PLA-CSF composites with different loads of ECSO and MCSO. All materials with either ECSO or MCSO show reduced elastic modulus values with regard to neat PLA. In relation to unreinforced (CSF) PLA, an addition of 7.5 wt.% ECSO and MCSO led to elastic modulus of 3.84 GPa and 3.86 GPa respectively, which are lower than neat PLA with an elastic modulus of 4.35 GPa. This decrease in elastic modulus represents a percentage decrease of about 11%.

In a similar way, the tensile strength follows the same trend, which means a decrease with ECSO or MCSO addition. In this case, the tensile strength is reduced from 65.9 MPa for neat PLA down to values of 47.3 MPa and 58.2 MPa for plasticized PLA with ECSO and MCSO respectively. It is worthy to note that this decrease is more pronounced for ECSO than for MCSO. As expected, the ductile properties are remarkably improved. In fact, the elongation at break changes from 3.7% for neat PLA up to values close to 165% for both ECSO- and MCSO-plasticized PLA. This indicates a clear decrease in brittleness.

These results are in total agreement with those reported by Ferri *et al.* by using maleinized linseed oil (MLO) to obtain toughened PLA formulations [30]. It is important to take into account that both ECSO and MCSO provide increased ductile properties of PLA without sacrificing mechanical resistant properties in a great extent. Previous studies have concluded that epoxy groups in ECSO can react with hydroxyl terminal groups in PLA, thus leading to a chain extension effect [32, 42]. Regarding maleic anhydride groups in MCSO, some studies suggested that in addition to a chain extension effect, some branching and/or crosslinking effects could be obtained as well. These overlapping phenomena could be responsible for the good balance between mechanical resistant and ductile properties [31, 43].

Table IV.6.2. Mechanical properties, tensile modulus (E_t), tensile strength (σ_t) and elongation at break (ϵ_b), of PLA-cottonseed composites with different loads of cottonseed oil (epoxidized-ECSO or maleinized-MCSO), and cottonseed flour (CSF).

Code	E_t (MPa)	σ_t (MPa)	ϵ_b (%)
PLA	4358 ± 89	65.9 ± 2.9	3.7 ± 0.5
PLA-7.5E	3846 ± 52	47.3 ± 0.6	163.9 ± 11.9
PLA-7.5M	3860 ± 138	58.2 ± 1.4	166.3 ± 29.7
PLA-15CSF	4328 ± 64	34.4 ± 1.1	26.8 ± 1.6
PLA-7.5E-15CSF	3556 ± 66	25.8 ± 1.2	75.3 ± 9.7
PLA-7.5M-15CSF	3698 ± 76	33.9 ± 0.7	75.8 ± 3.2

On the other hand, composites with 15 wt% cottonseed flour show a decrease in the elastic modulus when both epoxidized and maleinized cottonseed oil are added to PLA/CSF composites. Uncompatibilized PLA-15CSF composites show a similar elastic modulus to neat PLA of about 4.33 GPa. Addition of ECSO and MCSO decreases elastic modulus by almost 17%. With regard to tensile strength, a similar trend can be observed. The uncompatibilized PLA-15CSF composite shows a clear decrease in tensile strength with regard to PLA with a change from 65.9 MPa down to 34.4 MPa. This is due to the poor polymer-particle interaction, thus leading to a stress concentration effect. Addition of ECSO to this composite, gives lower tensile strength values of 25.8 MPa while MCSO addition does not provide any remarkable change in tensile strength. This could be related to the fact that ECSO provides higher plasticization effects on these composites, compared to MCSO. In addition, recent research works have revealed that some modified vegetable oils used as PLA modifiers could lead to somewhat phase separation as they do not show full miscibility. This phenomenon contributes to heterogeneity and, subsequently, mechanical resistant properties (directly related to cohesion) decrease [18-20, 23].

The changes in mechanical resistant properties of PLA-CSO composites are interesting but it is worthy to note the unexpected behaviour of the ductile properties. The elongation at break (ϵ_b) for both composites with ECSO or MCSO increases up to 75% which is almost triple the value of uncompatibilized composite. Silverajah *et al.* reported a good plasticization effect of epoxidized palm oil (EPO) on PLA due to lower intermolecular forces since EPO molecules are placed between PLA chains. This has a positive effect on chain mobility and, therefore, mechanical ductile properties are improved. They also conclude that epoxy groups in EPO can readily react with terminal

hydroxyl groups in PLA, leading to a chain extension effect in combination with a plasticization effect [18, 19]. Nevertheless, as the obtained results suggest, MCSO leads to slightly better overall properties as ductile properties are remarkably improved without compromising mechanical properties such as elastic modulus and tensile strength. It is important to take into account that both epoxy and maleic anhydride chemical groups contained in ECSO and MCSO can readily react with terminal hydroxyl groups in PLA chains leading to several potential reactions, *i.e.* chain extension, branching and, even, some crosslinking, which could be responsible for maintaining the overall good properties [43, 44].

Regarding mechanical behaviour in flexural conditions, results are summarized in **Table IV.6.3**. In the same way as in the previous analysis addition of either ECSO or MCSO to PLA leads to lower flexural modulus and strength values. Regarding flexural modulus, it changes from 3.5 GPa for neat PLA down to 3.3 GPa and 3.2 GPa for PLA formulations with 7.5 wt% ECSO and MCSO. It is worthy to note that, once again, MCSO addition keeps flexural strength values at higher levels than ECSO. Neat PLA shows a flexural strength of 96.3 MPa. This is remarkably reduced down to 45.4 GPa with 7.5 wt% ECSO thus indicating a clear plasticization effect. On the other hand, addition of 7.5 wt% MCSO maintains flexural strength at relatively high values of 67.1 MPa. This could be related to a combination of plasticization and other complex processes involving branching and/or crosslinking [18].

Table IV.6.3. Flexural properties, flexural modulus (E_f) and flexural strength (σ_f), of PLA-cottonseed composites with different loads of cottonseed oil (epoxidized-ECSO or maleinized-MCSO), and cottonseed flour (CSF).

Code	E_f (MPa)	σ_f (MPa)
PLA	3494 ± 108	96.3 ± 3.14
PLA-7.5E	3300 ± 123	45.4 ± 9.62
PLA-7.5M	3198 ± 124	67.1 ± 1.49
PLA-15CSF	3750 ± 14	58.9 ± 2.55
PLA-7.5E-15CSF	2599 ± 66	28.75 ± 2.16
PLA-7.5M-15CSF	2763 ± 26	42.1 ± 1.27

With regard to PLA-CSF composites, uncompatibilized PLA-15CSF composite shows an increase in modulus up to values of 3.7 GPa. In the same way as observed for

tensile properties, addition of ECSO and MCSO to PLA-15CSF leads to lower mechanical properties. In fact, both the flexural modulus and the flexural strength are reduced down to 2.6 GPa (E_f) and 28.75 MPa (σ_f) for PLA-15CSF with ECSO and to values of 2.8 GPa (E_f) and 42.1 MPa (σ_f) the MCSO modified PLA-CSF composite.

One of the main drawbacks of PLA is its high brittleness which gives low toughness. A direct estimation of the toughness can be carried out by impact tests. **Table IV.6.4** summarizes the main results obtained through Charpy impact test as well as the Shore D hardness values of PLA formulations with cottonseed derivatives (modified oils and flour). PLA is an intrinsically brittle polymer due to its high crystallinity and this is evidenced by a relatively low energy absorption in a Charpy test. Even though impact resistance seems to be a mechanical ductile property, the real situation is that it depends on both ductile properties (deformation ability) and resistant properties (strength). For this reason, MCSO improves in a remarkable way the overall impact strength by 67% while ECSO only increases this by 18%. If we go back to Table 3, it is possible to observe that the tensile strength of PLA-7.5MCSO is higher (58.2 MPa) than the value obtained for PLA-7.5ECSO (47.3 MPa) while the elongation at break (deformation ability) is almost the same at 163 – 166%. As we can see, as impact strength depends on both values, PLA-7.5MCSO gives higher values to those of PLA-7.5ECSO, as expected. In a quantitative way, the impact strength of neat PLA (26.8 kJ m⁻²) is slightly increased up to 31.6 kJ m⁻² with the addition of 7.5 wt% ECSO while the addition of the same amount of MCSO leads to a remarkable increase in impact strength up to values of 44.8 kJ m⁻². These results are in total accordance with the previous tensile and flexural characterization as MCSO contributes to balanced mechanical ductile and resistant properties [43].

On the other hand, as typical in a filled polymer, the addition of 15 wt% CSF leads to an embrittlement due to stress concentration phenomena. The impact strength is reduced down to 18.4 kJ m⁻² which represents a percentage decrease of about 31% with regard to neat PLA. Typically, lignocellulosic particles embedded in a polymer matrix provide an embrittlement phenomenon as these particles are randomly dispersed into the matrix with poor polymer-particle interactions. It is necessary to remark the high hydrophilic nature of the lignocellulosic filler which is opposite to the high hydrophobicity of the polymer matrix. This difference in polarity is responsible for poor particle-matrix interactions which, in turn, reduce material cohesion with a negative

effect on toughness. Addition of both modified vegetable oils provide an interesting behaviour against impact with a remarkable increase in toughness regarding the uncompatibilized composite. In fact, MCSO addition to PLA-15CSF provides impact strength values of almost 30 kJ m^{-2} which are even higher than those of neat PLA. But if we consider the nature of these composites, the results are very promising as both ECSO and MCSO counteract the embrittlement produced by the cottonseed flour. Some recent works of Balart *et al.* concluded that modified vegetable oils and, in particular, epoxidized linseed oil (ELO), can give a dual effect on PLA-lignocellulosic filler composites. On one hand, a clear plasticization is observed and on the other hand, a compatibilizing effect between the highly hydrophilic lignocellulosic particles and the highly hydrophobic matrix can be obtained. This could be possible though reaction of epoxy groups with hydroxyl groups contained in both PLA terminal chains and cellulose thus leading to a partial compatibilization [27, 34, 35, 45].

Table IV.6.4. Impact strength by Charpy impact test and Shore D hardness of PLA-cottonseed composites with different loads of cottonseed oil (epoxidized-ECSO or maleinized-MCSO), and cottonseed flour (CSF).

Code	Impact strength (kJ m^{-2})	Shore D hardness
PLA	26.8 ± 0.31	76.3 ± 2.0
PLA-7.5E	31.6 ± 0.94	77.2 ± 0.5
PLA-7.5M	44.8 ± 1.69	78.3 ± 0.7
PLA-15CSF	18.4 ± 0.51	78.3 ± 1.1
PLA-7.5E-15CSF	21.8 ± 0.45	75.3 ± 0.6
PLA-7.5M-15CSF	29.8 ± 0.59	75.3 ± 0.3

With regard to Shore D, the obtained results do not show a remarkable change and could be included within the standard deviation itself. Nevertheless, it is worthy to highlight the unusual increase in Shore D values for PLA with 7.5 wt% ECSO or 7.5 wt% MCSO which could be related to the above-mentioned branching and/or crosslinking reactions.

As a conclusion from mechanical characterization, it is convenient to stand out the improvement on ductility that both ECSO and MCSO could provide on both neat PLA and PLA composites with 15 wt% CSF. Although the performance of both ECSO and MCSO is positive on overall properties, it is necessary to highlight the excellent

properties MCSO can provide in terms of ductility (ε_b , impact strength) and mechanical resistant properties (E_t , σ_t , E_f , σ_f , HSD), as well. This superior effect on mechanical performance could be attributed to reaction of terminal hydroxyl groups in PLA with epoxy ring (in ECSO-based materials) and mainly with maleic anhydride (in MCSO-based materials). Although a clear plasticization effect is observed, some other overlapping reactions could lead to PLA chain-extension, branching and even, crosslinking [46].

■ Fracture morphology of PLA with cottonseed derivatives.

Analysis of the fractured samples from impact tests revealed the effect of all cottonseed derivatives on PLA formulations. **Figure IV.6.3[a] & [b]** shows the fracture surface of neat PLA. This fracture surface is smooth and homogeneous, typical of a brittle behaviour. **Figure IV.6.3[c] & [d]** shows the effect of the addition of 7.5 wt% ECSO to PLA. As evidenced in these images the fracture surface shows high density of spherical cavities/voids. These microvoids correspond to a ECSO-rich phase dispersed in the PLA matrix due to the restricted miscibility between them. Some studies have revealed that plasticizer saturation with vegetable oils ranges from 1 to 5 wt%. Nevertheless, loading over this saturation threshold can positively improve toughness due to the morphology of finely spherical domains which act as a rubber phase in high impact styrenic polymers [18, 42, 47-49]. In the same way, PLA with 7.5 wt% MCSO shows a biphasic morphology (**Figure IV.6.3[e] & [f]**). Some studies have revealed that addition of maleinized linseed oil (MLO) to PLA leads to phase separation as PLA saturation occurs at very low MLO loading. This phase separation can be observed as spherical shapes after fracture [31, 32, 43]. In both cases, the surface topography is smoother with microfibrils which indicate increased ductility.

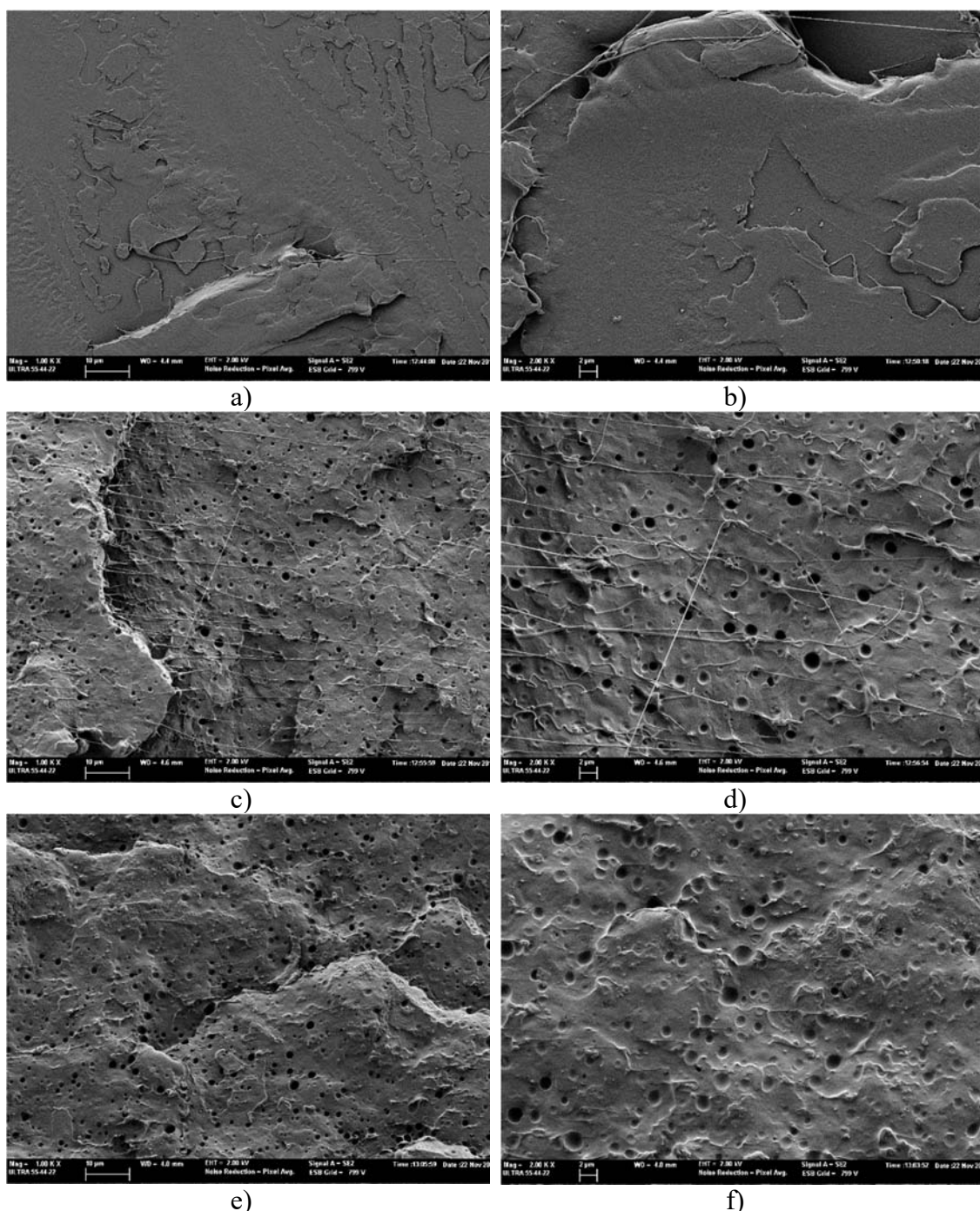


Figure IV.6.3. Field emission scanning electron microscopy (FESEM) images at different magnifications (1000x, left column and 2000x, right column) corresponding to neat PLA – a) & b), PLA with 7.5 wt.% ECSO – c) & d) and PLA with 7.5 wt.% MCSO – e) & f).

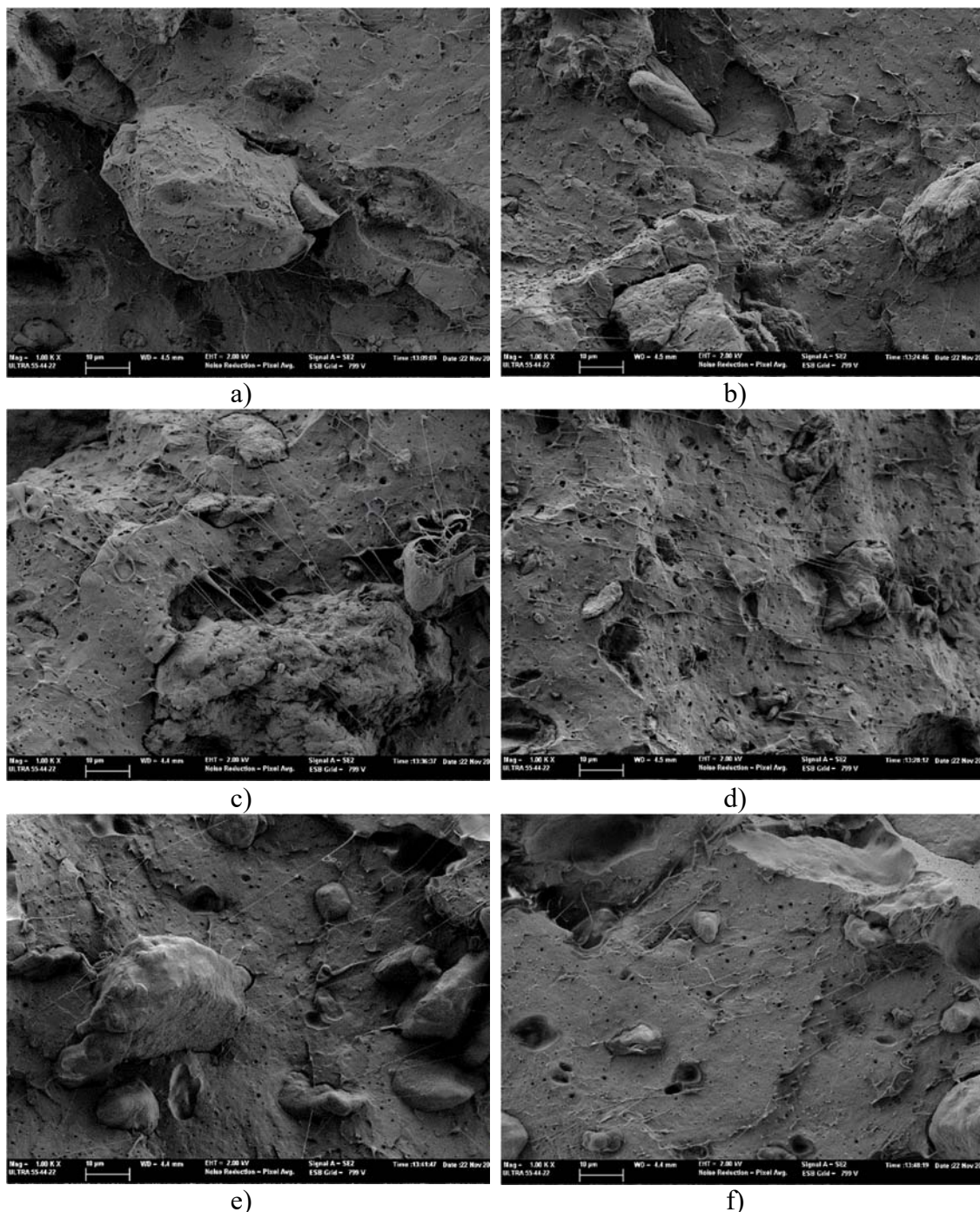


Figure IV.6.4. Field emission scanning electron microscopy (FESEM) images at 1000x corresponding to PLA composites with 15 wt.% CSF – a) & b), PLA composites with 15 wt.% CSF plus 7.5 wt.% ECSO – c) & d) and PLA composites with 15 wt.% CSF plus 7.5 wt.% MCSO – e) & f).

On the other hand, addition of 15 wt% lignocellulosic filler (CSF), gives completely different fracture morphologies. **Figure IV.6.4[a] & [b]** correspond to the uncompatibilized PLA composite with 15 wt% CSF (PLA-15CSF). The surface morphology is comprised of a smooth PLA matrix in which, relatively large CSF particles are randomly dispersed. Moreover, it is possible to observe a microgap between the CSF particle and the surrounding PLA matrix which is representative for lack (or poor) polymer-particle interaction. These microgaps contribute to break material cohesion and, subsequently, can act as stress concentrators. This morphology is in accordance with the previous mechanical results as the PLA-15CSF composite is more brittle than PLA.

Figure IV.6.4[c] & [d] shows the morphology of impact fractured PLA-15CSF composites with 7.5 wt% ECSO. The main difference regarding the uncompatibilized composite is the presence of microfibrils corresponding to a more flexible polymer matrix. In addition to this, it is important to highlight somewhat decrease of the gap between the particle and the surrounding PLA matrix which contributes to improve toughness. Similar findings can be observed for the PLA-15CSF composite with 7.5 wt% MCSO but in this case, both effects (microfibrils and gap reduction) are more accentuated. In fact, it is possible to observe full continuity between PLA matrix and embedded CSF particles. This is in total agreement with previous mechanical characterization that indicated a slightly superior effect of MCSO *versus* ECSO [44, 50].

■ Thermal and thermomechanical properties of PLA with cottonseed derivatives.

Table IV.6.5 shows the main thermal properties of PLA-based materials with cottonseed derivatives. Firstly, it is possible to see a slight plasticization effect with both ECSO and MCSO as the glass transition temperature (T_g) of neat PLA (66.7 °C) moves to lower values around 62 °C for both oils. This slight decrease indicates the restricted plasticization effect both ECSO and MCSO can provide to MLO as other primary plasticizers promote a T_g decrease of more than 15-20 °C for the same loading. On the other hand, PLA shows a cold crystallization process at 97 °C (peak) which is moved to 88 °C and 122 °C with 7.5 wt% ECSO and 7.5 wt% MCSO respectively. This is indicating

ECSO main effects is plasticization as it contributes to increase chain mobility with the subsequent decrease in both T_g and cold crystallization peak (T_{cc}). Nevertheless, the effect of MCSO is different. On one hand, we could observe some plasticization effect (slight decrease in T_g) while, on the other hand, some branching or crosslinking could be expected since the cold crystallization peak temperature is moved to higher values of 122 °C. Regarding the melt temperature (T_m), either addition of ECSO or MCSO does not change the melt process with a peak temperature located at 170 °C [50]. Both ECSO and MCSO lead to a decrease in the cold crystallization normalized enthalpies (ΔH_{cc}) which change from 20.03 J g⁻¹ for neat PLA down to values of 6.9 and 12.8 J g⁻¹ for ECSO and MCSO respectively. This suggests that the packing of PLA polymeric chains is favored by presence of modified vegetable oils as they provide increased chain mobility. Therefore, crystallite formation is favoured. By taking into account the cold crystallization normalized enthalpy (ΔH_{cc}) and the melt enthalpy (ΔH_m) it is possible to estimate the degree of crystallinity χ_c (%). As it can be seen in Table 5, addition of ECSO or MCSO into PLA gives increased crystallinity. In particular, the initial crystallinity of neat PLA (22%) increases to values around 32% for both ECSO or MCSO addition. This behaviour has been observed in previous works by Carbonell-Verdu *et al.* [32].

Table IV.6.5. Thermal properties obtained by differential scanning calorimetry (DSC) of PLA-cottonseed composites with different loads of cottonseed oil (epoxidized-ECSO or maleinized-MCSO), and cottonseed flour (CSF).

Code	T_g (°C)	T_{cc} PLA (°C)	ΔH_{cc} (J g⁻¹)	T_m (°C)	ΔH_m (J g⁻¹)	$\Delta H_m - \Delta H_{cc}$ (J g⁻¹)	χ_c (%)
PLA	66.8	97.2	20.03	169.9	39.08	19.05	22.1
PLA-7.5E	62.2	88.2	6.96	171.7	34.39	27.43	31.9
PLA-7.5M	62.0	122.3	12.84	168.4	40.43	27.59	32.07
PLA-15CSF	65.3	113.0	18.32	170.6	26.89	8.57	10.84
PLA-7.5E-15CSF	62.3	107.3	20.82	169.5	28.32	7.50	10.4
PLA-7.5M-15CSF	60.3	124.5	17.48	167.1	32.29	14.82	20.56

With regard to PLA composites with 15 wt% CSF, a negligible effect on T_g can be attributed to CSF addition (65.0 °C *versus* 66.8 °C). in the similar way, T_g values are slightly reduced by addition of ECSO or MCSO down to 62.3 °C (ECSO) and 60.3 °C (MCSO). We observe similar tendency with regard to the cold crystallization process. Once again, it seems ECSO main effect is plasticization (with a decrease of the cold

crystallization process from 113.0 °C down to 107.3 °C) while once again, MCSO provides an unusual behaviour with displacement of the cold crystallization process towards higher temperatures (124.5 °C) which could be indicating more complex interactions of MCSO with PLA. As described before, MCSO could provide a plasticization effect but, in addition, due to the high reactivity of maleic anhydride with hydroxyl groups (in terminal PLA chains and in cellulose), other overlapping process could occur, *i.e.* chain-extension, branching and crosslinking. The melt peak temperature is not highly affected by CSF and ECSO or MCSO and stands at 170 °C. Nevertheless, the finely dispersed CSF particles contribute to restriction in chain motion and, subsequently, the degree of crystallinity is reduced down to values of 10% while slightly higher crystallinity values are obtained by the addition of MCSO.

Differential scanning calorimetry is quite useful technique to evaluate all thermal transitions. Nevertheless, not all thermal transitions can be resolved equally. For example, the cold crystallization and the melt processes, which involve an enthalpy, are clearly resolved by DSC analysis. Despite this, some other thermal transitions that do not involve any enthalpy, such as the glass transition temperature are more difficult to observe or, at least, to give a precision value. For this reason, dynamic mechanical analysis (DMTA) has been carried out to clarify some unexpected behaviours detected by DSC.

Figure IV.6.5 shows the evolution of the storage modulus (G') and the damping factor ($\tan \delta$) for PLA with modified cottonseed oils (**Figure IV.6.5[a]**) and PLA-15CSF composites with modified cottonseed oils (**Figure IV.6.5[b]**). By following the evolution of the storage modulus (G') for neat PLA it is possible to observe a flat behaviour up to 50 °C when G' falls down by almost three orders of magnitude thus indicating the glass transition process. G' stabilizes at very low values and then, at about 90 °C it increases again by more than 1 fold. This increase in G' is directly related to the cold crystallization process as the packed structure is stiffer than the amorphous phase. The most important findings in **Figure IV.6.5[a]** indicate a decrease in the T_g from 65.4 °C (neat PLA) down to 61.2 °C for PLA with 7.5 wt% ECSO thus corroborating the main plasticization effect of ECSO on PLA [16, 17, 50, 51]. Nevertheless, the T_g obtained by the addition of 7.5 wt% MCSO increases up to values of 75.0 °C. These results are more coherent than those obtained by DSC for MCSO. As it has been reported by some authors, MCSO has more tendency to react with hydroxyl groups to give chain-extension,

branching and, potentially, crosslinking. All these phenomena lead to a restriction on chain mobility, with the subsequent increase in T_g and displacement of the cold crystallization process to higher temperatures. DSC revealed the displacement of the cold crystallization process towards higher temperatures but the T_g was lower (probably due to the sensitiveness of DSC to PLA T_g).

Nevertheless, DMTA reveals more coherence to the effects of ECSO and MCSO. ECSO has a main effect of plasticizing PLA and therefore, both the T_g and the cold crystallization process move to lower temperatures [42]. With regard to MCSO, in addition to plasticization, other complex reactions involving chain-extension, branching and crosslinking could overlap thus leading to a chain mobility restriction which, in turn, gives increased T_g values of 75 °C and a delayed cold crystallization process as observed in **Figure IV.6.5[a]**. With regard to PLA composites with 15 wt% CSF (Fig. 5b) similar effects can be detected.

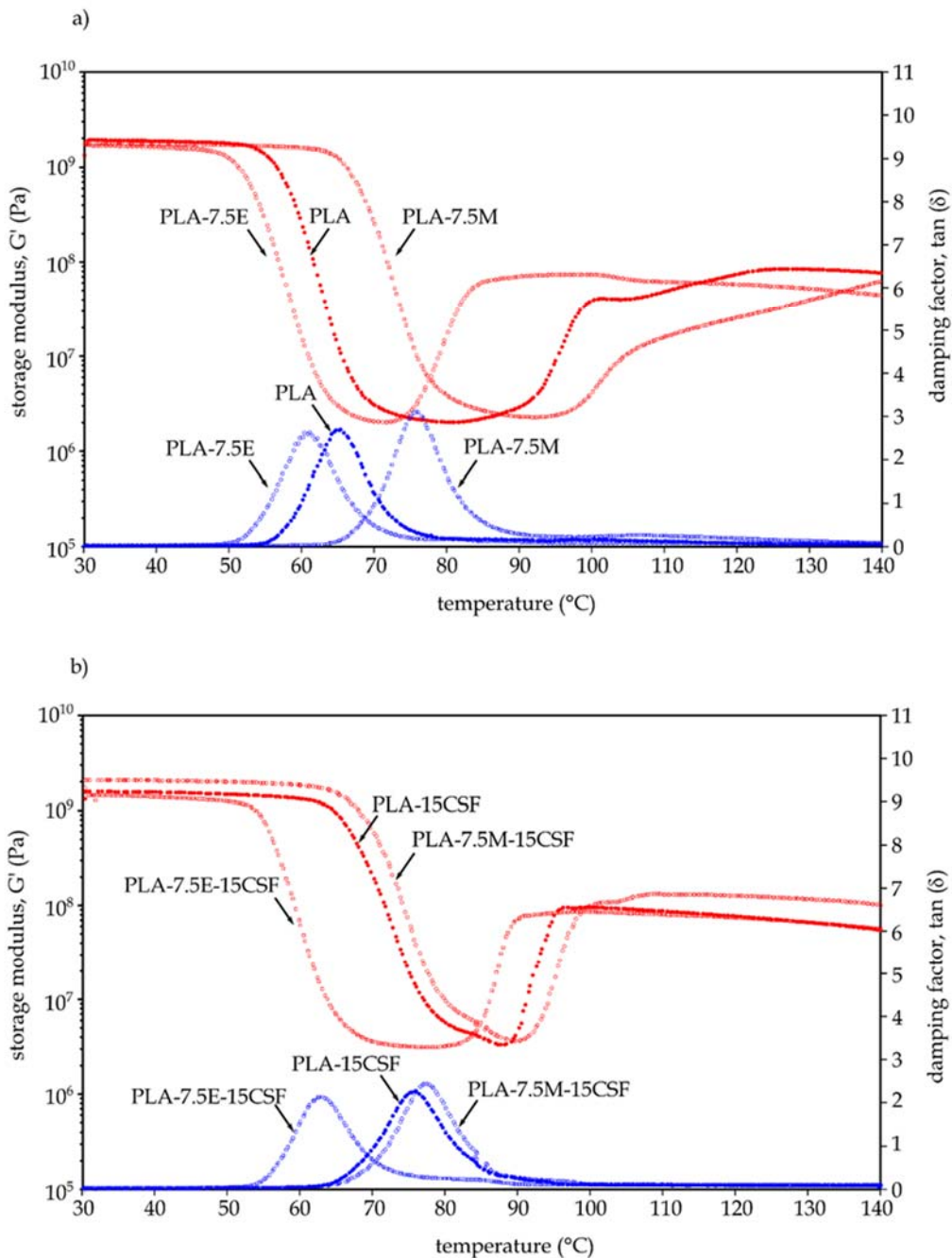


Figure IV.6.5. Plot evolution of the storage modulus, G' (red) and damping factor, $\tan \delta$ (blue) corresponding to a) PLA and PLA with 7.5 wt% ECSO and 7.5 wt% MCSO) and b) PLA composites with 15 wt% CSF with additional 7.5 wt% ECSO or 7.5 wt% MCSO.

Uncompatibilized PLA-15CSF composite shows a T_g of 76.7 °C and once again addition of 7.5 wt% ECSO leads to lowering T_g down to 63.1 °C [49], while the complex

reactions with maleic anhydride lead to an increase in T_g up to 78.0 °C [46]. As it can be seen in **Figure IV.6.5[b]**, the cold crystallization process is moved towards lower temperatures with ECSO and to higher temperatures with MCSO, thus giving coherence to the main effects of these two modified cottonseed oils. **Table IV.6.6** shows a summary of some properties obtained by DMTA characterization. It is worthy to note that the highest storage modulus, G' is obtained for the PLA composite with 15 wt% CSF and 7.5 wt% MCSO which is in total agreement with the above-mentioned overlapping reactions. It is also possible to see that the lowest G' values correspond to ECSO-containing PLA formulations, without (1.60 GPa) and with 15 wt% CSF (1.38 GPa).

Table IV.6.6. Summary of some thermomechanical properties, *i.e.* glass transition temperature (T_g) and storage modulus (G') obtained by dynamic mechanical thermal analysis (DMTA) on PLA formulations with cottonseed derivatives (CSF, ECSO and MCSO).

Code	T_g (°C) (peak tan δ)	Storage modulus, G' at 40 °C (GPa)
PLA	65.4	1.85
PLA-7.5E	61.2	1.60
PLA-7.5M	75.0	1.73
PLA-15CSF	76.7	1.67
PLA-7.5E-15CSF	63.1	1.38
PLA-7.5M-15CSF	78.0	2.04

IV.6.4. Conclusions.

This work has revealed the interesting properties of PLA-based materials with wastes coming from the cotton industry, *i.e.* cottonseed. Cottonseed meal or cottonseed flour (CSF), a by-product from oil extraction was added as a filler to PLA formulations to give high environmentally friendly wood plastic composites (WPC). On the other hand, the oil extracted by cold press from the seeds was subjected to two chemical modifications: on one hand epoxidation to obtain epoxidized cottonseed oil (ECSO) and on the other hand, maleinization to obtain maleinized cottonseed oil (MCSO). Different PLA-cottonseed derivatives were prepared by extrusion and subsequent injection

molding. PLA composites containing 15 wt% CSF showed embrittlement due to the poor particle-polymer interactions. To overcome this drawback ECSO and MCSO were added (7.5 wt%) to these composites. The main effect of ECSO is plasticization which gives increased elongation at break as well as a decrease in the cold crystallization process and the glass transition temperature (T_g). The obtained results suggest that composites with 7.5 wt% MCSO offer the best balanced properties in terms of mechanical ductile properties (impact strength, toughness, elongation at break) without compromising other mechanical properties (strength, modulus). In addition to the slight plasticization effect MCSO can provide, additional reactions between the maleic anhydride group and hydroxyl groups in both PLA and lignocellulosic filler (CSF), can take place, thus giving rise to the T_g and the cold crystallization process. PLA composites with 15 wt% CSF and 7.5 wt% MCSO represent an interesting solution from two different stand points: on one hand, cottonseeds are upgraded into high added value composite materials and, on the other hand, the bio-based content is close to 100% thus leading to high environmentally friendly materials with similar appearance to wood, with potential applications in furniture, automotive, construction and building, among others.

Acknowledgements.

This work received funding from the Ministry of Economy and Competitiveness (MINECO) (grant number MAT2017-84909-C2-2-R). A. Carbonell-Verdu wants to thank Universitat Politècnica de València for financial support through an FPI grant.

References.

- [1] J. Baffes, *Markets for cotton by-products: global trends and implications for african cotton producers.* (2010).
- [2] H.K. Knutson, L. Barregard, M. Bignami, B. Brueschweiler, S. Ceccatelli, M. Dinovi, L. Edler, B. Grasl-Kraupp, C. Hogstrand, L. Hoogenboom, C.S. Nebbia, I.P. Oswald, A. Petersen, M. Rose, A.-C. Roudot, T. Schwerdtle, C. Vleminckx, G. Vollmer, H. Wallace, J. Alexander, B. Cottrill, K. Mackay, E.P.C.F. Chain, "Presence of free gossypol in whole cottonseed", EFSA Journal (2017) **15**, 4850.
- [3] N. Hoda, "Optimization of biodiesel production from cottonseed oil by transesterification using NaOH and methanol", Energy Sources Part a-Recovery Utilization and Environmental Effects (2010) **32**, 434-441.
- [4] W.W. Song, K.B. He, J.X. Wang, X.T. Wang, X.Y. Shi, C. Yu, W.M. Chen, L. Zheng, "Emissions of EC, OC, and PAHs from cottonseed oil biodiesel in a heavy-duty diesel engine", Environmental Science & Technology (2011) **45**, 6683-6689.
- [5] M.L. Sanyang, S.M. Sapuan, M. Jawaid, M.R. Ishak, J. Sahari, "Development and characterization of sugar palm starch and poly(lactic acid) bilayer films", Carbohydrate Polymers (2016) **146**, 36-45.
- [6] S. Perinovic, B. Andricic, M. Erceg, "Thermal properties of poly(L-lactide)/olive stone flour composites", Thermochimica Acta (2010) **510**, 97-102.
- [7] T. Mukherjee, N. Kao, "PLA based biopolymer reinforced with natural fibre: a review", Journal of Polymers and the Environment (2011) **19**, 714-725.
- [8] O. Martin, L. Averous, "Poly(lactic acid): plasticization and properties of biodegradable multiphase systems", Polymer (2001) **42**, 6209-6219.
- [9] J. Lunt, "Large-scale production, properties and commercial applications of polylactic acid polymers", Polymer Degradation and Stability (1998) **59**, 145-152.

- [10] I. Chiulan, A.N. Frone, C. Brandabur, D.M. Panaiteescu, "Recent advances in 3D printing of aliphatic polyesters", Bioengineering (Basel, Switzerland) (2017) **5**, 2.
- [11] D. da Silva, M. Kaduri, M. Poley, O. Adir, N. Krinsky, J. Shainsky-Roitman, A. Schroeder, "Biocompatibility, biodegradation and excretion of polylactic acid (PLA) in medical implants and theranostic systems", Chemical Engineering Journal (2018) **340**, 9-14.
- [12] E. Lopez-Alba, S. Schmeer, F. Diaz, "Energy absorption capacity in natural fiber reinforcement composites structures", Materials (Basel, Switzerland) (2018) **11**, 418.
- [13] M. Patricia Arrieta, M. Dolores Samper, M. Aldas, J. Lopez, "On the use of PLA-PHB blends for sustainable food packaging applications", Materials (2017) **10**, 1008.
- [14] B. Tyler, D. Gullotti, A. Mangraviti, T. Utsuki, H. Brem, "Polylactic acid (PLA) controlled delivery carriers for biomedical applications", Advanced Drug Delivery Reviews (2016) **107**, 163-175.
- [15] M. Bocque, C. Voirin, V. Lapinte, S. Caillol, J.-J. Robin, "Petro-based and bio-based plasticizers: chemical structures to plasticizing properties", Journal of Polymer Science Part a-Polymer Chemistry (2016) **54**, 11-33.
- [16] J. Alam, M. Alam, M. Raja, Z. Abduljaleel, L.A. Dass, "MWCNTs-reinforced epoxidized linseed oil plasticized polylactic acid nanocomposite and its electroactive shape memory behaviour", International Journal of Molecular Sciences (2014) **15**, 19924-19937.
- [17] N. Prempeh, J. Li, D. Liu, K. Das, S. Maiti, Y. Zhang, "Plasticizing effects of epoxidized sun flower oil on biodegradable polylactide films: A Comparative Study", Polymer Science Series A (2014) **56**, 856-863.
- [18] V.S.G. Silverajah, N.A. Ibrahim, W.M.Z.W. Yunus, H. Abu Hassan, C.B. Woei, "A comparative study on the mechanical, thermal and morphological characterization of poly(lactic acid)/epoxidized palm oil blend", International Journal of Molecular Sciences (2012) **13**, 5878-5898.

- [19] V.S.G. Silverajah, N.A. Ibrahim, N. Zainuddin, W.M.Z.W. Yunus, H. Abu Hassan, "Mechanical, thermal and morphological properties of poly(lactic acid)/epoxidized palm olein blend", *Molecules* (2012) **17**, 11729-11747.
- [20] H. Liu, J. Zhang, "Research progress in toughening modification of poly(lactic acid)", *Journal of Polymer Science Part B-Polymer Physics* (2011) **49**, 1051-1083.
- [21] O. Fenollar, D. Garcia-Sanoguera, L. Sanchez-Nacher, J. Lopez, R. Balart, "Effect of the epoxidized linseed oil concentration as natural plasticizer in vinyl plastisols", *Journal of Materials Science* (2010) **45**, 4406-4413.
- [22] A. Carbonell-Verdu, D. Garcia-Sanoguera, A. Jordá-Vilaplana, L. Sanchez-Nacher, R. Balart, "A new biobased plasticizer for poly(vinyl chloride) based on epoxidized cottonseed oil", *Journal of Applied Polymer Science* (2016) **133**, 43642.
- [23] B.W. Chieng, N.A. Ibrahim, Y.Y. Then, Y.Y. Loo, "Epoxidized vegetable oils plasticized poly(lactic acid) biocomposites: mechanical, thermal and morphology properties", *Molecules* (2014) **19**, 16024-16038.
- [24] C. Xing, L.M. Matuana, "Epoxidized soybean oil-plasticized poly(lactic acid) films performance as impacted by storage", *Journal of Applied Polymer Science* (2016) **133**, 43201.
- [25] A. Carbonell-Verdu, M.D. Samper, D. Garcia-Garcia, L. Sanchez-Nacher, R. Balart, "Plasticization effect of epoxidized cottonseed oil (ECSO) on poly(lactic acid)", *Industrial Crops and Products* (2017) **104**, 278-286.
- [26] E.A.J. Al-Mulla, W.M.Z.W. Yunus, N.A.B. Ibrahim, M.Z. Ab Rahman, "Properties of epoxidized palm oil plasticized polylactic acid", *Journal of Materials Science* (2010) **45**, 1942-1946.
- [27] N. Petchwattana, S. Covavisaruch, "Mechanical and morphological properties of wood plastic biocomposites prepared from toughened poly(lactic acid) and rubber wood sawdust (*Hevea brasiliensis*)", *Journal of Bionic Engineering* (2014) **11**, 630-637.

- [28] D. Garcia-Garcia, O. Fenollar, V. Fombuena, J. Lopez-Martinez, R. Balart, "Improvement of mechanical ductile properties of poly(3-hydroxybutyrate) by using vegetable oil derivatives", Macromolecular Materials and Engineering (2017) **302**, 1600330.
- [29] J.M. Ferri, D. Garcia-Garcia, L. Sánchez-Nacher, O. Fenollar, R. Balart, "The effect of maleinized linseed oil (MLO) on mechanical performance of poly(lactic acid)-thermoplastic starch (PLA-TPS) blends", Carbohydrate Polymers (2016) **147**, 60-68.
- [30] J.M. Ferri, D. Garcia-Garcia, N. Montanes, O. Fenollar, R. Balart, "The effect of maleinized linseed oil as biobased plasticizer in poly (lactic acid)-based formulations", Polymer International (2017) **66**, 882-891.
- [31] A. Ruellan, A. Guinault, C. Sollogoub, G. Chollet, A. Ait-Mada, V. Ducruet, S. Domenek, "Industrial vegetable oil by-products increase the ductility of polylactide", Express Polymer Letters Polymers (2015) **9**, 1087-1103.
- [32] A. Carbonell-Verdu, D. Garcia-Garcia, F. Dominici, L. Torre, L. Sanchez-Nacher, R. Balart, "PLA films with improved flexibility properties by using maleinized cottonseed oil", European Polymer Journal (2017) **91**, 248-259.
- [33] A.K. Mohanty, M. Misra, L.T. Drzal, "Sustainable bio-composites from renewable resources: Opportunities and challenges in the green materials world", Journal of Polymers and the Environment (2002) **10**, 19-26.
- [34] R. Liu, Y. Peng, J. Cao, Y. Chen, "Comparison on properties of lignocellulosic flour/polymer composites by using wood, cellulose, and lignin flours as fillers", Composites Science and Technology (2014) **103**, 1-7.
- [35] A.A. Yussuf, I. Massoumi, A. Hassan, "Comparison of polylactic acid/kenaf and polylactic acid/rice husk composites: the influence of the natural fibers on the mechanical, thermal and biodegradability properties", Journal of Polymers and the Environment (2010) **18**, 422-429.
- [36] B.L. Shah, S.E. Selke, M.B. Walters, P.A. Heiden, "Effects of wood flour and chitosan on mechanical, chemical, and thermal properties of polylactide", Polymer Composites (2008) **29**, 655-663.

- [37] X. Li, S. Zhang, X. Zhang, S. Xie, G. Zhao, L. Zhang, "Biocompatibility and physicochemical characteristics of poly(epsilon-caprolactone)/poly(lactide-co-glycolide)/nano-hydroxyapatite composite scaffolds for bone tissue engineering", Materials & Design (2017) **114**, 149-160.
- [38] S. Pilla, S. Gong, E. O'Neill, R.M. Rowell, A.M. Krzysik, "Polylactide-pine wood flour composites", Polymer Engineering and Science (2008) **48**, 578-587.
- [39] Y. Du, T. Wu, N. Yan, M.T. Kortschot, R. Farnood, "Fabrication and characterization of fully biodegradable natural fiber-reinforced poly(lactic acid) composites", Composites Part B-Engineering (2014) **56**, 717-723.
- [40] D.P. Pfister, R.C. Larock, "Thermophysical properties of conjugated soybean oil/corn stover biocomposites", Bioresource Technology (2010) **101**, 6200-6206.
- [41] A. Carbonell-Verdu, L. Bernardi, D. Garcia-Garcia, L. Sanchez-Nacher, R. Balart, "Development of environmentally friendly composite matrices from epoxidized cottonseed oil", European Polymer Journal (2015) **63**, 1-10.
- [42] F. Ali, Y.-W. Chang, S.C. Kang, J.Y. Yoon, "Thermal, mechanical and rheological properties of poly (lactic acid)/epoxidized soybean oil blends", Polymer Bulletin (2009) **62**, 91-98.
- [43] L. Quiles-Carrillo, M.M. Blanes-Martinez, N. Montanes, O. Fenollar, S. Torres-Giner, R. Balart, "Reactive toughening of injection-molded polylactide pieces using maleinized hemp seed oil", European Polymer Journal (2018) **98**, 402-410.
- [44] L. Quiles-Carrillo, N. Montanes, C. Sammon, R. Balart, S. Torres-Giner, "Compatibilization of highly sustainable polylactide/almond shell flour composites by reactive extrusion with maleinized linseed oil", Industrial Crops and Products (2018) **111**, 878-888.
- [45] E. Petinakis, L. Yu, G. Edward, K. Dean, H. Liu, A.D. Scully, "Effect of matrix-particle interfacial adhesion on the mechanical properties of poly(lactic acid)/wood-flour micro-composites", Journal of Polymers and the Environment (2009) **17**, 83-94.
- [46] M.J. Garcia-Campo, L. Quiles-Carrillo, J. Masia, M.J. Reig-Perez, N. Montanes, R. Balart, "Environmentally friendly compatibilizers from soybean oil for ternary blends of poly(lactic acid)-

PLA, poly(epsilon-caprolactone)-PCL and poly(3-hydroxybutyrate)-PHB", Materials (Basel, Switzerland) (2017) 10, 1339.

- [47] S.C. Mauck, S. Wang, W. Ding, B.J. Rohde, C.K. Fortune, G. Yang, S.-K. Ahn, M.L. Robertson, "Biorenewable tough blends of polylactide and acrylated epoxidized soybean oil compatibilized by a polylactide star polymer", *Macromolecules* (2016) **49**, 1605-1615.
- [48] L. Quiles-Carrillo, S. Duart, N. Montanes, S. Torres-Giner, R. Balart, "Enhancement of the mechanical and thermal properties of injection-molded polylactide parts by the addition of acrylated epoxidized soybean oil", *Materials & Design* (2018) **140**, 54-63.
- [49] A. Carbonell-Verdu, M. Dolores Samper, D. Garcia-Garcia, L. Sanchez-Nacher, R. Balart, "Plasticization effect of epoxidized cottonseed oil (ECSO) on poly(lactic acid)", *Industrial Crops and Products* (2017) **104**, 278-286.
- [50] J.F. Balart, V. Fombuena, O. Fenollar, T. Boronat, L. Sanchez-Nacher, "Processing and characterization of high environmental efficiency composites based on PLA and hazelnut shell flour (HSF) with biobased plasticizers derived from epoxidized linseed oil (ELO)", *Composites Part B-Engineering* (2016) **86**, 168-177.
- [51] N. Burgos, V.P. Martino, A. Jimenez, "Characterization and ageing study of poly(lactic acid) films plasticized with oligomeric lactic acid", *Polymer Degradation and Stability* (2013) **98**, 651-658.



V. CONCLUSIONES



V.1. CONCLUSIONES PARCIALES.

V.1.1. Respecto a termoestables derivados del aceite de semilla de algodón epoxidado.

En relación al proceso de epoxidación del aceite de semilla de algodón (CSO) y la obtención de materiales termoestables derivados del ECSO es posible realizar las siguientes consideraciones finales:

Capítulo 1. *“Development of environmentally friendly composite matrices from epoxidized cottonseed oil”*

- 1.- La epoxidación del aceite de semilla de algodón con una ratio de peróxido: aceite de 3: 1 reflejó mejores resultados que con una ratio de 1,5: 1. A las 8 horas de epoxidación los valores del índice de oxígeno oxirano para el ratio 3: 1 se situaron en valores de 5,32% mientras que con un ratio de 1,5: 1 fueron en torno al 4%. En ambos casos la reacción se produjo rápidamente en las primeras dos horas debido a la alta disponibilidad de dobles enlaces.
- 2.- El valor del índice de oxígeno oxirano logrado para el ratio peróxido: aceite de 3: 1 con un índice de 5,32% es un resultado algo inferior al valor del aceite de soja epoxidado convencional (ESBO) aunque podría competir perfectamente en aplicaciones similares.
- 3.- El seguimiento del curado de la resina reveló que con una temperatura de curado de 110 °C durante 3 horas era suficiente para lograr resinas totalmente curadas.
- 4.- Es posible obtener interesantes resinas sólidas termoestables curando ECSO con anhídridos cíclicos. En particular, combinando un anhídrido flexible (anhídrido dodecenilsuccínico, DDSA) y un anhídrido rígido (anhídrido metil nadico, MNA) es posible adaptar las propiedades deseadas

en los materiales curados finales ya que DDSA confiere cierta flexibilidad mientras que MNA conduce a materiales más rígidos.

V.1.2. Respeto a los plastificantes derivados de aceite de semilla de algodón con aplicaciones en termoplásticos.

Capítulo 2. “*A new biobased plasticizer for poly (vinyl chloride), PVC base on epoxidized cottonseed oil (ECSO)*”

1.- Las propiedades mecánicas revelan el estado de curado de los plastisoles.

De este modo, es posible obtener plastisoles de PVC curados con valores de alargamiento superiores al 150 % y una resistencia a la tracción superior a 11 MPa.

2.- El perfil de curado a 220 °C y 10 min indica los valores óptimos en términos del mejor rendimiento mecánico; sin embargo, dado que el PVC es altamente sensible a la degradación térmica, el uso de temperaturas más bajas y tiempos de curado más altos, como 205 °C durante 15 min, podría ser una solución interesante ya que las condiciones de curado no son tan agresivas.

3.- Las coordenadas de color se presentan como un simple estudio, incluso aplicable durante un proceso de inspección de calidad o rutinario a nivel industrial, para conocer el grado de curado de los plastisoles.

4.- Las pruebas de extracción con disolventes, microscopía electrónica de barrido (SEM) y calorimetría diferencial de barrido (DSC) también son útiles para evaluar las condiciones óptimas de curado. Los plastisoles parcialmente curados se caracterizan por la presencia de plastificante libre que puede migrar fácilmente en un ensayo con disolventes, mostrar la presencia de

formas esféricas que pueden ser atribuidas a partículas de PVC hinchadas con ECSO en las imágenes SEM y picos endotérmicos entre -5 °C y 5 °C en los ensayos DSC.

Capítulo 3. “Plasticization effect of epoxidized cottonseed oil (ECSO) on poly(lactic acid)”

1.- El plastificante propuesto ECSO para el PLA mejora y facilita tanto el procesado con la extrusora de doble husillo como la posterior inyección de las probetas normalizadas

2.- En cuanto a las propiedades mecánicas la adición de un 10 % de ECSO mejoró el bajo alargamiento del PLA (9 %) hasta valores de 110,5 %. Ello supone un incremento de los valores de alargamiento de más del 1100 %. Para la citada formulación también se observó un notable aumento de la energía absorbida mediante los ensayos charpy.

3.- El análisis de la morfología de fractura mediante FESEM, pone en manifiesto la mejora de la ductilidad. Para un contenido bajo de plastificante se observa una buena miscibilidad mientras que, a medida que se aumenta la cantidad de ECSO, se puede observar separación de fases con algunas cavidades o huecos esféricos indicativos de una fase rica en ECSO disperso en la matriz de PLA.

4.- El análisis térmico mecánico dinámico (DMTA) y calorimetría diferencial de barrido (DSC) demostraron una clara disminución en la temperatura de transición vítrea con respecto al PLA puro a medida que aumentaba el contenido de ECSO. De hecho, la formulación PLA + 10 wt% ECSO ofrece una T_g de 60,74 °C, muy por debajo de la del PLA puro que se sitúa en 66,75 °C.

5.- Tras las pruebas previas llevadas a cabo antes de ejecutar la investigación, se observó que más del 10 wt% de ECSO provoca la saturación de plastificante y las propiedades mecánicas no mejoran.

Capítulo 4. “PLA films with improved flexibility properties by using maleinized cottonseed oil”

- 1.- La maleinización del aceite de semilla de algodón es viable desde el punto de vista del valor del índice de acidez. Durante las dos primeras horas, únicamente se alcanzó un valor de 16,9 mg KOH g⁻¹, aunque durante la tercera hora y favorecido por el incremento de la temperatura a los 220 °C, el índice de acidez se situó en 51,2 mg KOH g⁻¹ al finalizar el proceso de maleinización.
- 2.- Los aceites maleinizados también facilitaron las tareas de extrusión, tanto en el procesado en la extrusora de doble husillo como durante la obtención de los films, con respecto al PLA puro. Se comparó el efecto plastificante del MCSO con respecto al aceite de linaza maleinizado (MLO) y los resultados fueron satisfactorios.
- 3.- La caracterización térmica mediante DSC mostró un ligero efecto de la plastificación al reducirse la temperatura de transición vítrea en 2 °C en la formulación con un 10 % MCSO.
- 4.- La adición de plastificante también repercute en el incremento de las propiedades dúctiles. De hecho, la formulación de PLA con 7,5 wt% MCSO, ofrece un alargamiento a la rotura del 15,7 %; valor superior al PLA puro, con valores del 4 %. El alargamiento registrado al incorporar MLO prácticamente no demostró mejoras.
- 5.- El análisis de la morfología de fractura mediante microscopía FESEM pone en manifiesto las bajas propiedades logradas por el plastificante MLO. Las imágenes muestran separación de fases y por lo tanto se atribuyen a unos bajos valores de alargamiento con la incorporación de MLO. Por el contrario, las superficies analizadas de PLA con MCSO muestran una mayor ductilidad con mayores áreas de deformación plástica.
- 6.- Las pruebas de desintegración indican cómo la incorporación de los plastificantes maleinizados aceleran el proceso de desintegración con el

incremento del % de plastificante de 13 a 11 y 10 días para las formulaciones de PLA puro, 5 % MCSO y 7,5 % MCSO respectivamente.

V.1.3. Respecto a los efectos de aceites vegetales derivados de semilla de algodón en compatibilización y optimización de formulaciones derivadas de ácido poliláctico.

En relación al uso de los aceites vegetales derivados de la semilla de algodón y, en particular a los logrados a partir de la maleinización (MCSO) y epoxidación (ECSO) en aplicaciones como compatibilizantes y en la optimización de formulaciones derivadas del ácido poliláctico, es posible realizar las siguientes consideraciones finales para cada uno de los capítulos publicados:

Capítulo 5. “Manufacturing and compatibilization of PLA/PBAT binary blends by cottonseed oil-based derivatives”

1.- Los aceites maleinizados y epoxidados a partir del aceite de semilla de algodón ofrecen buenos resultados de compatibilización de los films 80 PLA/20 PBAT, con un notable aumento del alargamiento a la rotura sin comprometer otras propiedades de resistencia mecánica. De hecho, la mezcla compatibilizada con un 7,5 wt% de MCSO otorga unas propiedades mecánicas equilibradas con un alargamiento a la rotura del 123 % y un módulo de Young superior a 2250 MPa. Estas propiedades son incluso mejores que con el uso del oligómero de estireno acrílico Joncrys ADR 4368 proveniente del petróleo.

2.- Tan solo con la incorporación de un 1 wt. % Joncryl, 1 wt % ECSO y 1 wt % MCSO se logra incrementar el alargamiento en un 186,6 % 139,7 % y 107,2 % con respecto al PLA puro.

3.- El análisis de la morfología de fractura mediante FESEM proporciona diferencias entre los distintos compatibilizantes. Mientras que las mezclas con PLA/PBAT/1 ECSO muestran una superficie similar a las de la mezcla PLA/PBAT, la incorporación de un 1 % Joncryl o MCSO favorece la presencia de huecos.

4.- Según los análisis termomecánicos, la mezcla sin compatibilizantes muestra una baja miscibilidad, con un mínimo descenso de la T_g de 1,3 °C con respecto al PLA puro. Por otro lado, con la adición de un 1 wt% de los tres compatibilizadores utilizados en este estudio se obtuvo un significativo descenso en la T_g de aproximadamente 2 °C, lo que indica un cierto comportamiento de compatibilización.

5.- Según los resultados que revela la termogravimetría tanto ECSO como MCSO mejoran la estabilidad térmica de las formulaciones, aunque estos compatibilizantes no presentan un efecto relevante sobre la desintegración de los films.

Capítulo 6. “*Processing and characterization of environmentally friendly composites from poly(lactic acid) and cottonseed waste materials*”

1.- El uso de la harina de semilla de algodón, a parte de revalorizar un subproducto derivado directamente de la extracción del aceite de semilla de algodón, es viable desde el punto de vista del procesado mediante extrusión y posterior inyección.

2.- Los compuestos de PLA que contienen un 15 wt% de harina de semilla de algodón (CSF) mostraron fragilidad debido a las malas interacciones entre el polímero y las partículas de harina. De hecho, la formulación PLA-15CSF

ofrece el menor alargamiento a la rotura de todas las formulaciones, con un resultado del 26,8 %. No obstante, es un valor superior al PLA puro que se sitúa en el 3,7 %

3.- La incorporación de ECSO y MCSO (7,5 wt%) mejoró el incremento del alargamiento a la rotura hasta valores de 75,3 % y 75,8 % para las formulaciones de PLA-7,5E-15CSF y PLA-7,5M-15CSF. Si bien, los resultados obtenidos sugieren que los compuestos con 7,5 wt% de MCSO ofrecen un equilibrio de las propiedades mecánicas como resistencia al impacto y alargamiento a la rotura sin comprometer otras propiedades mecánicas como la resistencia y el módulo.

4.- Los resultados que ofrecen las técnicas de calorimetría diferencial de barrido demuestran un descenso de la temperatura de transición vítrea con la incorporación de los aceites de semilla de algodón modificados. Destaca una reducción en la formulación PLA-7,5M-15CSF de 6,5 °C con respecto al PLA puro, debido a un efecto plastificante provocado por la alta reactividad del grupo anhídrido maleico con el grupo hidroxilo de las cadenas terminales del PLA y la celulosa del CSF.

V.2. CONCLUSIONES FINALES.

De manera global, la hipótesis del trabajo inicial planteada ha sido validada con los resultados obtenidos a lo largo de todo el trabajo, y prueba de ello se refleja en las publicaciones logradas. Por lo tanto, en este sentido, es posible afirmar:

- 1.- Los subproductos de la planta de algodón, no aprovechados por los sectores textiles, pueden serlo para usos adicionales como el industrial, elaborando aceites de semilla de algodón modificados a partir de los cuales producir nuevos materiales respetuosos con el medio ambiente.
- 2.- Las resinas resultantes de la epoxidación del aceite de semilla de algodón ofrecen interesantes alternativas frente a algunas resinas epoxi derivadas del petróleo como resinas termoestables flexibles y aditivos para resinas epoxi de alta rigidez.
- 3.- El aceite de semilla de algodón epoxidado (ECSO) puede usarse como plastificante para conseguir plastisoles de PVC con una parte de origen bio.
- 4.- Con la incorporación de aceite de semilla de algodón epoxidado (ECSO) se obtuvieron nuevas formulaciones de PLA plastificado.
- 5.- El aceite de semilla de algodón maleinizado (MCSO) puede ser utilizado como un plastificante respetuoso con el medio ambiente para la elaboración de films de PLA. Incluso, si se compara el MCSO con un aceite comercial a partir del aceite de linaza maleinizado (MLO), el MCSO muestra un mejor rendimiento y resultados.
- 6.- Es posible indicar que MCSO es un plastificante altamente eficiente para la elaboración de films de PLA con gran interés desde el punto de vista técnico y ambiental.
- 7.- El uso de compatibilizantes derivados de aceites vegetales (aceites vegetales epoxidados y maleinizados) se destaca como una solución ecológica para mejorar la miscibilidad de mezclas de tipo poliéster con excelente

equilibrio entre propiedades mecánicas y térmicas. En definitiva, los compatibilizadores derivados de los aceites de semilla de algodón se presentan como aditivos ecológicos para mezclas binarias de PLA / PBAT, con mejores propiedades que el oligómero de estireno acrílico Joncryl proveniente del petróleo.

8.- Se observó que es factible el uso de materiales de PLA con desechos provenientes de la industria algodonera. En este caso, la harina de semilla de algodón, considerada como un subproducto de la extracción del aceite, se incorporó como una carga en las formulaciones de PLA para dar compuestos plásticos de madera altamente respetuosos (WPC).

Finalmente, y teniendo presentes los puntos citados anteriormente, se ha demostrado en esta investigación que tanto los aceites modificados químicamente a partir del aceite de semilla de algodón como los subproductos derivados del mismo proceso de extracción pueden ser usados en amplios sectores para lograr materiales respetuosos con el medio ambiente.